AD_____

Award Number: DAMD17-01-1-0781

TITLE: Mechanisms of α-Synuclein Aggregation and Toxicity

PRINCIPAL INVESTIGATOR: Benjamin Wolozin, Ph.D.

CONTRACTING ORGANIZATION: Boston University
Boston, MA 02118-2526

REPORT DATE: September 2006

TYPE OF REPORT: Final

PREPARED FOR: U.S. Army Medical Research and Materiel Command
Fort Detrick, Maryland 21702-5012

REPORT DOCUMENTATION PAGE

Form Approved
OMB No. 0704-0188

1. REPORT DATE	2. REPORT TYPE	3. DATES COVERED
01-09-2006	Final	1 Sepb 2001 – 31 Aug 2006

4. TITLE AND SUBTITLE

Mechanisms of α-Synuclein Aggregation and Toxicity

5a. CONTRACT NUMBER

5b. GRANT NUMBER
DAMD17-01-1-0781

5c. PROGRAM ELEMENT NUMBER

6. AUTHOR(S)

Benjamin Wolozin, Ph.D.

5d. PROJECT NUMBER

5e. TASK NUMBER

5f. WORK UNIT NUMBER

7. PERFORMING ORGANIZATION NAME(S) AND ADDRESS(ES)

Boston University
Boston, MA 02118-2526

8. PERFORMING ORGANIZATION REPORT NUMBER

9. SPONSORING / MONITORING AGENCY NAME(S) AND ADDRESS(ES)
U.S. Army Medical Research and Materiel Command
Fort Detrick, Maryland 21702-5012

10. SPONSOR/MONITOR'S ACRONYM(S)

11. SPONSOR/MONITOR'S REPORT NUMBER(S)

12. DISTRIBUTION / AVAILABILITY STATEMENT
Approved for Public Release; Distribution Unlimited

13. SUPPLEMENTARY NOTES

14. ABSTRACT

Alpha-synuclein is a protein implicated in the pathophysiology of Parkinson's disease. The purpose of this proposal is to study the regulation of synuclein aggregation by metals, the interaction of synuclein with other proteins associated with its pathophysiology and the effects of aggregated alpha-synuclein on the function of neuronal mitochondria. During the current year, we have studied the regulation of synuclein aggregation and toxicity in vitro. We examined the response of synuclein to metals, as well as to other toxins. We observed that inhibitors of mitochondrial complex I are the most effective agents for inducing synuclein fibrillization and toxicity in vivo (in C. elegans). We also used C. elegans to explore novel mechanisms of therapy. We demonstrated that D-ß-hydroxybutyrate, TUDCA and probucol were all protective against synuclein toxicity. Both TUDCA and probucol are FDA approved medications that could be readily translated towards clinical use.

15. SUBJECT TERMS
Protein aggregation, Lewy body, mitochondria, metals, mitochondria, complex I, C. elegans, therapy, neuroprotection

16. SECURITY CLASSIFICATION OF:				18. NUMBER OF PAGES	19a. NAME OF RESPONSIBLE PERSON
a. REPORT	b. ABSTRACT	c. THIS PAGE			USAMRMC
U	U	U	UU	90	19b. TELEPHONE NUMBER *(include area code)*

Table of Contents

Introduction

The goal of this grant proposal is to investigate the interaction of α-synuclein with metals. Our preliminary studies suggested that metals, such as iron, might promote synuclein aggregation. In this proposal, we sought to understand which metals interact with α-synuclein, how these metals might modulate α-synuclein aggregation, and how they might affect the interaction with other proteins relevant to Parkinson's disease. The work in the fourth year focused on examining how aggregation of α-synuclein, which is induced by iron or aging, affects its interaction with specific targets, such as the proteasome and the mitochondria. Much of this work has utilized the simple in vivo system of C. elegans, for which the MRC had previously approved expansion of our work.

Body:

Work from Aim 1 that was accomplished:

As mentioned in the progress report from 2003, we accomplished the work specified in Aim 1 during the 2002 – 2003 year. The articles related to this work were described in the last progress report, and will not be described in this report.

Work relevant to Aims 2:

In aim 2, we proposed to investigate how different metals might interact to affect α-synuclein aggregation, and how binding of α-synuclein to proteins altered the aggregation. In 2002, we had shown that iron potentiates synuclein aggregation while magnesium inhibits synuclein aggregation [1]. In 2003/4, we began examining proteins that bind α-synuclein and demonstrated that synuclein binds to the proteasomal S6' protein [2]. During the last year, we investigated the regulation of synuclein actions by its homologues. We published work investigating the regulation of synuclein aggregation by its homologues (ß and γ synuclein), showing that ß-synuclein competes with α-synuclein for interaction with the proteasome. This work is described in a manuscript by Snyder, et al, that was published in the Journal of Biological Chemistry [3].

Work relevant to Aims 3:

Work on Aim 3 focuses on the affects of α-synuclein on the mitochondria and the effects of α-synuclein in vivo. During the past year, we have expanded our work in vivo, using C. elegans. This work has proven to be very productive, and has resulted in a manuscript by Ved, et al, that was published in the Journal of Biological Chemistry. Using C. elegans, we made the surprising discovery that over-expressed α-synuclein causes a selective deficit in complex I of the mitochondria. We have demonstrated this in multiple ways, using toxicity assays, respiration, pharmacology and pathology. We also developed a novel therapeutic strategy for reversing inhibition of complex I using a combination of D-β-hydroxybutyrate (which augments the activity of complex II) and TUDCA, which prevents apoptosis. This work demonstrates a surprisingly strong connection between mitochondrial function and α-synuclein (and induction of pathology by inhibitors of mitochondrial complex I), and was published in the Journal of Biological Chemistry [4].

We have also examined the effects of α-synuclein on mammalian neurons from the A30P α-synuclein transgenic mice. We performed a proteomic study that resulted in identification of three proteins that show strong oxidation in brains of transgenic mice over-expressing α-synuclein. In work that is now in press, we demonstrated that aggregation of α-synuclein induces up-regulation of another protein related to Parkinson's disease, DJ-1 (see list of articles, below). This protein is up-regulated in astrocytes but also might be up-regulated in neurons, as shown by its ability to bind to tau protein.

Since beginning this proposal, an important new gene has been discovered – LRRK2. We have been studying LRRK2 and have made the surprising discovery that it exhibits strong control over anti-oxidant defenses. Based on our findings, we have identified biochemical approaches, based on the forkhead pathway, that can protect against toxicity caused by either α-synuclein, rotenone or LRRK2. Our future work will be examining this neuroprotective axis.

Key Research Accomplishments:

• Determined affinity and pH dependence of iron for α-synuclein
• Determined affinity of Cu(II), Mg(II), Zn(II) and Ca(II) for α-synuclein, and determined that Ni(II), Mn(II) and Al(III) do not bind α-synuclein.
• Performed electrospray ionization mass spectroscopy of α-synuclein.
• Demonstrated that iron causes α-synuclein aggregation in neurons, and that α-synuclein increases the vulnerability to iron of neurons.
• Demonstrated that magnesium inhibits α-synuclein aggregation and protects neurons against iron-mediated toxicity.
• Demonstrated that α-synuclein binds the proteasomal protein S6'.
• Demonstrated that β-synuclein inhibits binding of α-synuclein to the proteasome
• Demonstrated that γ-synuclein binds to a different part of the proteasome, the 20S proteasome.
• Demonstrated that aggregation of α-synuclein induces activation of JNK and hyperphosphorylation of tau protein.
• Demonstrated that the parkin binding protein, CHIP binds tau protein.
• Demonstrated that SEPT5_v2 binds parkin.
• Demonstrated that aggregation of α-synuclein induce up-regulation of DJ-1 protein.
• Developed an additional model for α-synuclein toxicity and aggregation using C. Elegans over-expressing α-synuclein, and demonstrated a selective vulnerability of mitochondrial complex I.
• Identified a chemical strategy for reversing the toxicity associated with inhibition of mitochondrial complex I, using DβHB and TUDCA.

Reportable Outcomes:

The research performed this year has resulted in publication of 4 articles relevant to α-synuclein. These articles are listed below, and are provided in the appendices.

Articles relevant to α-synuclein and the DAMD grant award that were published in last year:

1. Ved R, Saha S, Westlund B, Perier C, Burnam L, Sluder A, Hoener M, Rodrigues CM, Alfonso A, Steer C, Liu L, Przedborski S, Wolozin B. Similar patterns of mitochondrial vulnerability and rescue induced by genetic modification of alpha-synuclein, parkin, and DJ-1 in Caenorhabditis elegans. J Biol Chem. 2005 Dec 30;280(52):42655-68.

2. Poon HF, Frasier M, Shreve N, Calabrese V, Wolozin B, Butterfield DA. Mitochondrial associated metabolic proteins are selectively oxidized in A30P alpha-synuclein transgenic mice--a model of familial Parkinson's disease. Neurobiol Dis. 2005 Apr;18(3):492-8.

3. Frasier M, Walzer M, McCarthy L, Magnuson D, Lee JM, Haas C, Kahle P, Wolozin B. Tau phosphorylation increases in symptomatic mice overexpressing A30P alpha-synuclein. Exp Neurol. 2005 Apr;192(2):274-87.

4. Snyder H, Mensah K, Hsu C, Hashimoto M, Surgucheva IG, Festoff B, Surguchov A, Masliah E, Matouschek A, Wolozin B. beta-Synuclein reduces proteasomal inhibition by alpha-synuclein but not gamma-synuclein. J Biol Chem. 2005 Mar 4;280(9):7562-9. Epub 2004 Dec 9.

5. Snyder, H., Wolozin, B., Pathological proteins in Parkinson's disease: focus on the proteasome. J Mol Neurosci. 24:425-42 (2005).

6. Frasier, M., Frausto, S., Lewicki, D., Golbe, L., Wolozin, B., DJ-1 Expression Increases in Mice Over-Expressing A30P α-Synuclein (in press)

Conclusions:

α-Synuclein (AS) is one of the main proteins that accumulate in the brains of subjects with Parkinson disease (PD). The ability of mutant forms of AS to cause degenerative disease resembling PD indicates that abnormalities in AS biology are sufficient to cause degenerative disease and likely contribute to the pathophysiology of sporadic PD, which is the more common disorder afflicting Americans. The purpose of this grant proposal was to understand the mechanisms of α-synuclein (AS) toxicity. The work plan is presented below:

Work Plan:

Year 1 (completed)

1. Determine the buffer and pH dependence of iron - α-synuclein binding
2. Determine the stoichiometry of iron binding
3. Investigate the sequence requirements for binding of iron (FeII) to α-synuclein
4. Determine the role of metal binding binding in synuclein aggregation in neurons.

Year 2 (completed)

1. Determine the role of metal binding in synuclein aggregation in neurons.
2. Measure the levels of iron and proteins related to iron metabolism in cells over-expressing α-synuclein.
3. Measure binding of ions and nucleotides to α- and β-synuclein.
4. Determine how the interaction between co-factors affect binding patterns of α-synuclein.

Year 3 (current)

1. Investigate the domains of α-synuclein important for binding of nucleotides and metals.
2. Determine how cofactors affect the binding of α-synuclein to other proteins.
3. Determine how binding factors or analogues affect the aggregation of α-synuclein in vitro and in neurons.

Year 4 (planned)

1. Investigate the changes in mitochondrial function induced by synuclein aggregation.
2. Investigate how the levels of mitochondrial proteins change during synuclein aggregation.
3. Investigate how the distribution of mitochondrial proteins change during synuclein aggregation.

As a result of our study we have addressed many of the items in the work plan, although we were not able to determine some of the items in the work plan for technical reasons. The first part of the project (Year 1 from the work plan) focused on investigating the interaction between metals and AS. We accomplished many of the items in the aim. The methods that we used for this study and the actual results that we obtained are published in the article by Golts, et al [1]. These results demonstrated that metals bind to AS with three different patterns. The first class of metals include iron (Fe^{2+}) and copper (Cu^{2+}). These metals reduce the intrinsic tyrosine fluorescence in AS in response to binding, and exhibit what we would term a pathological pattern of binding. This pattern of binding exhibits an IC50 of 200 μM, and required an acidic environment, such as would occur within a vesicle, to occur. Binding of these metals causes AS to aggregate, which could be very important for the pathophysiology of PD. Deletion analysis demonstrated that the C-terminus of AS was critical for binding to iron (unpublished results) because an AS construct containing amino acids 1 – 113 showed greatly reduced binding of iron. A second class of metals, consisted of Magnesium, Zinc and Calcium. Binding of these metals to AS does not cause aggregation and increases rather than decreases the intrinsic tyrosine fluorescence. We studied binding of Mg the most because it produced very robust results. We observed that binding of Mg actually prevents aggregation of AS induced by iron. This observation is interesting and relates to the pathophysiology of PD because several reports suggest that Mg are reduced in neurons from subjects with PD

[5, 6]. Our findings raise the possibility that supplementing diets with Magnesium might delay the onset or progression of PD by reducing AS aggregation.

The work assigned to year 2 was the only work in this aim in which we did not make significant progress. In unpublished work, we used the tyrosine fluorescence assay to assess binding of nucleotides to AS. We observed that GTP is able to modulate the intrinsic fluorescence of AS. However, studies designed to pursue this intriguing observation suggested that the binding was quite weak and probably not biologically significant. First we use filter binding studies with radioactive GTP. We were unable to convincingly demonstrate that GTP binds AS; the radioactively labeled GTP never produced reactivity that remained attached to AS after washing. We also sent AS to a colleague at the University of Chicago who specializes in binding of G proteins. He performed an assay in which he determined whether AS promotes the hydrolysis of GTP, however he was unable to observe AS-stimulated hydrolysis. In parallel experiments performed as a positive control, he did show that Ras bindings GTP and promotes its hydrolysis. These studies led us to conclude that nucleotides do not play an important role in AS biology.

With respect to the work in Year 3, we made significant progress in understanding how binding of factors affects the function of AS. Increasing data suggests that degenerative diseases involve proteasomal inhibition, so we investigated the interaction of AS with the proteasome [2, 3]. We observed that aggregated AS potently inhibits the proteasome, and showed that the inhibiting is mediated by binding to the proteasomal protein S6'. AS has two homologues, β and γ-synuclein. We found that γ-synuclein also inhibits the proteasome, but the pattern of inhibition is different than that of AS. Inhibition of proteasomal activity by γ-synuclein does not require prior aggregation of the protein. Differences between the activities of AS and γ-synuclein also appeared when we examined the interaction with β-synuclein. We observed that β-synuclein potently antagonizes the proteasomal inhibition induced by AS, but had no effect on proteasomal inhibition induced by γ-synuclein. Our binding studies suggest that β-synuclein binds directly to AS, and we hypothesize that binding of the two proteins contributes to the mechanism of antagonism by β-synuclein. This work is important because it points to another possible therapeutic strategy, in which β-synuclein can be used to inhibit the toxic activity of AS. This hypothesis has gained some support from recent work out of Dr. Eliezer Masliah's, in which he showed that a lentiviral vector expressing β-synuclein could partially protect against AS toxicity [7] [8].

As part of this aim, we also examined the interactions of AS with the PD-related protein in vivo. First we examined the patterns of protein changes associated with AS aggregation in vivo [9]. We demonstrated that AS aggregation is associated with stimulation of the stress kinase c-Jun Kinase. We also showed that AS aggregation is associated with tau phosphorylation. The abnormally phosphorylated tau did not occur in the same neurons as the AS aggregates, which suggests that the deleterious effects of AS aggregation affect the brain more broadly than would be assumed by simply examining the neurons containing visible aggregates. This work is particularly interesting because polymorphisms in the tau gene are associated with PD [10]. We demonstrated a further linkage between tau protein and proteins implicated in PD in the work by Petrucelli et al [11]. This work demonstrates that parkin, and an associated protein, CHIP, regulate tau ubiquitination an degradation, which increases the links between tau protein and PD. DJ-1 is another protein that is associated with PD, and we observed that aggregation of AS is associated with DJ-1 accumulations, which are also not in the same cells as the AS aggregates; the DJ-1 accumulations occur in astrocytes. This work is being published as part of the proceedings of the AD/PD meeting from 2005. Finally, another paper performed by Petrucelli and colleagues in collaboration with my laboratory demonstrates that parkin can protect against AS toxicity [12].

The work in year 4 proposed to examine the interaction between AS and the mitochondria. We examined this question in two separate works by Ved et al, and by Poon et al, and we continue to examine this work in the laboratory [4] [13]. The work by Poon et al utilized a proteomic approach to examine which proteins are altered during the course of AS-mediated degeneration in a transgenic model of PD. This study identified three proteins that showed increased oxidation associated with AS-mediated degeneration, lactate dehyrogenase, α-enolase and carbonic anhydrase [13]. These results suggest that AS-aggregation might cause significant damage to the mitochondria because each of these proteins is associated with mitochondria. The focus on the

mitochondria was further enhanced by new technology that we imported into the laboratory. We have developed the capability to use C. elegans to examine biological mechanisms relevant to PD. Approaches using C. elegans were not described in the original grant proposal, but have proven to be very relevant to the aims of this grant proposal. In work published by Ved, et al, we demonstrated that abnormalities in the biology of AS, as well as two other PD-associated genes (parkin and DJ-1) all impair mitochondrial function [4]. We did this by directly monitoring oxygen consumption in the worms, and also by examining the pattern of vulnerability to toxins. We demonstrated that worms expressing PD-associated genes are selectively vulnerable to mitochondrial toxins, and in particular, to inhibitors of complex I. The knowledge that AS selectively targets mitochondria helped us to design a cocktail of neuroprotective compounds that appear to protect against mechanisms of toxicity associated with PD. We demonstrated that the compound D-betahydroxybutyrate (DbHB), which enhances the function of complex II, was able to partially protect against toxicity associated with AS toxicity. This work emphasizes the potential importance of mitochondrial dysfunction in PD. We also targeted apoptosis, which is another mitochondrial function. We observed that the compound tauroursodeoxycholic acid (TUDCA), which is clinically approved for use in liver failure, also partially protects against toxicity in our worm models. Combining the DbHB and the TUDCA provided complete protection [4]. This suggests that mitochondrial protection is a useful approach to examine for therapy of PD.

In summary, we have accomplished most of the tasks proposed in our report. We studied the interaction of metals with AS in vitro and in cells, and in the process identified metals that accelerate or slow the process of aggregation. We studied the regulation of AS physiology and pathophysiology in neurons discovering that AS inhibits the proteasome, possibly by binding to the S6' protein. We also developed a significant body of work demonstrating that AS impairs mitochondrial function. Finally, we developed three different strategies for therapeutic intervention: magnesium, β-synuclein and DbHB/TUDCA. Further work must be performed to determine whether these therapeutic approaches can be applied to the clinical treatments in humans.

I have included relevant publications from my laboratory along with this report.

Recommended changes: None.

References:

1. Golts, N., et al., Magnesium inhibits spontaneous and iron-induced aggregation of alpha- synuclein. J Biol Chem, 2002. 277: p. 16116-23.
2. Snyder, H., et al., Aggregated and monomeric alpha-synuclein bind to the S6' proteasomal protein and inhibit proteasomal function. J Biol Chem, 2003. 278: p. 11753-9.
3. Snyder, H., et al., beta-Synuclein reduces proteasomal inhibition by alpha-synuclein but not gamma-synuclein. J Biol Chem, 2005. 280: p. 7562-9.
4. Ved, R., et al., Similar Patterns of Mitochondrial Vulnerability and Rescue Induced by Genetic Modification of -Synuclein, Parkin and DJ-1 in *C. Elegans*. J Biol Chem, 2005. 280: p. 42655-68.
5. Barbiroli, B., et al., Phosphorus magnetic resonance spectroscopy in multiple system atrophy and Parkinson's disease. Mov Disord, 1999. 14: p. 430-5.
6. Uitti, R.J., et al., Regional metal concentrations in Parkinson's disease, other chronic neurological diseases, and control brains. Can J Neurol Sci, 1989. 16: p. 310-4.
7. Windisch, M., et al., Development of a new treatment for Alzheimer's disease and Parkinson's disease using anti-aggregatory beta-synuclein-derived peptides. Journal of Molecular Neuroscience, 2002. 19: p. 63-69.
8. Hashimoto, M., et al., beta-Synuclein Inhibits alpha-Synuclein Aggregation. A Possible Role as an Anti-Parkinsonian Factor. Neuron, 2001. 32: p. 213-23.
9. Frasier, M., et al., Tau phosphorylation increases in symptomatic mice overexpressing A30P alpha-synuclein. Exp Neurol, 2005. 192: p. 274-87.
10. Healy, D.G., et al., Tau gene and Parkinson's disease: a case-control study and meta-analysis. J Neurol Neurosurg Psychiatry, 2004. 75: p. 962-5.

11. Petrucelli, L., et al., CHIP and Hsp70 regulate tau ubiquitination, degradation and aggregation. Hum Mol Genet, 2004. 13: p. 703-14.
12. Petrucelli, L., et al., Parkin protects against the toxicity associated with mutant alpha-synuclein: proteasome dysfunction selectively affects catecholaminergic neurons. Neuron, 2002. 36: p. 1007-19.
13. Poon, H.F., et al., Mitochondrial associated metabolic proteins are selectively oxidized in A30P alpha-synuclein transgenic mice--a model of familial Parkinson's disease. Neurobiol Dis, 2005. 18: p. 492-8.

THE JOURNAL OF BIOLOGICAL CHEMISTRY
Vol. 277, No. 18, Issue of May 3, pp. 16116–16123, 2002

Printed in U.S.A.

Magnesium Inhibits Spontaneous and Iron-induced Aggregation of α-Synuclein*

Received for publication, August 15, 2001, and in revised form, February 13, 2002
Published, JBC Papers in Press, February 15, 2002, DOI 10.1074/jbc.M107866200

Natalie Golts, Heather Snyder, Mark Frasier, Catherine Theisler, Peter Choi, and Benjamin Wolozin‡

From the Department of Pharmacology, Loyola University Medical Center, Maywood, Illinois 60153

Multiple studies implicate metals in the pathophysiology of neurodegenerative diseases. Disturbances in brain iron metabolism are linked with synucleinopathies. For example, in Parkinson's disease, iron levels are increased and magnesium levels are reduced in the brains of patients. To understand how changes in iron and magnesium might affect the pathophysiology of Parkinson's disease, we investigated binding of iron to α-synuclein, which accumulates in Lewy bodies. Using fluorescence of the four tyrosines in α-synuclein as indicators of metal-related conformational changes in α-synuclein, we show that iron and magnesium both interact with α-synuclein. α-Synuclein exhibits fluorescence peaks at 310 and 375 nm. Iron lowers both fluorescence peaks, while magnesium increases the fluorescence peak only at 375 nm, which suggests that magnesium affects the conformation of α-synuclein differently than iron. Consistent with this hypothesis, we also observe that magnesium inhibits α-synuclein aggregation, measured by immunoblot, cellulose acetate filtration, or thioflavine-T fluorescence. In each of these studies, iron increases α-synuclein aggregation, while magnesium at concentrations >0.75 mM inhibits the aggregation of α-synuclein induced either spontaneously or by incubation with iron. These data suggest that the conformation of α-synuclein can be modulated by metals, with iron promoting aggregation and magnesium inhibiting aggregation.

Parkinson's disease (PD)[1] is a common motor disorder that affects about 1% of population over the age of 65 (1). The disease is characterized by progressive neurodegeneration predominantly affecting dopaminergic neurons in the nigrostriatal system (2). The degenerating neurons develop intracellular inclusions, termed Lewy bodies, which are composed of a dense core of filamentous and granular material (3). Recent studies indicate that α-synuclein is a major filamentous component of Lewy bodies (3, 4). Genetic studies suggest that α-synuclein plays a key role in the pathophysiology of PD, because mutations in α-synuclein, at A53T or A30P, are associated with early-onset familial PD (5, 6).

* This work was supported by NINDS Grant NS41786-01, United States Army Medical Research and Materiel Command Grant DAMD17-01-1-0781, Retirement Research Foundation, and Panacea Pharmaceuticals (to B. W.). The costs of publication of this article were defrayed in part by the payment of page charges. This article must therefore be hereby marked "*advertisement*" in accordance with 18 U.S.C. Section 1734 solely to indicate this fact.

‡ To whom correspondence should be addressed: Dept. of Pharmacology, Loyola University Medical Center, Bldg. 102, Rm. 3634, 2160 S. 1st Ave., Maywood, IL 60153. Tel.: 708-216-6195; Fax: 708-216-6596; E-mail: bwolozi@lumc.edu.

[1] The abbreviation used is: PD, Parkinson's disease.

The accumulation of aggregated protein underlies the pathophysiology of many neurodegenerative disorders, and increasing evidence suggests that aggregated α-synuclein plays a key role in the pathophysiology of PD. α-Synuclein has a strong tendency to aggregate and does so spontaneously *in vitro* at a slow rate (7–9). Both the A53T and the A30P mutations in PD increase the tendency of α-synuclein to aggregate. Many studies in cultured neurons, and some studies in transgenic animals, suggest that α-synuclein aggregation is linked to cellular toxicity and neurodegeneration (10–12). In cell culture, formation of α-synuclein aggregates correlates with cell injury (10). Overexpressing α-synuclein in *Drosophila* leads to an age-dependent accumulation of aggregated α-synuclein and associated neurodegeneration (12). Masliah and colleagues also observed that aggregated α-synuclein is associated with loss of markers in dopaminergic neurons, although other studies of α-synuclein overexpression in transgenic mice have been less conclusive (11, 13, 14). Thus, increasing lines of evidence suggest that aggregation of α-synuclein is associated with the degeneration of dopaminergic neurons and suggest that α-synuclein contributes to the neurodegenerative processes occurring in PD.

Recombinant α-synuclein aggregates spontaneously following prolonged incubation *in vitro*. Recently, we and others have shown that α-synuclein also aggregates rapidly following exposure to Fe(II) (10, 15). *In vitro*, Fe(II) accelerates the rate of α-synuclein aggregation. For example, similar amounts of aggregation are induced *in vitro* by incubating 23 μM α-synuclein alone for 30 days or with 50 μM $FeCl_2$ for only 3 days, suggesting that 50 μM Fe(II) increases the rate of α-synuclein aggregation about 10-fold (see discussion below). These observations suggest that interaction with iron could greatly accelerate α-synuclein aggregation.

The factors regulating α-synuclein aggregation in the brain are poorly understood. Some studies suggest that neurotoxins, such as the pesticide rotenone or paraquat, stimulate α-synuclein aggregation (16). The involvement of metals in PD suggests that metals might also play a role in the aggregation of α-synuclein and the pathophysiology of PD. Epidemiological studies have shown that exposure to metals is associated with PD. For instance, individuals with industrial exposure to iron, copper, and/or lead have high rates of PD (17). Neuropathological studies show that synucleinopathies are generally associated with iron accumulation, which is consistent with a pathological link between iron and α-synuclein (18). Brains from patients with PD, type I iron storage disease (Hallorvorden-Spatz disorder), and multiple systems atrophy all show increased iron content (19). In PD the levels of iron are increased over controls, and Fe(II) has been identified as a major component of Lewy bodies (20–26). How iron contributes to Lewy body formation and the pathophysiology of PD, though, is not

understood. In the experiments described below, we examine the regulation of α-synuclein aggregation using both spontaneous and iron-induced α-synuclein aggregation *in vitro* and show contrasting actions of iron and magnesium on α-synuclein aggregation. These studies have important implications for the pathophysiology of PD and other synucleionopathies.

EXPERIMENTAL PROCEDURES

Materials—α-Synuclein (wild-type, A53T, and A30P) was cloned into the *Nco*I/*Not*I site of the Pro-Ex His 6 vector (Invitrogen). To generate recombinant α-synuclein, BPer (Pierce) reagent was used to solubilize the recombinant α-synuclein from the isopropyl-1-thio-β-D-galactopyranoside-induced bacterial lysates, which were then passed over a nickel-agarose column for purification. All spectrophotometric analysis were repeated three to five times.

Immunoblotting—Cells were harvested with SDS lysis solution (2% SDS, 10 mM Tris, pH 7.4, 2 mM β-glycerol phosphate, 1 μM AEBSF). The amount of protein was determined using the BCA assay (Pierce), 5–30 μg per lane was run on 14% SDS-polyacrylamide gels and transferred to nitrocellulose (200 mA, 12 h). The nitrocellulose was then incubated 1 h in 5% I-block (Tropix)/phosphate-buffered saline, washed, incubated overnight in primary antibody, washed, then incubated 3 h in peroxidase-coupled secondary antibody and developed with chemiluminescent reagent (PerkinElmer Life Sciences).

Thioflavine-T Measurements—For analysis of aggregation using thioflavine-T, 23 nM α-synuclein was incubated in 10 μM thioflavine-T (in 50 mM glycine, pH 8.5) and measured by fluorescence (λ_{ex} = 440, λ_{em} = 450–600 nm).

Cellulose Acetate Assay—To analyze aggregation of α-synuclein by filtration, samples were diluted into 100 μl of water, filtered through cellulose acetate (0.2 μm pore size), washed with 200 μl phosphate-buffered saline, and then immunoblotted as described above.

RESULTS

Iron Quenches Tyrosine Fluorescence of α-Synuclein: Evidence of Association—To understand factors regulating α-synuclein aggregation, we investigated the interaction of different metals with α-synuclein using tyrosine fluorescence (27, 28). Tyrosine fluorescence has been used to monitor the association of various metals with a number of proteins, including Aβ, α-transducin and, more recently, α-synuclein (27–29). In these studies tyrosine fluorescence is used as an indicator of changes in protein conformation or binding of metals. Exciting tyrosine at 280 nm elicits fluorescence that peaks at 310 nm for monomeric tyrosine and at 350–400 nm for tyrosinate (30). The fluorescence spectrum of α-synuclein yielded fluorescence peaks at 310 and 375 nm (Fig. 1, *A* and *B*). Tyrosinate reactivity occurs when the phenolic hydroxyl group of tyrosine forms hydrogen bonds with carboxyl groups in nearby aspartates or glutamates. The fluorescence peak of α-synuclein at 375 nm showed a pH dependence similar to that of tyrosinate (Fig. 1*C*), which is consistent with the pH dependence of fluorescence due to tyrosinate. The peak at 375 nm had the highest intrinsic fluorescence at low pH and showed little change in fluorescence at pH > 7.0 (Fig. 1*C*). Further studies confirmed that the peak at 375 nm is not due to tyrosine dimerization, because both gel electrophoresis and mass spectrometry of the α-synuclein showed that the α-synuclein was monomeric (Fig. 1*D*, Coomassie gel of recombinant α-synuclein shown), and in addition, tyrosine dimerization of α-synuclein reduced its intrinsic fluorescence (Fig. 1, *E* and *F*, described further below). These results suggest that the peak at 375 nm is due to tyrosinate, which could result from proton transfer from the phenolic hydroxyl to aspartic or glutamic acid protein acceptors (30).

Metals Show Three Patterns of Interaction with α-Synuclein—Next we used the fluorescence to examine the interaction of α-synuclein with metals. We observed three classes of interaction with α-synuclein. Class I metals included iron (Fe(II) and Fe(III)) and copper (Cu(II)) and decreased the fluorescence at both 310 and 375 nm (Fig. 1*A*). Class II metals included magnesium, zinc, and calcium, and increased the fluorescence at 375 nm, but did not affect the fluorescence at 310 nm (Figs. 2*A* and 3*A*). Class III metals included nickel and manganese and did not affect α-synuclein fluorescence (data not shown). We proceeded to examine the fluorescence of α-synuclein in more detail to determine whether the metal induced changes α-synuclein fluorescence reflected interaction with metals or some other process, such as tyrosine dimerization. To examine whether the changes in fluorescence could be explained by tyrosine dimerization, we exposed monomeric α-synuclein to 312 nm light for 2 h (which is a process that induces tyrosine dimerization) and analyzed the emission fluorescence spectrum with excitation at either 280 or 315 nm. The emission spectrum derived using excitation at 280 nm showed that ultraviolet-irradiation reduced α-synuclein fluorescence strongly at 375 nm, but only weakly at 310 nm (Fig. 1*E*). The contrast between the changes in fluorescence induced by ultraviolet irradiation and by metals suggests that the changes in α-synuclein fluorescence induced by metals are not due to tyrosine dimerization. Analysis of the emission fluorescence spectrum of α-synuclein following excitation at 315 nm showed a reduced fluorescence at 380 nm for the ultraviolet-irradiated α-synuclein (Fig. 1*F*). In contrast, iron increased, rather than decreased, the fluorescence of α-synuclein as measured using the 315 nm excitation. These data indicate that the iron-induced quenching of α-synuclein fluorescence is not due to cross-linking of α-synuclein mediated by tyrosine dimerization.

Dose Dependence of Metal Binding—Plotting of the dose dependence of iron-induced fluorescence quenching showed a dose-dependent decrease in fluorescence, with an IC_{50} = 173 μM and a Hill coefficient of 1.0 (R2 = 1.0, $p < 0.0001$) (Fig. 1*B*), indicating one binding site or multiple binding sites with the same affinity and no cooperativity (Fig. 1, *A* and *B*). There is a small amount of binding of iron to α-synuclein between 1–10 μM Fe(II), which is a range that could be physiologically relevant (intracellular free iron is about 1.5 μM) (31).

The effect of magnesium on α-synuclein differed dramatically from that of iron. Magnesium increased the fluorescence at 375 nm but did not affect the fluorescence at 310 nm (Fig. 2*A*). Binding of magnesium to α-synuclein was also striking because the tyrosine fluorescence showed a sharp stepwise increase between 60 and 80 μM of magnesium indicating cooperative binding (Fig. 2*A*). The cooperative regulation of tyrosine fluorescence, specifically at 375 nm, suggests that magnesium causes a conformational change in synuclein differing from that induced by iron. Co-incubating 80 μM magnesium with iron did not prevent iron-induced quenching of α-synuclein tyrosine fluorescence and in fact increased affinity of α-synuclein for iron from 173 to 50 μM (Fig. 2*B*). These data suggest that iron and magnesium bind to different sites on α-synuclein.

Zinc and calcium also increased the fluorescence of α-synuclein at 375 nm, but showed a more graded pattern of interaction (Fig. 3*A*). Jensen and colleagues recently noted a similar pattern of binding of calcium to α-synuclein (29). Interestingly, immunoblots of recombinant α-synuclein following incubation with zinc showed that zinc induced formation of a prominent band at 32 kDa, consistent with formation of an SDS-resistant α-synuclein dimer (Fig. 3*B*). Neither magnesium nor calcium induced formation of SDS-resistant dimers identifiable by immunoblot (data not shown).

We also examined how the A53T mutation in human α-synuclein affected binding of iron and magnesium. The A53T mutation did not change the apparent affinity of iron for α-synuclein (data not shown), but did abolish the interaction between magnesium and α-synuclein (Fig. 2*C*). Previous stud-

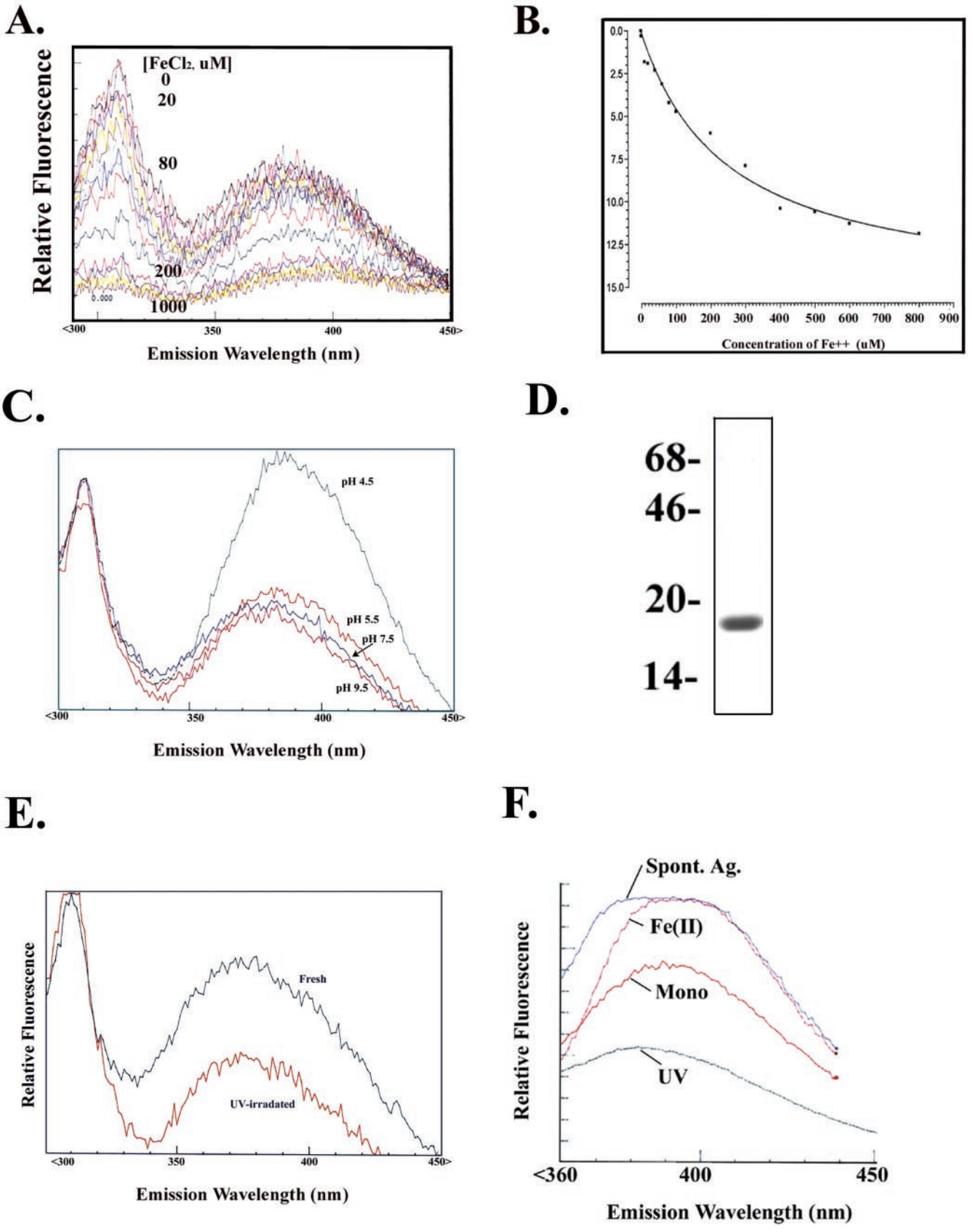

FIG. 1. **Interaction of iron with recombinant α-synuclein.** *A*, excitation of wild-type α-synuclein at λ_{ex} 280 nm produces a biphasic fluorescence spectrum with peaks at 310 and 375 nm. Incubating α-synuclein with increasing doses of $FeCl_2$ yields a progressive quenching of both peaks. *B*, quantification of the relative fluorescence from Fig. 1*A* of 1 μM α-synuclein at 310 nm during quenching by Fe(II). *C*, pH dependence of wild-type α-synuclein fluorescence using λ_{ex} 280 nm and λ_{em} 290–450 nm. The pH sensitivity of the fluorescence peak at 375 indicates that this fluorescence is due to the presence of tyrosinate. *D*, identification of recombinant α-synuclein following PAGE electrophoresis by staining with Coomassie Blue. The presence of a single α-synuclein band at 16 kDa shows that there is no dimerization. *E*, reduction in α-synuclein fluorescence following ultraviolet (UV) irradiation (2 h). The reduction in fluorescence of α-synuclein occurred mainly around the peak at 375 nm (λ_{ex} = 280 nm;

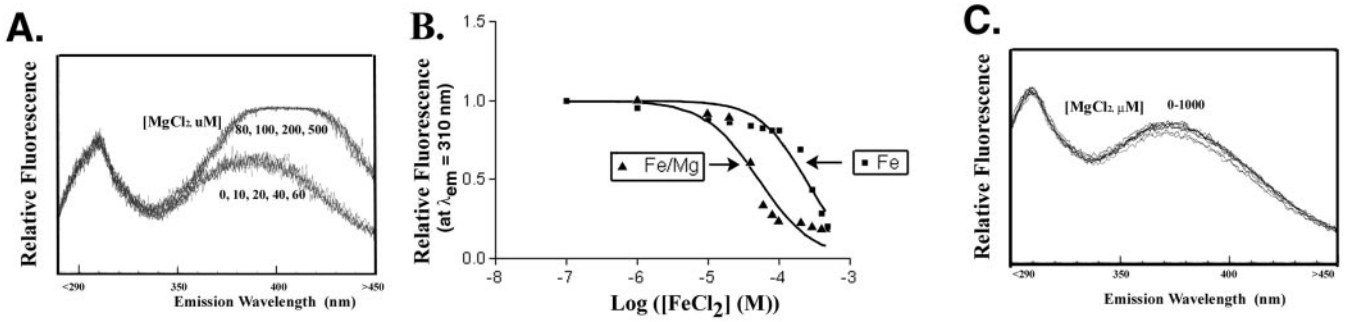

FIG. 2. A, fluorescence of wild-type α-synuclein in the presence of increasing doses of $MgCl_2$ shows increased fluorescence emission at 375 nm and no change at 310 nm, using an excitation wavelength of 280 nm (λex = 280 nm; λem 290–450 nm). *B*, a representative plot showing that magnesium increases the affinity of α-synuclein for iron. α-Synuclein shows an affinity for iron that is 5-fold lower when incubated in the presence of 100 μM $MgCl_2$. *C*, fluorescence emissions of A53T α-synuclein in the presence of increasing doses of $MgCl_2$ shows no change at 375 or 310 nm, using an excitation of 280 nm.

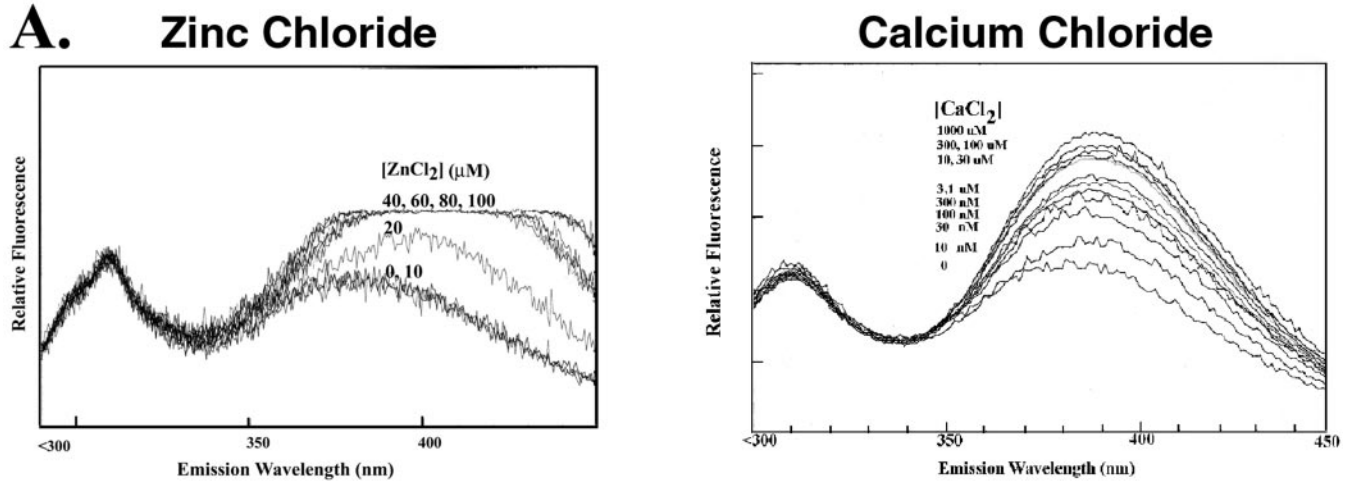

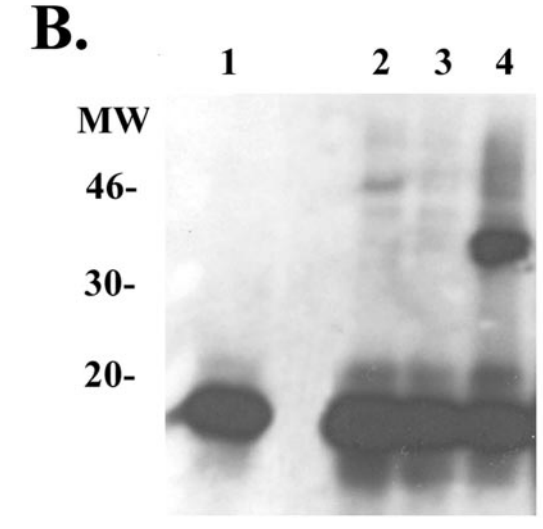

FIG. 3. **The effects of zinc on α-synuclein fluorescence and dimerization.** *A*, incubating zinc or calcium with recombinant α-synuclein increases the peak of α-synuclein emission fluorescence at 375 nm in a graded manner, using an excitation wavelength of 280 nm (λ_{ex} = 280 nm; λ_{em} 290–450 nm). *B*, immunoblot of recombinant α-synuclein after incubation with zinc shows formation of a 32-kDa band consistent with formation of an SDS-resistant α-synuclein dimer. *Lane 1*, 0 nM $ZnCl_2$; *lane 2*, 100 nM $ZnCl_2$; *lane 3*, 200 nM $ZnCl_2$; *lane 4*, 400 nM $ZnCl_2$.

ies have shown that the A53T mutation changes the conformation of α-synuclein by increasing its helical content (5). These conformational changes might either reduce binding of magnesium to α-synuclein or prevent the conformational change associated with binding of magnesium to α-synuclein.

Magnesium Inhibits α-Synuclein Aggregation—The differing effects of magnesium and iron on the fluorescence spectrum of α-synuclein suggested to us that magnesium and iron might

λ_{em} 290–450 nm), which contrasts with the changes in fluorescence induced by iron. *F*, UV irradiation (2 h) also reduces α-synuclein fluorescence following excitation at λ_{ex} = 315 nm; λ_{em} 350–450 nm. UV-induced inhibition of α-synuclein fluorescence contrasts with the increase in fluorescence induced by iron or spontaneous aggregation of α-synuclein.

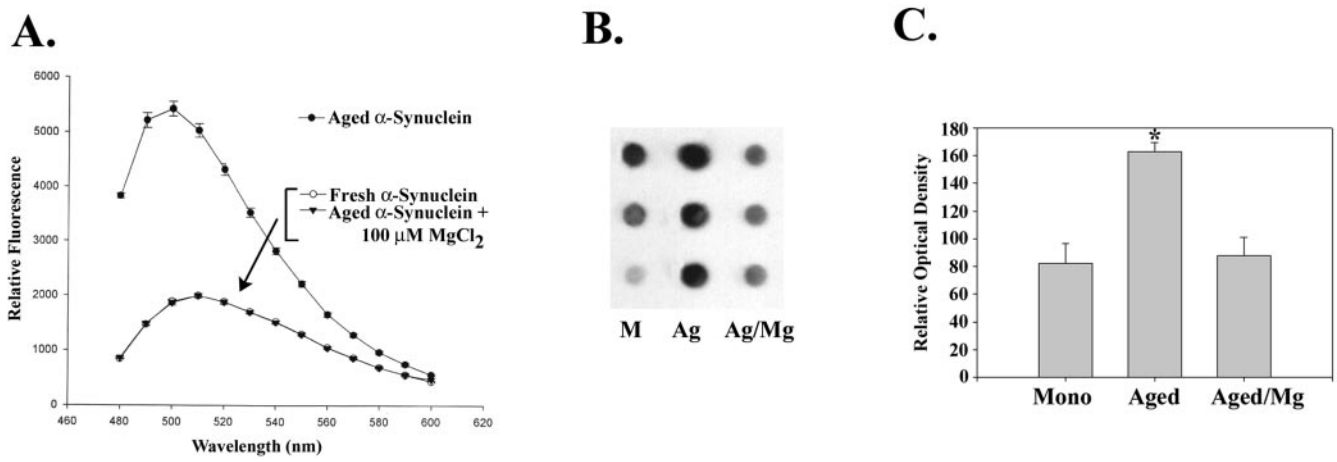

FIG. 4. **Magnesium inhibits the spontaneous aggregation of α-synuclein.** *A*, α-synuclein was prepared freshly (*Mono*) or aged 30 days at 37 °C to induce spontaneous aggregation (*Ag*) ± 0.8 mM Mg (*Ag/Mg*). Then the samples were then analyzed by Thioflavine-T fluorescence. The spontaneously aggregated α-synuclein gave strong fluorescence, while the sample aged in the presence of magnesium had a fluorescence curve identical to that of fresh α-synuclein. *B*, α-synuclein was prepared freshly (*M*, monomeric) or aged 30 days at 37 °C to induce spontaneous aggregation (*Ag*, aged) or aged 30 days at 37 °C in the presence of 0.8 mM $MgCl_2$ (*Ag/Mg*, aged plus Mg^{2+}). Then the samples were filtered through a cellulose acetate membrane and immunoblotted with rabbit anti-α-synuclein antibody. Incubating the α-synuclein with magnesium prevented formation of the large aggregates that are captured by the membrane. *C*, quantification of the optical density of the dot blots using the NIH Image program ($n = 6$, *, $p < 0.001$, analysis of variance factorial).

also induce different conformational states. We hypothesized that the conformational changes induced by binding of magnesium to α-synuclein might inhibit α-synuclein aggregation. To test this, we examined whether magnesium could inhibit the spontaneous aggregation of α-synuclein. α-Synuclein (23 μM) was incubated for 30 days at 37° ± $MgCl_2$ (500 μM). To measure the amount of aggregation, the α-synuclein was diluted to 23 nM in the presence of 10 μM thioflavine-T (in 50 mM glycine pH 8.5), and the fluorescence spectrum was measured. The solution of aged α-synuclein showed a strong fluorescence peak at 480, indicating the presence of abundant β-pleated sheet structures (Fig. 4*A*). Prior experiments have shown that the spontaneous aggregation of α-synuclein proceeds through a mechanism involving β-pleated sheet formation, and that thioflavine-T, which binds to proteins with β-pleated sheet structure, accurately measures α-synuclein aggregation (9). Using thioflavine-T we observed that samples incubated in the presence of magnesium showed only base-line levels of fluorescence, indicating that magnesium prevented the formation of β-pleated sheet structures and the aggregation of α-synuclein (Fig. 4*A*). To verify that the magnesium was inhibiting α-synuclein aggregation, we measured the amount of aggregated α-synuclein in each sample by capturing the aggregates with 0.2-μm cellulose acetate filters, measuring the amount of retained α-synuclein by dot blot, and quantitating the resulting optical density. The results of the cellulose acetate assay paralleled the thioflavine-T assay and showed that magnesium prevented the spontaneous aggregation of α-synuclein (Fig. 4, *B* and *C*). Thus, two independent methods show that magnesium inhibits the spontaneous aggregation of α-synuclein *in vitro*.

Magnesium was also able to prevent iron-induced α-synuclein aggregation. α-Synuclein (8 μM) was incubated with 50 μM $FeCl_2$ for 72 h and then analyzed by thioflavine-T fluorescence or cellulose acetate. In both cases, α-synuclein samples co-incubated with 500 μM magnesium chloride showed little aggregation (Fig. 5, *A* and *B*). The amount of thioflavine-T fluorescence induced by iron was less than that induced by spontaneously aggregated α-synuclein, which likely indicates that spontaneously induced α-synuclein contains more β-pleated sheet structure. Indeed analysis of iron-induced α-synuclein aggregates by circular dichroism did not show formation of β-pleated sheet structures, which suggests formation of a more amorphous aggregate (Fig. 5, *C* and *D*). These data suggest that magnesium inhibits the formation of α-synuclein aggregates containing either β-pleated sheet structure (via spontaneous aggregation) or amorphous structure (via iron-induced aggregation).

We also examined aggregation by immunoblot analysis, which has been successfully used to examine aggregation of α-synuclein, as well as aggregation of other proteins implicated in neurodegenerative disease, such as the huntingtin and PrP proteins (29, 32–35). In these assays, wild-type recombinant α-synuclein (8 μM) was incubated with 0–3 mM $FeCl_2$ and 0 or 100 μM $MgCl_2$ for 24 h at 37 °C. The samples were immunoblotted with anti-α-synuclein antibody, and the total amount of α-synuclein reactivity above 46 kDa (which includes structures larger than a dimers) was quantified by video densitometry (Fig. 6, *A* and *B*). We observed a reduction in formation of high molecular weight immunoreactivity of α-synuclein at all but the highest dose of iron ($n = 3$, $p < 0.0001$). These results support the hypothesis that magnesium inhibits aggregation of α-synuclein induced following treatment with iron.

Since we did not observe interaction between magnesium and A53T α-synuclein using tyrosine fluorescence, we tested whether aggregation of recombinant A53T α-synuclein was also insensitive to magnesium. We incubated recombinant A53T α-synuclein with 0–3 mM $FeCl_2$ and 0 or 100 μM $MgCl_2$ for 24 h, then immunoblotted the α-synuclein and quantified aggregation by video densitometry, as described above (Fig. 6, *C* and *D*). We did not observe consistent inhibition of iron-induced aggregation of A53T α-synuclein by magnesium. This suggests that magnesium cannot inhibit iron-induced aggregation of A53T α-synuclein.

DISCUSSION

These data demonstrate that iron (II), magnesium, zinc, and calcium all interact with α-synuclein. Our data primarily rely on tyrosine fluorescence as a measure of the interaction of α-synuclein with metals. The K_i of α-synuclein for iron is 173 μM, and the K_i of magnesium for α-synuclein is between 60 and 80 μM. These affinities are consistent with an affinity of α-synuclein for calcium, determined by Nielson and colleagues (29). Nielson and colleagues also confirmed their tyrosine flu-

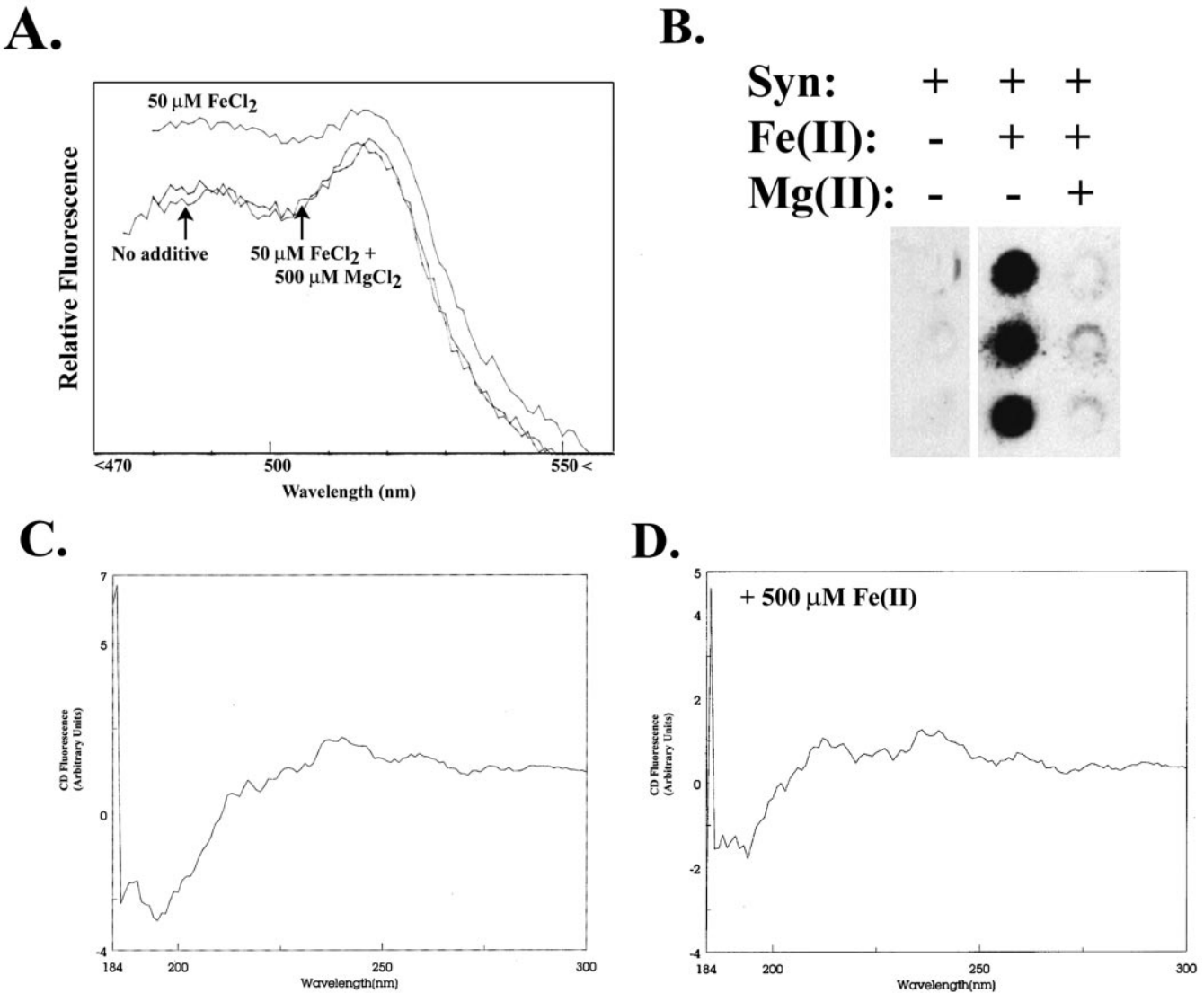

FIG. 5. **Magnesium inhibits iron-induced α-synuclein aggregation.** *A*, thioflavine-T fluorescence of α-synuclein (8 μM) following a 3-day incubation in the presence of 50 μM $FeCl_2$ ± 0.8 mM $MgCl_2$. *B*, analysis of the affects of magnesium on iron induced α-synuclein aggregation ± magnesium. α-Synuclein was prepared freshly (*Mono*) or aged 3 days at 37 °C in the presence of 50 μM $FeCl_2$ ± 0.8 mM $MgCl_2$. Then the samples were filtered through a cellulose acetate membrane and immunoblotted with rabbit anti-α-synuclein antibody. Cellulose acetate assay of spontaneously aggregated synuclein ± Mg^{2+}. *C*, circular dichroism spectrum of native α-synuclein (160 μg/ml). *D*, circular dichroism spectrum of α-synuclein (160 μg/ml) following incubation with 500 μM $FeSO_4$ for 5 days.

orescence studies using equilibrium dialysis; our attempts at using equilibrium dialysis were stymied by extensive binding of α-synuclein to dialysis membranes. However, the studies of Nielson and colleagues show that tyrosine fluorescence provides an accurate indication of metal-synuclein binding interactions. The apparent affinity of α-synuclein for magnesium is strong enough to allow interaction of α-synuclein with magnesium in living cells, where the average intracellular concentration of magnesium is about 0.5 mM. This suggests that this interaction could have physiological significance.

Although binding of magnesium to α-synuclein occurs at a concentration range that is physiologically significant, the concentration of free iron in the cell is much lower (<1.5 μM), which is far below the affinity of α-synuclein for iron that we observed (173 μM) (36). However, studies using cell culture and neuropathology both suggest that α-synuclein interacts with iron. Incubating cells with iron induces α-synuclein aggregation in viable cells, which suggests that the concentration of iron in a cell is sufficient to induce α-synuclein aggregation under some conditions. In addition, α-synuclein aggregates in iron type I storage disease, and iron co-localizes with α-synuclein in Lewy bodies (19). Although it is unclear how α-synuclein might interact with iron in the living cell, it is possible that cofactors increase the affinity of α-synuclein for iron sufficient to allow a physiological interaction. Many other factors might also affect the behavior of α-synuclein. For instance, binding to lipids and phosphorylation or binding to β-synuclein have all been shown to change the biochemistry of α-synuclein, and these agents might increase its affinity for iron (44). Our preliminary studies examining magnesium already provide a hint of modulation. The K_i of iron (II) drops to 50 μM in the presence of magnesium. Future studies might unravel the biochemistry of α-synuclein further.

Although binding of magnesium appears to introduce a conformation that promotes binding of iron, this same conformational change inhibits aggregation of α-synuclein. We hypothesize that magnesium either changes the conformation of α-synuclein to one that resists aggregation or induces dimerization to a structure that resists aggregation (Fig. 7). The ability of zinc to induce SDS-resistant α-synuclein dimers, cou-

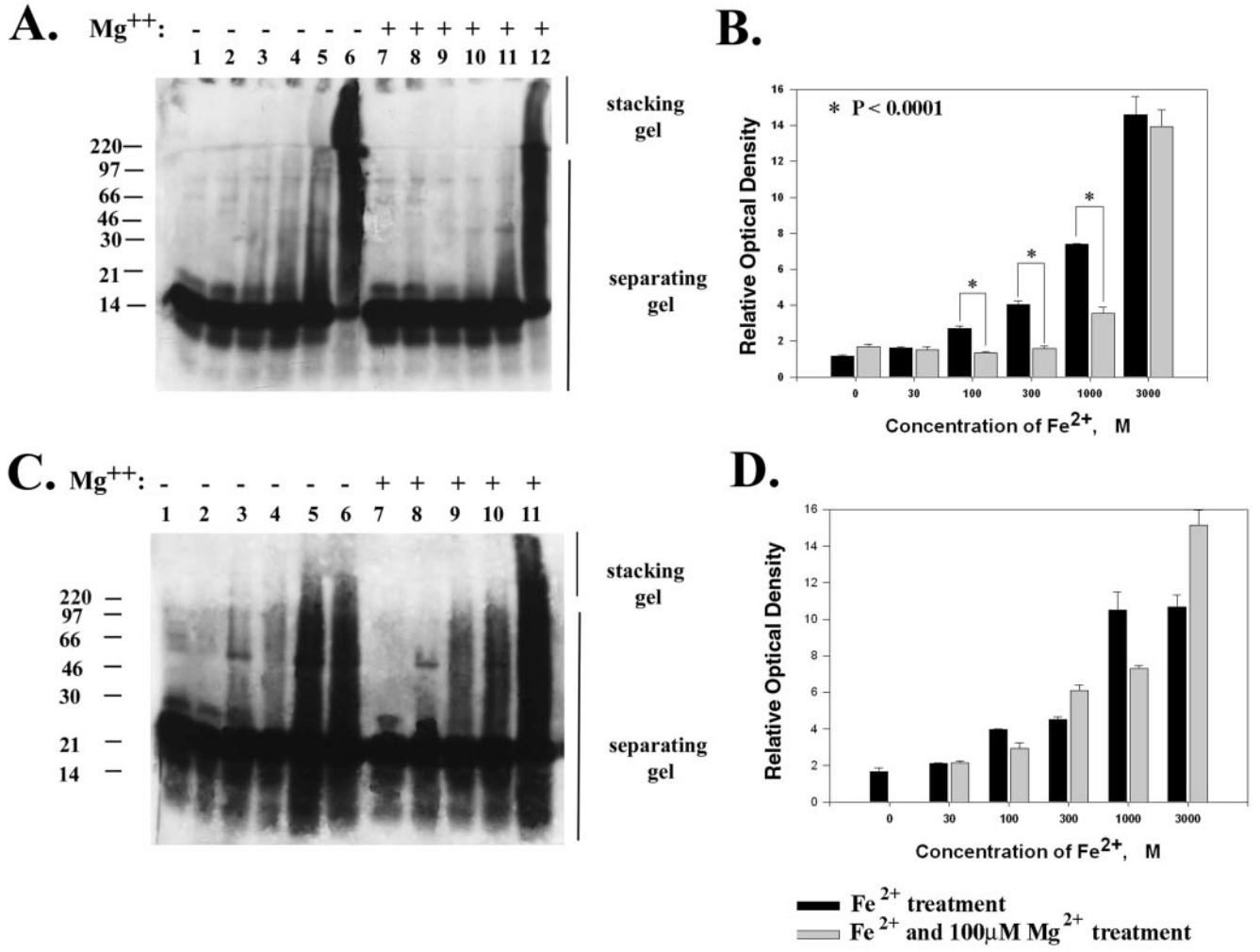

FIG. 6. **Immunoblotting of α-synuclein following incubation with varying doses of Fe(II) ± 100 μM $MgCl_2$.** *A*, immunoblotting of recombinant wild-type α-synuclein following treatment with 0–3 mM $FeCl_2$ plus 0.1 mM $MgCl_2$ for 1 day. The mean optical density above 46 kDa was quantified and used as an index of aggregation. Increasing doses of $MgCl_2$ reduced the formation of high molecular weight aggregates of α-synuclein. Concentrations (μM) of iron salts: 0 (*lanes 1* and *7*), 30 (*lanes 2* and *8*), 100 (*lanes 3* and *9*), 300 (*lanes 4* and *10*), 1000 (*lanes 5* and *11*); 3000 (*lanes 6* and *12*). Concentrations (μM) of $MgCl_2$: 0 (*lanes 1–6*), 100 (*lanes 7–12*). *B*, quantification of the aggregate formation by video densitometry showed a dose dependent decrease in aggregate formation that was statistically significant at 0.1 mM $MgCl_2$ ($n = 3$ for each point). *D*, immunoblotting of recombinant A53T α-synuclein following treatment with 0–3 mM $FeCl_2$ plus 0.1 mM $MgCl_2$ for 1 day. The mean optical density above 46 kDa was quantified and used as an index of aggregation. Increasing doses of $MgCl_2$ did not consistently inhibit formation of high molecular weight aggregates of α-synuclein. *E*, quantification of aggregate formation by video densitometry, showing that magnesium did not inhibit aggregation of A53T α-synuclein ($n = 3$ for each point).

pled with the similarity the changes in tyrosine fluorescence observed with magnesium and zinc, suggest that magnesium might induce dimerization of α-synuclein in a manner similar to that of zinc. Future studies using nuclear magnetic resonance spectroscopy will need to be performed to investigate further how magnesium affects the conformation of α-synuclein.

The most important observation made in this paper is that magnesium inhibits the aggregation of α-synuclein. This observation is supported by our use of four independent lines of investigation (immunoblot, cellulose acetate filtration, and thioflavine-T fluorescence). The type of aggregate measured by each assay likely differs slightly. Immunoblotting detects aggregates that are stable enough to resist both heating and SDS. Cellulose acetate filtration and thioflavine-T are more gentle methods that can detect both stable aggregates and also aggregates that might be re-dissolved by SDS. Thioflavine-T recognizes aggregate with a β-pleated sheet structure. Interestingly, spontaneously aggregated α-synuclein shows much more fluorescence by thioflavine-T than iron-induced aggregate, suggesting that the former has more β-pleated sheet structure. We have also taken care to examine two forms of α-synuclein aggregation: spontaneous and iron-induced aggregation. Many studies show that α-synuclein has a strong tendency to spontaneously aggregate, and this is the most widely accepted method for inducing α-synuclein aggregation (7–9). Metal-induced aggregation has only been investigated by a small number of groups, but is perhaps the only method currently available for inducing α-synuclein aggregation in cultured cells (10, 15, 37). The ability of magnesium to inhibit α-synuclein aggregation induced by both protocols (spontaneous and iron-induced) suggests that this is a robust phenomenon.

Increasing evidence suggests that metals play a pivotal role in the pathophysiology of neurodegenerative disorders. Zinc and copper greatly accelerate aggregation of β-amyloid and might play a critical role in neurotoxicity induced by β-amyloid (38, 39). Copper and manganese both bind to the prion protein and appear to influence the clinical course of prion-induced neurodegeneration (40, 41). Iron levels are increased in brains of patients with PD, and iron is present in Lewy bodies. Neu-

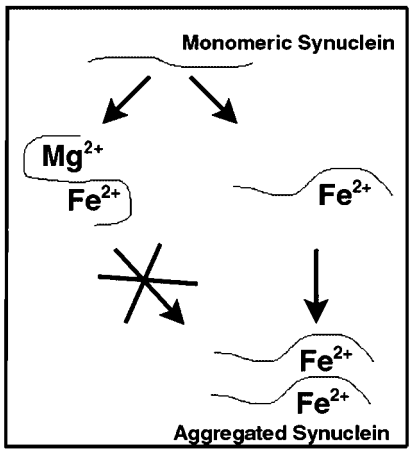

FIG. 7. **Model of interaction of iron and magnesium with α-synuclein.** In this model, iron binds to α-synuclein and promotes aggregation. Magnesium appears to bind to a different site than does iron and therefore does not inhibit binding of iron. We hypothesize that binding of magnesium to α-synuclein induces a conformational change that prevents formation of large α-synuclein aggregates.

romelanin selectively binds Fe(III) and might liberate Fe(II) as the Fe(III) is reduced to Fe(II) (via the Haber Weiss reaction) by free radicals produced in response to the oxidative stress associated with PD, providing a potential source of Fe(II) to accelerate α-synuclein aggregation (42, 43). On the other hand, magnesium levels are reduced in brains of patients with PD (21–26). If iron accelerates α-synuclein aggregation, then the abundance of iron in the substantia nigra could increase the tendency of Lewy bodies to accumulate in this region. In a companion paper,[2] we extend our studies from the test tube to neurons, and show that magnesium also inhibits aggregation of α-synuclein in neurons. Together, these data raise the possibility that iron and magnesium might also modulate α-synuclein aggregation in the brain.

Acknowledgments—We acknowledge the assistance of Alan Frankfater (Loyola University) and Brian Shoichet (Northwestern) and thank Matthew Farrer and John Hardy (Mayo Clinic) for providing the α-synuclein cDNA.

REFERENCES

1. Hoehn, M. M., and Yahr, M. D. (1998) *Neurology* **50,** 318–334
2. Gibb, W., and Lees, A. (1988) *J. Neurol. Neurosurg. Psych.* **51,** 745–752
3. Spillantini, M. G., Crowther, R. A., Jakes, R., Hasegawa, M., and Goedert, M. (1998) *Proc. Natl. Acad. Sci. U. S. A.* **95,** 6469–6473
4. Spillantini, M., Schmidt, M., VM-Y, L., Trojanowski, J., Jakes, R., and Goedert, M. (1997) *Nature* **388,** 839–840
5. Polymeropoulos, M. H., Lavedan, C., Leroy, E., Ide, S. E., Dehejia, A., Dutra, A., Pike, B., Root, H., Rubenstein, J., Boyer, R., Stenroos, E. S., Chandrasekharappa, S., Athanassiadou, A., Papapetropoulos, T., Johnson, W. G., Lazzarini, A. M., Duvoisin, R. C., Di Iorio, G., Golbe, L. I., and Nussbaum, R. L. (1997) *Science* **276,** 2045–2047
6. Kruger, R., Kuhn, W., Muller, T., Woitalla, D., Graeber, M., Kosel, S., Przuntek, H., Epplen, J., Schols, L., and Riess, O. (1998) *Nat. Genet.* **18,** 106–108
7. Hashimoto, M., Hsu, L., Sisk, A., Xia, Y., Takeda, A., Sundsmo, M., and Masliah, E. (1998) *Brain Res.* **799,** 301–306
8. Wood, S., Wypych, J., Steavenson, S., Louis, J., Citron, M., and Biere, A. (1999) *J. Biol. Chem.* **274,** 19509–19512
9. Conway, K. A., Lee, S. J., Rochet, J. C., Ding, T. T., Williamson, R. E., and Lansbury, P. T., Jr. (2000) *Proc. Natl. Acad. Sci. U. S. A.* **97,** 571–576
10. Ostrerova-Golts, N., Petrucelli, L., Hardy, J., Lee, J., Farrer, M., and Wolozin, B. (2000) *J. Neurosci.* **20,** 6048–6054
11. Masliah, E., Rockenstein, E., Veinbergs, I., Mallory, M., Hashimoto, M., Takeda, A., Sagara, Y., Sisk, A., and Mucke, L. (2000) *Science* **287,** 1265–1269
12. Feany, M. B., and Bender, W. W. (2000) *Nature* **404,** 394–398
13. Kahle, P. J., Neumann, M., Ozmen, L., Muller, V., Jacobsen, H., Schindzielorz, A., Okochi, M., Leimer, U., van Der Putten, H., Probst, A., Kremmer, E., Kretzschmar, H. A., and Haass, C. (2000) *J. Neurosci.* **20,** 6365–6373
14. van der Putten, H., Wiederhold, K. H., Probst, A., Barbieri, S., Mistl, C., Danner, S., Kauffmann, S., Hofele, K., Spooren, W. P., Ruegg, M. A., Lin, S., Caroni, P., Sommer, B., Tolnay, M., and Bilbe, G. (2000) *J. Neurosci.* **20,** 6021–6029
15. Paik, S. R., Shin, H. J., and Lee, J. H. (2000) *Arch. Biochem. Biophys.* **378,** 269–277
16. Uversky, V. N., Li, J., and Fink, A. L. (2001) *FEBS Lett.* **500,** 105–108
17. Gorell, J. M., Johnson, C. C., Rybicki, B. A., Peterson, E. L., Kortsha, G. X., Brown, G. G., and Richardson, R. J. (1999) *Neurotoxicology* **20,** 239–247
18. Duda, J. E., Lee, V. M., and Trojanowski, J. Q. (2000) *J. Neurosci. Res.* **61,** 121–127
19. Galvin, J. E., Giasson, B., Hurtig, H. I., Lee, V. M., and Trojanowski, J. Q. (2000) *Am. J. Pathol.* **157,** 361–368
20. Castellani, R., Siedlak, S., Perry, G., and Smith, M. (2000) *Acta Neuropathol.* **100,** 111–121
21. Mann, V. M., Cooper, J. M., Daniel, S. E., Srai, K., Jenner, P., Marsden, C. D., and Schapira, A. H. (1994) *Ann. Neurol.* **36,** 876–881
22. Griffiths, P. D., Dobson, B. R., Jones, G. R., and Clarke, D. T. (1999) *Brain* **122,** 667–673
23. Dexter, D., Carayon, A., Javoy-Agid, F., Agid, Y., Wells, F., Daniel, S., Lees, A., Jenner, P., and Marsden, C. (1991) *Brain* **114,** 1953–1975
24. Barbiroli, B., Martinelli, P., Patuelli, A., Lodi, R., Iotti, S., Cortelli, P., and Montagna, P. (1999) *Mov. Disord.* **14,** 430–435
25. Uitti, R. J., Rajput, A. H., Rozdilsky, B., Bickis, M., Wollin, T., and Yuen, W. K. (1989) *Can. J. Neurol. Sci.* **16,** 310–314
26. Durlach, J., Bac, P., Durlach, V., Rayssiguier, Y., Bara, M., and Guiet-Bara, A. (1998) *Magnes. Res.* **11,** 25–42
27. Garzon-Rodriguez, W., Yatsimirsky, A., and Glabe, C. (1999) *Bioorg. Med. Chem. Let.* **9,** 2243–2248
28. Phillips, W. J., and Cerione, R. A. (1988) *J. Biol. Chem.* **263,** 15498–15505
29. Nielsen, M. S., Vorum, H., Lindersson, E., and Jensen, P. H. (2001) *J. Biol. Chem.* **276,** 22680–22684
30. Szabo, A. G., Lynn, K. R., Krajcarski, D. T., and Rayner, D. M. (1978) *FEBS Lett.* **94,** 249–252
31. Thomson, A. M., Rogers, J. T., and Leedman, P. J. (1999) *Int. J. Biochem. Cell Biol.* **31,** 1139–1152
32. Giasson, B., Uryu, K., Trojanowski, J., and Lee, V. (1999) *J. Biol. Chem.* **274,** 7619–7622
33. Perrin, R. J., Woods, W. S., Clayton, D. F., and George, J. M. (2000) *J. Biol. Chem.* **275,** 34393–34398
34. Nucifora, F. C., Jr., Sasaki, M., Peters, M. F., Huang, H., Cooper, J. K., Yamada, M., Takahashi, H., Tsuji, S., Troncoso, J., Dawson, V. L., Dawson, T. M., and Ross, C. A. (2001) *Science* **291,** 2423–2428
35. Hegde, R. S., Mastrianni, J. A., Scott, M. R., DeFea, K. A., Tremblay, P., Torchia, M., DeArmond, S. J., Prusiner, S. B., and Lingappa, V. R. (1998) *Science* **279,** 827–834
36. Ponka, P., Beaumont, C., and Richardson, D. (1998) *Semin. Hematol.* **35,** 35–54
37. Hashimoto, M., LJ, H., Xia, Y., Takeda, A., Sisk, A., Sundsmo, M., and Masliah, E. (1999) *NeuroReport* **10,** 717–721
38. Atwood, C., Moir, R., Huang, X., Scarpa, R., Bacarra, N., Romano, D., Hartshorn, M., Tanzi, R., and Bush, A. (1998) *J. Biol. Chem.* **273,** 12817–12826
39. Bush, A. I., Pettingell, W. H., Multhaup, G., P. M.d, P. M., Vonsattel, J. P., Gusella, J. F., Beyreuther, K., Masters, C. L., and Tanzi, R. E. (1994) *Science* **265,** 1464–1467
40. Brown, D. R., Qin, K., Herms, J. W., Madlung, A., Manson, J., Strome, R., Fraser, P. E., Kruck, T., von Bohlen, A., Schulz-Schaeffer, W., Giese, A., Westaway, D., and Kretzschmar, H. (1997) *Nature* **390,** 684–687
41. Wadsworth, J. D., Hill, A. F., Joiner, S., Jackson, G. S., Clarke, A. R., and Collinge, J. (1999) *Nat. Cell Biol.* **1,** 55–59
42. Hirsch, E. C., Graybiel, A. M., and Agid, Y. (1989) *Acta Neurol. Scand. Suppl.* **126,** 19–22
43. Wolozin, B., and Golts, N. (2001) *Neuroscientist* **8,** 22–32
44. Hashimoto, M., Rockenstein, E., Mante, M., Mallory, M., and Masliah, E. (2001) *Neuron.* **32,** 213–223

[2] N. Golts, H. Snyder, M. Frasier, C. Theisler, P. Choi, and B. Wolozin, submitted for publication.

THE JOURNAL OF BIOLOGICAL CHEMISTRY
Vol. 277, No. 14, Issue of April 5, pp. 12334–12342, 2002

Printed in U.S.A.

α-Synuclein Interacts with Phospholipase D Isozymes and Inhibits Pervanadate-induced Phospholipase D Activation in Human Embryonic Kidney-293 Cells*

Received for publication, October 30, 2001, and in revised form, January 22, 2002
Published, JBC Papers in Press, January 30, 2002, DOI 10.1074/jbc.M110414200

Bong-Hyun Ahn,[a] Hyangshuk Rhim,[b] Shi Yeon Kim,[a] Young-Mo Sung,[c] Mun-Yong Lee,[d] Ju-Youn Choi,[b] Benjamin Wolozin,[e] Jong-Soo Chang,[f] Young Han Lee,[g] Taeg Kyu Kwon,[h] Kwang Chul Chung,[i] Shin-Hee Yoon,[a] Sang June Hahn,[a] Myung-Suk Kim,[a] Yang-Hyeok Jo,[a] and Do Sik Min[a,j]

From the [a]Department of Physiology, [b]Research Institute of Molecular Genetics, and [d]Anatomy, College of Medicine, The Catholic University of Korea, Seoul 137-701, Korea, the [c]Graduate School of Biotechnology, Korea University, Seoul 136-701, Korea, the [e]Department of Pharmacology, Loyola University Medical Center, Maywood, Illinois 60153, the [f]Department of Life Science, Daejin University, Pochon-gun 487-800, Kyeongggido, Korea, the [g]Department of Biochemistry and Molecular Biology, College of Medicine, Yeungnam University, Daegu 705-717, Korea, the [h]Department of Immunology, School of Medicine, Keimyung University, Daegu 700-712, Korea, and the [i]Department of Pharmacology, Yonsei University College of Medicine, Seoul 120-752, Korea

α-Synuclein has been implicated in the pathogenesis of many neurodegenerative diseases, including Parkinson's disease and Alzheimer's disease. Although the function of α-synuclein remains largely unknown, recent studies have demonstrated that this protein can interact with phospholipids. To address the role of α-synuclein in neurodegenerative disease, we have investigated whether it binds phospholipase D (PLD) and affects PLD activity in human embryonic kidney (HEK)-293 cells overexpressing wild type α-synuclein or the mutant forms of α-synuclein (A53T, A30P) associated with Parkinson's disease. Tyrosine phosphorylation of α-synuclein appears to play a modulatory role in the inhibition of PLD, because mutation of Tyr^{125} to Phe slightly increases inhibitory effect of α-synuclein on PLD activity. Treatment with pervanadate or phorbol myristate acetate inhibits PLD more in HEK 293 cells overexpressing α-synuclein than in control cells. Binding of α-synuclein to PLD requires phox and pleckstrin homology domain of PLD and the amphipathic repeat region and non-Aβ component of α-synuclein. Although biologically important, co-transfection studies indicate that the interaction of α-synuclein with PLD does not influence the tendency of α-synuclein to form pathological inclusions. These results suggest that the association of α-synuclein with PLD, and modulation of PLD activity, is biologically important, but PLD does not appear to play an essential role in the pathophysiology of α-synuclein.

α-Synuclein is a small, highly conserved presynaptic protein of unknown function that has been implicated in the development of neurodegenerative diseases, such as Alzheimer's (AD)[1] and Parkinson's disease (PD). α-Synuclein is known to be a structural component of the filaments in Lewy bodies of PD and dementia with Lewy bodies (1–5). α-Synuclein also contributes to the intracellular inclusions of multiple system atrophy (6, 7), and a fragment has been found in senile plaques in Alzheimer's disease. Two point mutations (A53T, A30P) in α-synuclein are genetically linked to familial PD (8, 9). However, the mechanism by which α-synuclein is involved in PD and in the accumulation in Lewy bodies remains elusive. The recent observation that both mice and flies expressing a human α-synuclein transgene recapitulate some characteristics of PD suggests that α-synuclein could be involved directly in the development of this disease (10, 11). Structurally, α-synuclein is a small acidic protein of 140 amino acid residues that contains three modular domain, including an amino-terminal lipid binding α-helix, an amyloid binding domain that encodes the non-Aβ component (NAC) of AD plaques, and a carboxyl-terminal acidic tail. The structure of α-synuclein allows the molecule to exist in either a random or a natively unfolded conformation or as an α-helix in the presence of phospholipids (12, 13), suggesting a highly dynamic regulation of α-synuclein function that depends on the local cellular milieu.

Reported binding targets for α-synuclein include Tau (14), 14-3-3 (15), protein kinase C (15), synphilin-1 (16), Elk (17), Tat-binding protein 1 (18). Recent studies have suggested various cellular roles for α-synuclein that include possible modifications of membrane and cell surface signaling events (19). Although normal cellular functions of α-synuclein are unknown, several observations suggest the synuclein may serve to integrate presynaptic signaling and membrane trafficking.

Recently, α-synuclein has been identified as a potent and selective inhibitor of phospholipase D2 (PLD2) *in vitro*. PLD hydrolyzes phosphatidylcholine to produce phosphatidic acid and diacylglycerol (20). This suggests that the level and modification of α-synuclein may affect phospholipase D2 activity *in vitro*, thereby modulating the cleavage of membrane lipids and membrane biogenesis (19). Thus far, two isoforms of PLD have

* This work was supported by a grant from the Korea Health 21 R & D Project, Ministry of Health & Welfare, Republic of Korea (01-PJ1-PG3-20900-0011) and by a research grant from the Ministry of Education (BK21). The costs of publication of this article were defrayed in part by the payment of page charges. This article must therefore be hereby marked "*advertisement*" in accordance with 18 U.S.C. Section 1734 solely to indicate this fact.

[j] To whom correspondence should be addressed. Tel.: 82-2-590-1165; Fax: 82-2-532-9575; E-mail: dsmin@cmc.cuk.ac.kr.

[1] The abbreviations used are: AD, Alzheimer's disease; PD, Parkinson's disease; PLD, phospholipase D; PLC, phospholipase C; PMA, phorbol 12-myristate 13-acetate; PKCα, protein kinase C α; DMEM, Dulbecco's modified Eagle's medium; HEK cells, human embryonic kidney cells; NAC, non-Aβ component of Alzheimer's disease plaques; GST, glutathione *S*-transferase; PBS, phosphate-buffered saline; H & E, hematoxylin and eosin; wt, wild-type.

been described, PLD1 and PLD2 (21–24). Activity of 120-kDa PLD1 is regulated by multiple inputs, including phosphatidylinositol 4,5-bisphosphate, protein kinase C, the Rho family proteins, and ADP-ribosylation factor proteins. PLD2 is a 106-kDa protein that share 50–55% homology with PLD1. PLD2 is reported to have a much higher basal activity than PLD1 and appears to be insensitive to further stimulation by the known activators of PLD1. The primary lipid product of PLD, phosphatidic acid, exhibits a number of biological activities *in vitro* and may be an important mediator of processes controlling vesicular transport and changes in cell morphology (25). In neuronal cells, PLD activation has been linked to pathways involved in cell growth, differentiation, and neurotransmitter release (26, 27). Although many studies continue to focus on the functional relationships and the isozyme specificities of the PLD isozymes, the molecular mechanism of the regulation of the PLDs has not been fully elucidated.

In this regard, the identification of PLD-binding partners may provide clues toward the understanding of complex regulatory mechanism of PLD in different cells. Since direct cell cytotoxicity of α-synuclein is still controversial, α-synuclein might interact with other proteins to cause neurodegeneration. The investigation of regulation of PLD by α-synuclein is required to gain insight into the role of these proteins under normal and pathological condition. As a step in this effort, we now report for the first time that α-synuclein binds to PLD1 and PLD2 and inhibits pervanadate-induced PLD activation in human embryonic kidney 293 cells. Moreover, we show that the state of tyrosine phosphorylation of α-synuclein plays a modulatory role in pervanadate-induced PLD activity.

EXPERIMENTAL PROCEDURES

Materials—Dulbecco's modified Eagle's medium (DMEM), fetal bovine serum, and LipofectAMINE were purchased from Invitrogen. Protein A-Sepharose and glutathione-Sepharose 4B were from Amersham Biosciences. Biotech. Hydrogen peroxide and sodium orthovanadate were from Sigma, and anti-phosphotyrosine antibody (Tyr(P)) (4G10) were from Upstate Biotechnology. The antibody to PKCα was purchased from Santa Cruz. Mouse monoclonal antibody to α-synuclein was generated using GST-α-synuclein as an antigen. Rabbit polyclonal antibody that recognizes both PLD1 and PLD2 was generated as described previously (28). Phosphatidylbutanol standard was from Avanti Polar Lipid. *myo*-[2-^{3}H]Inositol and [9,10-^{3}H]myristate were purchased from PerkinElmer Life Sciences. Silica gel 60 A thin layer chromatography plates were from Whatman. Horseradish peroxidase-conjugated anti-mouse IgG and anti-rabbit IgG were from Kirkegaard & Perry Laboratory (Gaithersburg, MD). The ECL Western blotting detection kit was from Amersham Biosciences.

Cell Culture and Transfection—HEK 293 cells were maintained in Hepes-buffered DMEM (Invitrogen) supplemented with 10% (v/v) fetal bovine serum under 5% CO_2. The cells were transfected with the indicated plasmid DNA and LipofectAMINE (Invitrogen) according to manufacturer's instructions. G418 (500 μg/ml) was used for selection.

Co-immunoprecipitation and Immunoblot—HEK 293 cells were lysed with lysis buffer (20 mM Hepes, pH 7.2, 1% Triton X-100, 1% sodium deoxycholate, 0.2% SDS, 150 mM NaCl, 1 mM Na_3VO_4, 1 mM NaF, 10% glycerol, 10 μg/ml leupeptin, 10 μg/ml aprotinin, 1 mM phenymethylsulfonyl fluoride) and precleared with preimmune IgG and protein A-Sepharose for 30 min at 4 °C with rocking. Protein concentrations were determined using the Bio-Rad Protein Assay with bovine serum albumin as a standard. Equal protein aliquots of precleared cell lysates (1 mg) were incubated with the indicated antibodies and 30 μl of a 1:1 slurry of protein A-Sepharose beads for 4 h at 4 °C. The immune complexes were collected by centrifugation and washed five times with a buffer (20 mM Tris, pH 7.5, 1 mM EDTA, 1 mM EGTA, 150 mM NaCl, 2 mM Na_3VO_4, 10% glycerol, and 1% Nonidet P-40) and resuspended in sample buffer. Immune complexes were subjected to SDS-PAGE and Western blot analysis using the indicated antibody. The protein bands were visualized using ECL (Amersham Biosciences).

Construction and Preparation of GST Fusion Proteins—The full-length cDNA of human PLD1 or PLD2 was digested into fragments containing specific domains. These individual PLD1 or PLD2 fragments were then ligated into the *Eco*RI or *Sma*I site of the pGEX4T1 vector. Subcloning and the polymerase chain reaction (PCR) were used to produce the expression vectors encoding the respective GST fusion proteins. *Escherichia coli* BL21 cells were transformed with individual expression vectors encoding the GST fusion proteins, and after harvesting the cells, the GST fusion protein expressed were purified by standard methods (29) using glutathione-Sepharose 4B (Amersham Biosciences).

Preparation of Rat Brain Extract—Rat brain (2 g) was homogenized in lysis buffer using a polytron homogenizer. After centrifugation at 100,000 × *g* for 1 h at 4 °C, the resulting supernatant was used to investigate potential α-synuclein or PLD binding domains. Protein concentrations were determined using the methods developed by Bradford (30).

In Vitro Binding Experiment—Clarified lysates (1 mg) of rat brain were incubated with 3 μg of GST fusion proteins immobilized on glutathione-Sepharose beads in a final volume of 500 μl of lysis buffer for 1.5 h at 4 °C. Protein complexes were collected by centrifugation and washed four times with washing buffer (1% Triton X-100, 150 mM NaCl, 20 mM Tris-HCl, pH 8.0, 20 mM NaF, 2 mM sodium orthovanadate, 1 mM PMSF, 10 μg/ml leupeptin, 10 μg/ml aprotinin). Associated protein complexes were resolved by SDS-PAGE and transferred to a nitrocellulose membrane. Immunoreactivity was detected using the indicated antibodies, horseradish peroxidase-conjugated secondary antibodies, and ECL according to the manufacturer's instructions.

Measurement of Phosphoinositides Hydrolysis by PLC—Cells were plated into 60-mm dishes at 5 × 10^5 cells per dish and grown for 1 day. The cells were then labeled with *myo*-[2-^{3}H]inositol (2 μCi/ml) in inositol-free DMEM for 20 h. Subsequently, the labeled cells were washed and pretreated with 20 mM LiCl for 15 min in DMEM containing 20 mM Hepes, pH 7.2, and 1 mg/ml bovine serum albumin. Stimulation was initiated by the addition of pervanadate for 50 min and terminated by the addition of ice-cold 5% $HClO_4$. After 30 min in an ice bath, extracts were centrifuged, diluted with distilled water, and applied to Bio-Rad Dowex AG 1-X8 anion exchanger column. The column was then washed with 10 ml of distilled water followed by 10 ml of 60 mM ammonium formate containing 5 mM of sodium tetraborate. Total inositol phosphates were eluted with a solution containing 1 M ammonium formate and 0.1 M formic acid.

Phospholipase D Assay—PLD activity was assessed by measuring the formation of [^{3}H]phosphatidylbutanol, the product of transphosphatidylation in the presence of 1-butanol. HEK 293 cells were subcultured in six-well plates at 2 × 10^5 cells/well. The cells were serum-starved in DMEM for 24 h before the start of the assay. For the final 20 h of serum starvation, the cells were labeled with 1 μCi/ml [9,10-^{3}H]myristic acid. The cells were washed three times with 5 ml of phosphate-buffered saline (PBS) and pre-equilibrated in serum-free DMEM for 1 h. For the final 10 min of preincubation, 0.3% butan-1-ol was included. At the end of the preincubation, cells were treated with pervanadate or PMA for the indicated times. Incubations were terminated by removing the medium, washing with 5 ml of ice-cold PBS, and adding 1 ml of ice-cold methanol. Cells were scraped off the plates using a policeman, and the lipids were extracted and separated with methanol/chloroform/0.1 N HCl (1:1:1) according to the method of Bligh and Dyer (31). The lower phase was dried under N_2, resuspended in 30 μl of chloroform/methanol (2:1), and spotted onto silica gel 60A thin layer chromatography plate (Whatman). The plates were developed in the upper phase of the solvent system of ethyl acetate/iso-octane/H_2O/acetic acid (55:25:50:10) and stained with iodine. A phosphatidylbutanol standard (Avanti Polar Lipids) was used to locate the bands, which were scraped into scintillation mixture. Radioactivity incorporated into total phospholipids was measured, and the results were presented as percentage of total lipid counts/min incorporated into phosphatidylbutanol to normalize the results.

Immunofluorescent Staining—To examine the co-localization of α-synuclein with PLD1, a double-immunofluorescence technique was used. Three male Sprague-Dawley rats (3–6 months old) were deeply anesthetized with 4% chloral hydrate (1 ml/100 mg) and were sacrificed by transcardial perfusion with a fixative containing 4% paraformaldehyde in 0.1 M phosphate buffer, pH 7.4. Cryostat coronal sections (25 μm thick) were cut throughout the mesencephalon and were processed for double-immunofluorescence histochemistry. Free floating sections were blocked in 10% normal donkey serum and normal goat serum in 0.01 M PBS for 1 h. Incubation with primary antibodies was performed with a mouse monoclonal antibody against α-synuclein and an affinity-purified anti-PLD1 antibody overnight at 4 °C. After washing in PBS, the sections were incubated with a mixture of fluorescein isothiocyanate-conjugated goat anti-mouse IgG (Jackson ImmunoResearch; diluted at 1:100) and Cy3-conjugated goat anti-rabbit IgG (Jackson Im-

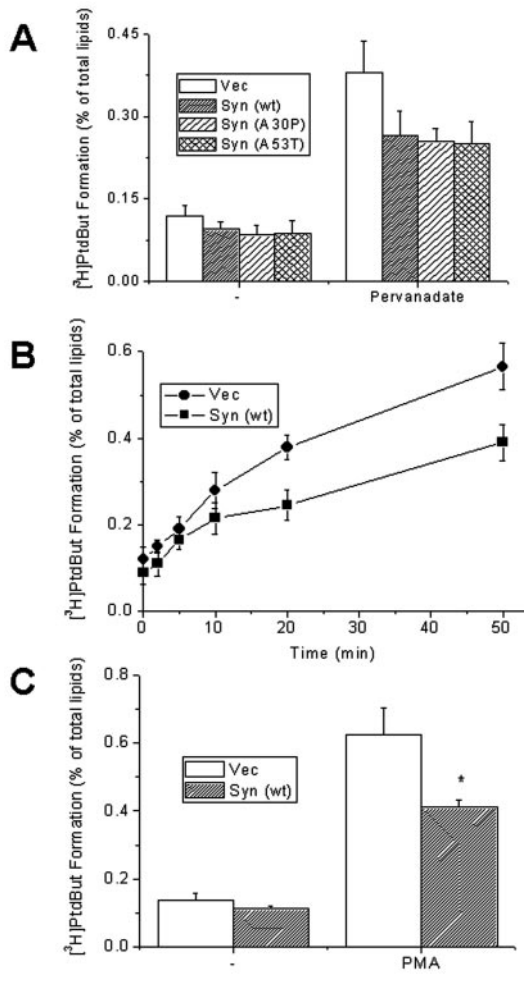

FIG. 1. **Overexpression of α-synuclein inhibits pervanadate-induced PLD activation in cells.** *A*, HEK 293 cells expressing wild-type (*wt*), A30P, and A53T α-synuclein as well as vector-transfected cells were cultured in six-well plates, labeled with [^{3}H]myristate, and treated with pervanadate (100 μM Na_3VO_4 and 0.5 mM H_2O_2) for 30 min. *B*, vector and α-synuclein HEK 293 cells were treated with pervanadate for different times. *C*, vector and α-synuclein HEK 293 cells were treated with PMA for 50 min. The radioactivity incorporated into phosphatidylbutanol was measured as described under "Experimental Procedures." Results are the means ± S.D of three independent experiments. *, $p < 0.05$ compared with PMA-treated control cells.

munoResearch; diluted at 1:100) for 2 h at room temperature. To test the specificity of immunostaining, control sections were processed in an identical manner but with the primary or secondary antibodies omitted. Slides were viewed using a confocal microscope (MRC-1024, Bio-Rad). Images were converted to TIFF format, and contrast levels of images were adjusted using Adobe Photoshop.

Formation of Eosinophilic Inclusions—We performed hematoxylin and eosin (H & E) staining according to standard cell biology techniques (16, 32). At 30 h post-transfection, the co-transfected HEK 293 cells were fixed with 3.7% formaldehyde-PBS buffer for 15 min at room temperature and hydrated with distilled water for 10 min. The hydrated cells were stained with Mayer's hematoxylin solution (Sigma) for 5 min and washed in distilled water. Cells were destained with 1% HCl in ethanol for 30 s and neutralized with 0.2% ammonia for 30 s. The processed cells were stained with eosin solution (Eosin Y, 0.5% aqueous solution, Sigma) for 1 min, followed by washing in distilled water. The cells were dehydrated by rinsing in the following concentration series of ethanol, 70, 80, and 100%, at room temperature and then mounted with 100% glycerol. All cells were counted in fields chosen at random from five different circles of the cell culture well (all cells were counted in five randomly selected fields under a light microscope at a magnification of ×400). Values are expressed as percentages of cells containing eosinophilic protein aggregates with pinkish color relative to total cells. Error bars shown in this study represent S.D. derived from means for three independent replicates.

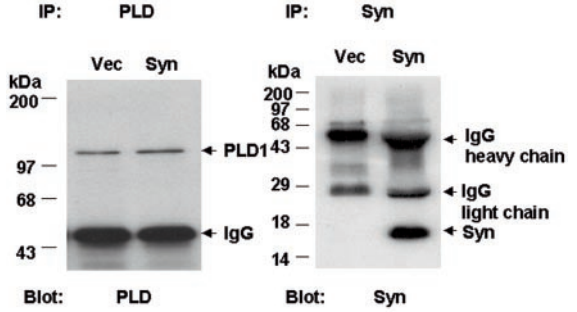

FIG. 2. **Expression of PLD1 in HEK 293 cells.** Vector or α-synuclein-expressing cells were lysed, and immunoprecipitates (*IP*) were prepared using anti-PLD or anti-α-synuclein (*Syn*) antibodies. Immunoprecipitants were analyzed by SDS-polyacrylamide gel electrophoresis, followed by transfer of proteins to nitrocellulose membrane and Western blotting (*Blot*) with anti-PLD or α-synuclein (*Syn*) antibodies. The results shown are representative of three separate experiments.

Statistical Analysis—Data are expressed as means ± S.D. The Student's *t* test was used where appropriate. A probability of $p < 0.05$ was considered statistically significant.

RESULTS

α-Synuclein Inhibits Pervanadate or PMA-induced PLD Activity in HEK 293 Cells—To investigate whether α-synuclein might affect PLD activity in human cell lines, we generated a line of 293 HEK cells overexpressing wild-type (wt), A30P, or A53T α-synuclein, as well as a vector transfected control cell line (Vec). Pervanadate, a complex of vanadate and hydrogen peroxide, is a competitive inhibitor of protein-tyrosine phosphatase that works by irreversible oxidation and functions on intact cells because of its cell permeability (33). Pervanadate is also known to stimulate PLD activity (34–36). Pervanadate stimulated PLD activity less in wild-type, A30P, or A53T α-synuclein cell lines than in the control cell line (Fig. 1*A*). Inhibition of pervanadate-stimulated PLD activity in α-synuclein HEK 293 cells occurred in a time dependent manner, compared with that of control cells (Fig. 1*B*). We also examined an effect of α-synuclein on another activator of PLD, PMA. PMA-induced PLD activation in cells expressing α-synuclein also was more reduced, compared with that of control cells (Fig. 1*C*). To examine the relative contribution of PLD protein to PLD activity in HEK cells, we investigated the expression level of PLD isozymes. By immunoprecipitation and Western blot analysis using anti-PLD antibody, cells overexpressing wild-type α-synuclein or vector-transfected cell line were found to express similar levels of PLD1 (Fig. 2). However, PLD2 was not detected in either cells (data not shown). Similar results were observed in HEK 293 cells stably transfected with A30P or A53T (data not shown). To further demonstrate the inhibitory effect of α-synuclein on the PLD activity, we transiently co-transfected α-synuclein and PLD1 or PLD2 into HEK 293 cells. Transfected cells were labeled with [^{3}H]myristic acid and then either left untreated or stimulated with pervanadate (100 μM sodium orthovanadate and 0.5 mM H_2O_2). Cells co-transfected with α-synuclein and PLD1 or PLD2 showed less pervanadate-induced PLD activation than cells transfected with PLD and vector (Fig. 4). These results demonstrate that α-synuclein inhibits both PLD1 and PLD2 activation induced by pervanadate in mammalian cells.

α-Synuclein Is Tyrosine-phosphorylated by Pervanadate in HEK 293 Cells—Protein-tyrosine phosphorylation plays a pivotal role for the functional properties of numorous proteins. α-Synuclein appears to contain four tyrosine residues, which are consensus sequences for tyrosine kinase-mediated phosphorylation. Recently, it was reported that α-synuclein is ty-

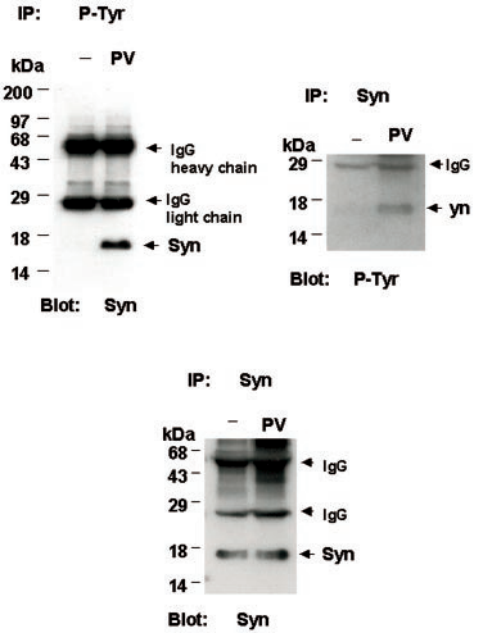

FIG. 3. **Pervanadate-induced tyrosine phosphorylation of α-synuclein in cells.** HEK cells overexpressing wild-type α-synuclein were treated with pervanadate (*PV*) (100 μM Na_3VO_4 and 0.5 mM H_2O_2) for 20 min. Cells were immunoprecipitated with anti-α-synuclein or anti-Tyr(P) antibody. Resulting immunoprecipitants were separated in duplicates by SDS-PAGE and transferred to nitrocellulose membranes using anti-Tyr(P) or α-synuclein (*Syn*) antibodies. The results shown are representative of three separate experiments.

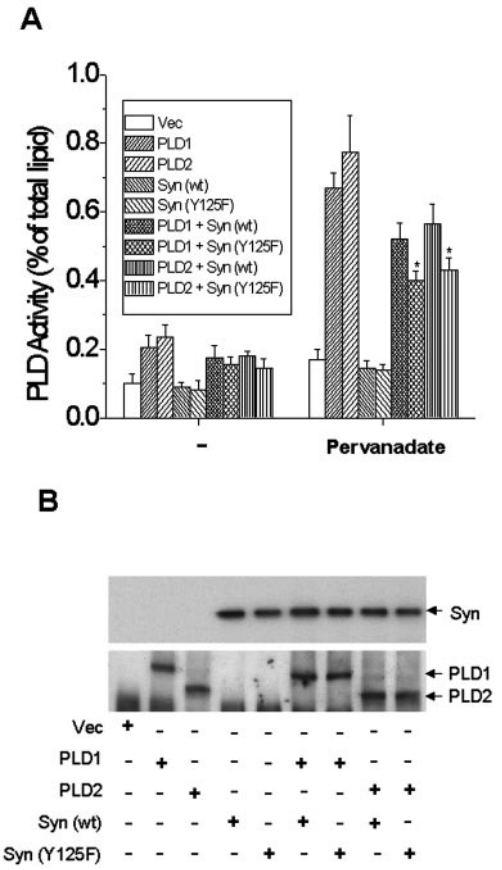

FIG. 4. **Effect of tyrosine phosphorylation state of α-synuclein on pervanadate-induced PLD activation.** *A*, HEK 293 cells were transiently transfected with various constructs and labeled with [^{3}H]myristic acid for 18 h. The cells were treated with or without pervanadate (100 μM Na_3VO_4 and 0.5 mM H_2O_2) for 30 min in the presence of 0.3% 1-butanol. The radioactivity incorporated into phosphatidylbutanol was measured as described under "Experimental Procedures." Results are the means ± S.D of three independent experiments. *, $p < 0.05$ compared with cells co-transfected with α-synuclein (*wt*) and PLD1 or PLD2 and treated with pervanadate. *B*, the lysates from the HEK 293 cells used in the experiments were analyzed by Western blotting as described under "Experimental Procedures."

rosine-phosphorylated by the Src family of protein-tyrosine kinases such as c-Src and Fyn (37). We investigated tyrosine phosphorylation of α-synuclein in transfected cells. Immunoprecipitated α-synuclein from either pervanadate-treated stably transfected HEK 293 cells expressing human α-synuclein was separated by SDS-PAGE in duplicate. Western blot analysis was then performed with phosphotyrosine specific antibody (4G10), or α-synuclein antibody, which specifically recognizes α-synuclein (Fig. 3). The cell lysates were also immunoprecipitated with anti-phosphotyrosine antibody and then analyzed by immunoblotting with anti-α-synuclein antibody. Pervanadate (100 μM sodium orthovanadate and 0.5 mM H_2O_2) induced tyrosine phosphorylation of α-synuclein.

Effect of Tyrosine Phosphorylation State of α-Synuclein on Pervanadate-induced PLD Activation—We investigated the effect of the tyrosine phosphorylation state of α-synuclein on pervanadate-induced PLD activity by mutating each of the tyrosines in α-synuclein. Mutation of Tyr^{125} to Phe was the only tyrosine mutation to alter the activity of α-synuclein. This reduced tyrosine phosphorylation to ~5% of the wild-type control, whereas other single amino acid changes do not change tyrosine phosphorylation significantly. Next, we examined the effect of tyrosine phosphorylation state on the ability of α-synuclein to inhibit PLD activity. The cells were co-transfected with PLD1 or PLD2 along with the Y125F mutant construct or wild-type control α-synuclein. After co-transfection, cells were trated with or without pervanadate (100 μM Na_3VO_4 and 500 μM H_2O_2). Mutation of Tyr^{125} to Phe slightly increased the inhibitory effect of α-synuclein on pervanadate-induced PLD activity. (Fig. 4*A*). The expression level of PLDs or α-synuclein was similar in these transfection experiment (Fig. 4*B*). Thus, the tyrosine phosphorylation state of α-synuclein appears to modulate PLD activity.

α-Synuclein Associates with PLD1 and PKCα—To explore the significance of this inhibition, we examined whether α-synuclein interacts with PLD isozymes. HEK 293 cells overexpressing α-synuclein were treated for 20 min with or without pervanadate. The lysates were immunoprecipitated with anti-PLD antibody, and the precipitates were probed with monoclonal anti-α-synuclein antibody (Fig. 5*A*). The presence of α-synuclein in the PLD immune complex was apparent. In a reciprocal experiment, α-synuclein was immunoprecipitated by antibody to α-synuclein. Subsequent immunoblotting with the anti-PLD1 revealed PLD1 expression (Fig. 5*A*). Interestingly, α-synuclein was constitutively associated with PLD1. Furtheremore, both α-synuclein and PLD1 proteins were associated with PKCα in cells overexpressing α-synuclein (Fig. 5, *B* and *C*). α-Synuclein was also associated with PLD2 in co-transfection experiments (Fig. 5*D*). Interestingly, pervanadate did not alter the interaction of α-synuclein with PKCα or PLD. To examine whether the effect of α-synuclein on PLD is specific, we investigated the effect of α-synuclein on the activity of other lipid modifying enzyme and their interaction (Fig. 6). Pervanadate induced an increase in PLC activity in the HEK 293 cells, but α-synuclein did not affect PLC activity (Fig. 6*A*) and did not associate with PLC-β1 (Fig. 6*B*) in cells overexpressing α-synuclein, suggesting that the effect of α-synuclein on PLD is specific.

Amphipathic Repeat Region and NAC Domain of α-Synuclein Is Involved in the Interaction with PLD1—To map the region on

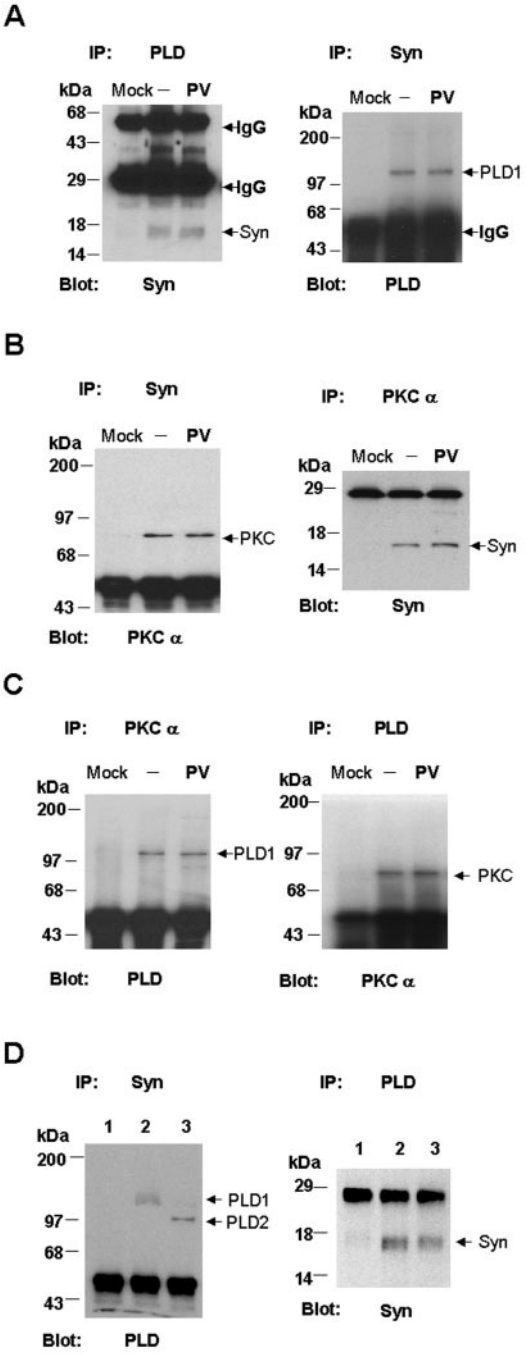

FIG. 5. **Interaction of α-synuclein with PLD and PKCα.** *A–C*, HEK 293 cells expressing α-synuclein were stimulated without or with pervanadate (*PV*) (100 μM Na_3VO_4 and 0.5 mM H_2O_2) for 20 min. The cells were then lysed, and immunoprecipitates (*IP*) were prepared using anti-PLD, anti-α-synuclein (*Syn*), or anti-PKCα antibody. The immunoprecipitates were analyzed by SDS-polyacrylamide gel electrophoresis, followed by transfer of proteins to nitrocellulose membranes and Western blotting (*Blot*) with anti-PLD, anti-α-synuclein (*Syn*), or anti-PKCα antibodies. *D*, HEK 293 cells were transiently transfected with the empty vector (*lane 1*), PLD1 and α-synuclein (*lane* 2), or PLD2 and α-synuclein (*lane* 3). After immunoprecipitation with the anti-PLD or anti-α-synuclein antibody, the immunoprecipitates were then immunoblotted with anti-α-synuclein or anti-PLD antibody. "*Mock*" represents a mock-precipitated control. The blots shown are representative of three independent experiments.

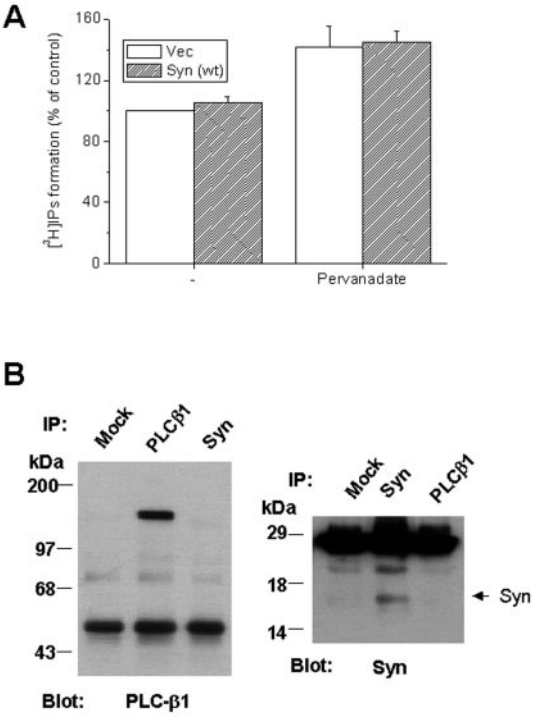

FIG. 6. **α-Synuclein does neither affect PLC activity nor interact with the enzyme.** *A*, subconfluent, quiescent cells were labeled with 2 μCi/ml *myo*-[2-^{3}H]inositol in inositol-free DMEM for 20 h and then stimulated with pervanadate (100 μM Na_3VO_4 and 0.5 mM H_2O_2) for 50 min in the presence of 20 mM LiCl, and total inositol phosphates were measured as described under "Experimental Procedures." Results are the means ± S.D of three independent experiments. *B*, the cells were then lysed, and immunoprecipitates (*IP*) were prepared using anti-PLCβ1 or anti-α-synuclein (*Syn*) antibody. The immunoprecipitates were then subjected to Western blotting (*Blot*) with anti-PLCβ1 or anti-α-synuclein (*Syn*). The blots shown are representative of three independent experiments.

the α-synuclein protein that is responsible for the interaction with PLD1, we prepared GST-fused human α-synuclein protein, GST-Syn-whole (amino acid residues 1–140), GST-Syn-N (amino acid residues 1–60), GST-Syn-NAC (amino acid residues 61–95), and GST-Syn-C (amino acid residues 96–140) and used them in *in vitro* binding experiments. As shown in Fig. 7, the GST-Syn-N and GST-Syn-NAC containing the amphipathic repeat region and the NAC domain, respectively, precipitated PLD1 from rat brain lysates. Thus, these data suggest that the amphipathic repeat region and the NAC domain might be involved in the interaction with PLD1.

α-Synuclein Associates with a Region (Amino Acids 1–331) of PLD1—Next, we analyzed the interaction site(s) of PLD1 with α-synuclein. To identify the PLD1 sequence involved in the α-synuclein binding, we constructed the GST fusion proteins shown in Fig. 8*A*. The lysates from rat brain were precipitated with GST-PLD1 fragments (Fig. 8*B*) and analyzed by Western blotting with anti-α-synuclein antibody. GST-PLD1 (amino acid 1–331) was found to be the region that most potently bound to α-synuclein. It appears, therefore, that the region between amino acids 1 and 331 containing the phox and pleckstrin homology domains may be important for the interaction with α-synuclein.

Interaction of PLD1 with the α-Synuclein in Rat Brain—As with HEK 293 cells overexpressing α-synuclein, we found that in rat brain tissues, PLD1 co-precipitates with endogeneous α-synuclein by using a co-immunoprecipitation method on rat brain (Fig. 9*A*). We tried to further check whether PLD1 co-localized with α-synuclein. Recently, we reported endogeneous PLD1 expression in neurons of the substantia nigra par compact (28), which are affected in PD. Expression of α-synuclein has been also reported in these neurons (38, 39). Therefore, rat brain sections were double-immunolabeled with anti-PLD1 and anti-α-synuclein antibodies to identify the co-localization of

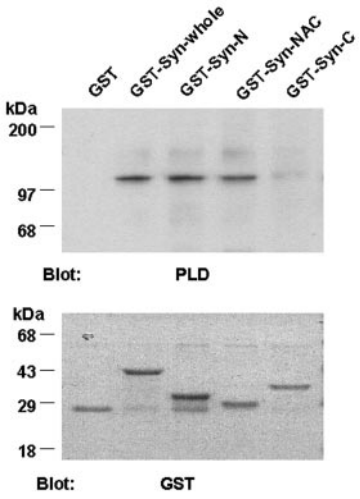

FIG. 7. **Amphipathic repeat region and NAC domain of α-synuclein interact with PLD1.** α-Synuclein was fragmented into individual domains consisting of NH_2 terminus (1–60), NAC (61–95), COOH terminus (96–140). The fragments and whole protein were cloned as GST fusion proteins, expressed in *E. coli*, and purified using glutathione-Sepharose beads. Equal amounts (1 mg) of GST or GST fusion proteins (GST-Syn fragment) were incubated with rat brain extract as described under "Experimental Procedures." The precipitated proteins were subjected to immunoblot analysis using antibody against PLD1 (*upper panel*). The amount of the GST fusion protein was visualized by Western blotting using anti-GST antibody (*lower panel*). The results shown are representative of three separate experiments.

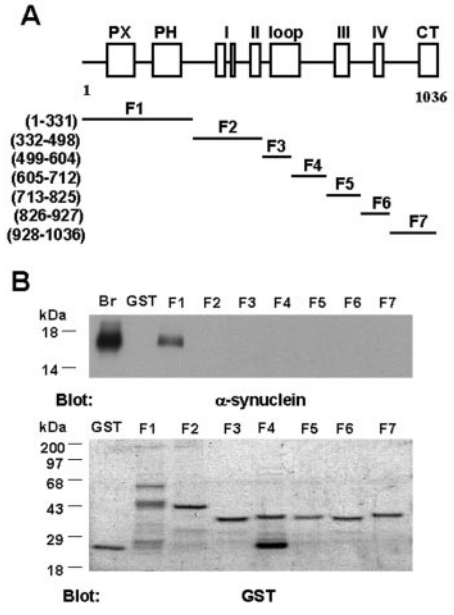

FIG. 8. **α-Synuclein associates with phox and pleckstrin homology domains of PLD1.** *A*, a schematic representation of the structure of PLD1 is shown on the *top*. The possible functions of each box have been proposed or demonstrated in Ref. 24. *Boxes* are the regions of highly conserved sequences in PLD. *PX*, phox domain; *PH*, pleckstrin homology-like domain; *I–IV*, conserved regions in the PLD family (24). *loop*, loop region, *CT*, COOH terminus. *B*, equal amounts (1 mg) of GST or GST fusion proteins (GST-PLD1 fragments, *F1–F7*) were incubated with rat brain extract as described under "Experimental Procedures." The precipitated proteins were subjected to immunoblot analysis using antibody against α-synuclein (*upper panel*). The amount of the GST fusion protein was visualized by Western blotting using anti-GST antibody (*lower panel*). The results shown are representative of three separate experiments.

α-synuclein with PLD1 in the same neuron. Examination with confocal microscopy revealed that all α-synuclein immunoreactive neurons in the substantia nigra pars compacta co-localized

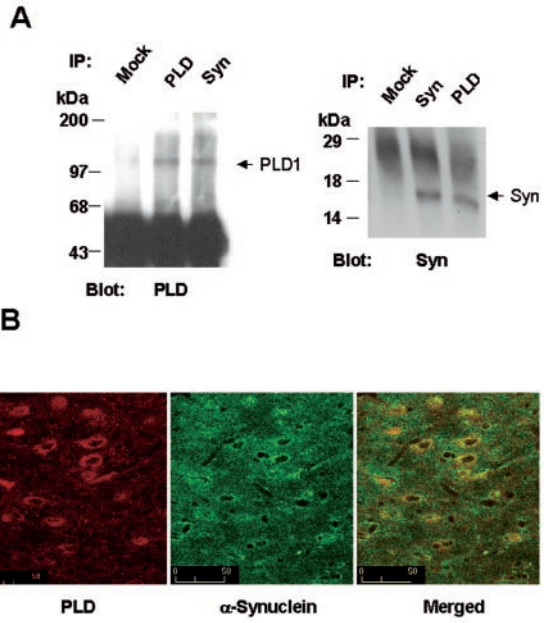

FIG. 9. **Interaction of PLD1 with α-synuclein in rat brain.** *A*, α-synuclein and PLD was co-immunoprecipitated from rat brain lysates using antibody to PLD or α-synuclein. The resulting immunoprecipitates were immunoblotted with antibodies to α-synuclein or PLD. *Mock* represents a mock-precipitated control. *B*, Cy3-labeled, PLD1 immunoreactive cells and fluorescein isothiocyanate-labeled, α-synuclein immunoreactive cells in the neuron of the substantia nigra pars compacta were visualized with confocal microscopy. Superimposed images display the co-localization of, respectively, PLD1-labeled and α-synuclein-labeled neurons in the substantia nigra pars compacta. *Scale bars*: 50 μm. The results shown are representative of two separative experiments.

with PLD1 immunoreactivity (Fig. 9*B*). Taken together, these results suggest that regulation of PLD by α-synuclein might occur through *in vivo* interaction.

Quantification of Eosinophilic Inclusions—Since α-synuclein was observed to interact with both PLD1 and PLD2, we assessed their functional significance in terms of the formation of intracellular cytoplasmic inclusions, which is pathological characteristics of PD (8, 9, 40, 41). The morphological composition of cells was determined by hematoxylin and eosin (H & E) staining to evaluate the formation of inclusion bodies in cells transfected with both PLD and α-synuclein proteins (Fig. 10*A*). Consistent with the previous result, we observed that ~6% cells out of total cell numbers had eosinophilic inclusion bodies in cytoplasm when HEK 293 cells were co-transfected with constructs encoding NAC and full-length synphilin-1, which were used as a positive control (Fig. 10*B*) (16). The percentage of cells that develop inclusion bodies is ~10–20%, out of cells expressing both NAC and synphilin-1 based on a transfection efficiency of 30–40%, which was calculated using a green fluorescent protein reporter plasmid. In contrast, cells co-transfected constructs encoding NAC and PLD1 or NAC and PLD2 exhibited only ~1–2% of eosinophilic inclusion bodies (Fig. 10*B*). In addition, cells co-expressing α-synuclein and PLD1 or PLD2 revealed same effect that was observed in cells co-exprexressing NAC and PLDs (data not shown). This is similar to the results that were obtained from cells expressing any protein alone, such as NAC, α-synuclein, PLD1, or PLD2 protein. These results suggest that the specific interaction between PLDs and α-synuclein might not be an essential feature in the formation of inclusion bodies in mammalian cells.

DISCUSSION

We demonstrate for the first time that α-synuclein binds to both PLD1 and PLD2 and inhibits its enzymatic activity in

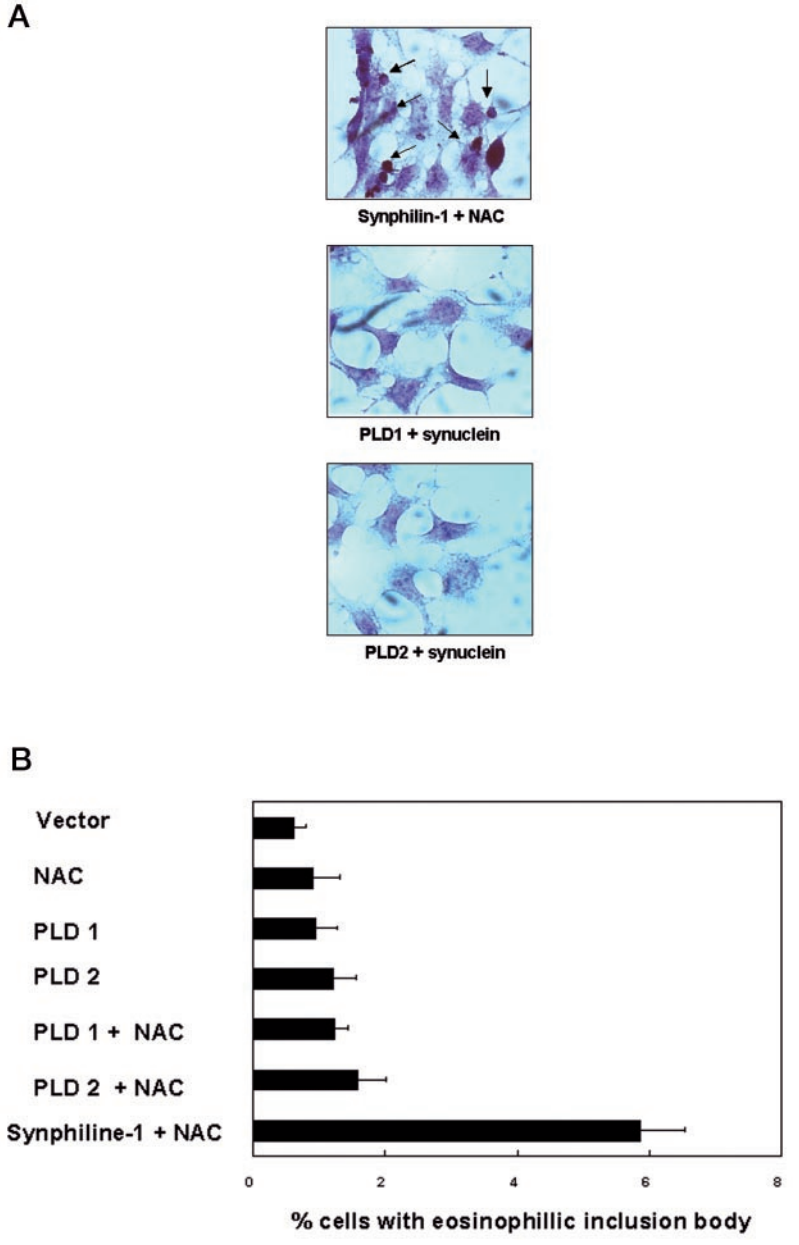

FIG. 10. **Formation of eosinophilic cytoplasmic inclusion bodies.** *A*, HEK 293 cells co-transfected with constructs encoding NAC (amino acids 61–95 of α-synuclein) and full-length synphilin-1 develop cytoplasmic eosinophilic inclusions when stained with H & E. The inclusions were hardly detected in cells co-transfected with constructs encoding NAC plus PLD1 or NAC plus PLD2. *B*, quantification of eosinophilic inclusion formation in HEK 293 cells transfected with various constructs. Approximately 6% of cells co-transfected with constructs encoding NAC and synphilin-1 co-stained eosinophilic inclusions, whereas co-transfection of constructs encoding NAC and PLD1 or PLD2 resulted in the formation of less than 1% of eosinophilic inclusion. Values are expressed as percentages of cells containing eosinophilic protein aggregates with *pinkish color* relative to total cells. Results are the means ± S.D of three independent experiments.

human cell lines. α-Synuclein has been implicated in Parkinson's and Alzheimer's disease. It is of great interest to determine the specific function(s) of α-synuclein because of its potential importance in the pathogenesis of these diseases. The link between α-synuclein and PLD appears to be particularly intriguing, because α-synuclein inhibits PLD2 activity *in vitro* (20), and PLD activity was significantly increased in in Alzheimer's disease brain tissues as compared with control tissues (42). Recently, we confirmed the increase in PLD1 protein in AD brain and also observed that PLD co-localized with β-amyloid (data not shown). Taken together, these results suggest that modulation of PLD by α-synuclein might play a role in some aspects of the pathophysiology of neurodegenerative diseases. Further investigations of the regulation of PLD by α-synuclein could provide valuable insights into the role of these proteins play in normal and pathological conditions.

To investigate this issue, we examined the regulation of PLD by α-synuclein in HEK 293 cells overexpressing α-synuclein. Pervanadate or PMA-stimulated PLD activation was decreased in cells overexpressing α-synuclein, compared with that of vector-transfected cells. Cells overexpressing $Ala^{53} \rightarrow Thr$ (A53T) and $Ala^{30} \rightarrow Pro$ (A30P) mutant α-synuclein, which have been associated with familial forms of PD, showed greater inhibition of PLD than vector-transfected cells. By immunoprecipitation and Western blot analysis using an anti-PLD antibody, the HEK 293 cells were found to express similar levels of ~120-kDa PLD1 protein. However, the 105-kDa PLD2 protein was not detected in any of the cell lines, indicating that the PLD activity shown in these cells is due to mainly to PLD1. Using *in vitro* studies, α-synuclein has been reported to inhibit PLD2 activity more potently than PLD1 activity (20). However, we found that in co-transfection experiments, α-synuclein inhibited pervanadate-stimulated PLD activity. This suggests that α-synuclein can inhibit both forms of PLD. The ability of α-synuclein to inhibit PLD1 in cells might reflect differences between *in vitro* and *in vivo* environments. Recently, α-synuclein was reported to inhibit PKC activity in HEK 293 cells (15), which could contribute to the inhibition of PLD activity. Inhibition of PKC by α-synuclein could contribute to the decrease in pervanadate-induced PLD activation in cells overexpressing α-synuclein. However, it is possible that this inhibition might also result from a direct interaction between

PLD and α-synuclein. Here we demonstrated that α-synuclein is constitutively associated with PLD1 in cells, and α-synuclein forms a triple complex with PLD and PKCα in a ligand-independent manner. The association between α-synuclein and PKC is consistent with prior results observed by Ostrerova and colleagues (15). We also demonstrated that α-synuclein associates with PLD2 in co-transfected cells. We found that α-synuclein co-immunoprecipitated with endogeneous PLD from rat brain tissue and is co-localized with PLD in neurons in the substantia nigra pars compacta of rat brain, indicating that these two proteins interact *in vivo*. The PLD1 binding site in α-synuclein resides in the amino acid residues 1–95 containing 6 or 7 conserved repeats with the consensus core sequence KTKEGV.

α-Synuclein has been shown to interact with phospholipids. This interaction is also facilitated mainly by a conserved NH_2-terminal 95 residues, which changes its structure from "unfolded" to α-helical upon binding to lipids (12). Because of α-synucleins ability to interact with lipids and their association with synaptic vesicles, it has been suggested that synucleins might be involved in intracellular vesicular trafficking (43). Tau interacts with the acidic COOH-terminal region (residues 89–140) of α-synuclein through its microtubule-binding domain. This opens the possibility that α-synuclein might have a bridging functions that might serve to bring different classes of ligands together. α-Synuclein binds to a region between amino acids 1 and 331 of PLD1. This region contains the NH_2-terminal pleckstrin homology and phox domains, which are known to be involved in protein-protein interaction as well as binding of phospholipids (44). The interaction sites of PLD2 with α-synuclein showed similar patterns as with PLD1 (data not shown). α-Synuclein did not affect the activity of PLC and other lipid-modifying enzymes and did not associate with PLC-β1 in cells overexpressing α-synuclein, suggesting that the effect of α-synuclein on PLD is specific.

Protein-tyrosine phosphorylation is thought to be important in regulating synaptic function and plasticity (45, 46). It was reported recently that α-synuclein can be tyrosine-phosphorylated by the Src family tyrosine kinase in a co-transfection experiment and *in vitro* using purified kinases (37). This tyrosine phosphorylation occurs primarily on tyrosine 125. It is difficult to speculate on the functional consequences of tyrosine phosphorylation of α-synuclein, because its normal function has not been elucidated definitively. The putative role of α-synuclein in regulating intracellular vesicular trafficking and signaling appears particularly interesting. Mice lacking α-synuclein show abnormal dopamine release (47). α-Synuclein exists in the cytoplasm in presynaptic neurons, but is also loosely associated with synaptic vesicles (48). Covalent modification, such as phosphorylation, is a likely candidate for regulation of α-synuclein at the synapse, and covalent modification could be important in modulating its function. Although the functional consequences of phosphorylation of the tyrosine 125 residue of α-synuclein remain to be elucidated, tyrosine phosphorylation could regulate the ability of α-synuclein to bind synaptic vesicles and thereby regulate protein-protein interactions. Here we demonstrate that the phosphorylation state of tyrosine 125 of α-synuclein modulates the activity of PLD. A mutation Tyr^{125} to Phe in α-synuclein (Y125F) that mimics dephosphorylation increases the ability of α-synuclein to inhibit pervanadate-induced PLD activation. This regulatory axis could affect exocytosis, because PLD is thought to be an important component of the exocytotic machinery (49).

The discovery of abnormal protein aggregates or accumulation has been described in a number of neurodegenerative diseases. We tried to investigate that the interaction between α-synuclein and PLD isozymes has a role in inclusion body formation in PD. Recently, it was reported that when constructs encoding portions of α-synuclein and synphilin-1 are co-transfected in mammalian cells, the cells formed eosinophilic cytosolic inclusions resembling the Lewy bodies of PD (16). Although α-synuclein aggregates by itself *in vitro*, it may be that aggregation *in vivo* is facilitated by an associated protein such as synphilin-1. When constructs encoding synphilin-1 and full-length α-synuclein or the non-Aβ component AD amyloid (NAC) portion of α-synuclein were co-transfected, we observed that ~6% of cells had cytosolic phase-dense inclusions. Cytosolic inclusions were eosinophilic when stained with H & E. In contrast, when constructs encoding PLD isozyme (PLD1 or PLD2) were co-transfected along with α-synuclein or NAC, only ~1–2% of cells had eosinophilic inclusions, which is similar to that present in control cells. Thus, our data suggest that PLD isozymes may not modulate α-synuclein aggregation.

In summary, our study suggests that α-synuclein modulates the activity of PLD by protein-protein interactions, but this interaction might not be involved in regulation of the formation of cytoplasmic inclusion bodies in mammalian cells. However, we cannot rule out the possibility that PLD does modulate α-synuclein aggregation in the brain, because the environment of HEK 293 cells differs from that of the aged human brain. Although the function of both α-synuclein and PLD remains largely unknown, identification of binding partners and examination of how and where the complexes form in the cell provide important tools for understanding the physiology of PD.

Acknowledgments—We thank Dr. Sung Ho Ryu for providing the GST-PLD expression vector, Dr. C. A. Ross for providing cDNA encoding synphilin-1, Dr. Robert L. Nussbaum for providing cDNA encoding mutant α-synuclein (Y125F), and Dr. John H. Exton for helpful comments in the preparation of this manuscript.

REFERENCES

1. Dickson, D. W. (2001) *Curr. Opin. Neurol.* **14,** 423–432
2. Goedert, M. (2001) *Nat. Rev. Neurosci.* **2,** 492–501
3. Baba, M., Nakajo, S., Tu, P. H., Tomita, T., Nakaya, K., Lee, V. M., Trojanowski, J. Q., and Iwatsubo, T. (1998) *Am. J. Pathol.* **152,** 879–884
4. Spillantini, M. G., Schmidt, M. L., Lee, V. M., Trojanowski, J. Q., Jakes, R., and Goedert, M. (1997) *Nature* **388,** 839–840
5. Spillantini, M. G., Growther, R. A., Jakes, R., Hasegawa, M., and Goedert, M. (1998) *Proc. Natl. Acad. Sci. U. S. A.* **95,** 6469–6473
6. Tu, P. H., Galvin, J. E., Baba, M., Giasson, B., Tomita, T., leight, S., Nakajo, S., Iwatsubo, T., Trojanowski, J. Q., and Lee, V. M. (1998) *Ann. Neurol.* **44,** 415–422
7. Dickson, D. W., Liu, W., Hardy, J., Farrer, M., Mehta, N., Uitti, R., Mark, M., Zimmerman, T., Golbe, L., Sage, J., Sima, A., D'Amato, C., Albin, R., Gilman, S., and Yen, S. H. (1999) *Am. J. Pathol.* **155,** 1241–1251
8. Polymeropoulus, M. H., Lavedan, C., Leroy, E., Ide, S. E., Dehejia, A., Dutra, A., Pike, B., Root, H., Rubenstein, J., Boyer, R., Stenroos, E. S., Chandrasekharappa, S., Athanassiadou, A., Papapetropolous, T., Johnson, W. G., Lazzarini, A. M., Duvoisin, R. C., Di Iorio, G., Golbe, L. I., and Nussbaum, R. L. (1997) *Science* **276,** 2045–2047
9. Kruger, R., Kuhn, W., Muller, T., Woitalla, D., Graeber, M., Kosel, S., Przunt, H., Epplen, J. T., Schols, L., and Riess, O. (1998) *Nat. Genet.* **18,** 106–108
10. Feany, M. B., and Bender, W. W. (2000) *Nature* **202,** 394–398
11. Masliah, E., Rockenstein, E., Veinbergs, I., Mallory, M., Hashimoto, M., Takeda, A., Sagara, Y., Sisk, A., and Mucke, L. (2000) *Science* **287,** 1265–1269
12. Davidson, W. S., Jonas, A., Clayton, D. F., and George, J. M. (1998) *J. Biol. Chem.* **273,** 9443–9449
13. Weinreb, P. H., Zhen, W., Poon, A. W., Conway, K. A., and Lansbury, P. T. J. (1996) *Biochemstry* **35,** 13709–13715
14. Jensen, P. H., Hager, H., Nielsen, M., Hojrup, P., Gliemann, J., and Jakes, R. (1999) *J. Biol. Chem.* **274,** 25481–25489
15. Ostrerova, N., Petrucelli, L., Farrer, M., Mehta, N., Choi, P., Hardy, J., and Wolozin, B. (1999) *J. Neurosci.* **19,** 5782–5791
16. Engelender, S., Kaminsky, Z., Guo, X., Sharp, A. H., Amaravi, R. K., Kleiderlein, J. J., Margolis, R. L., Troncoso, J. C., Lanahan, A. A., Worley, P. F., Dawson, V. L., Dawson, T. M., and Ross, C. A. (1999) *Nat. Genet.* **22,** 110–114
17. Iwata, A., Miura, S., Kanazawa, I., Sawada, M., and Nukina, N. (2001) *J. Neurochem.* **72,** 239–252
18. Ghee, M., Fournier, A., and Mallet, J. (2000) *J. Neurochem.* **75,** 2221–2224
19. Clayton, D. F., and George, J. M. (1999) *J. Neurosci. Res.* **58,** 120–129
20. Jenco, J. M., Rawlingson, A., Daniels, B., and Morris, A. J. (1998) *Biochemistry* **37,** 4901–4909
21. Hammond, S. M., Jenco, J. M., Nakashima, S., Cadwallader, K., Gu, Q-M., Cook, S., Nozawa, Y., Prestwich, G. D., Frohman, M. A., and Morris, A. J.

(1997) *J. Biol. Chem.* **272,** 3860–3868
22. Colley, W. C., Sung, R., Jenco, R. L., Hammond, S. M., Altshuller, Y., Bar-Sagi, D., Morris, A. J., and Frohman, M. A. (1997) *Curr. Biol.* **7,** 191–201
23. Min, D. S., Park, S. K., and Exton, J. H. (1998) *J. Biol. Chem.* **273,** 7044–7051
24. Sung, T. C., Zhang, Y., Morris, A. J., and Frohman, M. A. (1999) *J. Biol. Chem.* **274,** 3659–3666
25. Exton, J. H. (1997) *Physiol. Rev.* **77,** 303–320
26. Klein, J., Chalifa, V., Liscovitch, M., and Loffelholz, K. (1995) *J. Neurochem.* **6,** 1445–1455
27. Min, D. S., Ahn, B.-H., Rhie, D.-J., Yoon, S.-H., Hahn, S. J., Kim, M.-S., and Jo, Y-H. (2001) *Neuropharmacology* **41,** 384–391
28. Lee, M.-Y., Jo, Y.-H., Chun, M.-H., Chung, J.-W., Kim, M.-S., and Min, D. S. (2000) *Brain Res.* **864,** 52–59
29. Lee, C., Kim, S. R., Chung, J. K., Frohman, M. A., Kilimann, M. W., and Rhee, S. G. (2000) *J. Biol. Chem.* **275,** 18751–18758
30. Bradford, M. M. (1976) *Anal. Biochem.* **72,** 248–254
31. Bligh, E. G., and Dyer, W. J. (1959) *Can. J. Biochem. Physiol.* **37,** 911–917
32. David, L. S., Robert, D. G., and Leslie, A. L. (1998) *Cells: A Laboratory Manual*, pp. 98.6–98.13, Cold Spring Harbor Laboratory Press, Cold Spring Harbor, NY
33. Huyer, G., Liu, S., Kelly, J., Moffat, J., Payette, P., Kennedy, B., Tsaprailis, G., Gresser, M. J., and Ramachandran, C. (1997) *J. Biol. Chem.* **272,** 843–851
34. Min, D. S., Kim, E.-G., and Exton, J. H. (1998) *J. Biol. Chem.* **273,** 29986–29994
35. Rumenapp, U., Schmidt, M., Olesch, S., Ott, S., Eichel-Streiber, C. V., and Jakobs, K. H. (1998) *Biochem. J.* **334,** 625–631
36. Le Stunff, H., Dokhac, L., Harbon, S. (2000) *J. Pharmacol. Exp. Ther.* **292,** 629–637
37. Ellis, C. E., Schwartzberg, P. L., Grider, T. L., Fink, D. W., and Nussbaum, R. L. (2001) *J. Biol. Chem.* **276,** 3879–3884
38. Maroteaux, L., and Scheller, R. H. (1991) *Brain Res. Mol. Brain Res.* **11,** 335–343
39. Kholodilov, N. G., Neystat, M., Oo, T. F., Lo, S. E., Larsen, K. E., Sulzer, D., and Burke, R. E. (1999) *J. Neurochem.* **73,** 2586–2599
40. Forno, L. S. (1996) *J. Neuropathol. Exp. Neurol.* **55,** 259–272
41. Silva, H. R., Khan, N. L., and Wood, N. W. (2000) *Curr. Opin. Genet. Dev.* **10,** 292–298
42. Kanfer, J. N., Singh, I. N., Pettegrew, J. W., McCartney, D. G., and Sorrentino, G. (1996) *J. Lipid Mediat. Cell Signal.* **14,** 361–363
43. Lavedan, C. (1998) *Genome Res.* **8,** 871–880
44. Xu, Y., Seet, L.-F., Hanson, B., and Hong, W. (2001) *Biochem. J.* **360,** 513–530
45. Gurd, J. W. (1997) *Neurochem. Int.* **31,** 645–649
46. O'Dell, T. J., Kandel, E. R., and Grant, S. G. (1991) *Nature* **353,** 558–560
47. Abeliovich, A., Schmitz, Y., Farinas, I., Choi-Lundberg, D., Ho, W. H., Castillo, P. E., Shinsky, N., Verdugo, J. M., Armanini, M., Ryan, A., Hynes, M., Phillips, H., Sulzer, D., and Rosenthal, A. (2000) *Neuron* **25,** 239–252
48. Iwai, A., Yoshimoto, M., Masliah, E., and Saitoh, T. (1995) *Biochemistry* **34,** 10139–10145
49. Vitale, N., Caumont, A-S., Chasserot-Golaz, S., Du, G., Wu, S., Sciorra, V. A., Morris, A. J., Frohman, M. A., and Bader M-F. (2001) *EMBO J.* **20,** 2424–2434

Available online at www.sciencedirect.com
SCIENCE DIRECT
Molecular Brain Research 117 (2003) 179–189
MOLECULAR BRAIN RESEARCH
www.elsevier.com/locate/molbrainres

Research report

SEPT5_v2 is a parkin-binding protein

P. Choi[a,1], H. Snyder[a,1], L. Petrucelli[b], C. Theisler[a], M. Chong[a], Y. Zhang[c], K. Lim[c], K.K.K. Chung[c], K. Kehoe[c], L. D'Adamio[d], J.M. Lee[a], E. Cochran[e], R. Bowser[f], T.M. Dawson[c], B. Wolozin[a,*]

[a]*Department of Pharmacology, Loyola University Medical Center, Bldg. 102/3634, 2160 S. 1st Ave., Maywood, IL 60153, USA*
[b]*Department of Pharmacology, Mayo Clinic, Jacksonville, FL, USA*
[c]*Department of Neurology and Neuroscience, Johns Hopkins Medical Center, Baltimore, MD, USA*
[d]*Department of Microbiology and Immunology, Albert Einstein College of Medicine, The Bronx, NY, USA*
[e]*Department of Pathology, St. Lukes-Rush-Presbyterian Medical Center, Chicago, IL, USA*
[f]*Department of Pathology, University of Pittsburgh, Pittsburgh, PA, USA*

Accepted 24 June 2003

Abstract

Mutations in parkin are associated with various inherited forms of Parkinson's disease (PD). Parkin is a ubiquitin ligase enzyme that catalyzes the covalent attachment of ubiquitin moieties onto substrate proteins destined for proteasomal degradation. The substrates of parkin-mediated ubiquitination have yet to be completely identified. Using a yeast two-hybrid screen, we isolated the septin, human SEPT5_v2 (also known as cell division control-related protein 2), as a putative parkin-binding protein. SEPT5_v2 is highly homologous to another septin, SEPT5, which was recently identified as a target for parkin-mediated ubiquitination. SEPT5_v2 binds to parkin at the amino terminus and in the ring finger domains. Several lines of evidence have validated the putative link between parkin and SEPT5_v2. Parkin co-precipitates with SEPT5_v2 from human substantia nigra lysates. Parkin ubiquitinates SEPT5_v2 in vitro, and both SEPT5_v1 and SEPT5_v2 accumulate in brains of patients with ARJP, suggesting that parkin is essential for the normal metabolism of these proteins. These findings suggest that an important relationship exists between parkin and septins.

Theme: Disorders of the nervous system

Topic: Degenerative disease: Parkinson's

Keywords: Ubiquitination; Parkinson's disease; Lewy body; Ubiquitin proteasomal system; Autosomal recessive juvenile Parkinsonism; Substantia nigra; Dopamine; Dopaminergic neuron

1. Introduction

Parkinson's disease (PD) is the most common neurodegenerative movement disorder [21]. It is characterized by a classic group of symptoms: rigidity, resting state tremor, bradykinesia, and postural instability. Death of dopaminergic neurons in the substantia nigra with resultant severe dopamine depletion in the neostriatum is believed to underlie the motor symptoms of PD [21]. The cause of this neuronal degeneration is unknown. Recently, several genes have been identified to be associated with familial parkinsonism: α-synuclein, ubiquitin carboxy-terminal hydrolase L1 (UCH-L1), DJ-1, Nurr1 and parkin [3,10,18,20,22,25,29]. Mutations in α-synuclein (A53T and A30P) are associated with rare cases of autosomal dominant parkinsonism [20,29]. An I93M missense mutation in the ubiquitin C-terminal hydrolase, UCH-L1, a thiol protease deubiquitinating enzyme, has been identified in a German family with a history of familial PD [23]. Mutations in

Abbreviations: ARJP, autosomal recessive Juvenile Parkinsonism; PD, Parkinson's disease; SEPT5, cdc-rel1, cell division control-related protein 1; SEPT5_v2, SEPT5_v2, cell division control-related protein 2; UbcH, ubiquitin conjugating enzyme

*Corresponding author. Tel.: +1-708-216-6195; fax: +1-708-216-6596.
E-mail address: bwolozi@lumc.edu (B. Wolozin).
[1]Co-equal authors.

0169-328X/03/$ – see front matter
doi:10.1016/S0169-328X(03)00318-8

DJ-1 are associated with an early onset, autosomal recessive form of PD, while parkin is associated with autosomal recessive juvenile parkinsonism (ARJP) [3,18]. Mutations in Nurr1, an orphan nuclear receptor that is essential for the development of dopamine neurons, are associated with familial PD [22]. The most common mutations associated with Parkinsonism are mutations in *parkin*, including deletion and point mutations, which occur in many families affected by ARJP. The association of mutations in *parkin* with ARJP implicates *parkin* mutations in the etiology of familial parkinsonism [1,24,25]. In the most comprehensive genetic study to date by Lücking et al., 36 of 73 (49%) families with histories of early onset PD all had mutations in *parkin* that segregated with the disease [25]. In addition, mutations in parkin have also been recently linked to forms of adult-onset parkinsonism clinically indistinguishable from sporadic, non-inherited PD [8,19]. Thus, mutations in *parkin* are by far the most prevalent cause of inherited PD discovered to date.

The parkin structure contains a C-terminal RING-IBR-RING construct and an N-terminal region with homology to ubiquitin [18,31]. Recently, parkin was shown to possess ubiquitin ligase (E3) activity that catalyzes the covalent attachment of ubiquitin onto proteins targeted for degradation by the 26S proteasome [14,31,35]. Ubiquitination of proteins is thought to occur by action of a complex that includes E3 ligases, such as parkin, and ubiquitin conjugating enzymes (termed either UbcH or E2). Nine human UbcH enzymes have been identified to date, and parkin has been shown to associate with UbcH7 and UbcH8, via the RING-IBR-RING domain of parkin. Intense research has focused on identifying proteins that bind parkin and are ubiquitinated by parkin. Several parkin-binding proteins have been identified to date: cell division control-related protein 1, α-synuclein, Pael-R, Synphilin-1 and CHIP [6,13,14,32,36]. SEPT5 is a member of the septin family of proteins, which have roles in exocytosis and cell division [2]. Other septins include Nedd5, H5, Diff6, and SEPT5_v2 [2,17]. Wild-type parkin, but not mutant or truncated forms of parkin, increases SEPT5_v1 turnover in vitro, suggesting a central role of parkin in SEPT5_v1 regulation [36]. Parkin has also been shown to control the turnover of SEPT5_v1 and the Pael receptor (Pael-R) [14,36]. The interaction of parkin with CHIP suggests that it operates in the endoplasmic reticulum as part of the unfolded protein response [13,15]. We now report the identification of another parkin-binding protein, SEPT5_v2. Parkin ubiquitinates SEPT5_v2, and SEPT5_v2 steady state levels are increased in brains of patients with ARJP or in cells lacking parkin.

2. Materials and methods

2.1. Human brain samples

Post-mortem brain tissues were obtained from the Loyola University Chicago Brain Bank and from the Rush University Brain Bank. Paraffin-embedded tissues used for immunohistochemical analyses were treated with 10% buffered formalin. Human substantia nigra sections from PD cases and age-matched, neurologically normal controls were examined in this study. The ages and post-mortem interval of all the brains used are shown in Table 1. The mean ages and PMI of the control brains were 73.5±5.7 years and 7.6±1.8 h, while the means ages and post-mortem interval of the PD brains were 68.4±1.4 years and 7.0±1.1 h.

Paraffin-embedded brain sections were deparaffinized by incubation at 65 °C for 45 min. Sections were subsequently treated with three changes in xylene, 10 min each, then 3 min each in 100% ethanol, 95% ethanol, and 70% ethanol. Sections were then washed for 5 min in ddH_2O, placed in fresh ddH_2O, and autoclaved for 15 min at 121 °C. After slides cooled to room temperature, they were washed in 0.05 M PBS, pH 7.4, for 20 min, blocked in 10% FBS/PBS for 20 min, and incubated at 4 °C overnight in primary antibodies. This was followed by three 10-min washes in PBS, incubation with Cy2- and Cy3-tagged fluorescent antibodies (Jackson Immuno.) for 3 h at room temperature, and three 10-min washes in PBS. Slides were then dehydrated through ethanol, mounted with Depex, and cover-slipped.

2.2. Immunoblotting

For immunoblot analyses, protein gel loading buffer was added to 30 μg of total protein lysate per lane and resolved by 12% polyacrylamide gel electrophoresis. Protein bands were transferred to nitrocellulose matrix (Gibco/BRL) at 4 °C, 250 mA, for 10 h. Following blocking in 5% milk/tris-buffered saline plus 0.01% triton X-100 for 1 h at room temperature, blots were incubated with primary antibody overnight at 4 °C. Blots were then washed three times, 10 min each in tris-buffered saline plus 0.01% triton X-100, and incubated in biotinylated secondary antibody for 3 h at room temperature, washed again, and developed by chemiluminescence (DuPont).

Table 1
Brain samples

Case	PMI	Age	Sex	Diagnosis
1	5	64	M	Control
2	10.5	64	F	Control
3	11	79	F	Control
4	4	87	M	Control
5	5	64	F	PD
6	6	68	M	PD
7	4.5	72	M	PD
8	10	67	F	PD
9	9.5	71	M	PD
10	10	65 (17)		ARJP exon 3 deletion
11	18	62 (24)		ARJP exon 4 deletion
12	9	52 (14)		ARJP exon 4 deletion
13	10	68 (33)		ARJP exon 3 deletion

2.3. Antibodies

Park-1 polyclonal antibody (Southwest Immunology) was raised in goat, against an immunogen that corresponds to amino acids 83–97 of the N-terminus of the human parkin protein. Park-2 polyclonal antibody (Chemicon) was raised in rabbit, against an immunogen that corresponds to amino acids 305–323 of the human parkin protein. Park-3 polyclonal antibody was also raised in rabbit, against an immunogen corresponding to amino acids 391–405 of the parkin protein. Park-4 polyclonal antibody was raised against an epitope around amino acid 400 of parkin (Cell Signaling, no epitope sequence supplied). SP20 is a monoclonal antibody that recognizes SEPT5. Anti-α-actin monoclonal antibody (ICN) was used as an internal loading control in Western blot analyses. The anti-c-Myc antibody 9E10 was from Roche. Dilutions were done in tris-buffered saline plus 0.01% triton X-100+5% bovine serum albumin (Sigma). Dilutions: Park-1—1:300 for immunohistochemistry, and 1:5000 for immunoblotting; Park-2—1:1000 for immunohistochemistry; Park-3—1:500 for immunoblotting, and 1:200 for immunoprecipitation; Park-4—1:1500 for immunoblotting; SP20—1:10 for immunohistochemistry, and 1:100 for immunoblotting; anti-α-actin—1:2000 for immunoblotting; 9E10—1:1000 for immunoblotting, 1:200 for immunoprecipitation.

2.4. Plasmids

Wild-type and mutant parkin were cloned into pcDNA3 at the EcoRI/XbaI sites. Myc-parkin was generated by adding a myc epitope by PCR, and inserted into pcDNA3 at the EcoRI/NotI sites. SEPT5_v2a and myc-SEPT5_v2a were cloned into pcDNA3 at the XhoI/NotI sites. For production of recombinant SEPT5_v2a, the cDNA was also cloned into the proEX vector at the BamHI/SpeI sites, and purified with nickel agarose chromatography. UbcH7 and 8 were cloned into the pET3a vector. HA-Ubiquitin was obtained from Cecile Pickart (Johns Hopkins, Baltimore, MD, USA) and was cloned into the pMT123 vector. The parkin deletion constructs were in pRK5 and designed as described previously [36].

2.5. Cell culture

BE-M17 human neuroblastoma cells were maintained in Optimem (Gibco/BRL)+10% fetal bovine serum. SH-SY5Y human neuroblastoma cells were maintained in a 1:1 mixture of Ham's F12:EMEM (Gibco/BRL)+10% fetal bovine serum. Transfections were performed with Fugene (Roche) with 1 μg DNA+6 μl Fugene per ml in Optimem.

2.6. Immunoprecipitation

For immunoprecipitation experiments, approximately 2×10^6 cells were plated into sterile 10-cm Falcon dishes and grown to ≈80% confluence. Cells were harvested by trituration followed by low-speed centrifugation. Pellets were resuspended in lysis solution consisting of ice-cold 1% Triton-X in Tris-buffered saline, pH 7.4, with protease inhibitors (Sigma) and dismembranated via sonication. Protein concentration was determined by the BCA assay (Pierce). 500 μg of protein from each sample was diluted to a final volume of 1 ml in lysis solution. 25 μl protein A (Sigma) was added to pre-clear non-specific binding proteins, 1 h, 4 °C. Samples were centrifuged and supernatants were transferred to new sterile microcentrifuge tubes. 4 μg of primary antibody were added to each sample, followed by a 3-h shaking incubation at 4 °C. 30 μl protein A were then added to each sample and binding to immune complexes was performed by 2 h incubation at 4 °C with gentle agitation. Negative control consisted of 4 μg non-specific IgG plus control brain lysate and protein A. Samples were washed/centrifuged four times in ice-cold lysis solution. After final washing and centrifugation, samples were resuspended in protein loading buffer, heat denatured at 90 °C for 5 min, centrifuged again, and resolved by 12% polyacrylamide gel electrophoresis, 85 V, 90 min. Immunoblots were performed as detailed above.

2.7. Yeast two-hybrid

Assays were performed according to the manufacturer's protocol, using the Matchmaker (Clontech) LexA system. The cDNA library used for screening bait/prey interactions was derived from human brain, and consisted of 3.5×10^6 independent clones. We performed an interaction trap assay using parkin as the bait. Full-length parkin (465 amino acids; bait A), the amino-terminal 133 amino acids (bait B), the carboxy-terminal 332 amino acids (bait C), and the amino-terminal 257 amino acids (bait D) were cloned into plasmid pEG202 in-frame with the LexA DNA-binding domain. Two different reporter genes were used in the LexA system: one was a yeast Leu2 derivative and the other was the bacterial lacZ gene that encodes β-galactosidase and offers a quantitative method of measuring interactions. The LEU2 reporter is stably incorporated into the yeast strain, and has its normal regulatory sequences replaced by six LexA operator sequences. The lacZ reporter was introduced into the yeast strain on a plasmid (pSH18-34) and is also regulated by multiple upstream LexA operators.

2.8. In vitro ubiquitination

Constructs coding for myc-Parkin or myc-SEPT5_v2a were transfected into 293 cells, and immunoprecipitated from 4 mg of lysates with 4 μl 9E10 antibody and 50 μl of agarose coupled protein G. 7 μl of each immunoprecipitate was mixed with 100 ng E1 (Sigma), 200 ng Ubch7 (Affinity), and 5 μg ubiquitin (Sigma) in 50 μl buffer (50 mM Tris HCl pH 7.5, 10 mM DTT, 2 mM $MgCl_2$ and 4

mM ATP). The mixture was incubated for 1 h and then immunoblotted.

3. Results

3.1. Parkin binds to SEPT5_v2

We utilized the LexA yeast two-hybrid system to screen a human brain cDNA library for binding partners of parkin. We isolated positive clones coding for the septin, SEPT5_v2, in both splice variants, rel2a and rel2b (Fig. 1A, SEPT5_v2A shown). These clones collectively encoded sequences at the N-terminus of rel2a from amino acid 1 to 304, and the N-terminus of rel2b from amino acid 1 to 295, in multiple, in-frame overlapping prey cDNA hybrids, indicating that these amino acids mediate the parkin–SEPT5_v2 association. The amino terminus of

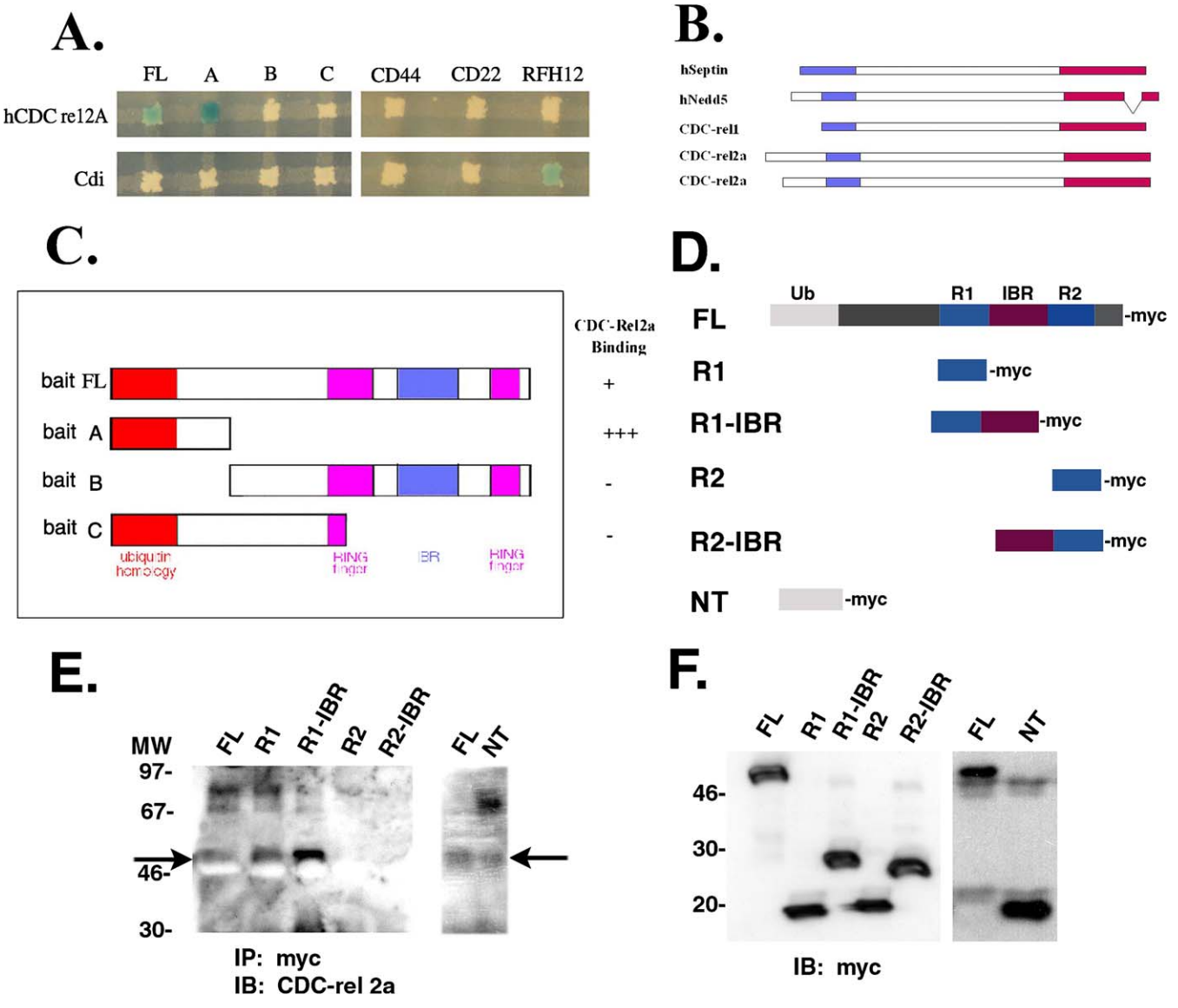

Fig. 1. (A) Yeast mating assay showing interaction between parkin and SEPT5_v2a. Blue represents a positive interaction. CDI is a control that should only interact with the RFH12 protein, thus demonstrating specificity for the assay. FL, full length parkin. (A, B, C) Parkin constructs shown below. CD44, CD22, and RFH12 are constructs that are not expected to interact with parkin, and act as negative controls. (B) Structure of septins. The structures of SEPT5_v2a, SEPT5_v2b, and SEPT5, are shown in relation to some other well-known septins, such as Septin, and Nedd5. Homologous regions are represented by the same color. Adapted from Kartmann and Roth [16]. (C) Structure of yeast parkin-binding constructs, and amount of binding to SEPT5_v2 on the right. (D) Structure of mammalian parkin deletion constructs. Myc-tagged constructs containing full-length parkin (FL), the R1 RING finger domain (R1), the R1 RING finger domain plus the 'In Between RING' finger domain (R1-IBR), the R2 RING finger domain (R2), the R2 RING finger domain plus the 'In Between RING' finger domain (R2-IBR), and the N-terminal ubiquitin homology domain (NT). (E) Co-immunoprecipitation of SEPT5_v2a with myc-tagged parkin deletion constructs. Left panel: SEPT5_v2a (arrow) co-immunoprecipitated with full-length parkin, the R1 RING finger domain and the R1 RING finger domain plus the 'In Between RING' finger domain (R1-IBR). Right panel: SEPT5_v2a (arrow) co-immunoprecipitated with full-length parkin (FL), the N-terminal ubiquitin domain (NT). (F) Immunoblots validating expression of the parkin deletion constructs in the HEK 293 cell lysates used for the immunoprecipitation in (E).

SEPT5_v2 shows minimal homology to other septins, including SEPT5_v1 (Fig. 1B). SEPT5_v2a and b are splice variants, with SEPT5_v2b lacking the first 19 amino acids of SEPT5_v2a (Fig. 1B). Interestingly, in the case of SEPT5, it is the carboxy terminal of parkin that associates with the carboxy terminal of SEPT5_v1 [36]. All further experiments were performed using the LexA yeast two-hybrid system and SEPT5_v2a as the interacting protein.

To understand better the nature of the interaction between parkin and SEPT5_v2, we generated a construct containing full-length parkin, and constructs of parkin truncated at either the amino or carboxy terminal (Fig. 1C). Yeast two-hybrid mating assays were subsequently performed to map the area of parkin responsible for SEPT5_v2a binding. SEPT5_v2a bound to full-length parkin and an amino terminal construct, but not a construct lacking the amino terminus (Fig. 1A and C). This suggests that the ubiquitin homology portion of parkin interacts with SEPT5_v2. Interestingly, no binding was seen to construct C that contained the amino two-thirds of parkin, possibly because of the altered conformation of this construct or inhibition of binding by downstream domains of parkin (Fig. 1C).

3.2. SEPT5_v2a binds to parkin at two sites in mammalian cells

Previous studies with SEPT5, a close homologue of SEPT5_v2a, showed binding to the carboxy region of parkin [36]. Because of the close homology between the two proteins, we examined the association of SEPT5_v2a with domains of parkin previously shown to bind SEPT5_v1, including the RING-IBR domains (Fig. 1C). Based on the yeast two-hybrid data suggesting binding of SEPT5_v2a to a domain near the amino terminus of parkin, we also designed a construct containing only the amino-terminal ubiquitin homology domain, and examined binding of SEPT5_v2a to this domain (Fig. 1C). HEK 293 cells were co-transfected with constructs coding for SEPT5_v2a and myc-tagged parkin deletion constructs corresponding to the amino or carboxy domains of parkin (Fig. 1D and E) [36]. We observed that SEPT5_v2a bound to full-length parkin, as well as parkin deletion constructs containing either the amino domain of parkin or the R1 RING finger (Fig. 1D and E). Binding of SEPT5_v2a to the R1 RING finger domain is consistent with prior studies showing that SEPT5_v1 binds to the R2 RING finger domain [36]. In addition, we observed that SEPT5_v2a binds to the amino domain of parkin, which contains the ubiquitin homology domain. Binding of SEPT5_v2a to the amino region of parkin concurs with the yeast two-hybrid studies, which also showed binding of this region. This indicates that both SEPT5_v1 and SEPT5_v2a associate with the RING finger domains, with SEPT5_v1 binding to the R2 domain and SEPT5_v2a binding to the R1 domain [36].

Although binding to the amino domain and the R1-IBR-R2 domain of parkin show binding to SEPT5_v2 in both the yeast two-hybrid assay and in mammalian cell immunoprecipitation assay, the two assays differ quantitatively in the amount of binding observed (Fig. 1C and E). One reason for the difference might result from the use of different parkin domains in the yeast two-hybrid study and the immunoprecipitation study. One discrepancy lies in the parkin R1-IBR-R2 domain. A construct containing the parkin R1-IBR-R2 domain showed no association with SEPT5_v2a in the yeast two-hybrid study, while a construct containing only the R1-IBR domain showed strong binding in the immunoprecipitation assay (Fig. 1C and E). The absence of an association in the yeast two-hybrid assay might derive from inhibition of SEPT5_v2 binding to parkin by the R2 domain when it is present. This hypothesis could explain why the immunoprecipitation assay showed no binding to a construct containing only the IBR-R2 domain and weak binding to full-length parkin (Fig. 1C and E). Binding to the parkin amino domain also showed a quantitative difference between the yeast two-hybrid assay and the immunoprecipitation assay. This difference could be due to differences in the size of the two constructs (Fig. 1D and F). The parkin amino domain construct used for the yeast two-hybrid studies was longer than that used for the immunoprecipitation studies (Fig. 1D and F). Binding of SEPT5_v2 close to the junction region between the ubiquitin homology domain and the rest of parkin could render it sensitive to interference from the anti-myc antibody used for the immunoprecipitation assay (Fig. 1C and E). Conversely, the increased length of the amino domain yeast two-hybrid construct might prevent interference with SEPT5_v2 binding.

3.3. SEPT5_v2a binds to parkin in human brain lysates

To validate our yeast two-hybrid analysis results, we investigated whether parkin interacts with SEPT5_v2 in human brain. SEPT5_v2a co-precipitated with parkin from human substantia nigra lysates (Fig. 2). Sepharose-coupled anti-parkin antibody P391 was used to immunoprecipitate parkin, and the immunoprecipitate was then immunoblotted with anti-SEPT5_v2a (Fig. 2, upper panel). As a negative control, the lysates were immunoprecipitated with sepharose coupled to non-specific IgG (Fig. 2, upper panel, lane 7). Nigral lysates from both control (Fig. 2, lanes 1–3) and PD (Fig. 2, lanes 4–6) cases were used in the immunoprecipitations to examine whether disease-associated differences in parkin-SEPT5_v2 binding exist. Immunoprecipitation revealed a single band migrating at the expected molecular weight of 52 kDa (Fig. 2). Although significant enrichment of SEPT5_v2a was observed by immunoprecipitation of parkin, indicative of high-affinity binding, there was no significant difference in the amount of co-precipitated rel2a between PD and control brains (Fig. 2). The amount of SEPT5_v2a in the lysates was also immunoblotted (Fig. 2, lower panel). The PD nigral lysates showed a trend toward greater SEPT5_v2a levels in PD than control lysates, but this difference did not reach

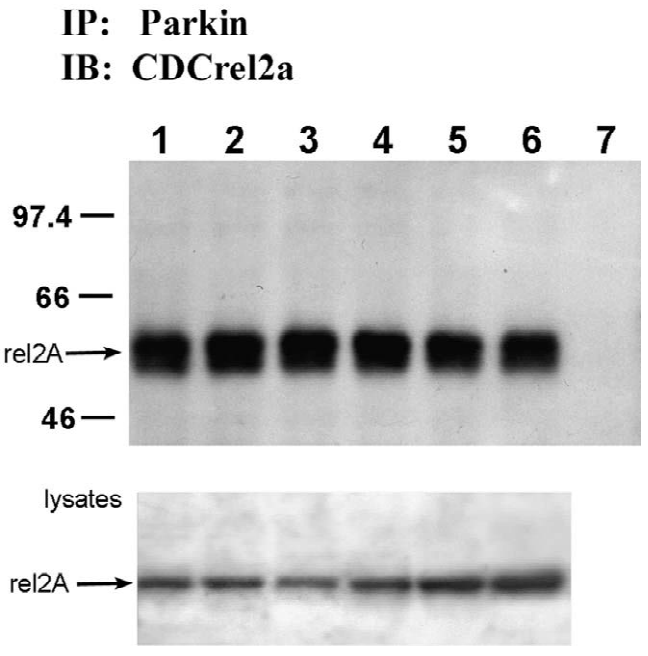

Fig. 2. Co-precipitation of SEPT5_v2a along with parkin from substantia nigra lysates. Sepharose-coupled anti-parkin antibody P391 was used to immunoprecipitate parkin. Immunoblotting the precipitate with the anti-SEPT5_v2a antibody revealed one band at 52 kDa, which is the expected molecular weight of SEPT5_v2a. The top panel shows the immunoprecipitate, while the bottom panel shows an immunoblot of the lysates with anti-SEPT5_v2a. Lanes 1–3 correspond to substantia nigra from three different control donors. Lanes 4–6 correspond to substantia nigra from three different PD donors. Lane 7 is an immunoprecipitation using non-specific rabbit IgG.

statistical significance ($P<0.1$, $N=9$ PD, 10 Control). Immunocytochemical experiments failed to detect any SEPT5_v2a in Lewy bodies (data not shown). The co-immunoprecipitation of parkin and SEPT5_v2a indicates that parkin associates with SEPT5_v2a in human brain tissue, and validates the yeast two-hybrid results.

3.4. Parkin levels affect levels of SEPT5_v2a

The association of SEPT5_v2a with parkin raises the possibility that the degradation of SEPT5_v2a is mediated by parkin. To investigate this, HEK 293 cells were transfected with plasmids coding for sense or anti-sense parkin plus SEPT5_v2a, HA-tagged ubiquitin and UbcH8. Three days following transfection, the cells were incubated with MG132 for 4 h to block proteasomal degradation. The cells were lysed, and centrifuged to separate soluble and insoluble material. Levels of SEPT5_v2a in both the pellet and supernatant were observed to vary with parkin levels. Cell pellets were immunoblotted with antibodies against HA (identifying ubiquitin), SEPT5_v2a, parkin or actin (Fig. 3A and B). Parkin expression was high in cells transfected with parkin cDNA and low in cells transfected with parkin anti-sense cDNA (Fig. 3A, bottom left panel). HA-ubiquitin immunoreactivity paralleled parkin expression (Fig. 3A, top left panel). The level of SEPT5_v2a was inversely related to parkin expression, and was low in cells transfected with parkin cDNA and high in cells transfected with parkin anti-sense cDNA (Fig. 3B, left panel). Finally, immunoblotting with anti-actin antibody showed that protein expression was similar in each lane (Fig. 3B, right panel).

3.5. Parkin ubiquitinates SEPT5_v2a

Next we examined whether SEPT5_v2a was ubiquitinated by parkin. To determine whether parkin was able to ubiquitinate SEPT5_v2a, we used an in vitro ubiquitination assay, similar to that used for the analysis of ubiquitination of Pael-R [14]. For the in vitro ubiquitination assay, HEK 293 cells were transfected cells with either myc-SEPT5_v2a or myc-parkin. After 48 h, the cells were harvested, and the myc-tagged proteins (SEPT5_v2a or parkin) were immunoprecipitated from the lysates. The parkin and SEPT5_v2a were then combined together along with recombinant UbcH8 and HA-ubiquitin, as well as ATP and buffer. Following 1 h of incubation, the mixture was immunoblotted with either anti-ubiquitin to detect ubiquitinated proteins or anti-SEPT5_v2a. SEPT5_v2a that had been incubated with parkin showed the presence of higher molecular weight bands, suggesting that it had been ubiquitinated. The anti-ubiquitin immunoblot showed increased levels of high molecular weight ubiquitin conjugates in lanes containing the SEPT5_v2a (Fig. 4A). Omission of parkin eliminated the high molecular weight bands seen with the SEPT5_v2a or ubiquitin antibodies, and omission of SEPT5_v2a eliminated all reactivity seen with anti-SEPT5_v2a and reduced the high molecular weight ubiquitin conjugated proteins. Omission of SEPT5_v2a would not have been expected to eliminate the high molecular weight ubiquitin proteins because parkin auto-ubiquitinates. In a parallel experiment, we performed in vitro ubiquitination and immunoblotted with antibody to SEPT5_v2a. High molecular weight bands were apparent only in the lanes containing SEPT5_v2a, parkin and other requisite reagents (Fig. 4B). Omission of SEPT5_v2a, parkin, Ubch8, or ubiquitin+E1 eliminated the bands. Quantification of the in vitro ubiquitination reactions is shown in Fig. 4C and D. These data suggest that parkin can ubiquitinate SEPT5_v2a.

3.6. Levels of SEPT5_v1 and SEPT5_v2a are increased in brains from patients with ARJP

The ability of parkin to modulate the ubiquitination and turnover of SEPT5_v2a in cell culture suggests that parkin might also regulate turnover of SEPT5_v2a in the brain. To investigate this question, we examined the levels of SEPT5_v2a in brains of patients who died with ARJP. Lysates were obtained from frontal cortex of ARJP brains ($N=4$), and age-matched control brains ($N=5$). Frontal

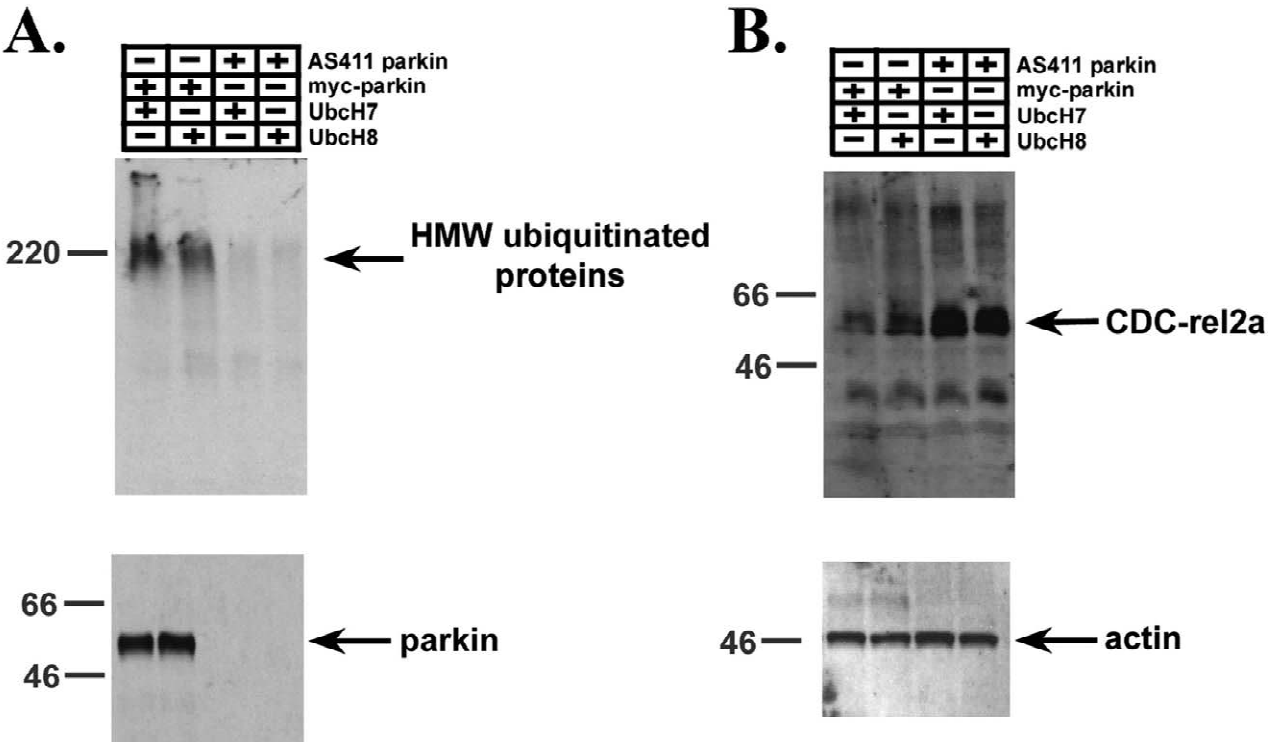

Fig. 3. (A, B) HEK 293 cells were transfected with SEPT5_v2a, parkin (sense or antisense), HA-ubiquitin and UbcH8. Two days after transfection, the cells were harvested and the lysates immunoblotted. (A) The top panel shows immunoblotting with anti-HA (recognizing ubiquitin), and the bottom panel shows immunoblotting with anti-parkin. Ubiquitination paralleled parkin expression. (B) In the same samples, immunoblots were performed with anti-SEPT5_v2a (top panel) and actin (bottom panel). Although the amount of protein did not vary, decreased parkin expression corresponded to increased SEPT5_v2a expression.

cortex was used because of the limited availability of substantia nigra from ARJP. We felt that analysis of cortical tissue in ARJP might be informative because parkin is expressed throughout the brain. Based on this distribution, loss of parkin might be expected to affect areas other than the substantia nigra, even though pathology (in the form of cell loss) is most severe in the substantia nigra. Consistent with this hypothesis, we observed that the levels of SEPT5_v2a were increased in brains from ARJP donors, although no change was seen in levels of actin (Fig. 5, top panel). Because SEPT5_v1 has also been shown to associate with parkin, we examined whether levels of SEPT5_v1 protein were increased in ARJP brain. We observed that SEPT5_v1 was also increased in three out of four cases of ARJP brain that were examined (Fig. 5, middle panel). No significant differences in actin were observed among the samples (Fig. 5, lower panel). These data suggest that parkin regulates the turnover of both SEPT5_v1 and SEPT5_v2a in vivo.

4. Discussion

Parkin is an E3 ligase, but its substrates are only beginning to be identified. Recently, SEPT5_v1 was shown to bind parkin and have its catabolism regulated by parkin [36]. The protein SEPT5_v2a is a member of the septin family of proteins, and is a close homologue of SEPT5_v1 [9]. We have now shown that parkin also binds SEPT5_v2a, ubiquitinates SEPT5_v2a, and can modulate the levels of SEPT5_v2a in cells. We also observe that levels of both SEPT5_v1 and SEPT5_v2a are increased in the brains of patients with ARJP. Septins are small proteins that can have GTPase activity and appear to function in membrane transport and exocytosis [2,9,26]. The ability of parkin to bind both SEPT5_v1 and SEPT5_v2 suggests a biochemical link between septins and parkin, although the functional consequences of the putative interaction between parkin and SEPT5_v1 proteins remain to be determined.

4.1. Parkin binds to specific domains on SEPT5_v2

Parkin appears to bind SEPT5_v2a at two different regions within the protein, the N-terminal ubiquitin-homology domain and the R1 RING finger domain. The RING finger domains appear to be important for binding and ubiquitination of ligase substrates. For instance, SEPT5, Synphilin-1 and Pael-R bind the R2 RING finger domain, and Tau all bind the R2-IBR domain [6,14,27,36]. In our experiments, we observed different binding patterns depending on whether we examined binding by yeast two-

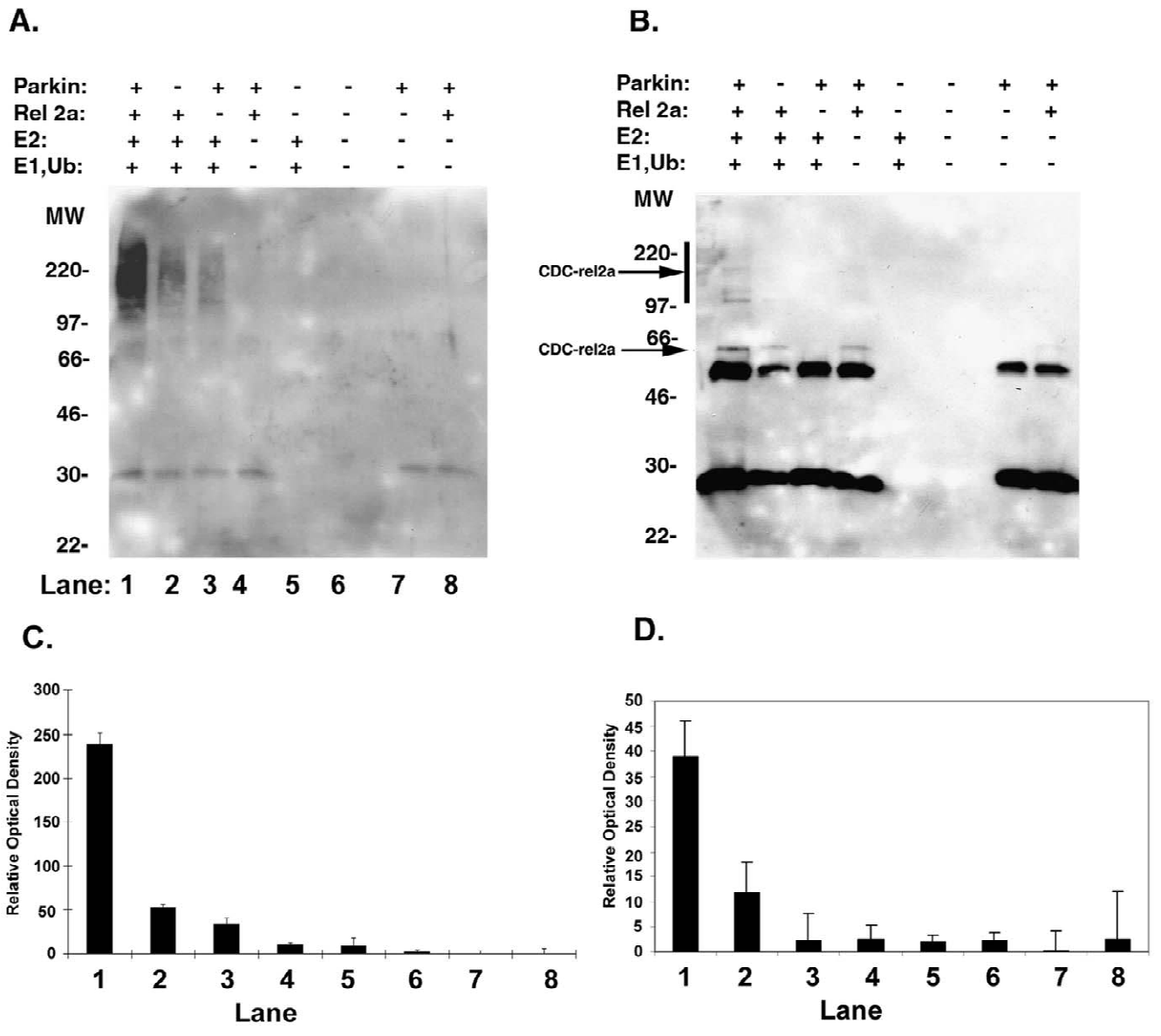

Fig. 4. In vitro ubiquitination of SEPT5_v2a by parkin. HEK cells were transfected with either myc-tagged SEPT5_v2a or myc-tagged parkin. The SEPT5_v2a and parkin were immunoprecipitated, combined, an in vitro ubiquitination was performed and the product was immunoblotted for anti-ubiquitin (A) or anti-SEPT5_v2a (B). High molecular weight bands positive for both ubiquitin and SEPT5_v2a were present in samples of SEPT5_v2a that had been co-transfected with parkin, suggesting that parkin lead to ubiquitination of SEPT5_v2a. Omission of any of the reaction components eliminated the ubiquitination. The prominent bands at 25 and 50 kDa represent the heavy and light chains of the anti-myc antibody used to immunoprecipitate the parkin and SEPT5_v2a proteins. Quantification of the in vitro ubiquitination for both ubiquitin reactivity and high molecular weight SEPT5_v2a reactivity is shown in panels (C) and (D), respectively ($n=3$).

hybrid analysis or by immunoprecipitation from mammalian cells. Binding in the yeast occurs only with the full-length construct or a construct containing only the N-terminal ubiquitin binding domain. Binding in mammalian cells is detected with constructs coding for either the N-terminal ubiquitin binding domain or constructs containing the RING1-IBR domain. Because other parkin substrates bind to the RING-IBR domains, the immunoprecipitation experiments appear more likely to reflect the true association that occurs in mammals. Several studies show that the RING-IBR-RING domain is required for ubiquitin ligase activity, which suggests that binding of SEPT5_v2 to this region is important for the ability of parkin to ubiquitinate the protein [36].

The N-terminal ubiquitin homology domains of ligases are important for the binding of ligases to other proteins in the ubiquitin proteasomal cascade. For instance, the ubiquitin homology domain is important for binding of ligases to proteasomal proteins [33]. The N-terminal ubiquitin homology domain of parkin also appears to be required for parkin function because mutations in this domain block the ubiquitin ligase activity of parkin, and

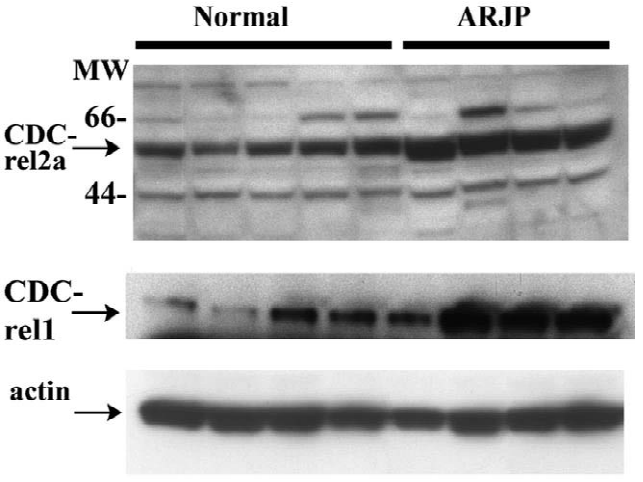

Fig. 5. Levels of SEPT5_v1 and SEPT5_v2 are increased in brains of patients with ARJP. Samples of cortex from cases of ARJP and age-matched controls were immunoblotted with anti-SEPT5_v2a (top panel), SP20 (middle panel), or anti-actin (bottom panel). Although the levels of actin were constant among the samples, the levels of SEPT5_v1 and 2a were increased in the ARJP brains.

are associated with ARJP [1,31,36]. By binding to the ubiquitin homology domain of parkin, SEPT5_v2a could modulate the association of parkin with other proteins or cellular organelles, such as the proteasome.

4.2. Parkin and disease

One of the critical tests of whether a protein is a substrate of parkin is determining whether loss of parkin function increases the steady state level of the protein. The levels of several parkin substrates, including glycosylated α-synuclein, synphilin-1 and Pael-R, are all increased in brains from ARJP donors [6,14,32]. We observed a similar phenomenon for both SEPT5_v1 and SEPT5_v2. Brains from subjects with ARJP show increased levels of SEPT5_v1 and SEPT5_v2 compared to controls, although SEPT5_v1 was increased in only three out of four ARJP brains examined. Unfortunately, insufficient knowledge is available to determine how elevated levels of SEPT5_v1 and SEPT5_v2 might contribute to the pathophysiology of ARJP.

Although mutations in parkin are associated with ARJP, parkin also appears to contribute to the pathophysiology of PD. Some parkin mutations are also associated with familial forms of PD that are indistinguishable from sporadic PD [1]. In addition, parkin accumulates in Lewy bodies [4,5,30]. The mechanism by which parkin accumulates in Lewy bodies is unknown, but could derive from the association of parkin with other proteins that accumulate in Lewy bodies. Shimura and colleagues observed that parkin associates with α-synuclein, but they observed that parkin only binds and ubiquitinates a glycosylated form of α-synuclein that represents only about 1% of the total α-synuclein pool [32]. Parkin also binds to other proteins that are present in LB, such as synphilin and cytochrome *c* [7,11]. Synphilin was recently shown to also bind and be a substrate for parkin [6]. Binding of parkin to α-synuclein and synphilin raises the possibility that parkin might appear in Lewy bodies due to its binding to synuclein and synphilin. In this context, it is interesting that we did not detect SEPT5_v2a in Lewy bodies (data not shown). The reason for the absence of SEPT5_v2a in Lewy bodies could simply result from antibodies that are not sufficiently sensitive to detect the protein in Lewy bodies. A recent study by Ihara and colleagues did identify septins in Lewy bodies [12]. This observation is consistent with a previous study showing the association of septins with inclusions in neurodegenerative diseases, because prior studies have identified the septins Nedd5, diff6 and H5 in neurofibrillary tangles in Alzheimer's disease [17]. These observations add septins to the list of proteins affected by the pathophysiology of PD.

Increasing evidence suggests that parkin might serve a neuroprotective function in the brain. As an ubiquitin ligase, parkin could promote the degradation of proteins that have been damaged by oxidation or other events that might denature the proteins. Studies show that parkin associates with a multi-protein complex that handles such denatured proteins [15]. Other studies show that over-expressing parkin protects against toxicity induced by α-synuclein in cell culture or in Drosophila [28,34]. Parkin also suppresses the toxicity of the Pael receptor, which is toxic when over-expressed and is present in elevated levels in subjects with ARJP [14,34]. The ability of septins to associate with particular vesicles suggests that they could function to target parkin to particular organelles, which could be important for controlling the proteins with which parkin associates [2]. Although we do not know whether SEPT5_v2 modulates parkin-mediated neuroprotection, the importance of parkin in neuroprotection suggests that this is an important line for further investigation.

References

[1] N. Abbas, C. Lücking, S. Ricard, A. Dürr, V. Bonifati, G. De Michele, S. Bouley, J. Vaughan, T. Gasser, R. Marconi, E. Broussolle, C. Brefel-Courbon, B. Harhangi, B. Oostra, E. Fabrizio, G. Böhme, L. Pradier, N. Wood, A. Filla, G. Meco, P. Denefle, Y. Agid, A. Brice, A wide variety of mutations in the parkin gene are responsible for autosomal recessive parkinsonism in Europe, Hum. Mol. Genet. 8 (1999) 567–574.

[2] C.L. Beites, H. Xie, R. Bowser, W.S. Trimble, The septin CDCrel-1 binds syntaxin and inhibits exocytosis, Nat. Neurosci. 2 (1999) 434–439.

[3] V. Bonifati, P. Rizzu, M.J. van Baren, O. Schaap, G.J. Breedveld, E. Krieger, M.C. Dekker, F. Squitieri, P. Ibanez, M. Joosse, J.W. van Dongen, N. Vanacore, J.C. van Swieten, A. Brice, G. Meco, C.M. van Duijn, B.A. Oostra, P. Heutink, Mutations in the DJ-1 gene associated with autosomal recessive early-onset parkinsonism, Science 299 (2003) 256–259.

[4] P. Choi, N. Golts, H. Snyder, L. Petrucelli, M. Chong, J. Hardy, D.

Sparkman, E. Cochran, J. Lee, B. Wolozin, Co-association of parkin and α-synuclein, NeuroReport 12 (2001) 2839–2844.
[5] P. Choi, N. Ostrerova-Golts, D. Sparkman, E. Cochran, J. Lee, B. Wolozin, Parkin is metabolized by the ubiquitin/proteosomal system, NeuroReport 11 (2000) 2635–2638.
[6] K. Chung, Y. Zhang, K. Lim, Y. Tanaka, H. Huang, J. Gao, C. Ross, V. Dawson, T. Dawson, Parkin ubiquitinates the α-synuclein-interacting protein, Synphilin-1: implications for Lewy body formation in Parkinson's disease, Nature Med. 7 (2001) 1144–1150.
[7] S. Engelender, Z. Kaminsky, X. Guo, A. Sharp, R. Amaravi, J. Kleiderlein, R. Margolis, J. Troncoso, A. Lanahan, P. Worley, V. Dawson, T. Dawson, C. Ross, Synphilin-1 associates with alpha-synuclein and promotes the formation of cytosolic inclusions, Nat. Genet. 22 (1999) 110–114.
[8] M. Farrer, P. Chan, R. Chen, L. Tan, S. Lincoln, D. Hernandez, L. Forno, K. Gwinn-Hardy, L. Petrucelli, J. Hussey, A. Singleton, C. Tanner, J. Hardy, J.W. Langston, Lewy bodies and parkinsonism in families with parkin mutations, Ann. Neurol. 50 (2001) 293–300.
[9] C.M. Field, D. Kellogg, Septins: cytoskeletal polymers or signalling GTPases?, Trends Cell Biol. 9 (1999) 387–394.
[10] B.S. Harhangi, M.J. Farrer, S. Lincoln, V. Bonifati, G. Meco, G. De Michele, A. Brice, A. Durr, M. Martinez, T. Gasser, B. Bereznai, J.R. Vaughan, N.W. Wood, J. Hardy, B.A. Oostra, M.M. Breteler, The Ile93Met mutation in the ubiquitin carboxy-terminal-hydrolase-L1 gene is not observed in European cases with familial Parkinson's disease, Neurosci. Lett. 270 (1999) 1–4.
[11] M. Hashimoto, A. Takeda, L. Hsu, T. Takenouchi, E. Masliah, Role of cytochrome *c* as a stimulator of α-synuclein aggregation in Lewy body disease, J. Biol. Chem. 274 (1999) 28849–28852.
[12] M. Ihara, H. Tomimoto, H. Kitayama, Y. Morioka, I. Akiguchi, H. Shibasaki, M. Noda, M. Kinoshita, Association of the cytoskeletal GTP-binding protein Sept4/H5 with cytoplasmic inclusions found in Parkinson's disease and other synucleinopathies, J. Biol. Chem. (2003).
[13] Y. Imai, M. Soda, S. Hatakeyama, T. Akagi, T. Hashikawa, K.I. Nakayama, R. Takahashi, CHIP is associated with Parkin, a gene responsible for familial Parkinson's disease, and enhances its ubiquitin ligase activity, Mol. Cell 10 (2002) 55–67.
[14] Y. Imai, M. Soda, H. Inoue, N. Hattori, Y. Mizuno, Y. Takahashi, An unfolded putative transmembrane polypeptide, which can lead to endoplasmic reticulum stress, is a substrate of parkin, Cell 105 (2001) 891–902.
[15] Y. Imai, M. Soda, R. Takahashi, Parkin suppresses unfolded protein stress-induced cell death through its E3 ubiquitin-protein ligase activity, J. Biol. Chem. 275 (2000) 35661–35664.
[16] B. Kartmann, D. Roth, Novel roles for mammalian septins: from vesicle trafficking to oncogenesis, J. Cell Sci. 114 (2001) 839–844.
[17] A. Kinoshita, M. Kinoshita, H. Akiyama, H. Tomimoto, I. Akiguchi, S. Kumar, M. Noda, J. Kimura, Identification of septins in neurofibrillary tangles in Alzheimer's disease, Am. J. Pathol. 153 (1998) 1551–1560.
[18] T. Kitada, S. Asakawa, N. Hattori, H. Matsumine, Y. Yamamura, S. Minoshima, M. Yokochi, Y. Mizuno, N. Shimizu, Mutations in the parkin gene cause autosomal recessive juvenile parkinsonism, Nature 392 (1998) 605–608.
[19] C. Klein, P.P. Pramstaller, B. Kis, C.C. Page, M. Kann, J. Leung, H. Woodward, C.C. Castellan, M. Scherer, P. Vieregge, X.O. Breakefield, P.L. Kramer, L.J. Ozelius, Parkin deletions in a family with adult-onset, tremor-dominant parkinsonism: expanding the phenotype, Ann. Neurol. 48 (2000) 65–71.
[20] R. Kruger, W. Kuhn, T. Muller, D. Woitalla, M. Graeber, S. Kosel, H. Przuntek, J. Epplen, L. Schols, O. Riess, Ala30Pro mutation in the gene encoding α-synuclein in Parkinson's disease, Nat. Genet. 18 (1998) 106–108.
[21] A. Lang, A. Lozano, Parkinson's disease, New Engl. J. Med. 339 (1998) 1044–1053.
[22] W.D. Le, P. Xu, J. Jankovic, H. Jiang, S.H. Appel, R.G. Smith, D.K. Vassilatis, Mutations in NR4A2 associated with familial Parkinson disease, Nat. Genet. 33 (2003) 85–89.
[23] E. Leroy, R. Boyer, G. Auburger, B. Leube, G. Ulm, E. Mezey, G. Harta, M. Brownstein, S. Jonnalagada, T. Chernova, A. Dehejia, C. Lavedan, T. Gasser, P. Steinbach, K. Wilkinson, M. Polymeropoulos, The ubiquitin pathway in Parkinson's disease, Nature 395 (1998) 451–452.
[24] C.B. Lucking, N. Abbas, A. Durr, V. Bonifati, A. Bonnet, T. de Broucker, G. De Michele, N.W. Wood, Y. Agid, A. Brice, Homozygous deletions in parkin gene in European and North African families with autosomal recessive juvenile parkinsonism, Lancet 352 (1999) 1355–1356.
[25] C.B. Lucking, A. Durr, V. Bonifati, J. Vaughan, G. De Michele, T. Gasser, B.S. Harhangi, P. Pollak, A.M. Bonnet, D. Nichol, M. DeMari, R. Marconi, E. Broussolle, O. Rascol, M. Rosier, I. Arnould, B.A. Oostr, M. Breteler, A. Filla, G. Meco, P. Denefle, N.W. Wood, Y. Agid, A. Brice, Association between early-onset parkinson's disease and mutations in the parkin gene, New Engl. J. Med. 342 (2000) 1560–1567.
[26] I.G. Macara, R. Baldarelli, C.M. Field, M. Glotzer, Y. Hayashi, S.C. Hsu, M.B. Kennedy, M. Kinoshita, M. Longtine, C. Low, L.J. Maltais, L. McKenzie, T.J. Mitchison, T. Nishikawa, M. Noda, E.M. Petty, M. Peifer, J.R. Pringle, P.J. Robinson, D. Roth, S.E. Russell, H. Stuhlmann, M. Tanaka, T. Tanaka, W.S. Trimble, J. Ware, N.J. Zeleznik-Le, B. Zieger, Mammalian septins nomenclature, Mol. Biol. Cell 13 (2002) 4111–4113.
[27] L. Petrucelli, K. Kehoe, Y. Tsuboi, T. Ishizawa, D. Dickson, R. Ved, J. Lewis, E. McGowan, G. Gonzalez-de-Chavez, P. Lockhart, C. O'Farrell, D. Hernandez, M. Van Slegtenhorst, M. Cookson, J. Lee, E. Cochran, P. Choi, M. Farrer, N. Hattori, Y. Mizuno, K. Chung, K. Lim, Y. Zhang, T. Dawson, J. Hardy, M. Hutton, B. Wolozin, Tau is a target for the E3 ligase activity of CHIP and parkin (submitted for publication).
[28] L. Petrucelli, C. O'Farrell, P.J. Lockhart, M. Baptista, K. Kehoe, L. Vink, P. Choi, B. Wolozin, M. Farrer, J. Hardy, M.R. Cookson, Parkin protects against the toxicity associated with mutant alpha-synuclein: proteasome dysfunction selectively affects catecholaminergic neurons, Neuron 36 (2002) 1007–1019.
[29] M.H. Polymeropoulos, C. Lavedan, E. Leroy, S.E. Ide, A. Dehejia, A. Dutra, B. Pike, H. Root, J. Rubenstein, R. Boyer, E.S. Stenroos, S. Chandrasekharappa, A. Athanassiadou, T. Papapetropoulos, W.G. Johnson, A.M. Lazzarini, R.C. Duvoisin, G. Di Iorio, L.I. Golbe, R.L. Nussbaum, Mutation in the alpha-synuclein gene identified in families with Parkinson's disease, Science 276 (1997) 2045–2047.
[30] M.G. Schlossmacher, M.P. Frosch, W.P. Gai, M. Medina, N. Sharma, L. Forno, T. Ochiishi, H. Shimura, R. Sharon, N. Hattori, J.W. Langston, Y. Mizuno, B.T. Hyman, D.J. Selkoe, K.S. Kosik, Parkin localizes to the lewy bodies of Parkinson disease and dementia with lewy bodies, Am. J. Pathol. 160 (2002) 1655–1667.
[31] H. Shimura, N. Hattori, S. Kubo, Y. Mizuno, S. Asakawa, S. Minoshima, N. Shimizu, K. Iwai, T. Chiba, K. Tanaka, T. Suzuki, Familial parkinson disease gene product, parkin, is a ubiquitin-protein ligase, Nat. Genet. 25 (2000) 302–305.
[32] H. Shimura, M.G. Schlossmacher, N. Hattori, M.P. Frosch, A. Trockenbacher, R. Schneider, Y. Mizuno, K.S. Kosik, D.J. Selkoe, Ubiquitination of a new form of alpha-synuclein by parkin from human brain: implications for Parkinson's disease, Science 293 (2001) 263–269.
[33] K.J. Walters, M.F. Kleijnen, A.M. Goh, G. Wagner, P.M. Howley, Structural studies of the interaction between ubiquitin family proteins and proteasome subunit S5a, Biochemistry 41 (2002) 1767–1777.
[34] Y. Yang, I. Nishimura, Y. Imai, R. Takahashi, B. Lu, Parkin suppresses dopaminergic neuron-selective neurotoxicity induced by Pael-R in Drosophila, Neuron 37 (2003) 911–924.
[35] D.M. Zhang, D. Levitan, G. Yu, M. Nishimura, F. Chen, A. Tandon, T. Kawarai, S. Arawaka, A. Supala, Y.Q. Song, E. Rogaeva, Y.

Liang, E. Holmes, P. Milman, C. Sato, L. Zhang, P. St George-Hyslop, Mutation of the conserved N-terminal cysteine (Cys92) of human presenilin 1 causes increased A beta42 secretion in mammalian cells but impaired Notch/lin-12 signalling in *C. elegans*, Neuroreport 11 (2000) 3227–3230.

[36] Y. Zhang, J. Gao, K.K. Chung, H. Huang, V.L. Dawson, T.M. Dawson, Parkin functions as an E2-dependent ubiquitin-protein ligase and promotes the degradation of the synaptic vesicle-associated protein, CDCrel-1, Proc. Natl. Acad. Sci. USA 97 (2000) 13354–13359.

Available online at www.sciencedirect.com

SCIENCE DIRECT

Experimental Neurology 192 (2005) 274–287

Experimental Neurology

www.elsevier.com/locate/yexnr

Tau phosphorylation increases in symptomatic mice overexpressing A30P α-synuclein

M. Frasier[a], M. Walzer[a,b], L. McCarthy[a], D. Magnuson[b], J.M. Lee[b], C. Haas[c], P. Kahle[c], B. Wolozin[a,*]

[a]*Department of Pharmacology, Loyola University Medical Center, Maywood, IL, United States*
[b]*Department of Pathology, Loyola University Medical Center, Maywood, IL, United States*
[c]*University of Munich, Germany*

Received 10 May 2004; revised 2 July 2004; accepted 21 July 2004
Available online 1 October 2004

Abstract

Mice overexpressing mutant α-synuclein develop a progressive loss of motor function associated with the accumulation of aggregated α-synuclein in neurons of the brainstem. Recent reports suggest that tau pathology might also be associated with Parkinson disease (PD) and aggregation of α-synuclein. We now report that mice overexpressing A30P α-synuclein develop abnormally phosphorylated tau in parallel with the accumulation of aggregated α-synuclein. Enhanced phosphorylation of tau occurs only in symptomatic mice that also harbor abundant aggregated α-synuclein. The increased phosphorylation of tau occurs at S396/404 and S202 as shown by immunoblotting and immunocytochemical studies with the antibodies PHF-1 and AT8. Neurons that accumulated α-synuclein occurred in the dorsal brainstem and did not show strong colocalization with neurons that showed abnormal tau phosphorylation, which largely occurred in the ventral brainstem. Aggregation of α-synuclein and phosphorylation of tau are associated with increased levels of phosphorylated c-jun kinase (JNK), which is a stress kinase known to phosphorylate tau protein. These results suggest that α-synuclein pathology can stimulate early pathological changes in tau.

Keywords: Aggregation; Parkinson disease; Lewy body; JNK; c-jun Kinase; GSK-3β; CDK5; Astrocytosis; Fibrillization

Introduction

The protein α-synuclein appears to play an important role in the pathophysiology of Parkinson disease (PD). Lewy bodies are a pathological hallmark of PD that are composed primarily of α-synuclein (Spillantini et al., 1997; Spillantini et al., 1998b). α-Synuclein is thought to play a critical role in the pathophysiology of PD because it accumulates in Lewy bodies and because genetic studies identified mutations in α-synuclein that are associated with familial PD (Kruger et al., 1998; Polymeropoulos et al., 1997; Singleton et al., 2003; Spillantini et al., 1998b; Zarranz et al., 2004). The A53T and A30P α-synuclein appear to be causative in PD by increasing the tendency of α-synuclein to aggregate. The mutations both increase the tendency of α-synuclein to aggregate spontaneously or in response to exogenous factors, such as metals and oxidative stress (Conway et al., 2000; Hashimoto et al., 1999; Kruger et al., 1998; Ostrerova-Golts et al., 2000; Paik et al., 1999, 2000; Polymeropoulos et al., 1997). The A53T and A30P mutations in α-synuclein also cause age-dependent α-synuclein aggregation and neuronal injury in transgenic mice and *Drosophila* (Feany and Bender, 2000; Giasson et al., 2002; Kahle et al., 2001; Masliah et al., 2000). These results emphasize the relevance of α-synuclein to the study of neurodegeneration.

α-Synuclein appears to have pleitropic actions. The α-synuclein protein contains regions of homology with the

* Corresponding author. Department of Pharmacology, Loyola University Medical Center, Building 102/3634, 2160 S. 1st Avenue, Maywood, IL 60153. Fax: +1 708 216 6596.
E-mail address: bwolozi@lumc.edu (B. Wolozin).

0014-4886/$ - see front matter © 2004 Elsevier Inc. All rights reserved.
doi:10.1016/j.expneurol.2004.07.016

protein chaperone 14-3-3, displays functions resembling a chaperone, and also binds many proteins recognized by 14-3-3 as well as other proteins (Ostrerova et al., 1999; Souza et al., 2000). The proteins bound by α-synuclein include 14-3-3, protein kinase C, phospholipase C δ, extracellular regulated kinase, synphilin-1, tyrosine hydroxylase, the dopamine transporter, SEPT4, and the S6′ proteasomal protein (Choi et al., 2001; Engelender et al., 1999; Ihara et al., 2003; Jenco et al., 1998; Lee et al., 2001a; Ostrerova et al., 1999; Perez et al., 2002; Pronin et al., 2000; Sharon et al., 2001; Snyder et al., 2003). α-Synuclein shows avid binding to lipids, and functional studies suggest that α-synuclein plays a role in vesicular exocytosis (Murphy et al., 2000; Sharon et al., 2001). However, the relationship between α-synuclein function and its role in neurodegeneration remain unclear.

The microtubule-associated protein tau is another protein implicated in the pathophysiology of many neurodegenerative diseases. Tau aggregation is a prominent feature in many diseases, including Alzheimer disease and frontotemporal dementias (Lee et al., 2001b). Increasing evidence suggests that many disorders exhibit both tau and α-synuclein aggregation. Tau and α-synuclein pathology both occur in Alzheimer disease, PD, Guam–Parkinson–ALS dementia complex, and PD caused by mutations α-synuclein (Duda et al., 2002; Forman et al., 2002; Ishizawa et al., 2003). Abnormal phosphorylated tau is present in Lewy bodies found in sporadic PD patients and occurs in neurons near areas containing α-synuclein pathology (Ishizawa et al., 2003). In vitro evidence also links α-synuclein and tau as α-synuclein binds tau in vitro, and stimulates tau phosphorylation by protein kinase A in vitro (Giasson et al., 2003; Jensen et al., 1999). Recent results indicate that α-synuclein enhances tau fibrillization in vitro and that abnormal tau fibrils are present in the brains of symptomatic transgenic mice overexpressing mutant A53T synuclein (Giasson et al., 2003). However, the mechanism by which tau and α-synuclein fibrillization might occur in the same diseases is poorly understood.

We set out to investigate whether A30P α-synuclein aggregation occurs alongside tau pathology and to explore potential mechanisms by which α-synuclein aggregation might occur in parallel with tau pathology in transgenic mice overexpressing A30P α-synuclein (Kahle et al., 2001). We report that symptomatic A30P α-synuclein transgenic mice exhibit abnormal tau phosphorylation and that the phosphorylation correlates with activation of a c-jun kinase.

Materials and methods

Animals

The human [A30P] α-synuclein transgene had been injected in hybrid B6/DBA oocytes (Kahle et al., 2000). Founders were extensively (7–10 generations) back-crossed into a C57Bl/6 background. Intercrossing of the highest expressing line 31 yielded a stable colony of homozygous 31H mice (Neumann et al., 2002). These were the animals used in the present study. The mice develop symptoms between 6 and 14 months. The symptoms begin with a tremor and progress to an end-stage phenotype characterized by muscular rigidity, postural instability, and ultimately, paralysis. Mice that progressed to end-stage symptoms were sacrificed by cervical dislocation, and their brains were hemisectioned. The right hemisphere was fixed in formalin and subsequently embedded in paraffin for immunohistochemistry. The left hemisphere was flash-frozen in methyl-2-butane and kept at −80°C for immunoblot analysis. Asymptomatic A30P α-synuclein transgenic mice were age-matched littermates (therefore from the same line as the transgenic A30P α-synuclein symptomatic mice) and were sacrificed at the same time. Nontransgenic control mice were C57Bl/6 mice and were also sacrificed at the same time as the symptomatic transgenic mice.

Antibodies and immunohistochemistry

Brains were sagittally sectioned at a thickness of 4 μm and mounted on Superfrost-plus slides (Fisher Scientific). Distinct monoclonal phospho-specific tau antibodies AT8 (Pierce Endogen, 1:200, Ser 199, 202, Thr 205) and PHF-1 (generously provided by P. Davies, 1:200, Ser 396, 404) were used to detect phosphorylated tau epitopes. Antibodies against α-synuclein included a mouse monoclonal anti-α-synuclein antibody directed against the N-terminus (Immunoblot: Transduction Labs: 1:1000, immunohistochemistry: Zymed, 1:100) and a rabbit polyclonal antibody directed against amino acids 116–131 (used for immunohistochemistry, 1:500) (Ostrerova-Golts et al., 2000). Other antibodies used were: anti-glial fibrillary acidic protein (Dako, 1:500), rabbit polyclonal anti-phospho CDK5 antibody (Tyr15) (Santa Cruz Biotechnology, Santa Cruz, CA, 1:50), anti-phospho-GSK-3β (Serine-9) (Santa Cruz Biotechnology, 1:500), anti-phospho-GSK-3α/β (Tyr216) (BioSource, 1:200), anti-phospho-SAPK/JNK (Thr183/Tyr185) G9 monoclonal antibody (Cell Signaling, 1:1000), and rabbit polyclonal anti-ubiquitin antibody (Dako, 1:500). Immunofluorescence was performed using the same antibody concentrations as above. For immunofluorescence, sections were first treated with 70% formic acid at room temperature for 15 min, rinsed in PBS for 10 min, and then blocked for 20 min in 2% fetal bovine serum and 1% normal goat serum in PBS at room temperature. Primary antibody was incubated on the sections overnight at 4°C and followed by two 10-min washes in PBS. Fluorescent cy2 anti-mouse (1:2500) and rhodamine anti-rabbit (1:200) secondary antibodies (Jackson Immunology) were incubated on the sections for 1 h at room temperature in the dark. Following two more 10-min washes in PBS, coverslips were applied using the Fluormount G mounting media (Electron Microscopy Sciences, Washington, PA).

Brain tissue extraction

Brain tissue extraction was performed as previously described by Sahara et al. (2002) with minor modifications. Left hemibrains were weighed and homogenized in three volumes of TBS (TBS, pH 7.4, 1 mM EDTA, 5 mM sodium pyrophosphate, 30 mM glycerol 2-phosphate, 30 mM sodium fluoride, 1 mM EDTA) containing a protease inhibitor cocktail (Sigma-Aldrich). Protein content was determined via the BCA method, and total protein and concentration were adjusted with the homogenization buffer to be equal between samples. Samples were then centrifuged at 150,000 × *g* for 15 min at 4°C in a Beckman TLA 1004 rotor (Beckman, Palo Alto, CA). The resulting pellet was rehomogenized in three volumes of a salt sucrose buffer (10 mM Tris-HCl, pH 7.4, 0.8 M NaCl, 10% sucrose, 1 mM EDTA) with a protease inhibitor cocktail added immediately before use, while the supernatant was labeled as S1 and frozen at −80°C. The resuspended pellet was again centrifuged at 150,000 × *g* for 15 min at 4°C; this time, the pellet was discarded, and the supernatant was brought to a 1% sarkosyl solution and incubated at 37°C for 1 h with gentle shaking. After centrifugation (150,000 × *g* for 30 min at 4°C), the supernatant was kept, labeled as S2, and frozen at −80°C. The pellet was resuspended in Tris/EDTA (10 mM Tris HCl, pH 7.4, 1 mM EDTA), washed once more with 1% sarkosyl solution, and frozen at −80°C.

Immunoblot analysis

Samples were separated on a gradient 8–16% SDS–PAGE, transferred to PVDF membranes, and stained with either a monoclonal α-synuclein antibody (Transduction Labs, 1:1000) or a phospho-dependent tau monoclonal antibody (PHF-1 or AT8, 1:200) followed by anti-mouse HRP-conjugated secondary antibody (Santa Cruz Biotechnology) and detected with SuperSignal™ West Pico Enhanced Chemiluminescence Kit (Pierce), followed by exposure to Kodak film.

Quantification of immunoblots

Densitometry analysis was performed using ImageJ software. Bands were analyzed and normalized to actin levels. Unpaired student *t* tests were used to determine statistical significance between expression levels in the animals ($n = 5$ for both the transgenic symptomatic and nontransgenic animals).

Results

Symptomatic A30P mice exhibit synuclein and ubiquitin aggregates in the brainstem

As reported previously, mice overexpressing the A30P α-synuclein transgene developed symptoms between 6 and 14 months (Kahle et al., 2001). The clinical phenotype presented with tremor followed by increasing bradykinesia, first manifest as hind limb impairment. As the clinical phenotype progressed, the mice developed postural instability and ultimately paralysis. For most experiments, we sacrificed mice when they developed an end-stage phenotype, which consisted of paralysis, postural instability, and absence of grooming behavior. The clinical phenotype evolved over a time course of 3–4 weeks.

Mice exhibiting an end-stage phenotype were sacrificed, and their brains were analyzed by biochemistry and immunoblotting. For the these studies, whole brain tissue was homogenized, and protein aggregates were partially purified based on insolubility in the presence of the detergent sarkosyl, as described previously (Giasson et al., 2002; Kahle et al., 2001). The samples were separated into three fractions: aqueous-soluble, sarkosyl-soluble, and sarkosyl-insoluble. All fractions showed more monomeric α-synuclein in the transgenic mice compared to the nontransgenic mice. The sarkosyl-insoluble fraction from symptomatic transgenic mice showed extensive higher molecular weight α-synuclein reactivity that was not apparent in sarkosyl-insoluble fractions from either age-matched nontransgenic or asymptomatic transgenic mice (Fig. 1A). These higher molecular weight bands likely represent oligomeric and aggregated α-synuclein as reported previously (Giasson et al., 2002; Kahle et al., 2001).

To determine where aggregated α-synuclein was present in the brain, we performed immunohistochemistry on sagittally cut brain sections. Aggregated α-synuclein accumulated mainly in large neurons in the rostral part of the reticular formation and as punctate inclusions in the neuropil throughout the reticular formation of transgenic symptomatic mice (Fig. 1C, panel a). α-Synuclein staining in age-matched nontransgenic mice was weaker and showed fewer inclusions (Fig. 1C, panel d). α-Synuclein staining in large neurons of symptomatic transgenic mice also showed strong diffuse expression, which was not observed in nontransgenic or asymptomatic mice (Fig. 1C, panel a). These neurons also contained α-synuclein inclusions (Fig. 1C, panels a and c, arrows). Double staining demonstrated that these inclusions also stained positively with anti-ubiquitin antibody indicating that they contain ubiquitin (Fig. 1C, panels b and c, arrows). No reactivity was seen with preimmune serum (Fig. 1C, panel e).

Symptomatic A30P mice exhibit increased pathological phosphorylation of tau

Phosphorylation of tau protein can be detected by the PHF-1 and AT8 antibodies, and is associated with tau pathology (Spillantini et al., 1998a). Brain sections from mice exhibiting end-stage motor impairment (defined as tremor, muscular rigidity, and full paralysis) were analyzed by immunoblot for the presence of abnormally phosphorylated tau with the phospho-specific antibody PHF-1, which

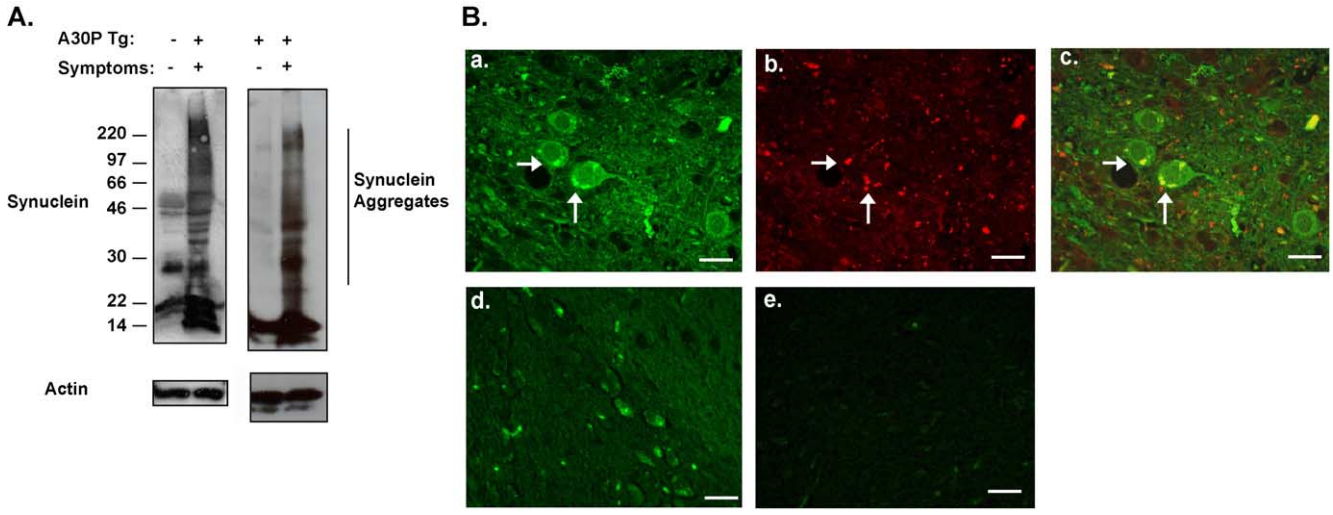

Fig. 1. Accumulation of aggregated α-synuclein. (A) The amount of aggregated α-synuclein observed in the sarkosyl-insoluble fraction from symptomatic A30P transgenic mice (lanes 2 and 4, from a 14-month female mouse shown) is much greater than the amount present in an age-matched nontransgenic female mouse (lane 1) or old asymptomatic transgenic A30P α-synuclein female mouse (lane 3). (B) Immunocytochemical analysis of a symptomatic A30P transgenic mouse shows neurons in the dorsal pons exhibiting both diffuse and punctate accumulation of α-synuclein (a). This region also shows an increase in ubiquitin immunoreactivity (b) that partly colocalizes with the α-synuclein reactivity (c, arrows). Less α-synuclein immunoreactivity is seen in the same region from an age-matched nontransgenic α-synuclein mouse (d), and no α-synuclein immunoreactivity is seen in the same region from a symptomatic A30P transgenic mouse following preadsorption of antibody (e). Bar = 20 μm.

detects phosphorylation of serine at amino acids 396/404. (Lewis et al., 2001) Immunoblots of whole brain homogenates demonstrated over a fourfold increase in PHF-1 reactivity in symptomatic transgenic mice compared to nontransgenic controls (Fig. 2A). In addition, some of the PHF-1-reactive tau migrated at a higher molecular weight, which is characteristic of abnormally phosphorylated tau in diseased brain (Fig. 2A). The total amount of tau as detected by the Tau-5 antibody, however, did not differ among the groups (Figs. 2A and B). Abnormally phosphorylated tau in disease brain often shifts to an insoluble pool as the tau fibrillizes. To determine whether such a shift was apparent in the symptomatic transgenic mice, we performed stepwise solubility fractionation to separate salt-soluble, sarkosyl-soluble, and sarkosyl-insoluble fractions. All brain tissue fractions of symptomatic transgenic mice showed increased PHF-1 signal compared to age-matched nontransgenic mice as analyzed by PHF-1 immunoblot. A representative immunoblot of the sarkosyl-insoluble fraction in Fig. 2C (left panel) shows increased S396 and S404 phosphorylation detected with the PHF-1 antibody in a symptomatic transgenic mouse. A similar pattern of reactivity was observed when the insoluble fraction was probed with the Tau-5 antibody, an antibody that recognizes tau from Arg221 to Leu282 and is independent of phosphorylation state (Fig. 2C, right panel). The increased total tau reactivity observed in the insoluble fraction from symptomatic transgenic mice compared to control mice reflects the tendency of abnormally phosphorylated tau to shift to the sarkosyl-insoluble fraction, which could be due to fibrillization of tau or association with other species that are aggregating. Immunoblotting with anti-actin antibody confirmed equal protein loading among the different samples (Fig. 2C). Immunohistochemical analysis using the MC1 and Alz-50 antibodies that detect a conformational change in tau associated with tangles did not stain positively in the symptomatic transgenic animals (data not shown), suggesting that the phosphorylated tau is in a "pretangle" state. Further washing of the insoluble fraction did not remove either the PHF-1-positive or Tau-5-positive tau, which indicates that the presence of the tau in the insoluble fraction was not due to carryover of sample from the soluble fraction (data not shown).

To further characterize the pathological phosphorylation of tau in these animals, we utilized AT8, another phospho-tau antibody that recognizes tau phosphorylated on amino acids Ser199, Ser202, and Thr205 (Drewes et al., 1992). The results paralleled those seen with the PHF-1 antibody. Immunoblot analysis showed more reactivity in the sarkosyl-insoluble fraction from the symptomatic transgenic mice than in asymptomatic transgenic control mice or nontransgenic mice (Fig. 2D, asymptomatic mouse data shown). In addition, tau from the symptomatic transgenic mice migrated at a slightly higher molecular weight (Fig. 2D, AT8 and Tau-5 panels). The sarkosyl-soluble fractions also showed increased AT8 signal in the symptomatic transgenic mice compared to nontransgenic mice (Fig. 2D). The size of the shift in tau varied among experiments but was often more apparent with Tau-5, perhaps because the PHF-1 and AT8 only detect tau that has already been phosphorylated. No difference in actin reactivity was observed among the lanes demonstrating that there was equal protein among the samples (Fig. 2D).

To determine whether tau phosphorylation is found in the same brain regions as the synuclein pathology, we

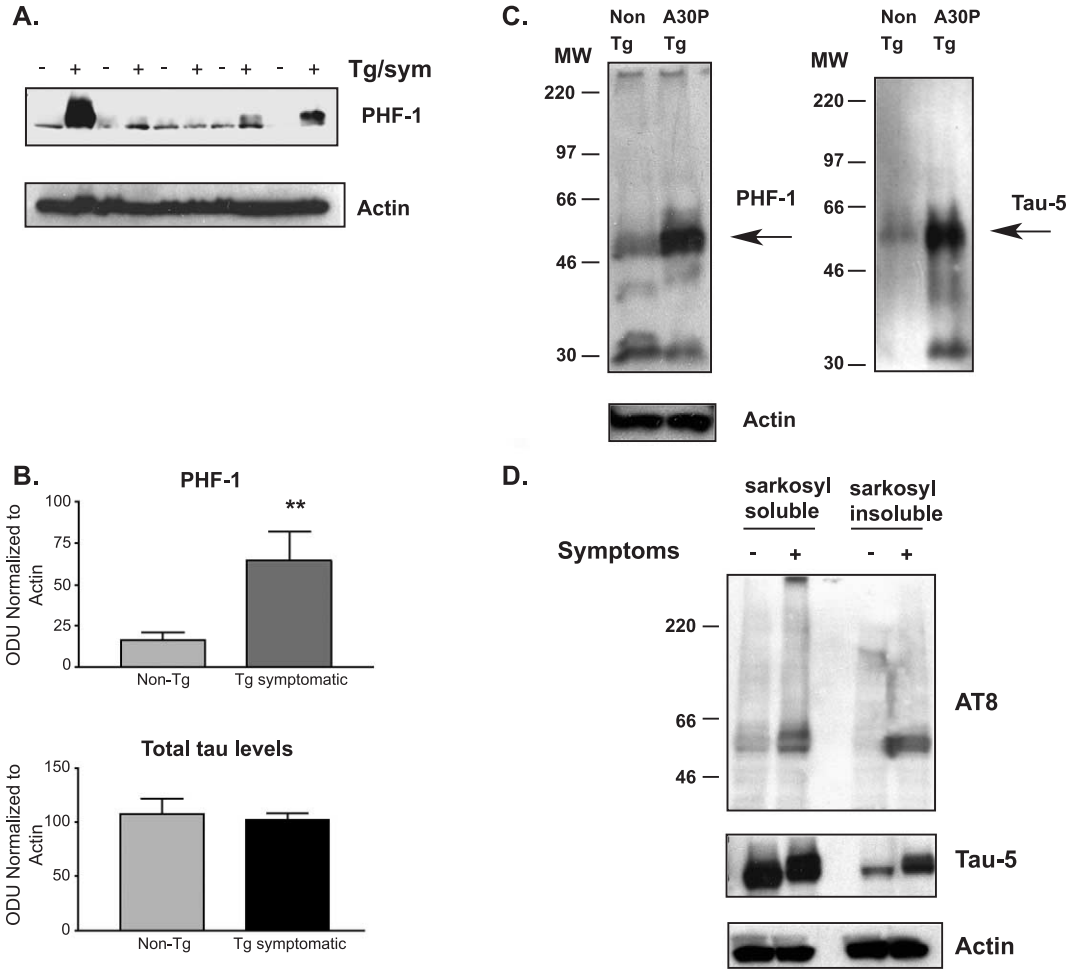

Fig. 2. Induction of phosphorylated PHF-1 and AT8-reactive tau protein. (A) PHF-1 immunoblot of nonfractionated whole brain homogenates from transgenic symptomatic (+) or age-matched nontransgenic mice. The blot was stripped and reprobed with tau-5 antibody which recognizes total tau, indicating similar total tau levels between animals. Actin immunoblot demonstrates equal protein loading. (B) Quantification of differences in PHF-1 and total tau immunoreactivity in the homogenates. ImageJ densitometric analysis of the PHF-1 immunoreactivity normalized to actin levels in each animal (**$P = 0.0035$ in PHF-1, $n = 5$) No significant difference in tau levels detected by Tau-5 existed between transgenic symptomatic and nontransgenic animals. (C) Immunoblot of the sarkosyl-insoluble fraction from a symptomatic A30P transgenic mouse showed increased PHF-1-reactive tau protein compared to the same fraction from an age-matched nontransgenic mouse (arrow). Also, note the electrophoretic shift in the PHF-1 immunoreactive band in the symptomatic transgenic mouse corresponding to increased phosphorylation. The lower panel shows actin immunoreactivity as a loading control. (D) Immunoblot of fractionated samples in old (12 months, lanes 2 and 4) symptomatic A30P transgenic mouse and young (2 months, lanes 1 and 3) asymptomatic A30P transgenic mouse. Sarkosyl-soluble fractions are lanes 1 and 2, while insoluble fractions are lanes 3 and 4. AT8 antibody demonstrates increased phosphorylation of tau in the symptomatic mouse compared to the asymptomatic mouse. Tau-5 immunoreactivity of the same immunoblot shows a shift in tau mobility in the symptomatic mouse likely due to an increased phosphorylated tau protein which migrates more slowly on SDS–PAGE

performed double-label immunofluorescence analysis. Double-labeling immunofluorescence analysis with antibodies to synuclein and phosphorylated tau (PHF-1, Ser396, and Ser404) demonstrated increased labeling of neurons in the brainstems of symptomatic animals compared to age-matched nontransgenic mice (Fig. 3A). Many neurons in the brainstem exhibited both diffuse cytoplasmic PHF-1 reactivity and punctate PHF-1 labeling within neurons (Fig. 2A, panel e). Much less PHF-1 staining was observed in the same region from nontransgenic mice. The neurons that were diffusely positive for PHF-1 staining showed either no α-synuclein staining or a small amount of punctate α-synuclein staining (Fig. 2A, panels d and f). PHF-1-positive neurons were most abundant in the ventral brainstem. In contrast, the neurons that stained strongly for α-synuclein were large neurons located in the dorsal reticular formation (Fig. 1C). A merge of the pictures showing strong PHF-1 tau inclusions showed only occasional colocalized with punctate α-synuclein inclusions (Fig. 2B, panel f, white arrows). The age-matched nontransgenic mouse displayed weaker staining of synuclein and phosphorylated tau (Fig. 2B, panels a and b). These results suggest that the neurons that develop phosphorylated tau at Ser395/404 do not contain large aggregations or accumulations of α-synuclein protein.

Immunofluorescence analysis with AT8 antibody also showed increased tau pathology in the ventral forebrain. AT8 reactivity associated with phosphorylation on residues

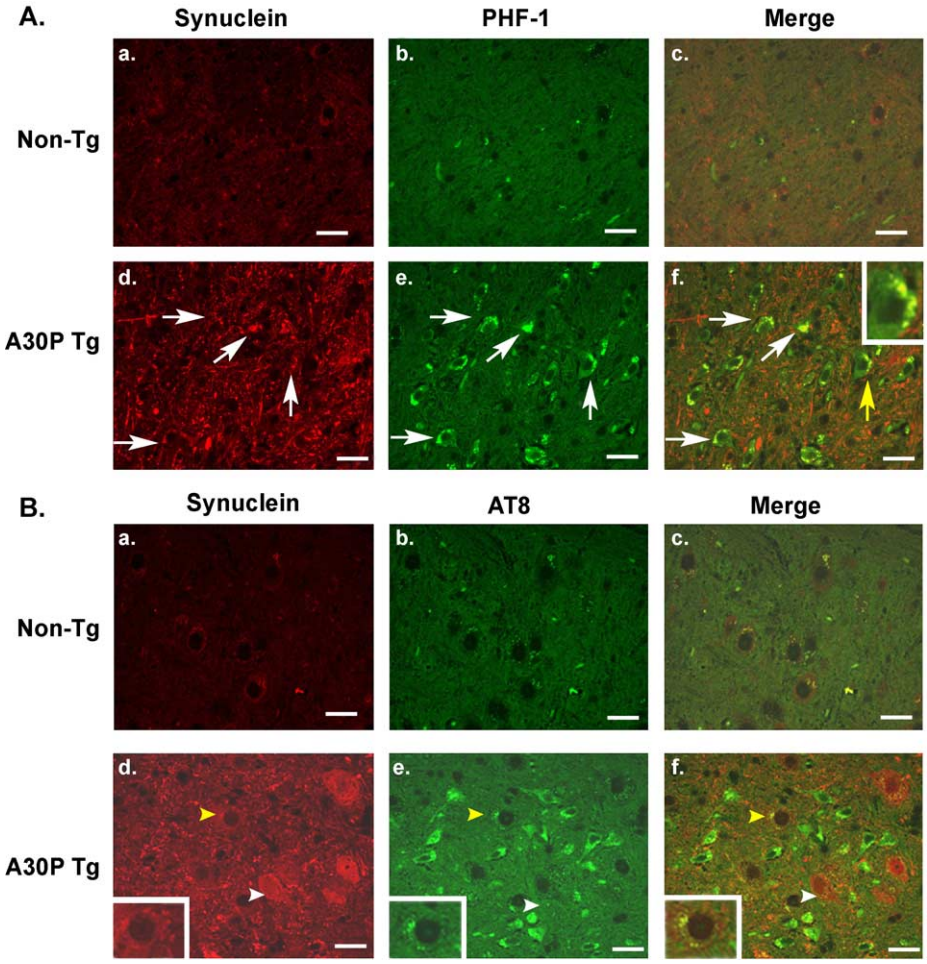

Fig. 3. Phosphorylated tau and α-synuclein aggregates can occur independently. (A) Immunocytochemical analysis of α-synuclein and PHF-1 immunoreactivity in the ventral pons. Staining of ventral pons from an aged nontransgenic mouse showed little α-synuclein (a, c) or PHF-1 (b, c) reactivity. In contrast staining of a symptomatic A30P, transgenic mouse showed an increase in punctate α-synuclein staining (d), and both diffuse and punctate staining for PHF-1 (e). Merging of the pictures shows that some of the α-synuclein staining occurred in neurons containing the PHF-1 reactivity (f, arrows). Inset highlights α-synuclein and PHF-1 colocalization of a single neuron (yellow arrow). Bar = 20 μm. (B) Immunocytochemical analysis of an aged nontransgenic mouse shows little staining of α-synuclein (a, c) or AT8 (b, c). In contrast staining of a symptomatic A30P, transgenic mouse shows an increase in punctate α-synuclein labeling (d), and neurons in the ventral pons with both diffuse and punctate accumulation of AT8 (e). Merging of the pictures shows that some of the α-synuclein staining occurs in neurons containing the AT8 reactivity (f, arrows). Bar = 20 μm.

199, 202, 205 was apparent in small neurons of the pontine reticular formation of symptomatic transgenic mice (Fig. 3B, panel e). Staining with an antibody to α-synuclein showed large neurons in this area that exhibited diffuse anti-α-synuclein reactivity (Fig. 3B, panel d). In addition, there was some punctate α-synuclein staining present both in the large neurons and throughout the neuropil (Fig. 3B, panel d). The neurons that were diffusely positive for AT8 were small neurons that did not colocalize with the neurons showing diffuse α-synuclein accumulation (Fig. 3B, panel f). Some of the large, synuclein-positive neurons also harbored punctate AT8-positive inclusions (Fig. 3B, panel f, arrow heads). The nontransgenic animal exhibited weaker staining with both synuclein and AT8 (Fig. 3B, panels a, b, and c), and colocalization was not evident. These results parallel those observed with PHF-1 and indicate that neurons that develop phosphorylated tau at Ser202/204 do not contain large aggregations or accumulations of α-synuclein protein.

Increased activity of cellular stress kinases in symptomatic transgenic mice

Three kinases are commonly associated with PHF-1 reactivity including cyclin-dependent kinase 5 (CDK5), c-jun kinase (JNK), and glycogen synthase kinase 3β (GSK-3β) (Godemann et al., 1999; Paudel, 1997; Wang et al., 1998). We examined whether any of these kinases are activated as the A30P α-synuclein mice develop motor impairment. We obtained tissue sections from symptomatic and nonsymptomatic A30P α-synuclein mice and age-matched nontransgenic control mice. The tissue was probed with antibodies to the activated c-jun kinase (JNK, phospho-Thr183/Tyr185), tyrosine 216, or Serine 9 of glycogen

synthase kinase 3β, and p25, the cellular activator of cdk5. The antibody recognizing activated JNK exhibited higher reactivity in the symptomatic animals compared to age-matched nontransgenic controls, although no change was observed in the level of total JNK (Figs. 4A and B, phospho-JNK data shown). Reactivity for phospho-GSK-3β Serine 9 was increased (Figs. 4C and D), while reactivity for phospho-GSK-3β tyrosine Y216 was unchanged (Fig. 4E). Phosphorylation of Serine 9 of GSK-3β is associated with inactivation of the protein, while phosphorylation of tyrosine 216 is associated with activation of GSK-3β (Fang et al., 2000; Wang et al., 1994). Immunoblotting with antibody to p25, the activator of CDK5, also failed to show a difference between transgenic and nontransgenic animals (Figs. 4F and G).

We performed immunofluorescence analysis to determine if the activated p-JNK is located in the same neurons of either phosphorylated tau or α-synuclein aggregates. Double labeling revealed p-JNK and α-synuclein colocalization (Fig. 5A) in neurons of the dorsal brainstem area

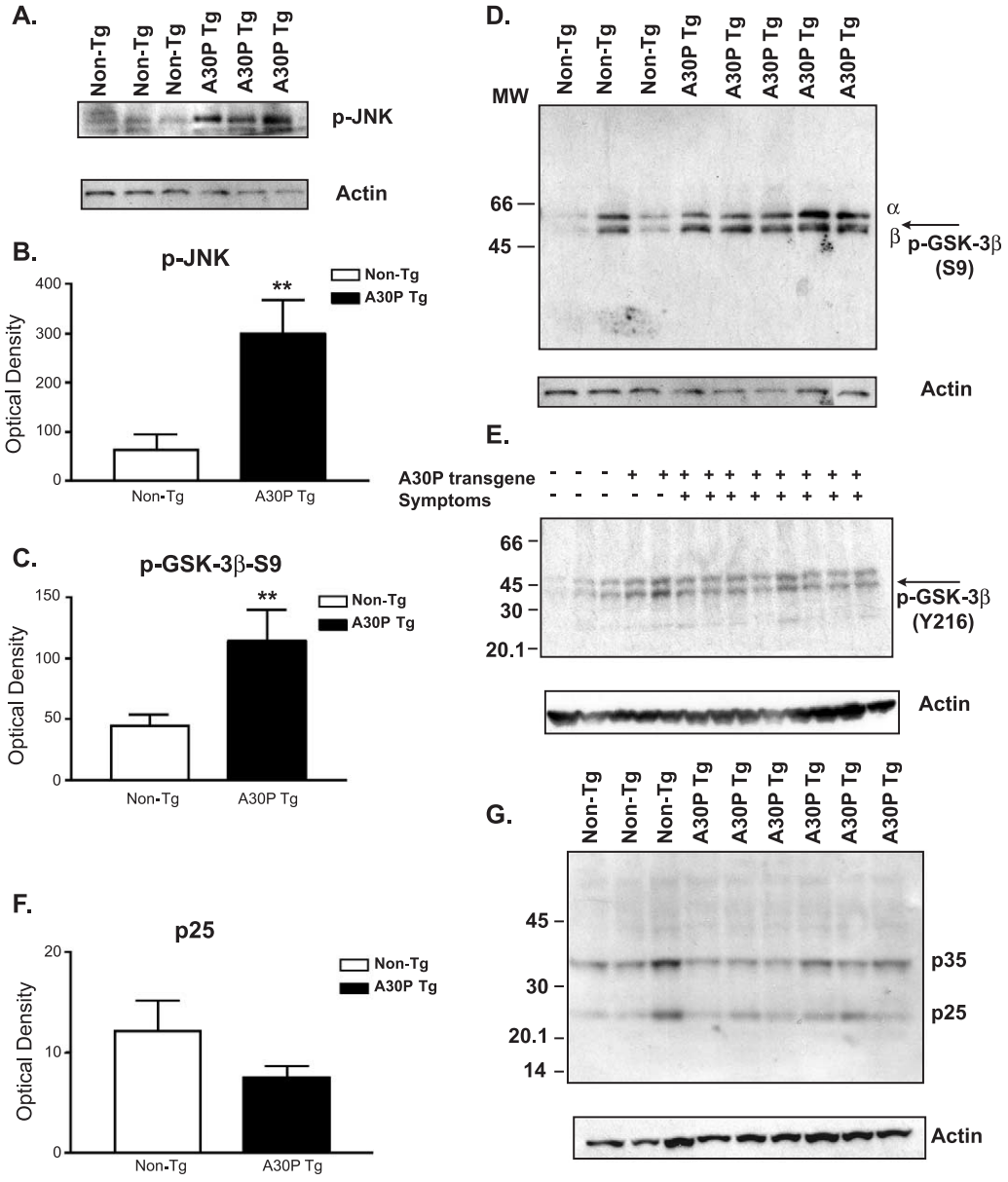

Fig. 4. Levels of activated c-jun kinase increase in symptomatic A30P α-synuclein mice. (A) Immunoblot of brainstem homogenates probed with an antibody recognizing activated JNK. Activated JNK reactivity (upper panel) is increased in motor-impaired animals relative to nontransgenic control animals; actin levels (lower panel) were used to normalize for protein loading. (B) Densitometric analysis demonstrates a significant increase in the levels of activated JNK in symptomatic animals when normalized to actin. (C and D) Levels of GSK-3β phosphorylated at Serine-9 are increased in symptomatic animals when normalized to actin; phosphorylation at Serine-9 is a modification that inhibits GSK-3β activity. (E) Phosphorylation at Y216 of GSK-3β is not changed in symptomatic transgenic animals compared to nontransgenic controls. (F and G) Immunoblot of p25, the activator of cdk5, shows no significant change in p25 levels between symptomatic and asymptomatic animals. Actin is used to demonstrate equal protein loading for all protein analyses. $^{**}P < 0.05$.

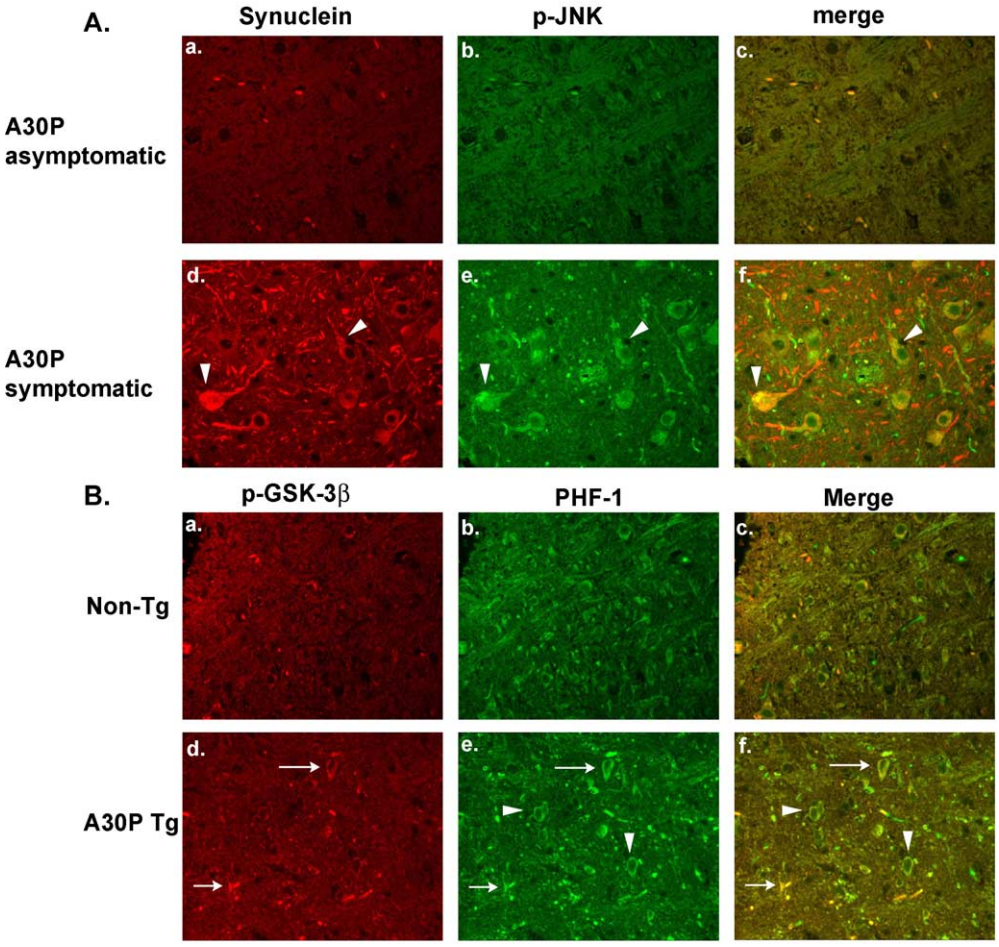

Fig. 5. Phosphorylated-JNK and GSK-3β-S9 are localized in neurons containing α-synuclein or PHF-1 phospho-tau reactivity. (A) Immunocytochemical analysis comparing tissue from an age-matched asymptomatic transgenic animal (top panels) to a motor-impaired transgenic animal (second panel). Staining in the dorsal pons for α-synuclein (a, d) and phospho-JNK (b, e) reveals weak staining in the asymptomatic animal compared to the motor-impaired animal. Merge of the two (c, f) shows moderate co-occurrence. Arrowheads point to colocalization. (B) Immunocytochemical analysis of the dorsal pons region of a nontransgenic mouse (upper panel) and a symptomatic transgenic mouse (lower panel). Antibodies towards phospho-GSK-3β Serine-9 (red, a and d) and PHF-1 (green, b and e) show increased reactivity in the symptomatic animal compared to the age-matched nontransgenic animal. Merging the two (c and f) reveals some colocalization of PHF-1 and GSK-3β S9 reactivity in the symptomatic animals (designated by arrows) and other PHF-1-positive neurons that do not show GSK-3β S9 reactivity (designated by arrowheads). Magnification ×40.

where neurons were diffusely positive for α-synuclein in symptomatic transgenic mice. In areas with fewer α-synuclein-positive neurons, such as the ventral brainstem, anti-phospho-JNK reactivity appeared to colocalize with PHF-1 reactivity rather than anti-α-synuclein reactivity. Serial sections with antibodies towards p-JNK and PHF-1 showed similar patterns of staining in the ventral brainstem in symptomatic transgenic mice (Figs. 6a and b). This suggests that p-JNK reactivity does not always occur in neurons that have overt accumulation of α-synuclein. In contrast, staining for p-JNK and PHF-1 in the asymptomatic transgenic mice (Figs. 6c and d) or nontransgenic mice (Figs. 6e and f) was weak. Studies with antibodies towards phospho-GSK-3β, showed no increase in reactivity (data not shown), although reactivity with antibody identifying phospho-Ser9 of GSK-3β showed some colocalization with PHF-1 in the ventral portion of the brainstem of motor-impaired animals (Fig. 5B, lower panel, arrows), while very little staining is present in age-matched nontransgenic mice (Fig. 5B, upper panel).

Increased reactivity for glial fibrillary acidic protein in symptomatic transgenic mice

Because gliosis has not been reported on in this line of A30P α-synuclein mice, and to assess other signs of injury, we performed immunohistochemistry with an antibody directed against glial fibrillary (GFAP) acidic protein to detect astrocytosis, which is a classic marker for neuronal injury. We observed a massive increase in GFAP reactivity present throughout the brainstem of symptomatic A30P α-synuclein mice (Fig. 7B, c.) compared to nonsymptomatic A30P α-synuclein transgenic mice (Fig. 7B, b.) or nontransgenic mice (Fig. 7B,

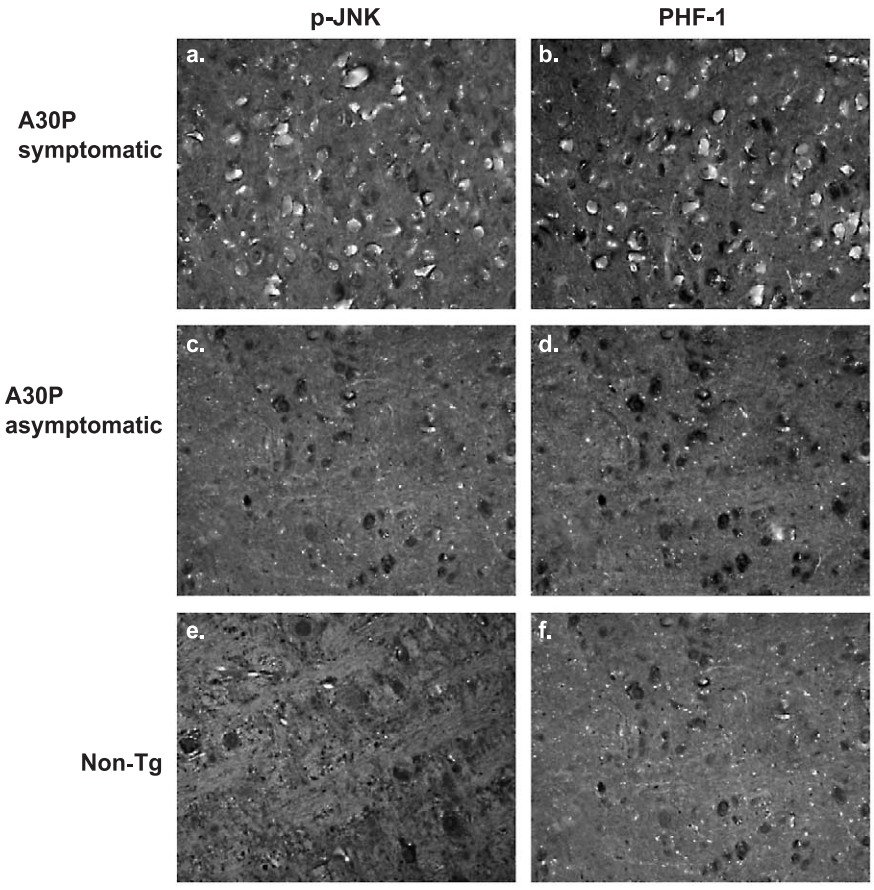

Fig. 6. Phosphorylated-JNK is present in neurons similar to those exhibiting PHF-1 phospho-tau reactivity in the ventral brainstem. Serial sections of brain tissue from symptomatic transgenic A30P α-synuclein transgenic mice showed staining for both phosphorylated-JNK (a) and PHF-1 (b) in similar neurons observed in serial sections. No staining for either antibody was observed in sections from asymptomatic A30P α-synuclein transgenic mice (c and d) or aged, nontransgenic mice (e and f). Magnification ×40.

a). The presence of the GFAP reactivity throughout contrasted sharply with the focal loci of reactivity seen with the phospho-tau or α-synuclein immunoreactivity (Figs. 1B, 2B, and 3B).

Discussion

Transgenic mice overexpressing α-synuclein develop an age-dependent accumulation of α-synuclein in neurons of the brainstem (Giasson et al., 2002; Kahle et al., 2001). Our study confirms the observations of α-synuclein aggregation observed by Kahle et al. (2000, 2001), as well as by other groups studying mice overexpressing A53T or wild-type α-synuclein. We also observed the surprising finding that transgenic α-synuclein mice with impaired motor function accumulate tau that is phosphorylated at Ser202/Thr205 (detected with the AT8 antibody) and Ser396/Ser404 (detected with the PHF-1 antibody).

Phosphorylation of tau at Ser202/Thr205 and Ser396/Ser404 is commonly observed in neurodegenerative diseases that are associated with tau pathology including FTDP-17, AD, and PSP (Godemann et al., 1999; Jicha et al., 1997; Paudel, 1997; Wang et al., 1998). Abnormal tau phosphorylation was readily apparent by both immunohistochemistry and immunoblot. Biochemical analyses of the brain homogenates indicate that hyperphosphorylated tau was present in both sarkosyl-soluble and the sarkosyl-insoluble fractions of whole brain homogenates. The presence of tau in the sarkosyl-insoluble fraction suggests that some of the tau is either self-aggregated or associated with another aggregate, such as aggregated α-synuclein. Indeed, we demonstrated that some of the tau coassociates with α-synuclein in the symptomatic transgenic mice but not in the nontransgenic or asymptomatic transgenic mice. The presence of tau with pathological phosphorylation but lacking conformational epitopes associated with neurofibrillary tangles suggests that the tau exists at a stage characteristic of pretangles or early tangle formation. Incomplete tangle formation has been observed in aged mice expressing the human amyloid precursor protein APP 717 or Swedish mutations (Games et al., 1995; Hsiao et al., 1996). Progression to full tangle formation might not occur in mice because mouse tau does not appear to have the same tendency as human tau to aggregate in vivo (Lewis et al., 2000, 2001; Tatebayashi et al., 2002).

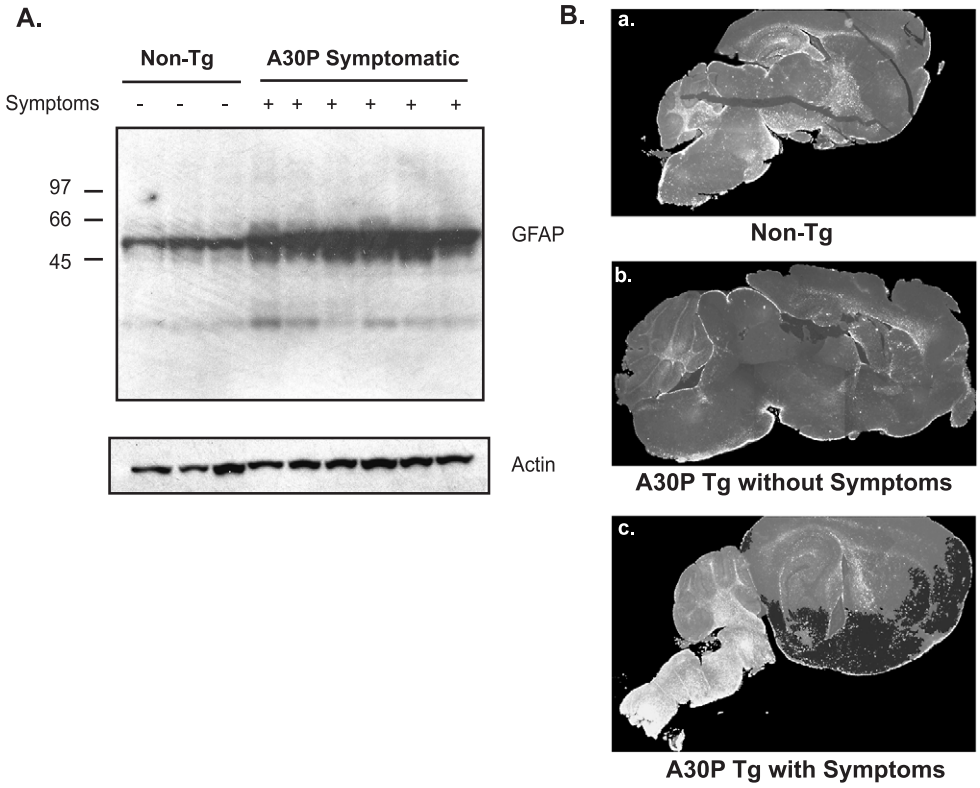

Fig. 7. GFAP activity increases in symptomatic A30P α-synuclein mice. (A) Immunoblot of whole brain homogenates with an antibody against glial fibrillary acidic protein. GFAP reactivity is elevated in symptomatic animals compared to nontransgenic animals. Actin is used as a loading control. (B) Immunocytochemistry of sagittally cut brains from nontransgenic, asymptomatic transgenic, or symptomatic transgenic mice. Abundant immunoreactivity against GFAP was apparent in the brainstem from a 12-month-old symptomatic A30P α-synuclein mouse (c) using an antibody against activated GFAP, while little GFAP reactivity was apparent in tissue sections from a 4-month-old nonsymptomatic A30P α-synuclein mouse (b) and a 12-month-old nontransgenic mouse (a). Magnification ×2.

One surprising aspect of tau pathology in the A30P α-synuclein mice is that the phospho-tau appears to form predominantly in neurons that did not overtly accumulate α-synuclein. This observation is consistent with recent studies of pathological tau and α-synuclein aggregates in human and mouse tissues. Tau can be detected in some Lewy bodies in PD substantia nigra, but many Lewy bodies do not contain pathological tau (Ishizawa et al., 2003). Pathological tau can also be detected in brain tissue from human PD subjects caused by the A53T α-synuclein mutation as well as in transgenic mice coexpressing P301L tau and A53T α-synuclein; however, the tau and α-synuclein are not always colocalized (Duda et al., 2002; Giasson et al., 2003). Duda et al. found tau in a halo shape surrounding α-synuclein inclusions in the brains of patients overexpressing A53T α-synuclein, which indicates that the two proteins can aggregate in close proximity. Giasson et al. reported approximately 25% of α-synuclein inclusions contained tau threads in mice overexpressing A53T α-synuclein. These results are therefore consistent with our observation that only a fraction of pathological tau colocalizes with α-synuclein accumulations. The amount of colocalization might vary depending on extrinsic factors, such as the oxidative stress present in neurons of patients with PD, and on intrinsic factors, such as the type of mutation that is present; the P301L tau mutation, A53T α-synuclein, and A30P α-synuclein mutations might impact colocalization of tau and α-synuclein aggregates differentially. Previous studies examining tau pathology in mice developing amyloid accumulations also observed tau phosphorylation occurring at a distance from the amyloid accumulation. Mice transgenic for both amyloid precursor protein and P301L tau develop tau pathology in some regions that are separate from the amyloid accumulation (Lewis et al., 2001). Following injection of Aβ, tau pathology also develops at some sites distant from the injection site (Gotz et al., 2001; Sigurdsson et al., 1997). The separation of tau and synuclein pathology that we observed in this study might reflect similar processes. The presence of pathological tau in neurons that do not show α-synuclein accumulation could result from the presence of small amounts of fibrillar α-synuclein in these neurons, which might either directly stimulate the stress kinases or might stimulate aggregation of tau. Alternatively, the pathological tau might derive from distant signals. Neurons that have been injured by the accumulation of large amounts of α-synuclein might secrete factors such as cytokines that would stimulate tau phosphorylation, as well as gliosis. Neurons containing large

amounts of α-synuclein accumulation might also generate free radicals and/or might fail to send out trophic signals required by neighboring neurons.

Other proteins known to be involved in the neurodegenerative pathology appear to accumulate along with the α-synuclein. Lewy bodies are composed primarily of the proteins α-synuclein and ubiquitin, but other proteins are present in some Lewy bodies in smaller amounts, such as parkin, Synphilin-1, SEPT4, torsin, and neurofilament (Choi et al., 2001; Goldman and Yen, 1986; Schlossmacher et al., 2002; Sharma et al., 2001; Wakabayashi et al., 2000). Interestingly, we did not observe increases in parkin associated with the α-synuclein accumulation (data not shown). Ubiquitin is the protein most commonly associated with Lewy bodies, and we observed that the A30P α-synuclein mice show concomitant accumulation of ubiquitin. The ubiquitin that accumulates appears to occur in only a subset of the neurons that accumulate α-synuclein as shown by double-staining sections from the brainstem of affected mice using antibodies to both α-synuclein and ubiquitin. The lower prevalence of ubiquitin accumulations suggests that ubiquitin accumulation occurs after that of α-synuclein and is consistent with a prior study indicating that the accumulation of α-synuclein precedes the accumulation of ubiquitin in these mice (Kahle et al., 2001). Astrocytosis is another common indicator of neuronal injury, and immunocytochemical staining for GFAP showed a massive increase in GFAP reactivity throughout the brainstem of symptomatic A30P transgenic mice. The pattern of GFAP reactivity is striking because the distribution is much broader than that observed for α-synuclein accumulation or phospho-tau immunoreactivity. Because the Thy1 promoter, which is neuron-specific, drives the human A30P α-synuclein transgene, we hypothesize that the astrocytosis occurs in response to the neuronal injury. The widespread gliosis suggests that the neuronal injury is either more widespread than is apparent by immunocytochemical analysis, determined with antibodies to α-synuclein, or that the injured neurons secrete diffusible signals, such as cytokines. Astrocytosis has been noted in another transgenic α-synuclein mouse model, in MPTP toxicity and in PD with dementia, but is not a prevalent feature of rotenone-induced toxicity or of classic cases of Parkinson disease (Gomez-Isla et al., 2003; Muramatsu et al., 2003; Tsuchiya et al., 2002). The presence of astrocytosis in the α-synuclein transgenic mice distinguishes an important difference between this transgenic mouse model of PD and actual PD in humans.

Our studies suggest that the mechanism of increased phosphorylation of tau may involve selective activation of JNK. The kinases glycogen synthase kinase 3β, CDK5, and c-jun kinase are all activated by oxidative stress (Nemoto et al., 2000; Shaw et al., 1998; Strocchi et al., 2003). JNK, GSK-3β, and CDK5 all phosphorylate tau at S396 and S404 (Godemann et al., 1999; Paudel, 1997; Wang et al., 1998). In our study, the increased tau phosphorylation correlated with increased phosphorylation of JNK but not with phosphorylation of GSK-3β (at Tyr216) or CDK5. Interestingly, we also observed some increase in phosphorylation of GSK-3β at Ser9, which is associated with reduced activity (Wang et al., 1988, 1998). This pattern or reactivity differs somewhat from the pattern of reactivity seen in Alzheimer disease. Hyperphosphorylation of tau is associated with increased activity of both CDK5 and GSK3β in CNS neurons in Alzheimer disease and in Niemann-Pick disease (Bu et al., 2002; Takashima et al., 1996; Vincent et al., 1997). The identification of JNK as a pathway that is selectively associated with α-synuclein pathology in the A30P α-synuclein mice in vivo provides a useful tool for identifying the biochemical pathways associated with α-synuclein pathology. Our results contradict findings by Hashimoto et al. (2002) that show cells overexpressing α-synuclein inactivate JNK in response to oxidative stress. This discrepancy could reflect differences between in vitro and in vivo studies. Hashimoto overexpressed wild-type α-synuclein in cell culture, while we utilized mice overexpressing mutant A30P α-synuclein. The A30P mutation may disrupt the ability of α-synuclein to inactivate JNK, or aggregated α-synuclein may prevent the JNK inactivation in the animals. Activation of JNK by α-synuclein might explain how α-synuclein pathology leads to abnormal phosphorylation of tau in the A30P α-synuclein mice. Because phosphorylation of tau predisposes tau to aggregation, the phosphorylation could provide a mechanism that contributes to the increased fibrillization of tau observed in synucleinopathies (Giasson et al., 2003). In addition, activation of JNK through a transsynaptic mechanism (perhaps due to trophic withdrawal or release of reactive oxygen species) might also explain how abnormal phosphorylation and fibrillization of tau occur in neurons without large amounts of aggregated α-synuclein, such as is observed in this study and other studies (Giasson et al., 2003).

Increasing evidence suggests common mechanisms of neurodegeneration among different diseases. In Alzheimer disease, Parkinson disease, frontotemporal dementias, and polyglutamine disorders such as Huntington disease, protein aggregation appears to drive neurodegeneration. In each case, in vitro studies show that the proteins that accumulate have a inherent tendency to aggregate (Conway et al., 1998; DiFiglia et al., 1997; Hong et al., 1998; Hutton et al., 1998; Lewis et al., 2000). Many of these proteins have also been shown to stimulate concomitant aggregation of proteins prone to aggregate. Human tau aggregates as Aβ accumulates in vivo, Aβ stimulates aggregation of α-synuclein, α-synuclein coaggregates with proteins containing expanded polyglutamine regions, and α-synuclein stimulates tau aggregation (Charles et al., 2000; Furlong et al., 2000; Giasson et al., 2003; Lewis et al., 2001; Masliah et al., 2001). In addition, the formation of protein aggregates appears to stimulate similar pathological reactions, including formation of free radicals, activation of stress kinases, and inhibition of proteasomal activity. In our study, we observed that the tau and synuclein pathology can occur at spatially distinct sites. Because formation of microaggre-

gates (also known as protofibrils) and activation of stress responses often occur in parallel, the exact mechanism of tau pathology in the A30P α-synuclein mice remains to be determined. However, our data provide in vivo support for the hypothesis that accumulation and aggregation of α-synuclein can stimulate pathological changes in tau protein.

Acknowledgments

We would like to thank Nancy Muma (Loyola) for her useful suggestions. This research was supported by grants to BW from NINDS (NS41786-01), NIA (AG17485), and USAMRC (DAMD17-01-1-0781).

References

Bu, B., Klunemann, H., Suzuki, K., Li, J., Bird, T., Jin, L.W., Vincent, I., 2002. Niemann-Pick disease type C yields possible clue for why cerebellar neurons do not form neurofibrillary tangles. Neurobiol. Dis. 11, 285–297.

Charles, V., Mezey, E., Reddy, P.H., Dehejia, A., Young, T.A., Polymeropoulos, M.H., Brownstein, M.J., Tagle, D.A., 2000. alpha-Synuclein immunoreactivity of huntingtin polyglutamine aggregates in striatum and cortex of Huntington's disease patients and transgenic mouse models. Neurosci. Lett. 289, 29–32.

Choi, P., Golts, N., Snyder, H., Petrucelli, L., Chong, M., Hardy, J., Sparkman, D., Cochran, E., Lee, J., Wolozin, B., 2001. Co-association of parkin and α-synuclein. NeuroReport 12, 2839–2844.

Conway, K., Harper, J., Lansbury, P., 1998. Accelerated in vitro fibril formation by a mutant alpha-synuclein linked to early-onset Parkinson disease. Nat. Med. 4, 1318–1320.

Conway, K.A., Lee, S.J., Rochet, J.C., Ding, T.T., Williamson, R.E., Lansbury Jr., P.T., 2000. Acceleration of oligomerization, not fibrillization, is a shared property of both alpha-synuclein mutations linked to early-onset Parkinson's disease: implications for pathogenesis and therapy. Proc. Natl. Acad. Sci.U. S. A. 97, 571–576.

DiFiglia, M., Sapp, E., Chase, K., Davies, S., Bates, G., Vonsattel, J., Aronin, N., 1997. Aggregation of huntingtin in neuronal intranuclear inclusions and dystrophic neurites in brain. Science 277, 1990–1993.

Drewes, G., Lichtenberg-Kraag, B., Doring, F., Mandelkow, E., Biernat, J., Goris, J., Doree, M., Mandelkow, E., 1992. Mitogen activated protein (MAP) kinase transforms tau protein into an Alzheimer-like state. EMBO J. 11, 2131–2138.

Duda, J.E., Giasson, B.I., Mabon, M.E., Miller, D.C., Golbe, L.I., Lee, V.M., Trojanowski, J.Q., 2002. Concurrence of alpha-synuclein and tau brain pathology in the Contursi kindred. Acta Neuropathol. (Berl.) 104, 7–11.

Engelender, S., Kaminsky, Z., Guo, X., Sharp, A., Amaravi, R., Kleiderlein, J., Margolis, R., Troncoso, J., Lanahan, A., Worley, P., Dawson, V., Dawson, T., Ross, C., 1999. Synphilin-1 associates with alpha-synuclein and promotes the formation of cytosolic inclusions. Nat. Genet. 22, 110–114.

Fang, X., Yu, S.X., Lu, Y., Bast Jr., R.C., Woodgett, J.R., Mills, G.B., 2000. Phosphorylation and inactivation of glycogen synthase kinase 3 by protein kinase A. Proc. Natl. Acad. Sci.U. S. A. 97, 11960–11965.

Feany, M.B., Bender, W.W., 2000. A *Drosophila* model of Parkinson's disease. Nature 404, 394–398.

Forman, M.S., Schmidt, M.L., Kasturi, S., Perl, D.P., Lee, V.M., Trojanowski, J.Q., 2002. Tau and alpha-synuclein pathology in amygdala of Parkinsonism–dementia complex patients of Guam. Am. J. Pathol. 160, 1725–1731.

Furlong, R.A., Narain, Y., Rankin, J., Wyttenbach, A., Rubinsztein, D.C., 2000. alpha-Synuclein overexpression promotes aggregation of mutant huntingtin. Biochem. J. 346 (Pt. 3), 577–581.

Games, D., Adams, D., Alessandrini, R., Barbour, R., Berthelette, P., Blackwell, C., Carr, T., Clemens, J., Donaldson, T., Gillespie, F., Guido, T., Hagopian, S., Johnson, M., Wood, K., Khan, K., Lee, M., Leibowitz, P., Lieberburg, I., Little, S., Masliah, E., McConlogue, L., Montoya-Zavala, M., Mucke, L., Paganini, L., Penniman, E., Power, M., Schenk, D., Seubert, P., Snyder, B., Soriano, F., Tan, H., Vitale, J., Wadsworth, S., Wolozin, B., Zhao, J., 1995. Development of neuropathology similar to Alzheimer's disease in transgenic mice overexpressing the 717V-F β-amyloid precursor protein. Nature 373, 523–527.

Giasson, B.I., Duda, J.E., Quinn, S.M., Zhang, B., Trojanowski, J.Q., Lee, V.M., 2002. Neuronal alpha-synucleinopathy with severe movement disorder in mice expressing A53T human alpha-synuclein. Neuron 34, 521–533.

Giasson, B.I., Forman, M.S., Higuchi, M., Golbe, L.I., Graves, C.L., Kotzbauer, P.T., Trojanowski, J.Q., Lee, V.M., 2003. Initiation and synergistic fibrillization of tau and alpha-synuclein. Science 300, 636–640.

Godemann, R., Biernat, J., Mandelkow, E., Mandelkow, E.M., 1999. Phosphorylation of tau protein by recombinant GSK-3beta: pronounced phosphorylation at select Ser/Thr-Pro motifs but no phosphorylation at Ser262 in the repeat domain. FEBS Lett. 454, 157–164.

Goldman, J.E., Yen, S.H., 1986. Cytoskeletal protein abnormalities in neurodegenerative diseases. Ann. Neurol. 19, 209–223.

Gomez-Isla, T., Irizarry, M.C., Mariash, A., Cheung, B., Soto, O., Schrump, S., Sondel, J., Kotilinek, L., Day, J., Schwarzschild, M.A., Cha, J.H., Newell, K., Miller, D.W., Ueda, K., Young, A.B., Hyman, B.T., Ashe, K.H., 2003. Motor dysfunction and gliosis with preserved dopaminergic markers in human alpha-synuclein A30P transgenic mice. Neurobiol. Aging 24, 245–258.

Gotz, J., Chen, F., van Dorpe, J., Nitsch, R.M., 2001. Formation of neurofibrillary tangles in P301l tau transgenic mice induced by Abeta 42 fibrils. Science 293, 1491–1495.

Hashimoto, M., LJ, H., Xia, Y., Takeda, A., Sisk, A., Sundsmo, M., Masliah, E., 1999. Oxidative stress induces amyloid-like aggregate formation of NACP/α-synuclein in vitro. NeuroReport 10, 717–721.

Hashimoto, M., Hsu, L.J., Rockenstein, E., Takenouchi, T., Mallory, M., Masliah, E., 2002. alpha-Synuclein protects against oxidative stress via inactivation of the c-Jun N-terminal kinase stress-signaling pathway in neuronal cells. J. Biol. Chem. 277, 11465–11472.

Hong, M., Zhukareva, V., Vogelsberg-Ragaglia, V., Wszolek, Z., Reed, L., Miller, B., Geschwind, D., Bird, T., McKeel, D., Goate, A., Morris, J., Wilhelmsen, K., Schellenberg, G., Trojanowski, J., Lee, V., 1998. Mutation-specific functional impairments in distinct tau isoforms of hereditary FTDP-17. Science 282, 1914–1917.

Hsiao, K., Chapman, P., Nilsen, S., Eckman, C., Harigaya, Y., Younkin, S., Yang, F., Cole, G., 1996. Correlative memory deficits, Abeta elevation, and amyloid plaques in transgenic mice. Science 274, 99–102.

Hutton, M., Lendon, C., Rizzu, P., Baker, M., Froelich, S., Houlden, H., Pickering-Brown, S., Chakraverty, S., Isaacs, A., Grover, A., Hackett, J., Adamson, J., Lincoln, S., Dickson, D., Davies, P., Petersen, R., Stevens, M., de Graaff, E., Wauters, E., van Baren, J., Hillebrand, M., Joosse, M., Kwon, J., Nowotny, P., Heutink, P., al, e., 1998. Association of missense and 5′-splice-site mutations in tau with the inherited dementia FTDP-17. Nature 393, 702–705.

Ihara, M., Tomimoto, H., Kitayama, H., Morioka, Y., Akiguchi, I., Shibasaki, H., Noda, M., Kinoshita, M., 2003. Association of the cytoskeletal GTP-binding protein Sept4/H5 with cytoplasmic inclusions found in Parkinson's disease and other synucleinopathies. J. Biol. Chem. 278, 24095–24102.

Ishizawa, T., Mattila, P., Davies, P., Wang, D., Dickson, D.W., 2003. Colocalization of tau and alpha-synuclein epitopes in Lewy bodies. J. Neuropathol. Exp. Neurol. 62, 389–397.

Jenco, J., Rawlingson, A., Daniels, B., Morris, A., 1998. Regulation of phospholipase D2: selective inhibition of mammalian phospholipase D isoenzymes by a and b synucleins. Biochemistry 37, 4901–4909.

Jensen, P.H., Hager, H., Nielsen, M.S., Hojrup, P., Gliemann, J., Jakes, R., 1999. alpha-Synuclein binds to tau and stimulates the protein kinase A-catalyzed tau phosphorylation of serine residues 262 and 356. J. Biol. Chem. 274, 25481–25489.

Jicha, G.A., Lane, E., Vincent, I., Otvos Jr., L., Hoffmann, R., Davies, P., 1997. A conformation- and phosphorylation-dependent antibody recognizing the paired helical filaments of Alzheimer's disease. J. Neurochem. 69, 2087–2095.

Kahle, P.J., Neumann, M., Ozmen, L., Muller, V., Jacobsen, H., Schindzielorz, A., Okochi, M., Leimer, U., van Der Putten, H., Probst, A., Kremmer, E., Kretzschmar, H.A., Haass, C., 2000. Subcellular localization of wild-type and Parkinson's disease-associated mutant alpha-synuclein in human and transgenic mouse brain. J. Neurosci. 20, 6365–6373.

Kahle, P.J., Neumann, M., Ozmen, L., Muller, V., Odoy, S., Okamoto, N., Jacobsen, H., Iwatsubo, T., Trojanowski, J.Q., Takahashi, H., Wakabayashi, K., Bogdanovic, N., Riederer, P., Kretzschmar, H.A., Haass, C., 2001. Selective insolubility of alpha-synuclein in human Lewy body diseases is recapitulated in a transgenic mouse model. Am. J. Pathol. 159, 2215–2225.

Kruger, R., Kuhn, W., Muller, T., Woitalla, D., Graeber, M., Kosel, S., Przuntek, H., Epplen, J., Schols, L., Riess, O., 1998. Ala30Pro mutation in the gene encoding α-synuclein in Parkinson's disease. Nat. Genet. 18, 106–108.

Lee, F.J., Liu, F., Pristupa, Z.B., Niznik, H.B., 2001a. Direct binding and functional coupling of alpha-synuclein to the dopamine transporters accelerate dopamine-induced apoptosis. FASEB J. 15, 916–926.

Lee, V.M., Goedert, M., Trojanowski, J.Q., 2001b. Neurodegenerative tauopathies. Annu. Rev. Neurosci. 24, 1121–1159.

Lewis, J., McGowan, E., Rockwood, J., Melrose, H., Nacharaju, P., Van Slegtenhorst, M., Gwinn-Hardy, K., Paul Murphy, M., Baker, M., Yu, X., Duff, K., Hardy, J., Corral, A., Lin, W.L., Yen, S.H., Dickson, D.W., Davies, P., Hutton, M., 2000. Neurofibrillary tangles, amyotrophy and progressive motor disturbance in mice expressing mutant (P301L) tau protein. Nat. Genet. 25, 402–405.

Lewis, J., Dickson, D.W., Lin, W.L., Chisholm, L., Corral, A., Jones, G., Yen, S.H., Sahara, N., Skipper, L., Yager, D., Eckman, C., Hardy, J., Hutton, M., McGowan, E., 2001. Enhanced neurofibrillary degeneration in transgenic mice expressing mutant tau and APP. Science 293, 1487–1491.

Masliah, E., Rockenstein, E., Veinbergs, I., Mallory, M., Hashimoto, M., Takeda, A., Sagara, Y., Sisk, A., Mucke, L., 2000. Dopaminergic loss and inclusion body formation in alpha-synuclein mice: implications for neurodegenerative disorders. Science 287, 1265–1269.

Masliah, E., Rockenstein, E., Veinbergs, I., Sagara, Y., Mallory, M., Hashimoto, M., Mucke, L., 2001. beta-Amyloid peptides enhance alpha -synuclein accumulation and neuronal deficits in a transgenic mouse model linking Alzheimer's disease and Parkinson's disease. Proc. Natl. Acad. Sci.U. S. A. 25, 25.

Muramatsu, Y., Kurosaki, R., Watanabe, H., Michimata, M., Matsubara, M., Imai, Y., Araki, T., 2003. Cerebral alterations in a MPTP-mouse model of Parkinson's disease—An immunocytochemical study. J. Neural Transm. 110, 1129–1144.

Murphy, D.D., Rueter, S.M., Trojanowski, J.Q., Lee, V.M., 2000. Synucleins are developmentally expressed, and alpha-synuclein regulates the size of the presynaptic vesicular pool in primary hippocampal neurons. J. Neurosci. 20, 3214–3220.

Nemoto, S., Takeda, K., Yu, Z.X., Ferrans, V.J., Finkel, T., 2000. Role for mitochondrial oxidants as regulators of cellular metabolism. Mol. Cell. Biol. 20, 7311–7318.

Neumann, S., Kahle, P.J., Giasson, B.I., Ozmen, L., Borroni, E., Spooren, W., Muller, V., Odoy, S., Fujiwara, H., Hasegawa, M., Iwatsubo, T., Trojanowski, J.Q., Kretzschmar, H.A., Haass, C., 2002. Misfolded proteinase K-resistant hyperphosphorylated alpha-synuclein in aged transgenic mice with locomotor deterioration and in human alpha-synucleinopathies. J. Clin. Invest. 110, 1429–1439.

Ostrerova, N., Petrucelli, L., Farrer, M., Mehta, N., Alexander, P., Choi, P., Palacino, J., Hardy, J., Wolozin, B., 1999. α-Synuclein shares physical and functional homology with 14-3-3 proteins. J. Neurosci. 19, 5782–5791.

Ostrerova-Golts, N., Petrucelli, L., Hardy, J., Lee, J., Farrer, M., Wolozin, B., 2000. The A53T α-synuclein mutation increases iron-dependent aggregation and toxicity. J. Neurosci. 20, 6048–6054.

Paik, S., Shin, H., Lee, J., Chang, C., Kim, J., 1999. Copper(II)-induced self-oligomerization of α-synuclein. Biochem. J. 340, 821–828.

Paik, S.R., Shin, H.J., Lee, J.H., 2000. Metal-catalyzed oxidation of alpha-synuclein in the presence of copper(II) and hydrogen peroxide. Arch. Biochem. Biophys. 378, 269–277.

Paudel, H.K., 1997. The regulatory Ser262 of microtubule-associated protein tau is phosphorylated by phosphorylase kinase. J. Biol. Chem. 272, 1777–1785.

Perez, R.G., Waymire, J.C., Lin, E., Liu, J.J., Guo, F., Zigmond, M.J., 2002. A role for alpha-synuclein in the regulation of dopamine biosynthesis. J. Neurosci. 22, 3090–3099.

Polymeropoulos, M.H., Lavedan, C., Leroy, E., Ide, S.E., Dehejia, A., Dutra, A., Pike, B., Root, H., Rubenstein, J., Boyer, R., Stenroos, E.S., Chandrasekharappa, S., Athanassiadou, A., Papapetropoulos, T., Johnson, W.G., Lazzarini, A.M., Duvoisin, R.C., Di Iorio, G., Golbe, L.I., Nussbaum, R.L., 1997. Mutation in the alpha-synuclein gene identified in families with Parkinson's disease. Science 276, 2045–2047.

Pronin, A.N., Morris, A.J., Surguchov, A., Benovic, J.L., 2000. Synucleins are a novel class of substrates for G protein-coupled receptor kinases. J. Biol. Chem. 275, 26515–26522.

Sahara, N., Lewis, J., DeTure, M., McGowan, E., Dickson, D.W., Hutton, M., Yen, S.H., 2002. Assembly of tau in transgenic animals expressing P301L tau: alteration of phosphorylation and solubility. J. Neurochem. 83, 1498–1508.

Schlossmacher, M.G., Frosch, M.P., Gai, W.P., Medina, M., Sharma, N., Forno, L., Ochiishi, T., Shimura, H., Sharon, R., Hattori, N., Langston, J.W., Mizuno, Y., Hyman, B.T., Selkoe, D.J., Kosik, K.S., 2002. Parkin localizes to the Lewy bodies of Parkinson disease and dementia with Lewy bodies. Am. J. Pathol. 160, 1655–1667.

Sharma, N., Hewett, J., Ozelius, L.J., Ramesh, V., McLean, P.J., Breakefield, X.O., Hyman, B.T., 2001. A close association of torsinA and alpha-synuclein in Lewy bodies: a fluorescence resonance energy transfer study. Am. J. Pathol. 159, 339–344.

Sharon, R., Goldberg, M.S., Bar-Josef, I., Betensky, R.A., Shen, J., Selkoe, D.J., 2001. alpha-Synuclein occurs in lipid-rich high molecular weight complexes, binds fatty acids, and shows homology to the fatty acid-binding proteins. Proc. Natl. Acad. Sci. U. S. A. 98, 9110–9115.

Shaw, M., Cohen, P., Alessi, D.R., 1998. The activation of protein kinase B by H_2O_2 or heat shock is mediated by phosphoinositide 3-kinase and not by mitogen-activated protein kinase-activated protein kinase-2. Biochem. J. 336 (Pt. 1), 241–246.

Sigurdsson, E.M., Lee, J.M., Dong, X.W., Hejna, M.J., Lorens, S.A., 1997. Laterality in the histological effects of injections of amyloid-beta 25–35 into the amygdala of young Fischer rats. J. Neuropathol. Exp. Neurol. 56, 714–725.

Singleton, A.B., Farrer, M., Johnson, J., Singleton, A., Hague, S., Kachergus, J., Hulihan, M., Peuralinna, T., Dutra, A., Nussbaum, R., Lincoln, S., Crawley, A., Hanson, M., Maraganore, D., Adler, C., Cookson, M.R., Muenter, M., Baptista, M., Miller, D., Blancato, J., Hardy, J., Gwinn-Hardy, K., 2003. alpha-Synuclein locus triplication causes Parkinson's disease. Science 302, 841.

Snyder, H., Mensah, K., Theisler, C., Lee, J., Matouschek, A., Wolozin, B., 2003. Aggregated and monomeric alpha-synuclein bind to the S6′ proteasomal protein and inhibit proteasomal function. J. Biol. Chem. 278, 11753–11759.

Souza, J.M., Giasson, B.I., Lee, V.M., Ischiropoulos, H., 2000. Chaperone-like activity of synucleins. FEBS Lett. 474, 116–119.

Spillantini, M., Schmidt, M., VM-Y, L., Trojanowski, J., Jakes, R., Goedert, M., 1997. α-Synuclein in Lewy bodies. Nature 388, 839–840.

Spillantini, M.G., Bird, T.D., Ghetti, B., 1998a. Frontotemporal dementia and parkinsonism linked to chromosome 17: a new group of tauopathies. Brain Pathol. 8, 387–402.

Spillantini, M.G., Crowther, R.A., Jakes, R., Hasegawa, M., Goedert, M., 1998b. α-Synuclein in filamentous inclusions of Lewy bodies from Parkinson's disease and dementia with Lewy bodies. Proc. Natl. Acad. Sci. U. S. A. 95, 6469–6473.

Strocchi, P., Pession, A., Dozza, B., 2003. Up-regulation of cDK5/p35 by oxidative stress in human neuroblastoma IMR-32 cells. J. Cell. Biochem. 88, 758–765.

Takashima, A., Noguchi, K., Michel, G., Mercken, M., Hoshi, M., Ishiguro, K., Imahori, K., 1996. Exposure of rat hippocampal neurons to amyloid beta peptide (25–35) induces the inactivation of phosphatidyl inositol-3 kinase and the activation of tau protein kinase I/glycogen synthase kinase-3 beta. Neurosci. Lett. 203, 33–36.

Tatebayashi, Y., Miyasaka, T., Chui, D.H., Akagi, T., Mishima, K., Iwasaki, K., Fujiwara, M., Tanemura, K., Murayama, M., Ishiguro, K., Planel, E., Sato, S., Hashikawa, T., Takashima, A., 2002. Tau filament formation and associative memory deficit in aged mice expressing mutant (R406W) human tau. Proc. Natl. Acad. Sci. U. S. A. 99, 13896–13901.

Tsuchiya, K., Ikeda, K., Niizato, K., Watabiki, S., Anno, M., Taki, K., Haga, C., Iritani, S., Matsushita, M., 2002. Parkinson's disease mimicking senile dementia of the Alzheimer type: a clinicopathological study of four autopsy cases. Neuropathology 22, 77–84.

Vincent, I., Jicha, G., Rosado, M., Dickson, D.W., 1997. Aberrant expression of mitotic cdc2/cyclin B1 kinase in degenerating neurons of Alzheimer's disease brain. J. Neurosci. 17, 3588–3598.

Wakabayashi, K., Engelender, S., Yoshimoto, M., Tsuji, S., Ross, C.A., Takahashi, H., 2000. Synphilin-1 is present in Lewy bodies in Parkinson's disease. Ann. Neurol. 47, 521–523.

Wang, Y.H., Fiol, C.J., DePaoli-Roach, A.A., Bell, A.W., Hermodson, M.A., Roach, P.J., 1988. Identification of phosphorylation sites in peptides using a gas-phase sequencer. Anal. Biochem. 174, 537–547.

Wang, Q.M., Fiol, C.J., DePaoli-Roach, A.A., Roach, P.J., 1994. Glycogen synthase kinase-3 beta is a dual specificity kinase differentially regulated by tyrosine and serine/threonine phosphorylation. J. Biol. Chem. 269, 14566–14574.

Wang, J.Z., Wu, Q., Smith, A., Grundke-Iqbal, I., Iqbal, K., 1998. Tau is phosphorylated by GSK-3 at several sites found in Alzheimer disease and its biological activity markedly inhibited only after it is prephosphorylated by A-kinase. FEBS Lett. 436, 28–34.

Zarranz, J.J., Alegre, J., Gomez-Esteban, J.C., Lezcano, E., Ros, R., Ampuero, I., Vidal, L., Hoenicka, J., Rodriguez, O., Atares, B., Llorens, V., Tortosa, E.G., Del Ser, T., Munoz, D.G., De Yebenes, J.G., 2004. The new mutation, E46K, of alpha-synuclein causes Parkinson and Lewy body dementia. Ann. Neurol. 55, 164–173.

Available online at www.sciencedirect.com

SCIENCE DIRECT

Experimental Neurology 192 (2005) 244–250

Experimental Neurology

www.elsevier.com/locate/yexnr

Commentary

α-Synuclein: A potent inducer of tau pathology

James W. Geddes*

Spinal Cord and Brain Injury Research Center and Sanders-Brown Center on Aging, University of Kentucky, 800 South Limestone Street, Lexington, KY 40536-0230, USA

Revised 12 October 2004; accepted 1 December 2004

Lewy bodies and other filamentous α-synuclein inclusions characterize the neuropathology of Parkinson's disease and other 'synucleinopathies,' but are also present in approximately 50% of Alzheimer's disease (AD) cases, for which tau-immunoreactive neurofibrillary tangles and β-amyloid deposits in senile plaques are the defining pathologies. Whether the α-synuclein inclusions in AD represent a co-evolving pathology or contribute to the formation of plaques and tangles has been a subject of debate. The report of Frasier et al., 2004 in this issue demonstrates that α-synuclein aggregation can induce both the fibrillization and aberrant phosphorylation of tau. Overexpression of A30P α-synuclein in a transgenic mouse model resulted in the appearance of phosphorylated tau inclusions. Tau phosphorylated at AT8 and PHF-1 epitopes was detected in sarkosyl-insoluble as well as soluble fractions. In comparison, transgenic mouse models of β-amyloid deposition do not result in the formation of insoluble tau aggregates without the co-expression of mutant human tau. As illustrated by the results of Frasier et al., α-synuclein inclusions are not innocent bystanders, but are potent inducers of tau pathologies in AD and other synucleinopathies. This commentary will review the evidence for, and implications of, this close interrelationship between α-synuclein and tau pathologies in neurodegenerative disorders.

Synucleinopathies and tauopathies. The identification of mutations in α-synuclein in some rare familial Parkinson's disease cases (Kruger et al., 1998; Polymeropoulos et al., 1997) led to the identification of this protein as a principal component of Lewy bodies and related inclusions in disorders collectively referred to as 'synucleinopathies' [(Spillantini et al., 1997), for review, see (Jellinger, 2003)]. The α-synuclein immunoreactive Lewy bodies and filamentous neuritic aggregates (Lewy neurites) are found in neurons in Parkinson's disease, dementia with Lewy bodies, and in both neurons and oligodendrocytes in Neurodegeneration with Brain Iron Accumulation Type 1 (NBIA1; Hallervorden–Spatz syndrome) and multiple system atrophy (Jellinger, 2003). In these synucleinopathies, the sarkosyl-insoluble α-synuclein is phosphorylated, nitrated, and often ubiquitinated (Duda et al., 2000; Hasegawa et al., 2002).

Prior to the discovery of its involvement in Parkinson's disease, α-synuclein pathology was identified in AD. Ueda et al. (1993) identified a 35-amino acid peptide which represented a non-Aβ component (NAC) of insoluble amyloid. The corresponding full-length 140 amino acid protein (NACP) was later shown to be identical to α-synuclein (Iwai et al., 1995). The NAC sequence, residues 61 to 95 of α-synuclein, contains the domain required for α-synuclein self-aggregation and is not conserved in β- and γ-synuclein (Iwai, 2000). Subsequent studies have not found a direct association of α-synuclein and extracellular Aβ, although α-synuclein is detected in the dystrophic neurites decorating senile plaques (Bayer et al., 1999; Culvenor et al., 1999; Wirths et al., 2000) and as neuronal inclusions in familial and sporadic AD cases (Kotzbauer et al., 2001; Lippa et al., 1998).

Insoluble, filamentous neuronal or glial aggregates of hyperphosphorylated tau and neurodegeneration characterize 'tauopathies,' which include AD, corticobasal degeneration (CBD), progressive supranuclear palsy (PSP), Pick's disease, and hereditary frontotemporal dementia and parkinsonism linked to chromosome 17 (FTDP-17) (for review see (Lee et al., 2001). For the sporadic tauopathies CBD and PSP, inherited tau polymorphisms that do not influence the amino acid sequence or splice sites influence susceptibility (Baker et al., 1999; Conrad et al., 1997; Conrad et al., 2004).

Six isoforms of tau are present in the adult human CNS, generated by alternate splicing of a single gene located on

* Fax: +1 859 323 2866.
E-mail address: jgeddes@uky.edu.

doi:10.1016/j.expneurol.2004.12.002

chromosome 17. The tau isoforms prevalent in the sarkosyl-insoluble fraction, and the physical characteristics of the tau filaments formed, differ among the various tauopathies (Buee and Delacourte, 1999). In each of the disorders, the insoluble tau filaments are extensively phosphorylated (for review see (Avila et al., 2004; Buee and Delacourte, 1999). Although 30 phosphorylation sites have been described on the longest tau isoform (441 amino acids), the few sites within the microtubule-binding domains appear to have the greatest influence on tau pathology. Phosphorylation within the microtubule-binding domain (S262, S285, S305, S324, S352, and S356) disrupts tau's ability to stabilize microtubules and promote their assembly. Following detachment from microtubules, tau may self-assemble into paired helical filaments (Alonso et al., 2001), a process facilitated by polyanions and lipids (Barghorn and Mandelkow, 2002; Gamblin et al., 2000; Goedert et al., 1996). However, the relationship between the tau phosphorylation and aggregation is unclear. Tau hyperphosphorylation may promote its aggregation into paired helical filaments (Alonso et al., 2001), or may inhibit PHF assembly (Schneider et al., 1999), depending on the oxidation state or other conditions (Gamblin et al., 2000; Gomez-Ramos et al., 2004; Schweers et al., 1995). Tau phosphorylation is sequential, with some epitopes (T231, S262, T153) being phosphorylated in pre-tangle inclusions, and additional epitopes being phosphorylated in intracellular and extracellular NFTs (Augustinack et al., 2002). Additional tangle-related tau epitopes are conformation dependent and recognized by the MC1 and Alz-50 antibodies (Weaver et al., 2000). Normal tau can be phosphorylated at many of the same sites as PHF tau in situ. However, normal tau is rapidly dephosphorylated postmortem in contrast to PHF tau (Matsuo et al., 1994; Schwab et al., 1994) which is more extensively phosphorylated.

Overlap between tauopathies and synucleinopathies. Although early studies suggested a clear distinction between 'tauopathies' and 'synucleinopathies' (Harrington et al., 1994; Strong et al., 1995), more recent studies demonstrate that there is often an overlap in the clinical symptoms and pathological findings in these disorders. Tau-immunoreactive pathology has been found in each of the synucleinopathies. The incidence of NFTs in Parkinson's disease is much greater than in an age-matched population (Boller et al., 1980). Tau-immunoreactive Lewy bodies are detected in the medulla of 80% of individuals with sporadic Parkinson's disease or dementia with Lewy bodies, where tau is often localized towards the periphery of the Lewy body (Arima et al., 1999; Ishizawa et al., 2003). In familial PD, tau lesions and insoluble tau filaments have been detected in brain tissue obtained at autopsy from two members of the Contursi kindred with the A53T α-synuclein mutation (Duda et al., 2002; Kotzbauer et al., 2004). Tau-immunoreactive NFT's can also be found in NBIA1 (Saito et al., 2000). In multiple system atrophy, hyperphosphorylated tau is associated with a subset of the glial cytoplasmic inclusions, where tau appears to decorate the α-synuclein aggregates (Giasson et al., 2003b).

In AD, Lewy bodies composed largely of α-synuclein are detected in up to 60% of sporadic cases where they are found most frequently in the amygdala (Arai et al., 2001; Hamilton, 2000; Parkkinen et al., 2003). Similarly, amygdala Lewy bodies are found in 63% of familial AD and 50% of aged Down syndrome cases (Lippa et al., 1998, 1999). Additional non-Lewy body α-synuclein-positive inclusions are most prevalent in the hippocampus of AD cases, a region in which few Lewy bodies are typically found (Arai et al., 2001). Of interest is that some neurons appear to have predilection to develop Lewy bodies, while other neurons are more susceptible to NFTs. In neurons vulnerable to Lewy bodies, tau immunoreactivity is localized towards the periphery of the lesion. In neurons prone to develop NFTs, the α-synuclein immunoreactive inclusions are smaller than Lewy bodies. Rare examples of filaments containing both tau and α-synuclein have been identified, but in most cases, the two proteins are segregated to distinct filaments.

In tauopathies other than AD, α-synuclein inclusions have only rarely been found. In a report from Takeda et al. (2000), an antibody against the C-terminus of α-synuclein immunostained neuronal and glial tau inclusions in CBD, PSP, and Pick's disease following protease K pretreatment of paraffin sections, However, antibodies against other domains of α-synuclein were negative. Tsuboi et al. (2003) identified mild α-synuclein pathology in the anterior olfactory nucleus in a small subset of individuals with PSP. These rare reports of α-synuclein pathology in tauopathies contrast with the almost ubiquitous presence of tau pathology in synucleinopathies.

Transgenic models. The frequent co-localization of α-synuclein and tau immunoreactivity in synucleinopathies and AD could reflect a synergistic relationship between the two proteins in promoting pathology, influence of a common underlying mechanism on the two proteins, or the effects of independent age-related mechanisms. Transgenic mouse models of both tauopathies and synucleinopathies have provided important insights into the relationship between tau and α-synuclein.

Overexpression of familial AD mutations in mice, including amyloid precursor protein (APP), presenilin 1 (PS1), and presenilin 2, has resulted in several excellent models of senile plaque pathology (Gotz et al., 2004), but not in neurofibrillary tangles or α-synuclein deposits. Phosphorylated tau epitopes can be detected in dystrophic neurites near the Aβ deposits (Kurt et al., 2003; Moechars et al., 1999; Sturchler-Pierrat et al., 1997), but there is no evidence of the formation of insoluble tau filaments (Xu et al., 2002). Transgenic mice expressing human mutant tau display many aspects of tau pathology in AD and other tauopathies, including the appearance of straight or helical filaments, hyperphosphorylation, and ubiquitination (for review, see (Gotz et al., 2004; Lee et al., 2001). However,

inclusions of α-synuclein or accumulations of β-amyloid have not been identified in any of the tau/FTDP-17 single-transgenic models.

Overexpression of mutant human A53T or A30P, but not wild-type α-synuclein, in mice results in the appearance of detergent insoluble α-synuclein, cytoplasmic inclusions, and motor dysfunction (Giasson et al., 2003a,b; Kahle et al., 2001; Lee et al., 2002; Sampathu et al., 2003). Within the inclusions, α-synuclein is phosphorylated and often ubiquitinated (Giasson et al., 2002; Neumann et al., 2002), closely resembling α-synuclein inclusions in human synucleinopathies. Approximately half of the brains from one line of symptomatic A53T mice exhibited tau-immunoreactive inclusions in the form of threads, grains, spheroids, and pre-tangle neurons (Giasson et al., 2003a). These were occasionally co-localized with α-synuclein inclusions in affected regions (pons, midbrain, spinal cord), but could also be found independent of α-synuclein pathology. The tau inclusions were detected using a rabbit polyclonal antibody that does not provide information on tau phosphorylation, and the solubility of tau was not evaluated.

The Frasier et al. study in this issue is the first to demonstrate the appearance of phosphorylated, sarkosyl-insoluble, tau in a transgenic mouse model of synucleinopathy (Frasier et al., 2004). Mice overexpressing A30P α-synuclein and symptomatic for motor abnormalities developed tau-immunoreactive inclusions and detergent-insoluble tau that were immunoreactive with PHF-1 (pS396/S404 epitope) and AT8 (pS202/T205 epitope) antibodies. The neurons that accumulated tau inclusions were spatially distinct from those exhibiting α-synuclein inclusions, although some of the PHF-1-positive neurons exhibited punctate α-synuclein immunoreactivity. This is similar to human synucleinopathies and AD, where neurons appear to show a predilection for either α-synuclein or tau pathology.

Tau pathology in P301L transgenic mice is observed primarily in the brainstem and spinal cord. However, when P301L tau is expressed along with hAPP in double- or triple (hAPP/hPS1/htau) transgenic models, both plaque and tangle-like structures are detected in the cortex and hippocampus (Lewis et al., 2001; Oddo et al., 2003). The tangle-like tau inclusions are not localized to the vicinity of the β-amyloid deposits, but in neurons that project to the deposits (Lewis et al., 2001; Oddo et al., 2003). These studies provide strong support for the amyloid cascade hypothesis (Hardy and Higgins, 1992) and demonstrate that Aβ not only facilitates the development of tau pathology, but also shifts the localization of the tau-immunoreactive lesions to limbic and cortical areas that did not exhibit tangles in singly transgenic P301L mice. Similarly, in double transgenic mice expressing wild type human α-synuclein and wild-type human APP, α-synuclein inclusions are detected in neocortical regions in contrast to their brain stem localization in mice overexpressing wild type human α-synuclein (Masliah et al., 2001). This is similar to the results obtained with mice expressing hAPP and P301L tau (Lewis et al., 2001; Oddo et al., 2003) and demonstrates that β-amyloid can enhance both α-synuclein and tau pathology, and shift the lesions to limbic and cortical structures. Conversely, α-synuclein and tau overexpression does not alter β-amyloid pathology.

Similarities between α-synuclein, tau, and β-amyloid. Tau and α-synuclein share many physical and biochemical properties (Dickson, 1999; Lee et al., 2004). Both are natively unfolded, heat stable proteins (Syme et al., 2002). Both are abundant in neurons and enriched in presynaptic locations, with tau being prevalent in axons (Binder et al., 1985) and α-synuclein localized to presynaptic terminals (Iwai et al., 1995). Both proteins aggregate through their hydrophobic domains that form the core of the resultant fibrils (Giasson et al., 2001; Ksiezak-Reding and Yen, 1991). The fibrils formed from both proteins exhibit protease resistance and sarkosyl insolubility. Moreover, the insoluble fibrils of both proteins are hyperphosphorylated (Grundke-Iqbal et al., 1986; Hasegawa et al., 2002; Ihara et al., 1986), nitrated (Horiguchi et al., 2003), and more mature forms of the aggregated fibrils are ubiquitinated (Hasegawa et al., 2002; Iqbal et al., 1998). Tau fibrillization can be induced by α-synuclein, but not by β- or γ-synuclein, and tau can enhance α-synuclein fibrillization in vitro. Following co-incubation of tau and α-synuclein, homopolymers of 10–15 nm filaments predominate although co-polymers can be detected (Giasson et al., 2003a).

Oligomeric aggregates of α-synuclein have properties similar to oligomers of amyloid β-protein. Both are recognized by a polyclonal antibody developed against Aβ oligomers, and fibrillar forms of both proteins contain β-pleated sheets (Kayed et al., 2003). When applied to cell membranes, oligomers of both proteins form pores that resemble those caused by bacterial toxins such as lysozyme, and result in increased membrane conductance, possibly due to membrane permeabilization (Glabe et al., 2004; Lashuel et al., 2002).

Other amyloidogenic proteins. With physical properties of α-synuclein aggregates resembling aspects of both tau and β-amyloid, which property is responsible for the tau aggregation and phosphorylation observed in the A30P transgenic mice? Hints are obtained from other amyloidogenic proteins, including prion proteins and the aBri protein which accumulates in familial British dementia.

Prion proteins and aBRi can form soluble oligomers similar to those formed by β-amyloid and α-synucleinand cause similar toxicity in cultured cells (El-Agnaf et al., 2001; Kayed et al., 2003; Srinivasan et al., 2004). α-Synuclein immunoreactive deposits are found close to, but not co-localized with, prion aggregates in several animal and human prion disorders (Haik et al., 2002). One familial prion disorder, Gerstmann–Sträussler–Scheinker syndrome

(GSS), is associated with prion-immunoreactive cerebral amyloid deposits and with neurofibrillary tangles in some families (Ghetti et al., 1994; Ishizawa et al., 2002). Familial British dementia is a rare form of cerebral amyloidosis caused by a mutation in the stop codon for the BRI gene. resulting in accumulation of the abnormal C-terminal amyloidogenic fragment ABri (Kim et al., 1999). Tau-positive neurofibrillary tangles and neuropil threads are found in the brain regions that accumulate ABri (Holton et al., 2001), but the presence or absence of α-synuclein aggregates has not been evaluated. Together, these results indicate that amyloidogenic proteins other than Aβ can induce both tau and α-synuclein pathology.

Summary, conclusions, and speculation. The report of Frasier et al., 2004 in this issue, combined with previous studies, demonstrate that α-synuclein aggregation is a potent inducer of tau aggregation and tau phosphorylation. Tau pathology has been identified in each of the synucleinopathies and in transgenic mouse models of these disorders. The tau pathology observed in the A30P mouse was greater than that detected in any of the hAPP transgenic models that do not also express human tau, leading to the conclusion that α-synuclein is a more potent inducer of tau pathology than β-amyloid.

The potency of α-synuclein as a promoter of tau pathology may reflect both its tau-like and Aβ-like properties. In vitro, α-synuclein can promote tau aggregation and can also aggregate into oligomers that form annular pore-like protofibrils, similar to Aβ, prion protein, and ABri (Sokolowski et al., 2003). Intracellular accumulations of each of these proteins are associated with the formation of neurofibrillary tangles composed of tau protein. Prion and Aβ aggregates are also associated with α-synuclein pathology, in the form of Lewy bodies or other inclusions.

The presence of tau pathology in each of the α-synucleinopathies, and the presence of both tau and α-synuclein pathology in most disorders associated with the intracellular or extracellular accumulation of amyloidogenic proteins, leads to the conclusion that α-synuclein aggregates play an essential role in the development of tau pathology. One argument against this is that α-synuclein inclusions have not been found in all AD cases, although they are identified in up to 60% of both sporadic and familial AD cases. However, increasing evidence suggests that the oligomers of α-synuclein represent the toxic form (el-Agnaf and Irvine, 2002; Lashuel et al., 2002), with larger aggregates possibly being protective. This is strikingly similar to the role of oligomers in β-amyloid toxicity (Klein et al., 2001). As noted by Frasier et al, phosphorylated tau inclusions in A30P α-synuclein mice were detected in neurons in which α-synuclein aggregates were either punctate or not detected. Neurons that contained larger α-synuclein inclusions did not exhibit the phosphorylated tau inclusions. Oligomeric forms of α-synuclein are likely not detected in AD, suggesting that α-synuclein may contribute to tau pathology even in cases in which larger α-synuclein inclusions are not found.

It is tempting to speculate on the mechanisms linking the α-synuclein, tau, and Aβ pathologies. One attractive possibility mentioned briefly by Frasier et al., 2004 is proteasome inhibition. β-amyloid, tau, and α-synuclein can each be degraded via the 26S proteasome, and their aggregates can inhibit proteasome activity (Bennett et al., 1999; Gregori et al., 1995; Keck et al., 2003; Lindersson et al., 2004; Lopez Salon et al., 2003). Recently, Oddo et al. (2004) elegantly demonstrated that removal of β-amyloid deposits by immunotherapy also allows phosphorylated tau in early stage tangles to be degraded via the proteasome. There is also ample evidence linking proteasome inhibition to the accumulation and aggregation of α-synuclein (McNaught et al., 2004; Rideout et al., 2001). Proteasome inhibition also results in the activation of c-jun N-terminal kinase (JNK) (Ishizawa et al., 2004; Sang et al., 2002), implicated by Frasier et al., 2004 in the tau phosphorylation observed in A30P mice. In addition to the α-synuclein mutations, mutations in other components of the ubiquitin-proteasome system, such as parkin and ubiquitin C-terminal hydrolase L1, are associated with familial PD and the accumulation of α-synuclein (Kitada et al., 1998; Liu et al., 2002).

Together, the above results suggest the following model. Deposits of Aβ and similar proteins result in proteasome inhibition, leading to the accumulation of α-synuclein and tau, and JNK activation. α-Synuclein aggregation facilitates tau fibrillization, although the spatial separation of α-synuclein and tau pathologies in the A30P mice and in synucleinopathies suggests that small oligomers of α-synuclein may be the primary culprit. The α-synuclein oligomers cause further proteasome inhibition and impair cellular transport, exacerbating tau accumulation and promoting the aggregation of tau into filamentous structures.

In summary, inclusions of α-synuclein in human disorders and transgenic animal models, in the presence or absence of β-amyloid or similar proteins, are invariably associated with tau pathologies. In contrast, tau inclusions in FTDP-17 tauopathies and related animal models do not result in the accumulation of β-amyloid and only rarely are associated with α-synuclein pathology. Together, the results demonstrate that α-synuclein aggregates are potent inducers of tau pathologies in synucleinopathies, including the most prevalent synucleinopathy-AD.

References

Alonso, A., Zaidi, T., Novak, M., Grundke-Iqbal, I., Iqbal, K., 2001. Hyperphosphorylation induces self-assembly of tau into tangles of paired helical filaments/straight filaments. Proc. Natl. Acad. Sci. U. S. A. 98, 6923–6928.

Arai, Y., Yamazaki, M., Mori, O., Muramatsu, H., Asano, G., Katayama, Y., 2001. Alpha-synuclein-positive structures in cases with sporadic Alzheimer's disease: morphology and its relationship to tau aggregation. Brain Res. 888, 287–296.

Arima, K., Hirai, S., Sunohara, N., Aoto, K., Izumiyama, Y., Ueda, K., Ikeda, K., Kawai, M., 1999. Cellular co-localization of phosphorylated tau- and NACP/alpha-synuclein-epitopes in Lewy bodies in sporadic Parkinson's disease and in dementia with Lewy bodies. Brain Res. 843, 53–61.

Augustinack, J.C., Schneider, A., Mandelkow, E.M., Hyman, B.T., 2002. Specific tau phosphorylation sites correlate with severity of neuronal cytopathology in Alzheimer's disease. Acta Neuropathol. (Berl.) 103, 26–35.

Avila, J., Lucas, J.J., Perez, M.A.R., Hernandez, F., 2004. Role of tau protein in both physiological and pathological conditions. Physiol. Rev. 84, 361–384.

Baker, M., Litvan, I., Houlden, H., Adamson, J., Dickson, D., Perez-Tur, J., Hardy, J., Lynch, T., Bigio, E., Hutton, M., 1999. Association of an extended haplotype in the tau gene with progressive supranuclear palsy. Hum. Mol. Genet. 8, 711–715.

Barghorn, S., Mandelkow, E., 2002. Toward a unified scheme for the aggregation of tau into Alzheimer paired helical filaments. Biochemistry 41, 14885–14896.

Bayer, T.A., Jakala, P., Hartmann, T., Havas, L., McLean, C., Culvenor, J.G., Li, Q.X., Masters, C.L., Falkai, P., Beyreuther, K., 1999. Alpha-synuclein accumulates in Lewy bodies in Parkinson's disease and dementia with Lewy bodies but not in Alzheimer's disease beta-amyloid plaque cores. Neurosci. Lett. 266, 213–216.

Bennett, M.C., Bishop, J.F., Leng, Y., Chock, P.B., Chase, T.N., Mouradian, M.M., 1999. Degradation of alpha-synuclein by proteasome. J. Biol. Chem. 274, 33855–33858.

Binder, L.I., Frankfurter, A., Rebhun, L.I., 1985. The distribution of tau in the mammalian central nervous system. J. Cell Biol. 101, 1371–1378.

Boller, F., Mizutani, T., Roessmann, U., Gambetti, P., 1980. Parkinson disease, dementia, and Alzheimer disease: clinicopathological correlations. Ann. Neurol. 7, 329–335.

Buee, L., Delacourte, A., 1999. Comparative biochemistry of tau in progressive supranuclear palsy, corticobasal degeneration, FTDP-17 and Pick's disease. Brain Pathol. 9, 681–693.

Conrad, C., Andreadis, A., Trojanowski, J.Q., Dickson, D.W., Kang, D., Chen, X., Wiederholt, W., Hansen, L., Masliah, E., Thal, L.J., Katzman, R., Xia, Y., Saitoh, T., 1997. Genetic evidence for the involvement of tau in progressive supranuclear palsy. Ann. Neurol. 41, 277–281.

Conrad, C., Vianna, C., Schultz, C., Thal, D.R., Ghebremedhin, E., Lenz, J., Braak, H., Davies, P., 2004. Molecular evolution and genetics of the Saitohin gene and tau haplotype in Alzheimer's disease and argyrophilic grain disease. J. Neurochem. 89, 179–188.

Culvenor, J.G., McLean, C.A., Cutt, S., Campbell, B.C., Maher, F., Jakala, P., Hartmann, T., Beyreuther, K., Masters, C.L., Li, Q.X., 1999. Non-Abeta component of Alzheimer's disease amyloid (NAC) revisited. NAC and alpha-synuclein are not associated with Abeta amyloid. Am. J. Pathol. 155, 1173–1181.

Dickson, D.W., 1999. Tau and synuclein and their role in neuropathology. Brain Pathol. 9, 657–661.

Duda, J.E., Giasson, B.I., Chen, Q., Gur, T.L., Hurtig, H.I., Stern, M.B., Gollomp, S.M., Ischiropoulos, H., Lee, V.M., Trojanowski, J.Q., 2000. Widespread nitration of pathological inclusions in neurodegenerative synucleinopathies. Am. J. Pathol. 157, 1439–1445.

Duda, J.E., Giasson, B.I., Mabon, M.E., Miller, D.C., Golbe, L.I., Lee, V.M., Trojanowski, J.Q., 2002. Concurrence of alpha-synuclein and tau brain pathology in the Contursi kindred. Acta Neuropathol. (Berl.) 104, 7–11.

el-Agnaf, O.M., Irvine, G.B., 2002. Aggregation and neurotoxicity of alpha-synuclein and related peptides. Biochem. Soc. Trans. 30, 559–565.

El-Agnaf, O.M., Nagala, S., Patel, B.P., Austen, B.M., 2001. Non-fibrillar oligomeric species of the amyloid ABri peptide, implicated in familial British dementia, are more potent at inducing apoptotic cell death than protofibrils or mature fibrils. J. Mol. Biol. 310, 157–168.

Frasier, M., Walzer, M., McCarthy, L., Magnuson, D., Lee, J.M., Haas, C., Kahle, P., Wolozin, B., 2001. Tau phosphorylation increases in symptomatic mice over-expressing A30P α-synuclein. Exp. Neurol. 192, 274–287 (doi:10.1016/j.expneurol.2004.07.016).

Gamblin, T.C., King, M.E., Kuret, J., Berry, R.W., Binder, L.I., 2000. Oxidative regulation of fatty acid-induced tau polymerization. Biochemistry 39, 14203–14210.

Ghetti, B., Tagliavini, F., Giaccone, G., Bugiani, O., Frangione, B., Farlow, M.R., Dlouhy, S.R., 1994. Familial Gerstmann–Straussler–Scheinker disease with neurofibrillary tangles. Mol. Neurobiol. 8, 41–48.

Giasson, B.I., Murray, I.V., Trojanowski, J.Q., Lee, V.M., 2001. A hydrophobic stretch of 12 amino acid residues in the middle of alpha-synuclein is essential for filament assembly. J. Biol. Chem. 276, 2380–2386.

Giasson, B.I., Duda, J.E., Quinn, S.M., Zhang, B., Trojanowski, J.Q., Lee, V.M., 2002. Neuronal alpha-synucleinopathy with severe movement disorder in mice expressing A53T human alpha-synuclein. Neuron 34, 521–533.

Giasson, B.I., Forman, M.S., Higuchi, M., Golbe, L.I., Graves, C.L., Kotzbauer, P.T., Trojanowski, J.Q., Lee, V.M., 2003a. Initiation and synergistic fibrillization of tau and alpha-synuclein. Science 300, 636–640.

Giasson, B.I., Mabon, M.E., Duda, J.E., Montine, T.J., Robertson, D., Hurtig, H.I., Lee, V.M., Trojanowski, J.Q., 2003b. Tau and 14-3-3 in glial cytoplasmic inclusions of multiple system atrophy. Acta Neuropathol. (Berl.) 106, 243–250.

Glabe, C.G., Kayed, R., Sokolov, Y., Hall, J., 2004. Common structure and mechanism of soluble amyloid oligomer pathogenesis in degenerative diseases. Neurobiol. Aging 25, 75.

Goedert, M., Jakes, R., Spillantini, M.G., Hasegawa, M., Smith, M.J., Crowther, R.A., 1996. Assembly of microtubule-associated protein tau into Alzheimer-like filaments induced by sulphated glycosaminoglycans. Nature 383, 550–553.

Gomez-Ramos, A., Smith, M.A., Perry, G., Avila, J., 2004. Tau phosphorylation and assembly. Acta Neurobiol. Exp. (Wars) 64, 33–39.

Gotz, J., Streffer, J.R., David, D., Schild, A., Hoerndli, F., Pennanen, L., Kurosinski, P., Chen, F., 2004. Transgenic animal models of Alzheimer's disease and related disorders: histopathology, behavior and therapy. Mol. Psychiatry 9, 664–683.

Gregori, L., Fuchs, C., Figueiredo-Pereira, M.E., Van Nostrand, W.E., Goldgaber, D., 1995. Amyloid beta-protein inhibits ubiquitin-dependent protein degradation in vitro. J. Biol. Chem. 270, 19702–19708.

Grundke-Iqbal, I., Iqbal, K., Tung, Y.C., Quinlan, M., Wisniewski, H.M., Binder, L.I., 1986. Abnormal phosphorylation of the microtubule-associated protein tau (tau) in Alzheimer cytoskeletal pathology. Proc. Natl. Acad. Sci. U. S. A. 83, 4913–4917.

Haik, S., Privat, N., Adjou, K.T., Sazdovitch, V., Dormont, D., Duyckaerts, C., Hauw, J.J., 2002. Alpha-synuclein-immunoreactive deposits in human and animal prion diseases. Acta Neuropathol. (Berl.) 103, 516–520.

Hamilton, R.L., 2000. Lewy bodies in Alzheimer's disease: a neuropathological review of 145 cases using alpha-synuclein immunohistochemistry. Brain Pathol. 10, 378–384.

Hardy, J.A., Higgins, G.A., 1992. Alzheimer's disease: the amyloid cascade hypothesis. Science 256, 184–185.

Harrington, C.R., Perry, R.H., Perry, E.K., Hurt, J., McKeith, I.G., Roth, M., Wischik, C.M., 1994. Senile dementia of Lewy body type and Alzheimer type are biochemically distinct in terms of paired helical filaments and hyperphosphorylated tau protein. Dementia 5, 215–228.

Hasegawa, M., Fujiwara, H., Nonaka, T., Wakabayashi, K., Takahashi, H., Lee, V.M., Trojanowski, J.Q., Mann, D., Iwatsubo, T., 2002. Phosphorylated alpha-synuclein is ubiquitinated in alpha-synucleinopathy lesions. J. Biol. Chem. 277, 49071–49076.

Holton, J.L., Ghiso, J., Lashley, T., Rostagno, A., Guerin, C.J., Gibb, G., Houlden, H., Ayling, H., Martinian, L., Anderton, B.H., Wood, N.W., Vidal, R., Plant, G., Frangione, B., Revesz, T., 2001. Regional distribution of amyloid-Bri deposition and its association with neuro-

fibrillary degeneration in familial British dementia. Am. J. Pathol. 158, 515–526.
Horiguchi, T., Uryu, K., Giasson, B.I., Ischiropoulos, H., LightFoot, R., Bellmann, C., Richter-Landsberg, C., Lee, V.M., Trojanowski, J.Q., 2003. Nitration of tau protein is linked to neurodegeneration in tauopathies. Am. J. Pathol. 163, 1021–1031.
Ihara, Y., Nukina, N., Miura, R., Ogawara, M., 1986. Phosphorylated tau protein is integrated into paired helical filaments in Alzheimer's disease. J. Biochem. (Tokyo) 99, 1807–1810.
Iqbal, K., Alonso, A.C., Gong, C.X., Khatoon, S., Pei, J.J., Wang, J.Z., Grundke-Iqbal, I., 1998. Mechanisms of neurofibrillary degeneration and the formation of neurofibrillary tangles. J. Neural Transm. 53, 169–180 (Suppl.).
Ishizawa, K., Komori, T., Shimazu, T., Yamamoto, T., Kitamoto, T., Shimazu, K., Hirose, T., 2002. Hyperphosphorylated tau deposition parallels prion protein burden in a case of Gerstmann–Straussler–Scheinker syndrome P102L mutation complicated with dementia. Acta Neuropathol. (Berl.) 104, 342–350.
Ishizawa, T., Mattila, P., Davies, P., Wang, D., Dickson, D.W., 2003. Colocalization of tau and alpha-synuclein epitopes in Lewy bodies. J. Neuropathol. Exp. Neurol. 62, 389–397.
Ishizawa, J., Yoshida, S., Oya, M., Mizuno, R., Shinojima, T., Marumo, K., Murai, M., 2004. Inhibition of the ubiquitin-proteasome pathway activates stress kinases and induces apoptosis in renal cancer cells. Int. J. Oncol. 25, 697–702.
Iwai, A., 2000. Properties of NACP/alpha-synuclein and its role in Alzheimer's disease. Biochim. Biophys. Acta 1502, 95–109.
Iwai, A., Masliah, E., Yoshimoto, M., Ge, N., Flanagan, L., de Silva, H.A., Kittel, A., Saitoh, T., 1995. The precursor protein of non-A beta component of Alzheimer's disease amyloid is a presynaptic protein of the central nervous system. Neuron 14, 467–475.
Jellinger, K.A., 2003. Neuropathological spectrum of synucleinopathies. Mov. Disord. 18 (Suppl. 6), S2–S12.
Kahle, P.J., Neumann, M., Ozmen, L., Muller, V., Odoy, S., Okamoto, N., Jacobsen, H., Iwatsubo, T., Trojanowski, J.Q., Takahashi, H., Wakabayashi, K., Bogdanovic, N., Riederer, P., Kretzschmar, H.A., Haass, C., 2001. Selective insolubility of alpha-synuclein in human Lewy body diseases is recapitulated in a transgenic mouse model. Am. J. Pathol. 159, 2215–2225.
Kayed, R., Head, E., Thompson, J.L., McIntire, T.M., Milton, S.C., Cotman, C.W., Glabe, C.G., 2003. Common structure of soluble amyloid oligomers implies common mechanism of pathogenesis. Science 300, 486–489.
Keck, S., Nitsch, R., Grune, T., Ullrich, O., 2003. Proteasome inhibition by paired helical filament-tau in brains of patients with Alzheimer's disease. J. Neurochem. 85, 115–122.
Kim, S.H., Wang, R., Gordon, D.J., Bass, J., Steiner, D.F., Lynn, D.G., Thinakaran, G., Meredith, S.C., Sisodia, S.S., 1999. Furin mediates enhanced production of fibrillogenic ABri peptides in familial British dementia. Nat. Neurosci. 2, 984–988.
Kitada, T., Asakawa, S., Hattori, N., Matsumine, H., Yamamura, Y., Minoshima, S., Yokochi, M., Mizuno, Y., Shimizu, N., 1998. Mutations in the parkin gene cause autosomal recessive juvenile parkinsonism. Nature 392, 605–608.
Klein, W.L., Krafft, G.A., Finch, C.E., 2001. Targeting small Abeta oligomers: the solution to an Alzheimer's disease conundrum. Trends Neurosci. 24, 219–224.
Kotzbauer, P.T., Trojanowsk, J.Q., Lee, V.M., 2001. Lewy body pathology in Alzheimer's disease. J. Mol. Neurosci. 17, 225–232.
Kotzbauer, P.T., Giasson, B.I., Kravitz, A.V., Golbe, L.I., Mark, M.H., Trojanowski, J.Q., Lee, V.M., 2004. Fibrillization of alpha-synuclein and tau in familial Parkinson's disease caused by the A53T alpha-synuclein mutation. Exp. Neurol. 187, 279–288.
Kruger, R., Kuhn, W., Muller, T., Woitalla, D., Graeber, M., Kosel, S., Przuntek, H., Epplen, J.T., Schols, L., Riess, O., 1998. Ala30Pro mutation in the gene encoding alpha-synuclein in Parkinson's disease. Nat. Genet. 18, 106–108.
Ksiezak-Reding, H., Yen, S.H., 1991. Structural stability of paired helical filaments requires microtubule-binding domains of tau: a model for self-association. Neuron 6, 717–728.
Kurt, M.A., Davies, D.C., Kidd, M., Duff, K., Howlett, D.R., 2003. Hyperphosphorylated tau and paired helical filament-like structures in the brains of mice carrying mutant amyloid precursor protein and mutant presenilin-1 transgenes. Neurobiol. Dis. 14, 89–97.
Lashuel, H.A., Petre, B.M., Wall, J., Simon, M., Nowak, R.J., Walz, T., Lansbury Jr., P.T., 2002. Alph-synuclein, especially the Parkinson's disease-associated mutants, forms pore-like annular and tubular protofibrils. J. Mol. Biol. 322, 1089–1102.
Lee, V.M., Goedert, M., Trojanowski, J.Q., 2001. Neurodegenerative tauopathies. Annu. Rev. Neurosci. 24, 1121–1159.
Lee, M.K., Stirling, W., Xu, Y., Xu, X., Qui, D., Mandir, A.S., Dawson, T.M., Copeland, N.G., Jenkins, N.A., Price, D.L., 2002. Human alpha-synuclein-harboring familial Parkinson's disease-linked Ala-53- > Thr mutation causes neurodegenerative disease with alpha-synuclein aggregation in transgenic mice. Proc. Natl. Acad. Sci. U. S. A. 99, 8968–8973.
Lee, V.M., Giasson, B.I., Trojanowski, J.Q., 2004. More than just two peas in a pod: common amyloidogenic properties of tau and alpha-synuclein in neurodegenerative diseases. Trends Neurosci. 27, 129–134.
Lewis, J., Dickson, D.W., Lin, W.L., Chisholm, L., Corral, A., Jones, G., Yen, S.H., Sahara, N., Skipper, L., Yager, D., Eckman, C., Hardy, J., Hutton, M., McGowan, E., 2001. Enhanced neurofibrillary degeneration in transgenic mice expressing mutant tau and APP. Science 293, 1487–1491.
Lippa, C.F., Fujiwara, H., Mann, D.M., Giasson, B., Baba, M., Schmidt, M.L., Nee, L.E., O'Connell, B., Pollen, D.A., St George-Hyslop, P., Ghetti, B., Nochlin, D., Bird, T.D., Cairns, N.J., Lee, V.M., Iwatsubo, T., Trojanowski, J.Q., 1998. Lewy bodies contain altered alpha-synuclein in brains of many familial Alzheimer's disease patients with mutations in presenilin and amyloid precursor protein genes. Am. J. Pathol. 153, 1365–1370.
Lippa, C.F., Schmidt, M.L., Lee, V.M., Trojanowski, J.Q., 1999. Antibodies to alpha-synuclein detect Lewy bodies in many Down's syndrome brains with Alzheimer's disease. Ann. Neurol. 45, 353–357.
Lindersson, E., Beedholm, R., Hojrup, P., Moos, T., Gai, W., Hendil, K.B., Jensen, P.H., 2004. Proteasomal inhibition by alpha-synuclein filaments and oligomers. J. Biol. Chem. 279, 12924–12934.
Liu, Y., Fallon, L., Lashuel, H.A., Liu, Z., Lansbury Jr., P.T., 2002. The UCH-L1 gene encodes two opposing enzymatic activities that affect alpha-synuclein degradation and Parkinson's disease susceptibility. Cell 111, 209–218.
Lopez Salon, M., Pasquini, L., Besio Moreno, M., Pasquini, J.M., Soto, E., 2003. Relationship between beta-amyloid degradation and the 26S proteasome in neural cells. Exp. Neurol. 180, 131–143.
Masliah, E., Rockenstein, E., Veinbergs, I., Sagara, Y., Mallory, M., Hashimoto, M., Mucke, L., 2001. beta-amyloid peptides enhance alpha-synuclein accumulation and neuronal deficits in a transgenic mouse model linking Alzheimer's disease and Parkinson's disease. Proc. Natl. Acad. Sci. U. S. A. 98, 12245–12250.
Matsuo, E.S., Shin, R.W., Billingsley, M.L., Van de Voorde, A., O'Connor, M., Trojanowski, J.Q., Lee, V.M., 1994. Biopsy-derived adult human brain tau is phosphorylated at many of the same sites as Alzheimer's disease paired helical filament tau. Neuron 13, 989–1002.
McNaught, K.S., Perl, D.P., Brownell, A.L., Olanow, C.W., 2004. Systemic exposure to proteasome inhibitors causes a progressive model of Parkinson's disease. Ann. Neurol. 56, 149–162.
Moechars, D., Dewachter, I., Lorent, K., Reverse, D., Baekelandt, V., Naidu, A., Tesseur, I., Spittaels, K., Haute, C.V., Checler, F., Godaux, E., Cordell, B., Van Leuven, F., 1999. Early phenotypic changes in transgenic mice that overexpress different mutants of amyloid precursor protein in brain. J. Biol. Chem. 274, 6483–6492.
Neumann, M., Kahle, P.J., Giasson, B.I., Ozmen, L., Borroni, E., Spooren, W., Muller, V., Odoy, S., Fujiwara, H., Hasegawa, M., Iwatsubo, T., Trojanowski, J.Q., Kretzschmar, H.A., Haass, C., 2002. Misfolded

proteinase K-resistant hyperphosphorylated alpha-synuclein in aged transgenic mice with locomotor deterioration and in human alpha-synucleinopathies. J. Clin. Invest. 110, 1429–1439.

Oddo, S., Caccamo, A., Shepherd, J.D., Murphy, M.P., Golde, T.E., Kayed, R., Metherate, R., Mattson, M.P., Akbari, Y., LaFerla, F.M., 2003. Triple-transgenic model of Alzheimer's disease with plaques and tangles: intracellular Abeta and synaptic dysfunction. Neuron 39, 409–421.

Oddo, S., Billings, L., Kesslak, J.P., Cribbs, D.H., LaFerla, F.M., 2004. Abeta immunotherapy leads to clearance of early, but not late, hyperphosphorylated tau aggregates via the proteasome. Neuron 43, 321–332.

Parkkinen, L., Soininen, H., Alafuzoff, I., 2003. Regional distribution of alpha-synuclein pathology in unimpaired aging and Alzheimer disease. J. Neuropathol. Exp. Neurol. 62, 363–367.

Polymeropoulos, M.H., Lavedan, C., Leroy, E., Ide, S.E., Dehejia, A., Dutra, A., Pike, B., Root, H., Rubenstein, J., Boyer, R., Stenroos, E.S., Chandrasekharappa, S., Athanassiadou, A., Papapetropoulos, T., Johnson, W.G., Lazzarini, A.M., Duvoisin, R.C., Di Iorio, G., Golbe, L.I., Nussbaum, R.L., 1997. Mutation in the alpha-synuclein gene identified in families with Parkinson's disease. Science 276, 2045–2047.

Rideout, H.J., Larsen, K.E., Sulzer, D., Stefanis, L., 2001. Proteasomal inhibition leads to formation of ubiquitin/alpha-synuclein-immunoreactive inclusions in PC12 cells. J. Neurochem. 78, 899–908.

Saito, Y., Kawai, M., Inoue, K., Sasaki, R., Arai, H., Nanba, E., Kuzuhara, S., Ihara, Y., Kanazawa, I., Murayama, S., 2000. Widespread expression of alpha-synuclein and tau immunoreactivity in Hallervorden–Spatz syndrome with protracted clinical course. J. Neurol. Sci. 177, 48–59.

Sampathu, D.M., Giasson, B.I., Pawlyk, A.C., Trojanowski, J.Q., Lee, V.M., 2003. Ubiquitination of alpha-synuclein is not required for formation of pathological inclusions in alpha-synucleinopathies. Am. J. Pathol. 163, 91–100.

Sang, C., Kobayashi, Y., Du, J., Katsumo, M., Adachi, H., Doyu, M., Sobue, G., 2002. c-Jun N-terminal kinase pathway mediates lactacystin-induced cell death in a neuronal differentiated Neuro2a cell line. Brain Res. Mol. Brain Res. 108, 7–17.

Schneider, A., Biernat, J., von Bergen, M., Mandelkow, E., Mandelkow, E.M., 1999. Phosphorylation that detaches tau protein from microtubules (Ser262, Ser214) also protects it against aggregation into Alzheimer paired helical filaments. Biochemistry 38, 3549–3558.

Schwab, C., Bondada, V., Sparks, D.L., Cahan, L.D., Geddes, J.W., 1994. Postmortem changes in the levels and localization of microtubule-associated proteins (tau, MAP2 and MAP1B) in the rat and human hippocampus. Hippocampus 4, 210–225.

Schweers, O., Mandelkow, E.M., Biernat, J., Mandelkow, E., 1995. Oxidation of cysteine-322 in the repeat domain of microtubule-associated protein tau controls the in vitro assembly of paired helical filaments. Proc. Natl. Acad. Sci. U. S. A. 92, 8463–8467.

Sokolowski, F., Modler, A.J., Masuch, R., Zirwer, D., Baier, M., Lutsch, G., Moss, D.A., Gast, K., Naumann, D., 2003. Formation of critical oligomers is a key event during conformational transition of recombinant syrian hamster prion protein. J. Biol. Chem. 278, 40481–40492.

Spillantini, M.G., Schmidt, M.L., Lee, V.M., Trojanowski, J.Q., Jakes, R., Goedert, M., 1997. Alpha-synuclein in Lewy bodies. Nature 388, 839–840.

Srinivasan, R., Marchant, R.E., Zagorski, M.G., 2004. ABri peptide associated with familial British dementia forms annular and ring-like protofibrillar structures. Amyloid 11, 10–13.

Strong, C., Anderton, B.H., Perry, R.H., Perry, E.K., Ince, P.G., Lovestone, S., 1995. Abnormally phosphorylated tau protein in senile dementia of Lewy body type and Alzheimer disease: evidence that the disorders are distinct. Alzheimer Dis. Assoc. Disord. 9, 218–222.

Sturchler-Pierrat, C., Abramowski, D., Duke, M., Wiederhold, K.H., Mistl, C., Rothacher, S., Ledermann, B., Burki, K., Frey, P., Paganetti, P.A., Waridel, C., Calhoun, M.E., Jucker, M., Probst, A., Staufenbiel, M., Sommer, B., 1997. Two amyloid precursor protein transgenic mouse models with Alzheimer disease-like pathology. Proc. Natl. Acad. Sci. U. S. A. 94, 13287–13292.

Syme, C.D., Blanch, E.W., Holt, C., Jakes, R., Goedert, M., Hecht, L., Barron, L.D., 2002. A Raman optical activity study of rheomorphism in caseins, synucleins and tau. New insight into the structure and behaviour of natively unfolded proteins. Eur. J. Biochem. 269, 148–156.

Takeda, A., Hashimoto, M., Mallory, M., Sundsumo, M., Hansen, L., Masliah, E., 2000. C-terminal alpha-synuclein immunoreactivity in structures other than Lewy bodies in neurodegenerative disorders. Acta Neuropathol. (Berl.) 99, 296–304.

Tsuboi, Y., Wszolek, Z.K., Graff-Radford, N.R., Cookson, N., Dickson, D.W., 2003. Tau pathology in the olfactory bulb correlates with Braak stage, Lewy body pathology and apolipoprotein ε4. Neuropathol. Appl. Neurobiol. 29, 503–510.

Ueda, K., Fukushima, H., Masliah, E., Xia, Y., Iwai, A., Yoshimoto, M., Otero, D.A., Kondo, J., Ihara, Y., Saitoh, T., 1993. Molecular cloning of cDNA encoding an unrecognized component of amyloid in Alzheimer disease. Proc. Natl. Acad. Sci. U. S. A. 90, 11282–11286.

Weaver, C.L., Espinoza, M., Kress, Y., Davies, P., 2000. Conformational change as one of the earliest alterations of tau in Alzheimer's disease. Neurobiol. Aging 21, 719–727.

Wirths, O., Weickert, S., Majtenyi, K., Havas, L., Kahle, P.J., Okochi, M., Haass, C., Multhaup, G., Beyreuther, K., Bayer, T.A., 2000. Lewy body variant of Alzheimer's disease: alpha-synuclein in dystrophic neurites of A beta plaques. NeuroReport 11, 3737–3741.

Xu, G., Gonzales, V., Borchelt, D.R., 2002. Abeta deposition does not cause the aggregation of endogenous tau in transgenic mice. Alzheimer Dis. Assoc. Disord. 16, 196–201.

Human Molecular Genetics, 2004, Vol. 13, No. 7 ***703–714***
DOI: 10.1093/hmg/ddh083
Advance Access published on February 12, 2004

CHIP and Hsp70 regulate tau ubiquitination, degradation and aggregation

Leonard Petrucelli[1], Dennis Dickson[1], Kathryn Kehoe[1], Julie Taylor[1], Heather Snyder[2], Andrew Grover[1], Michael De Lucia[1], Eileen McGowan[1], Jada Lewis[1], Guy Prihar[1], Jungsu Kim[1], Wolfgang H. Dillmann[3], Susan E. Browne[4], Alexis Hall[5], Richard Voellmy[5], Yoshio Tsuboi[6], Ted M. Dawson[7,8,9], Benjamin Wolozin[2], John Hardy[10] and Mike Hutton[1,*]

[1]Mayo Clinic, Jacksonville, FL 32224, USA, [2]Loyola University School of Medicine, Department of Pharmacology, Maywood, IL 60153, USA, [3]University of California, Department of Medicine, La Jolla, CA, USA, [4]Weill Medical College of Cornell University, New York, NY 10021, USA, [5]University of Miami School of Medicine, Miami, FL 33136, USA, [6]Fukuoka University, Department of Internal Medicine, Japan, [7]Institute for Cell Engineering, [8]Department of Neurology, [9]Department of Neuroscience, Johns Hopkins University School of Medicine, Baltimore, MD 21205, USA and [10]National Institutes of Health, Department of Neurogenetics, Bethseda, MD 20892, USA

Received November 17, 2003; Revised and Accepted January 30, 2004

Molecular chaperones, ubiquitin ligases and proteasome impairment have been implicated in several neurodegenerative diseases, including Alzheimer's and Parkinson's disease, which are characterized by accumulation of abnormal protein aggregates (e.g. tau and α-synuclein respectively). Here we report that CHIP, an ubiquitin ligase that interacts directly with Hsp70/90, induces ubiquitination of the microtubule associated protein, tau. CHIP also increases tau aggregation. Consistent with this observation, diverse of tau lesions in human postmortem tissue were found to be immunopositive for CHIP. Conversely, induction of Hsp70 through treatment with either geldanamycin or heat shock factor 1 leads to a decrease in tau steady-state levels and a selective reduction in detergent insoluble tau. Furthermore, 30-month-old mice overexpressing inducible Hsp70 show a significant reduction in tau levels. Together these data demonstrate that the Hsp70/CHIP chaperone system plays an important role in the regulation of tau turnover and the selective elimination of abnormal tau species. Hsp70/CHIP may therefore play an important role in the pathogenesis of tauopathies and also represents a potential therapeutic target.

INTRODUCTION

Neurodegenerative diseases as diverse as Alzheimer's disease (AD) and Parkinson's disease (PD) share an obvious common feature—aggregation and accumulation of abnormal proteins. A large group of these diseases, known as the tauopathies, are characterized by filamentous lesions in neurons and sometimes in glia that are composed of aggregates of hyperphosphorylated microtubule-associated protein tau (tau).

Tau promotes microtubule (MT) assembly, reduces MT instability and plays a role in maintaining neuronal integrity and axonal transport (1,2). Human tau protein is encoded by a single gene on chromosome 17q21 that consists of 16 exons, and central nervous system isoforms are generated by alternative splicing involving 11 of these exons (3–7). Tau is a phosphoprotein, predominantly expressed in neurons, where it is largely localized in axons (8). During the development of tau pathology, tau becomes hyperphosphorylated, detaches from the axonal microtubules and aggregates. The abnormal tau eventually accumulates in filamentous inclusions within neuronal cell bodies and processes. The precise sequence of events and the mechanisms involved in this process are not fully understood, but it is clear that abnormal tau accumulation and aggregation are sufficient to cause neurodegeneration. This in turn leads progressively to the onset of clinical symptoms. The primary tauopathies include Pick's disease (PiD), corticobasal degeneration (CBD), progressive supranuclear palsy (PSP) and frontotemporal dementia and parkinsonism linked to chromosome 17 (FTDP-17). Tau also accumulates in AD, where where the tau neurofibrillary pathology (e.g. tangles and

*To whom correspondence should be addressed at: Department of Neuroscience, 4500 San Pablo Road, Jacksonville, FL 32224, USA. Email: hutton.michael@mayo.edu

neuropil threads) occurs with a second protein aggregate, the amyloid plaque. The identification of exonic and intronic tau gene mutations associated with FTDP-17 established that tau dysfunction can cause neurodegeneration (9–11).

Unfolded or misfolded protein generated under diverse conditions must be either refolded by molecular chaperones, for instance Hsc/Hsp70 and Hsp40, or eliminated by the ubiquitin proteasomal system (UPS) through an energy-dependent process and concerted action of a number of molecules, including specific ubiquitin ligases. CHIP (carboxyl terminus of the Hsc70-interacting protein) is a molecule with dual function: (i) a co-chaperone of Hsp70 linked through the tetratricopeptide repeat (TPR) domain of CHIP; and (ii) possessing intrinsic E3 ubiquitin ligase activity (U-box domain) which promotes ligation/chain elongation for substrates (12–16). It is structurally similar to RING finger motifs typical of E3 ligases, like parkin. CHIP interacts functionally and physically with the stress-responsive ubiquitin-conjugating (E2 conjugase) enzyme family UBCH5. Thus CHIP is a bona fide ubiquitin ligase which provides a direct link between the chaperone and UPS and has been suggested to contribute in regulating the cellular balance between folding and degradation (17).

Recently, Imai *et al.* (18,19) showed that CHIP, Hsp70, parkin and PAELR formed a complex *in vitro* and *in vivo*. Unfolded PAELR is a substrate of the E3 ubiquitin ligase parkin and accumulation of non-ubiquitinated PAELR in the endoplasmic reticulum (ER) of dopaminergic neurons induces ER stress, leading to neurodegeneration (19). CHIP promotes the dissociation of Hsp70 from parkin and PAELR, thus facilitating parkin-mediated PAELR ubiquitination. Moreover, CHIP enhances parkin-mediated *in vitro* ubiquitination of PAELR in the absence of Hsp70. CHIP also enhances the ability of parkin to inhibit cell death induced by PAELR (18).

The role of the chaperones Hsp70/90 in tau biology has previously been examined by Dou *et al.* (20), who found an inverse relationship between tau aggregation and chaperone levels. Specifically, transgenic mice harboring the V337M tau mutation, which develop hippocampal tau aggregates, had lower levels of Hsp90 than control mice, suggesting that Hsp90 might be degraded along with aggregated tau. In addition, a small number of neurons in the hippocampus that were devoid of aggregated tau were observed to have significantly higher levels of Hsp90. The same relationship between Hsp90 and Hsp70 and tau aggregates in post-mortem samples from a single human AD brain were also reported (20).

In cell cultures transfected with tau constructs increased levels of both Hsp70 and 90, induced by treatment with geldanamycin, led to an ~80% reduction in levels of aggregated, detergent-insoluble tau. This reduction, however, was not accompanied by a decrease in total tau levels, but rather by a redistribution of tau from the insoluble fraction to the soluble fraction. The increased levels of soluble tau were accompanied by an increase in microtubule-bound tau. Reduction of Hsp70 or Hsp90 by RNAi caused the levels of the microtubule-bound tau to decrease (20).

Overall, these studies suggest that abnormal tau accumulation might be associated with perturbation of the major components of the cellular protein quality control machinery—molecular chaperones and the UPS. Hsp70/90 and other chaperones identify proteins that require proper folding, whereas aberrant unfolded proteins are directed to the UPS. CHIP is a ubiquitin E3 ligase that is involved in ubiquitination of Hsp70-bound proteins; this generally results in their targeting to the proteasome. This is a tandem event (chaperone and UPS activity) such that perturbation in either of these systems might play a role in tau accumulation. Moreover, evidence suggests that the Hsp70/90 chaperones and ubiquitin ligases are neuroprotective and can suppress the toxicity associated with abnormal protein accumulation in *Drosophila* and mouse models of disease (21–24).

In the present study we examined the relationship between CHIP/Hsp70 and tau and the role of this chaperone system in tau degradation, ubiquitination and aggregation. We show that CHIP associates with tau through the microtubule-binding domain, is able to ubiquitinate tau and increases the level of insoluble aggregated tau. In addition, a diversity of neuronal and glial tau-related lesions in several neurodegenerative disorders have CHIP immunoreactivity. This suggests that CHIP may play a role in the formation of, or cellular response to, fibrillary tau lesions. Hsp70 also binds to tau, but has opposing effects. Hsp70 decreases tau steady-state levels and selectively reduces insoluble and hyperphosphorylated tau species. Together, these data suggest that the Hsp70–CHIP chaperone system plays an important role in tau biology and in the pathogenesis of tauopathies.

RESULTS

CHIP interacts with tau

Because Hsp70 is known to interact with tau, the major protein species in neurofibrillary pathology, we investigated whether the Hsp70 co-chaperone CHIP, an E3 ubiquitin ligase, was able to interact with and ubiquitinate tau. Although CHIP has several known substrates, none of these have been associated with neurodegenerative disease.

To determine if CHIP and tau interact we first conducted co-immunoprecipitation experiments. Myc-tagged CHIP, parkin and Hsp70 were separately co-transfected with V5-tagged tau into HEK293 cells and then immunoprecipitation was performed with the V5 antibody. Detection of co-immunoprecipitating species was performed by western blotting with the Myc-tag antibody. Tau was found to co-immunoprecipitate with CHIP and Hsp70 (Fig. 1A). Tau also co-immunoprecipitated with parkin, an E3 ligase associated with autosomal recessive juvenile parkinsonism (25). This was not surprising given that parkin has previously been shown to interact with CHIP and that there is considerable structural homology between these two E3 ligases. To determine whether CHIP and tau interact *in vivo*, we performed co-immunoprecipitation using an antibody against CHIP in brain homogenates from transgenic mice (JNPL3 line) expressing mutant (P301L) tau (26). Western blot analysis was then performed with an antibody against tau (Fig. 1B). Tau co-immunoprecipitated with CHIP (Fig. 1B). These data clearly support the physiological and potential pathological relevance of the observed CHIP–tau interaction.

Using co-immunoprecipitation and *in vitro* binding assays, we next examined which regions of CHIP are necessary for the

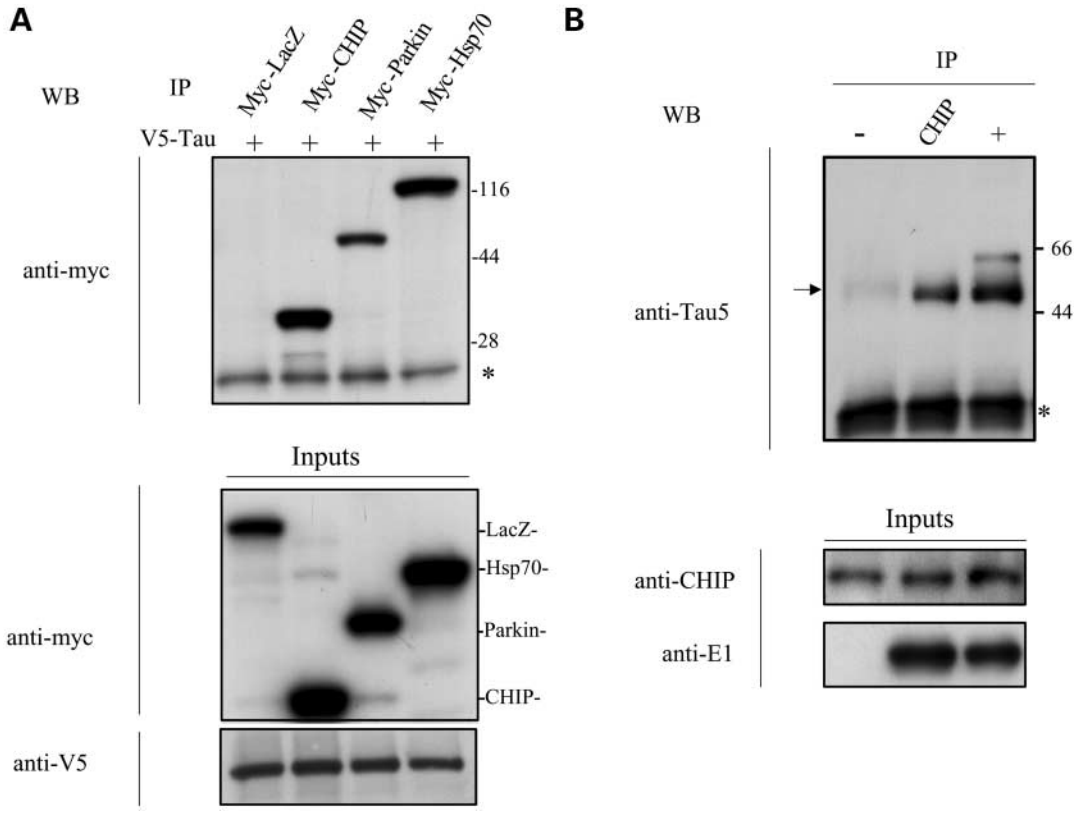

Figure 1. Tau associates with CHIP. (**A**) Interaction of Tau with CHIP, Hsp70 and parkin. Lysates from HEK293 cells transfected with an LacZ vector (Control), myc-tagged CHIP, myc-tagged Hsp70 or myc-tagged parkin and V5-tagged tau were immunoprecipitated with anti-V5 antibody. Immunoprecipitates (IP) and total soluble lysates (total lysate) were analyzed by western blotting (WB). (**B**) *In vivo* interaction of tau with CHIP in brain tissue. Mouse brain tissue from P301L transgenic mice (JNPL3) was homogenized as described in Experimental Procedures. The supernatant fractions were immunoprecipitated with anti-CHIP (CHIP), anti-E1 (+) or an irrelevant (−) polyclonal antibody. The co-precipitated tau was detected by western blotting using Tau5. An asterisk indicates the IgG light chain. The arrow indicates native tau species.

interaction with tau. CHIP contains two major structural motifs—a TPR motif and a U-box domain. The TPR motif is required for interaction with Hsc70 and Hsp90, while the U-box domain has ubiquitin ligase activity (Fig. 2A). To determine the site of interaction of CHIP with tau, we monitored the interaction of tau with these two domains of CHIP. The TPR mutant (C1; 1–189 amino acids) and U-box mutant (C2; 145-303 amino acids) both failed to bind to tau; in contrast, full-length CHIP bound strongly to tau (Fig. 2C). Although these results did not reveal a specific binding domain of CHIP with tau, it is conceivable that the interaction with tau requires both domains, as might be expected if complex formation with Hsp70 is required for the tau–CHIP interaction, or one of these domains and a third undefined region of CHIP. A series of truncated tau constructs were also generated to determine the domain of tau that interacted with CHIP (Fig. 2B). These experiments demonstrated that residues 187–311 contain the region of the tau protein necessary for interaction with CHIP. This includes the microtubule binding domains and the region immediately N-terminal (Fig. 2C).

CHIP ubiquitinates tau

To ascertain whether CHIP or parkin ubiquitinates tau, HEK293 cells were transfected with myc-tagged parkin or myc-tagged CHIP, V5-tagged tau and HA-tagged ubiquitin (Fig. 3A). Two days later, immunoprecipitation was performed with an antibody against V5 and probed with an antibody against HA to assess the degree of tau ubiquitination. Immunoprecipitated tau showed prominent anti-HA (ubiquitin) immunoreactivity in CHIP-transfected cells, with ubiquitin positive species appearing as mulitple higher molecular weight species, possibly representing oligomeric and multimeric ligations (Fig. 3A). To characterize the effect of Hsp70 on CHIP-mediated tau ubiquitination, cells were transfected as described above; however, they were also transfected with myc-tagged Hsp70 in the presence of CHIP. As shown in Figure 3B, Hsp70 attenuates CHIP activity, suggesting that Hsp70 antagonizes CHIP ubiquitination of tau. We further explored which ubiquitin lysine linkage (K48 or K68) was primarily responsible for ubiquitination of tau. Ubiquitin linkage through K48 is associated with proteasome targeting, while K68 ubiquitin linkage appears to be involved in cellular signaling/DNA repair (27). HEK293 cells were transfected with myc-tagged CHIP, V5-tagged tau and HA-tagged wild-type ubiquitin, K48 or K63 constructs. K48 and K63 refer to the particular lysine amino acid used to link the ubiquitins to each other. CHIP-mediated ubiquitination of tau did not discriminate between K48 or K63 type ubiquitin linkage suggesting that both types of linkage occur in tau (Fig. 3C). This has potential functional implications for the role of ubiquitination in tau biology. A further study showed that

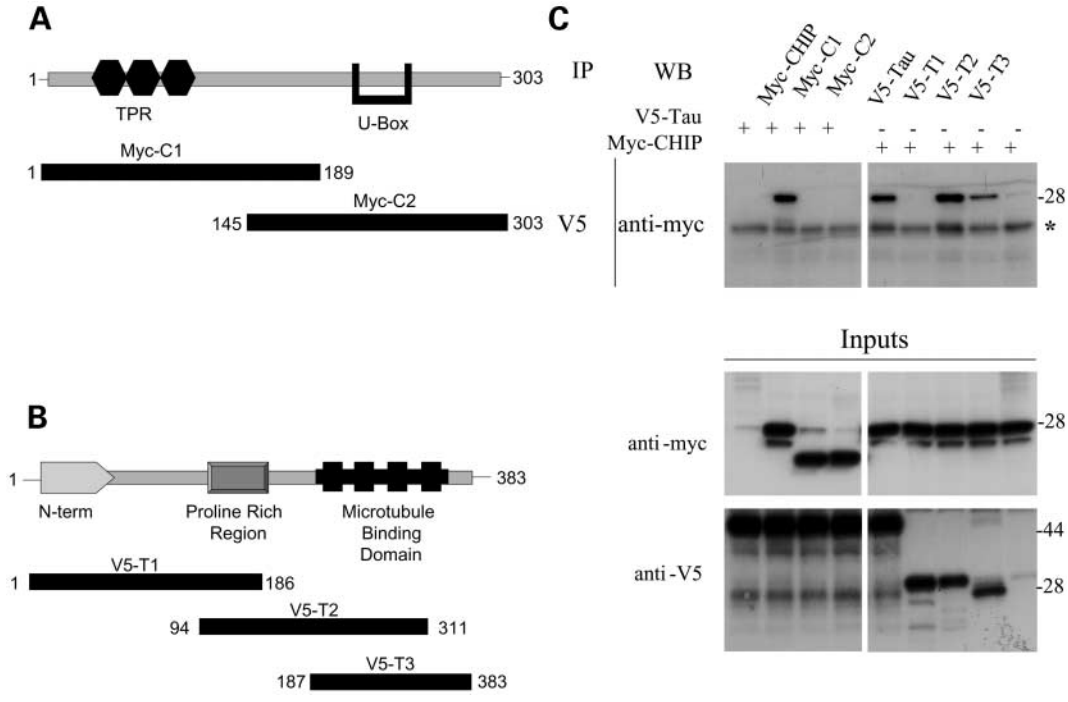

Figure 2. CHIP preferentially interacts with the microtubule-binding domain of tau and tau binding requires full-length CHIP. (**A**) Diagrammatically representation of full-length CHIP and the two structural domains (C1 and C2) used to determine the Tau binding. (**B**) Diagrammatically representation of tau and the three domains (T1, T2 and T3) used to determine the CHIP binding domain. (**C**) Lysates prepared from HEK293 cells transfected with V5-tagged tau and various myc-tagged CHIP domain constructs and various V5-tagged tau domains constructs and myc-CHIP and subjected to IP with anti-V5 followed by anti-myc immunoblotting. Lysates (inputs) were immunoblotted with either anti-V5 or anti-myc antibodies. The asterisk indicates IgG light chain. A representative result from three experiments is shown.

the amount of multimeric ubiquitinated tau (>200 kDa) increased dramatically after the cells were treated with the proteasome inhibitor MG-132, suggesting that a proportion of tau is degraded through the proteasome (Fig. 3D). In particular, it would appear that tau carrying long ubiquitin chains in the soluble fraction is degraded by the proteasome.

To verify the functional interaction between CHIP and tau, we reconstituted the ubiquitination reaction *in vitro*. In this experiment, immunoprecipitated CHIP or parkin and recombinant His-tagged tau were combined with other essential components for *in vitro* ubiquitination, including ATP and E2 conjugases. Again, immunoprecipitated CHIP, but not parkin, ubiquitinated tau (Fig. 4), demonstrating that tau is a substrate of CHIP. Further, when the western blot was re-probed with an antibody against the His-tag on tau, a ladder of species was observed, confirming that tau was directly ubiquitinated by CHIP. Finally, we observed that, in the absence of additional cellular components, Hsp70 had no impact on tau ubiquitination by CHIP; this is in contrast to the attenuation associated with increased Hsp70 activity observed in the *in vivo* ubiquitination studies. This suggests that *in vivo* an additional component of the complex or a particular Hsp70 conformation is required to down regulate tau ubiquitination by CHIP.

CHIP immunoreactivity in human neurodegenerative tauopathies

To evaluate the potential pathological significance of the interaction between tau and CHIP, we examined the immunolocalization of CHIP in postmortem brain sections of different human tauopathies, including AD, PSP, CBD, FTDP-17 and PiD, as well as JNPL3 transgenic mice that express mutant (P301L) tau. CHIP immunoreactivity was detected in a wide range of tau-positive lesions in both neurons and glia, including neurofibrillary tangles (NFTs; Fig. 5A) and dystrophic neurites in neuritic plaques (Fig. 5B) of AD, Pick bodies in PiD (Fig. 5C), globose NFTs (Fig. 5D) and tufted astrocytes (Fig. 5E) in PSP, and oligodendroglial coiled bodies and thread-like processes in CBD (Fig. 5F).

To confirm CHIP co-localization with tau lesions, serial sections from PiD, were immunostained with anti-phospho-tau (CP13; Fig. 5G) and with antibodies anti-CHIP (Fig. 5H), and to ubiquitin 3–39 (Fig. 5I).

The degree of CHIP immunoreactivity correlated to the predominant isoform of tau in the lesions, with 3R tauopathies showing more immunoreactivity than 3R+4R tauopathies or 4R tauopathies. Specifically, there was more robust CHIP immunoreactivity in Pick bodies (3R) than in NFTs in AD (3R+4R). Almost all Pick bodies were also ubiquitin-immunoreactive on adjacent sections stained for ubiquitin. In adjacent sections of AD stained for ubiquitin, most of the CHIP-positive NFTs were also ubiquitin-immunoreactive. The major exception was extracellular NFT, which had no CHIP-immunoreactivity yet variable ubiquitin immunoreactivity. Pre-tangles, neurons with non-fibrillar abnormal phospho-tau immunoreactivity, were negative for CHIP (data not shown). There were only a few NFTs stained in PSP, CBD and FTDP-17. These were all 4R tauopathies and neurofibrillary lesions in these disorders had

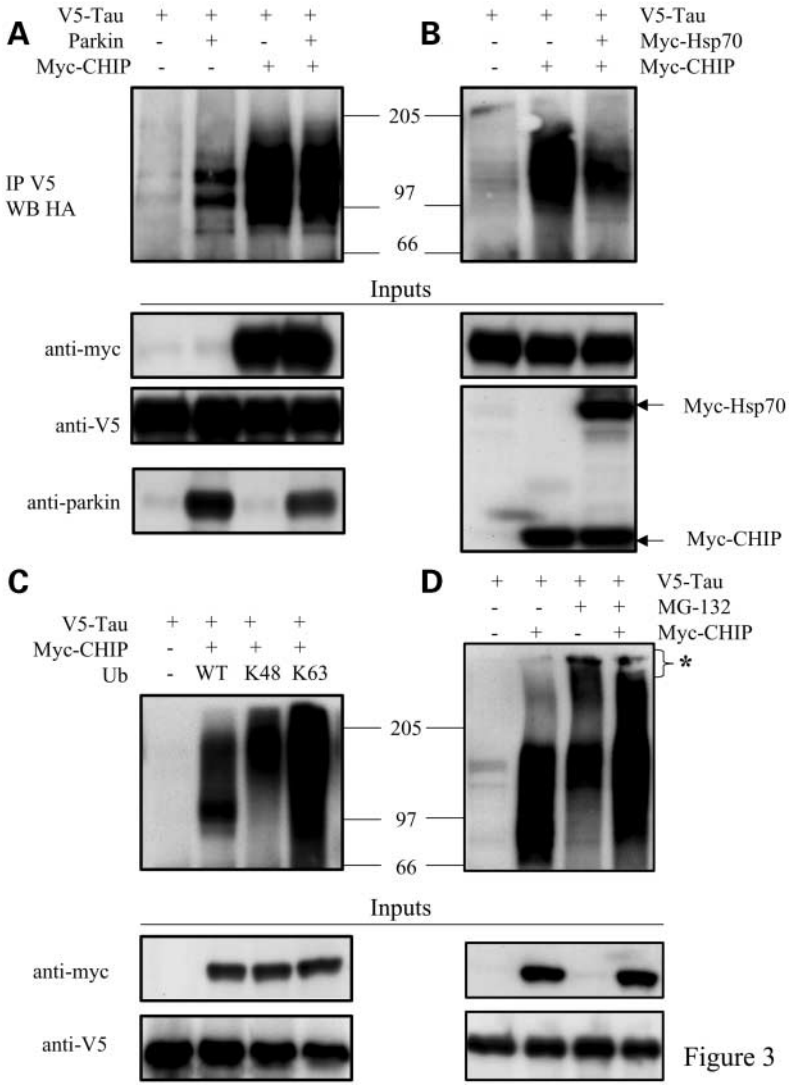

Figure 3. Tau tends to be ubiquitinated *in vivo.* (**A**) CHIP, not parkin, mediates tau ubiquitination. V5-tagged Tau cDNA combined with empty vector, untagged parkin or myc-tagged CHIP and HA-Ub construct were transfected into HEK293 cells. Immunoprecipitates with anti-V5 mAb (V5-IP) immunoblotted with HA mAb to assess the amount of ubiquitination. Total soluble lysates (inputs) were analyzed by western blotting using anti-myc, anti-V5 or anti-parkin. (**B**) Hsp70 attenuates CHIP activity. V5-tagged Tau cDNA combined with empty vector, myc-tagged CHIP and myc-tagged Hsp70 and HA-Ub construct were transfected into HEK293 cells. Immunoprecipitates with anti-V5 mAb immunoblotted with HA mAb to assess the amount of ubiquitination. Total soluble lysates (inputs) were analyzed by western blotting using anti-myc, anti-V5 or anti-parkin. (**C**) CHIP ubiquitinates tau through K48 and K63 ubiquitin linkages. V5-tagged Tau cDNA combined with myc-tagged CHIP (or vector as a control) and HA-tagged wild type or K48 or K63 ubiquitin mutants were transfected into HEK293 cells. Immunoprecipitates with anti-V5 mAb immunoblotted with HA mAb to assess the amount of ubiquitination. Total soluble lysates (inputs) were analyzed by western blotting using anti-myc or anti-V5. (**D**) Proteasome inhibition increases CHIP-mediated ubiquitination of tau. V5-tagged Tau cDNA combined with either empty vector or myc-tagged CHIP and HA-tagged ubiquitin were transfected into HEK293 cells. Thirty-six hours post-transfection cells were exposed to MG132 (5 μM, 12 h). Immunoprecipitates with anti-V5 and immunoblotted with HA mAb to access the amount of ubiquitination. Total soluble lysates (inputs) were analyzed by western blotting using anti-myc or anti-V5.

almost no ubiquitin immunoreactivity. Only a few glial lesions in the latter 4R tauopathies were CHIP-immunoreactive. Overall, the number of CHIP immunoreactive lesions was 50–70% for PiD, 5–10% for AD and 1–5% for both PSP and CBD. These data suggest a role for CHIP in pathologies involving tauopathies in humans. Similar to humans, neurofibrillary lesions in spinal cord sections of JNPL3 mice, which contain mutant 4R tau, were weakly immunoreactive for CHIP and ubiquitin, yet strongly positive for phospho-tau (data not shown).

Controls for specificity of CHIP included omission of primary antibody and absorption with CHIP synthetic peptide. These sections showed no immunoreactivity in Pick bodies (Fig. 5K) or NFTs (data not shown).

Effects of CHIP and Hsp70 on accumulation of detergent-insoluble tau

To examine the impact of CHIP-mediated ubiquitination on tau aggregation, COS-7 cells were transfected with a mutant

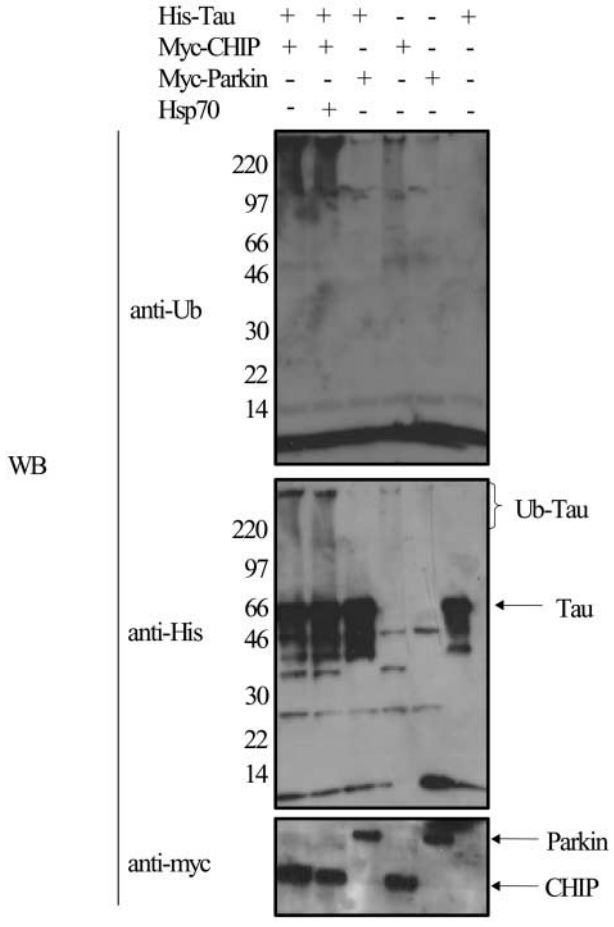

Figure 4. *In vitro* ubiquitination of tau by CHIP. The ubiquitination of Tau by CHIP (or parkin) was reconstituted by using immunoprecipitated myc-tagged parkin and myc-tagged CHIP from transfected HEK293 cells with the addition of purified UBCH7 or UBCH5b and the additional essential components for *in vitro* ubiquitination (see Materials and Methods). The reaction products were analyzed by western blot analysis with both anti-ubiquitin and anti-His antibodies. Inputs were immunoblotted with anti-myc antibodies. Brackets and molecular marker at 220 kDa indicate both Tau and ubiquitin-positive high molecular species. All experiments were replicated twice with similar results.

(P301L) tau expression construct in the absence or presence of either CHIP or Hsp70. Total tau was extracted and then fractionated into triton-soluble and insoluble pools. Transfection of CHIP dramatically increased the accumulation of high molecular weight aggregated tau species in the detergent (triton) insoluble fraction (Fig. 6), detected by western blot analysis with the Tau5 and E1 antibodies. The apparent molecular weight of these aggregated tau species ranged from ~90 kDa to large enough to be retained in the stacking gel. In contrast, expression of Hsp70 selectively reduced the amount of detergent insoluble tau to the point where little or no tau partitioned into the detergent-insoluble fraction. Although the level of insoluble tau was selectively reduced by Hsp70 transfection, there was no corresponding increase in detergent-soluble tau levels, which were also reduced relative to non-transfected cells (Fig. 6).

Induction of Hsp70 reduces tau levels *in vitro* and *in vivo*

To further explore the relationship between Hsp70 and tau steady-state levels *in vitro* we upregulated Hsp70 through geldanamycin (GA) treatment and activated heat shock factor 1 [(HSF-1 (+)] transfection (28). GA is a naturally occurring benzoquinone ansamycin that specifically binds to and interferes with the activity of the molecular chaperone Hsp90 (29), a negative regulator of heat-shock factor 1 (HSF-1), which regulates the transcription of several molecular chaperones, including Hsp70 (28,30). M17 human neuroblastoma cells, which express significant levels of endogenous tau, were either treated with GA or transfected with a mutant (constitutive active) form of HSF-1 (mHSF-1). As shown in Figure 7, treatment with GA reduced tau levels in a dose-dependent manner. Similar results were observed in cells transfected with mHSF-1. Both GA and mHSF-1 increased Hsp70 levels, with mHSF-1 causing the greater induction of the molecular chaperones (Fig. 7). HSF-1 (+), but not GA, also caused an increase in Hsp40 levels, suggesting that Hsp40 is unlikely to be necessary for the reduction of steady-state tau levels produced by these two treatments.

Based on the results described above, Hsp70 appears likely to be involved in regulating tau metabolism, especially the turnover of triton-insoluble species. To obtain additional evidence supporting this idea, we assessed the amount of endogenous tau in the brains of old mice overexpressing the inducible form of Hsp70 (31). There was no significant difference in age between transgenic and control littermates (30.6 ± 5.1 and 28.3 ± 2.1 months of age for non-transgenic and TgHsp70i mice, respectively). Whole brain homogenates from three non-transgenic and three tgHsp70 mice were homogenized and separated into 1% Triton X-100-soluble or -insoluble fractions. The fractions were then immunoblotted using Tau46, a polyclonal antibody to a carboxyl terminal epitope in tau that detects all forms of human and mouse tau (Fig. 8A). The amount of tau was normalized to β-actin levels in the brain of each mouse. Tau levels in TgHsp70 mice in both the soluble and insoluble fractions were significantly lower (~50% lower in both fractions) compared with NT mice (Fig. 8A and B). Moreover, high molecular weight triton-insoluble tau species present in the stacking gel that were observed in the very old NT mice were absent in the age-matched TgHsp70 mice (Fig. 8B). Tau levels were normalized to β-actin from the same gel from either the soluble or insoluble fractions with all the mice in the study. Statistical significance was estimated using Student's *t*-test for difference between NT and tgHsp70i mice in both fractions ($*P < 0.01$, $**P < 0.001$).

DISCUSSION

In the current study, we identified tau as a substrate for the ubiquitin ligase–chaperone protein CHIP. We concluded that tau is an authentic substrate of CHIP from the following evidence: first, CHIP interacts with tau and is specifically ubiquitinated by CHIP *in vivo* and *in vitro* in the presence of the E2 conjugase, UbcH5b. Second, proteasome inhibition augmented CHIP-mediated tau ubiquitination and promoted the insolubility of tau in triton-X-100 detergent. Finally, CHIP

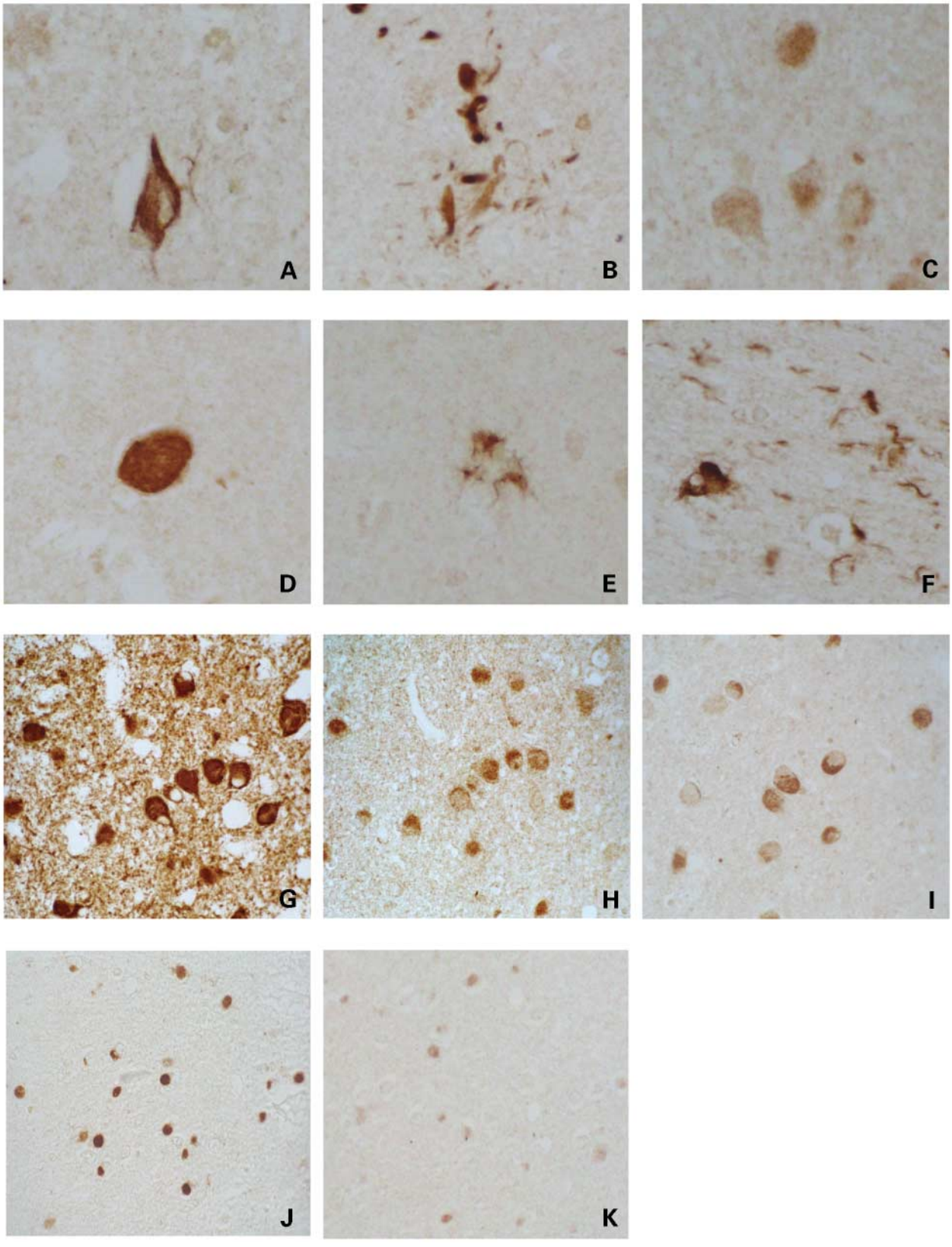

Figure 5. CHIP immunoreactivity is present in a diversity of neurodegenerative tauopathies. Immunostaining of CHIP in several tauopathies. (**A**) NFT in AD, (**B**) dystrophic neurites in senile plaques in AD, (**C**) Pick bodies in PiD, (**D**) globose NFT in PSP, (**E**) tufted astrocyte in PSP and (**F**) oligodendroglial coiled bodies and threads in CBD. CHIP co-localization with tau and ubiquitin was visualized using serial sections immunostained for phospho-tau with CP13 (**G**), CHIP (**H**) and anti-ubiquitin 3–39 (**I**). CHIP staining in PiD case (**J**) and preabsorption with CHIP synthetic peptide (**K**).

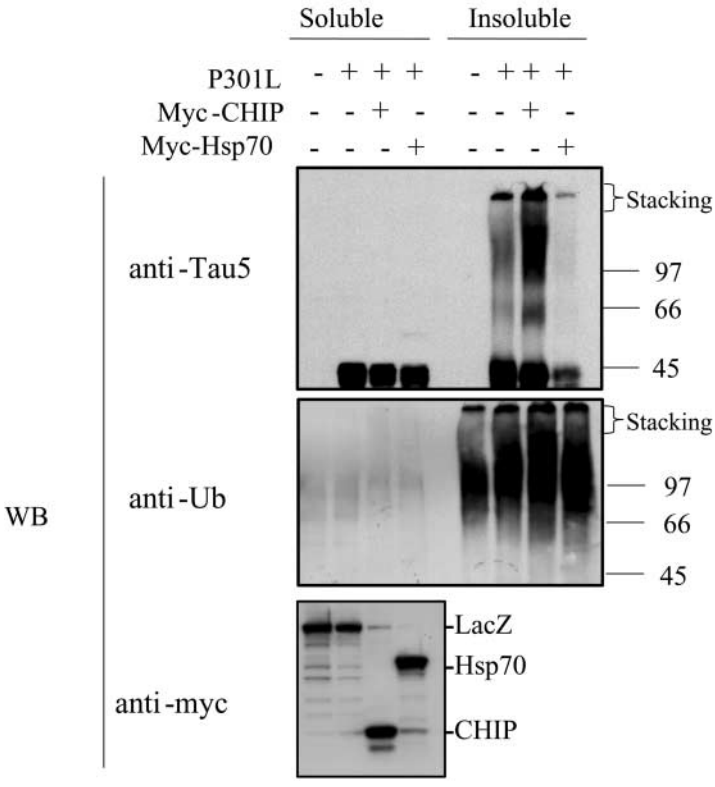

Figure 6. CHIP increases, Hsp70 suppresses tau aggregation. CHIP increases and Hsp70 decreases the accumulation of insoluble Tau in the COS7 cells. Cells transfected with vector plasmid (lacZ) or construct for mutant tau (P301L) combined with construct for mock (Control), myc-tagged CHIP or myc-Hsp70, were lysed and separated into 1% Triton X-100-soluble (S) or -insoluble (I) fractions, then immunoblotted with Tau5. Membrane was stripped and re-probed with anti-ubiquitin. Soluble fraction was used to demonstrate expression of respective constructs.

immunoreactivity was present in a range of tau lesions in several neurodegenerative tauopathies, especially those in which 3R tau is present in pathologic lesions, such as PiD and AD. The tauopathies with CHIP immunoreactivity were also those that have been shown in other studies to have ubiquitin-positive lesions (32). In contrast, disorders such as PSP or CBD in which lesions show almost no ubiquitin immunoreactivity were also negative for CHIP (35–38).

In this study, we found that CHIP mediated ubiquitination of tau. Moreover, both CHIP and Hsp70 interact with tau, suggesting that these two proteins act in concert to control tau metabolism. In fact, overexpression of Hsp70, in cells, attentuated the ubiquitination of tau induced by CHIP (Fig. 3B). These results suggest that Hsp70 and CHIP interact at the functional and/or cellular level. Interestingly the negative effect of Hsp70 on tau ubiquitination was not observed with *in vitro* assays, suggesting that additional chaperones that interact with the Hsp70/CHIP complex might play a role *in vivo*. Furthermore, it appears that a proportion of the tau ubiquitinated by CHIP via K48 ubiquitin linkage is consistent with the observed evidence of proteasome degradation of poly-ubiquitinated tau; however, tau was also ubiquitinated via K63 ubiquitin linkage, suggesting an alternative cellular fate for these species possibly including altered distribution and aggregation.

Although Dou *et al.* (20) reported that increased levels of Hsp70 reduce tau aggregation, which is in accord with results of the present study, they did not determine if this was a result of a reduction in tau levels (Figs 7 and 8), as our data indicate, rather than a redistribution of tau. Our data would further suggest that the CHIP and Hsp70 levels are critical to tau physiology such that excess CHIP would promote tau aggregation whereas Hsp70 would suppress it. In our model systems, insoluble tau aggregates represented a small fraction of total tau protein, which is a consistent observation in several tauopathies, including AD. Hsp/Hsc70 may protect against tau aggregation, neurofibrillary degeneration and neurotoxicity. Our data argue that Hsp70 (with CHIP) may be a critical determinant of normal tau degradation and may possibly be involved in the pathogenesis of human tauopathy. In this scheme, molecular chaperones would mediate tau degradation and directly or indirectly prevent tau aggregation and the toxicity associated with this protein. The balance between CHIP and Hsp70 levels may well be critical. Dai *et al.* (33) have recently shown that CHIP regulates activation of Hsp70 through induced trimerization and transcriptional activation of HSF-1. The activation of HSF-1 by CHIP emphasizes that a single protein (i.e. CHIP) within the complex can regulate major and often diametrically opposed chaperone activities (Hsp70) to alter the metabolism of substrate, in this case tau (33).

Although CHIP has been implicated in the ubiquitination of several substrates, including unfolded CFTR, glucocorticoid receptor and androgen receptor (14–16), tau is the first CHIP substrate that has been implicated in a number of

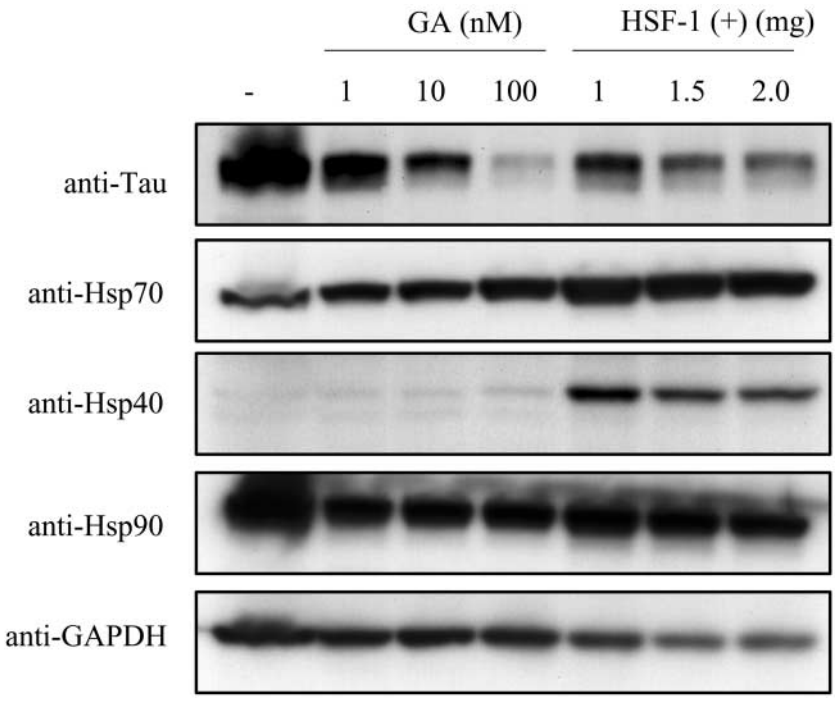

Figure 7. Induction of molecular chaperones decreases tau steady-state levels. M17 human neuroblastoma cell lines expressing endogenous tau were treated with geldanamycin (GA) at 1, 10 and 100 nM or transfected with activated heat shock factor 1 at 1, 1.5 and 2 μg DNA for 48 h. Cells were lysed and immunoblotted with Tau5 mAb. Membranes were stripped and sequentially re-probed with monoclonal antibodies to Hsp70, Hsp40, Hsp90 and GADPH (for protein loading).

neurodegenerative diseases. It is also clear that the another member of this chaperone complex, Hsp70, is involved in tau metabolism. Although many questions remain, the multiple effects of the Hsp70/CHIP chaperone system on tau biology make it of interest as a potential therapeutic target for the human tauopathies including AD.

MATERIALS AND METHODS

Expression vectors, cell culture and antibodies

cDNAs for parkin, tau (4R0N ± P301L), Hsp70 and CHIP were cloned into the mammalian expression vector pcDNA31.1 (Myc- or V5-tagged). Deletion constructs targeted for the respective domains were cloned into similar expression vectors. Ubiquitin constructs were obtained from Dr Ted Dawson (Johns Hopkins). A mutated cDNA sequence encoding an HSF1 lacking residues 203–315 was inserted into vector pcDNA3.1 to prepare expression construct HSF1(+). The integrity of all constructs was confirmed by automated sequencing.

COS-7 and HEK-293 cells were maintained in Optimem (Life Technologies) supplemented with 10% fetal bovine serum (Life Technologies), heat inactivated. Cells were transfected using Lipofectamine 2000 (Life Technologies) or FuGene6 (Roche) incubated for 48 h and treated as previously described. Human M17 Neuroblastoma cell lines stably overexpressing vector, wild-type tau (4R0N) and P301L cell lines were maintained in DMEM (Life Technologies) supplemented with 10% fetal bovine serum heat inactivated, glutamine, and 500 μg ml^{-1} G418.

CHIP polyclonal antibody was obtained from Abcam; HA and Myc antibodies was obtained from Roche; parkin antibody was obtained from Cell Signaling; Tau5 was generously provided by Dr Binder (Northwestern University); Hsp70 antibody was obtained from Stressgen abs; E1, human specific tau and Tau46 antibody were obtained from Dr Shu-Hui Yen (Mayo Clinic); CP13 (phospho-tau ser202) was obtained from Peter Davies (Albert Einstein College of Medicine) and ubiquitin 3–39 from Signet. HRP-coupled anti-mouse and anti-rabbit secondary antibodies were obtained from Jackson Immunoresearch. Ubiquitin polyclonal antibodies were obtained from Dako. His monoclonal antibody was obtained from Calbiochem. LB509 to α-synuclein (Zymed, San Francisco, CA, USA). Hsp40 and Hsp90 were obtained from BD Transduction laboratories. Hsp70 was obtained from Stressgen.

Ubiquitination assays

In vitro. Reactions were performed in 50 μl mixture containing 50 mM Tris–HCl, pH 7.5, 2.5 mM MgCl, 10 mM DTT, 4 mM ATP, 10 μg ubiquitin (Sigma), 500 ng of E1 (Calbiochem, San Diego, CA, USA), 200 ng of UbcH7 or UbcH5b (Affinti-Research, Exeter, UK), immunoprecipitated myc-tagged parkin or myc-tagged CHIP and 2 μg recombinant monomeric his-tagged tau (Dr Binder). Reactions were carried out for 2 h at 37°C before terminating with an equal volume of 2× SDS sample buffer. The reaction products were then subjected to western blot analysis with anti-ubiquitin (Dako, Carpinteria, CA, USA), Tau5 or anti-His antibodies.

In vivo. HEK293 cells were transfected with 4 μg of V5-tagged tau or 4 μg Myc-tagged parkin, Myc-tagged CHIP or Myc-tagged CHIP and Myc-tagged Hsp70 and 4 μg of

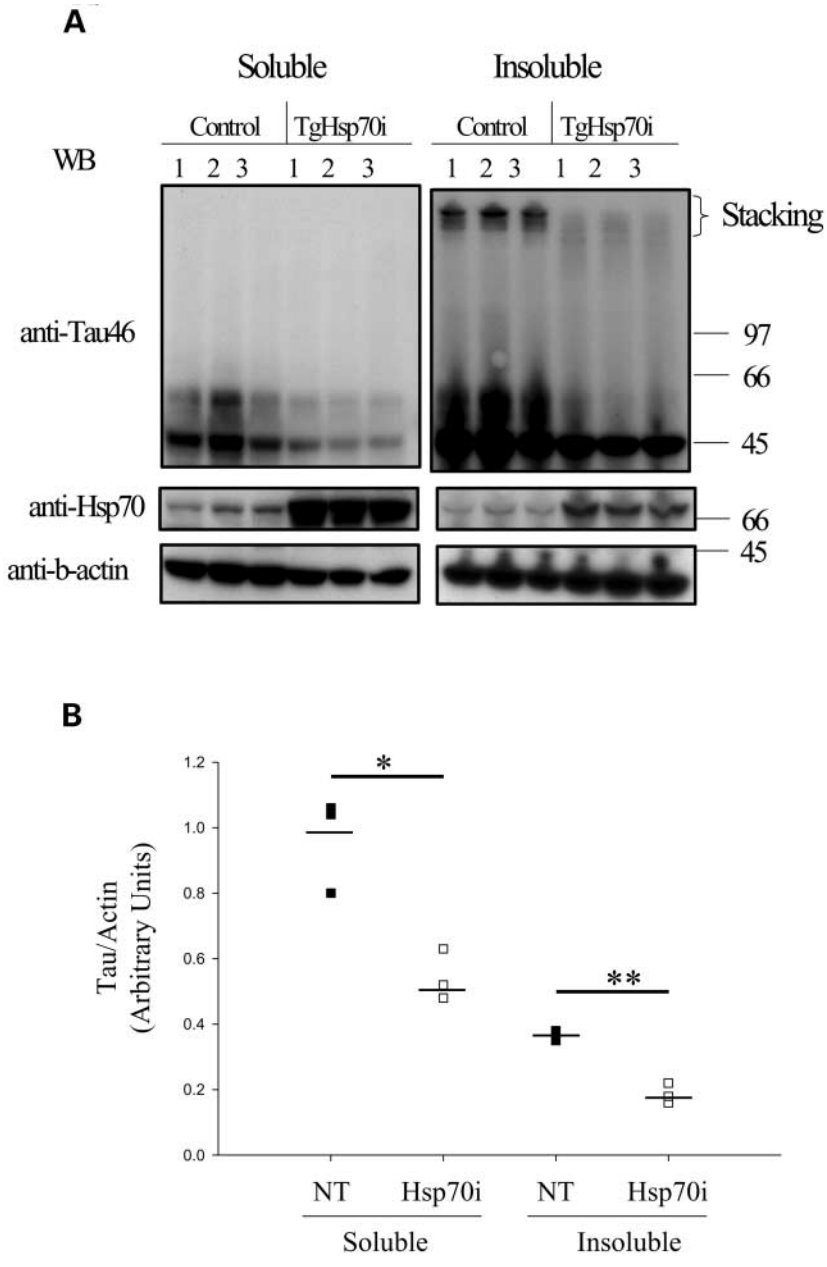

Figure 8. Tau levels in brains of mice overexpressing inducible form of Hsp70. (**A**, **B**) Whole brain tissues from 30-month-old normal (NT) or transgenic mice expressing the Hsp70 transgene were separated into 1% Triton X-100-soluble or -insoluble fractions, then immunoblotted with Tau46. Membrane was stripped and re-probed with anti-Hsp70 and anti-β-actin (control for protein loading). There was no significant difference between mice (30.6 ± 5.1 and 28.3 ± 2.1 months of age for NT and TgHsp70i, respectively). Tau normalized to β-actin from the same gel from either the soluble or insoluble fractions on all mice examined. Statistical significance was estimated using Student's *t*-test for difference between NT and tgHsp70i mice in both fractions. $^{*}P < 0.01$; $^{**}P < 0.001$.

pRK5–HA–wild-type ubiquitin, pRK5–HA–K48–ubiquitin, or pRK5–HA–K63–ubiquitin plasmids. After 48 h, immunoprecipitation was performed with an antibody against V5. The precipitates were submitted to western blotting with an antibody against HA.

Co-immunoprecipitation

For co-immunoprecipitation from cell cultures, HEK293 cells were transfected with 4 μg of each plasmid. After 48 h, cells were washed with cold PBS and harvested in immunoprecipitation buffer (0.1% Triton X-100, 2 μg/ml aprotinin, 100 μg/ml PMSF, 100 mM NaCl in 50 mM Tris–HCl, pH 7.2). The lysate was sonicated, pre-cleared for 1 h at 4°C with 25 μl of protein G (Pierce) and centrifuged at 14 000 rpm. The supernatants were incubated with 2 μg of an antibody against V5 (Life Technologies) and 60 μl of protein G and rocked at 4°C overnight. The protein G beads were pelleted and washed three times with immunoprecipitation buffer. The precipitates were resolved on SDS–PAGE gel and subjected to western blot

analysis. Bands were visualized with chemiluminescence (Pierce, Rockford, IL, USA).

For co-immunoprecipitation of proteins from mice, whole brains from adult mice expressing the P301L transgene brain (or non-transgenic mice as controls) were homogenized in 4 vols of ice-cold PBS containing 320 mM sucrose and 0.1% Triton X-100 with protease inhibitor cocktail (Sigma). The tissue homogenate was centrifuged at 37 000*g* at 4°C for 20 min. The supernatant was collected and 500 µg of protein was used for immunoprecipitation with one of the following antibodies: anti-CHIP, anti-E1 or anti-GFP (irrelevant antibody). The precipitates were subjected to western blot analysis and immunoblotted with Tau5.

M17 human neuroblastoma cells were either treated with GA (100 nM) or transfected with mHSF-1 (1, 1.5 and 2 µg DNA) for 48 h. Cells lysates were 1% Triton–PBS plus protease inhibitors. The precipitates were subjected to western blot analysis and immunoblotted with Tau5 and HSPs 70, 40 and 90.

Immunohistochemistry

Pre-absorption and specificity testing of polyclonal anti-CHIP antibody. CHIP peptide was re-suspended in 1% BSA in PBS to a concentration of 1 mg mL^{-1}. The peptide solution was added to diluted CHIP antibody in TBST to obtain a final dilution of 1 : 500. The mixture was rocked for 1 h at room temperature. The mixture was centrifuged at 13 500*g* for 2 min. The supernatant was separated from the pellet. Serial sections (5 µm thick) from a PiD case were deparaffinized and rehydrated in xylene and graded series of alcohol (100, 100, 95 and 70%). Antigen retrieval was performed in dH_2O in steam bath for 30 min. The sections were allowed to cool. The supernatant and diluted CHIP antibody (1 : 500 in TBST) were used for immunohistochemistry on the DAKO Autostainer (DakoCytomation, Carpinteria, CA, USA) using the DAKO EnVision HRP system on the serial sections. DAKO Liquid DAB Substrate–Chromogen system was the chromogen. The slides were then dehydrated and coverslipped.

Single antibody staining. Paraffin serial sections (5 µm thick) were used for immunohistochemistry from, diffuse Lewy body disease ($n = 6$), multiple system atrophy ($n = 2$) JNPL3 and littermate control mice (one each), AD ($n = 2$), PiD ($n = 4$), PSP ($n = 2$), CBD ($n = 2$), and FTDP_17 ($n = 2$). The sections were then processed the same as above. Primary antibodies used in the serial sections were: CHIP (1 : 250), CP13 (1 : 500) and 3–39 (1 : 200 000). In Lewy body disease and multiple system atrophy cases anti-synuclein (LB509, 1 : 100) replaced CP13. All antibodies were diluted in DAKO Antibody Diluent with background reducing components.

Fractionation experiments

For triton soluble/insoluble fractionation experiments, cells or tissue were lysed in a buffer containing PBS with 1% Triton X-100 and a cocktail of protease inhibitors. After sonication, cells were centrifuged at 100 000 *g* at 4°C for 30 min. Triton X-100 insoluble pellets were dissolved in a buffer containing 1% Triton X-100/1% SDS. The soluble and insoluble fractions were used in western blot analysis using the antibodies described in the figure legend.

ACKNOWLEDGEMENTS

This work was supported by NINDS grant RO1-NS41816-01.

NOTE ADDED IN PROOF

Very recently Shimura *et al.* (34) reported that tau binds to Hsc70 and phosphorylation is a requirement for ubiquitination by CHIP. In addition, CHIP was able to rescue phosphorylated tau-induced toxicity. Our data, while generally consistent with the findings of Shimura *et al.*, extends our understanding of the interaction between the Hsp70/CHIP chaperone system and tau by demonstrating the *in vivo* co-localization of CHIP with tau lesions in human patients with tauopathy and further by exploring the antagonistic action of Hsp70 and CHIP on tau ubiquitination and aggregation. In addition, while Shimura *et al.* report that CHIP ubiquitination is dramatically enhanced by GSK-3β driven phosphorylation of tau, our data show that GSK-3β phosphorylation is not absolutely required for CHIP to ubiquitinate tau.

REFERENCES

1. Ebneth, A., Godemann, R., Stamer, K., Illenberger, S., Trinczek, B. and Mandelkow, E. (1998) Overexpression of tau protein inhibits kinesin-dependent trafficking of vesicles, mitochondria, and endoplasmic reticulum: implications for Alzheimer's disease. *J. Cell Biol.*, **143**, 777–794.
2. Hirokawa, N. (1994) Microtubule organization and dynamics dependent on microtubule-associated proteins. *Curr. Opin. Cell. Biol.*, **6**, 74–81.
3. Andreadis, A., Brown, W.M. and Kosik, K.S. (1992) Structure and novel exons of the human tau gene. *Biochemistry*, **31**, 10626–10633.
4. Neve, R.L., Harris, P., Kosik, K.S., Kurnit, D.M. and Donlon, T.A. (1986) Identification of cDNA clones for the human microtubule-associated protein tau and chromosomal localization of the genes for tau and microtubule-associated protein 2. *Brain Res.*, **387**, 271–280.
5. Goedert, M., Wischik, C.M., Crowther, R.A., Walker, J.E. and Klug, A. (1988) Cloning and sequencing of the cDNA encoding a core protein of the paired helical filament of Alzheimer disease: identification as the microtubule-associated protein tau. *Proc. Natl Acad. Sci. USA*, **85**, 4051–4055.
6. Goedert, M., Spillantini, M.G., Potier, M.C., Ulrich, J. and Crowther, R.A. (1989) Cloning and sequencing of the cDNA encoding an isoform of microtubule-associated protein tau containing four tandem repeats: differential expression of tau protein mRNAs in human brain. *EMBO J.*, **8**, 393–399.
7. Goedert, M., Spillantini, M.G., Jakes, R., Rutherford, D. and Crowther, R.A. (1989) Multiple isoforms of human microtubule-associated protein tau: sequences and localization in neurofibrillary tangles of Alzheimer's disease. *Neuron*, **3**, 519–526.
8. Kanemaru, K., Takio, K., Miura, R., Titani, K. and Ihara, Y. (1992) Fetal-type phosphorylation of the tau in paired helical filaments. *J. Neurochem.*, **58**, 1667–1675.
9. Poorkaj, P., Bird, T.D., Wijsman, E., Nemens, E., Garruto, R.M., Anderson, L., Andreadis, A., Wiederholt, W.C., Raskind, M. and Schellenberg, G.D. (1998) Tau is a candidate gene for chromosome 17 frontotemporal dementia. *Ann. Neurol.*, **43**, 815–825.
10. Spillantini, M.G., Murrell, J.R., Goedert, M., Farlow, M.R., Klug, A. and Ghetti, B. (1998) Mutation in the tau gene in familial multiple system tauopathy with presenile dementia. *Proc. Natl Acad. Sci. USA*, **95**, 7737–7741.
11. Hutton, M., Lendon, C.L., Rizzu, P., Baker, M., Froelich, S., Houlden, H., Pickering-Brown, S., Chakraverty, S., Isaacs, A., Grover, A.*et al.* (1998) Association of missense and 5′-splice-site mutations in tau with the inherited dementia FTDP-17. *Nature*, **393**, 702–705.

12. Ballinger, C.A., Connell, P., Wu, Y., Hu, Z., Thompson, L.J., Yin, L.Y. and Patterson, C. (1999) Identification of CHIP, a novel tetratricopeptide repeat-containing protein that interacts with heat shock proteins and negatively regulates chaperone functions. *Mol. Cell. Biol.*, **19**, 4535–4545.
13. Jiang, J., Ballinger, C.A., Wu, Y., Dai, Q., Cyr, D.M., Hohfeld, J. and Patterson, C. (2001) CHIP is a U-box-dependent E3 ubiquitin ligase: identification of Hsc70 as a target for ubiquitylation. *J. Biol. Chem.*, **276**, 42938–42944.
14. Cardozo, C.P., Michaud, C., Ost, M.C., Fliss, A.E., Yang, E., Patterson, C., Hall, S.J. and Caplan, A.J. (2003) C-terminal Hsp-interacting protein slows androgen receptor synthesis and reduces its rate of degradation. *Arch. Biochem. Biophys.*, **410**, 134–140.
15. Connell, P., Ballinger, C.A., Jiang, J., Wu, Y., Thompson, L.J., Hohfeld, J. and Patterson, C. (2001) The co-chaperone CHIP regulates protein triage decisions mediated by heat-shock proteins. *Nat. Cell. Biol.*, **3**, 93–96.
16. Meacham, G.C., Patterson, C., Zhang, W., Younger, J.M. and Cyr, D.M. (2001) The Hsc70 co-chaperone CHIP targets immature CFTR for proteasomal degradation. *Nat. Cell. Biol.*, **3**, 100–105.
17. McClellan, A.J. and Frydman, J. (2001) Molecular chaperones and the art of recognizing a lost cause. *Nat. Cell. Biol.*, **3**, E51–53.
18. Imai, Y., Soda, M., Hatakeyama, S., Akagi, T., Hashikawa, T., Nakayama, K.I. and Takahashi, R. (2002) CHIP is associated with Parkin, a gene responsible for familial Parkinson's disease, and enhances its ubiquitin ligase activity. *Mol. Cell.*, **10**, 55–67.
19. Imai, Y., Soda, M. and Takahashi, R. (2000) Parkin suppresses unfolded protein stress-induced cell death through its E3 ubiquitin-protein ligase activity. *J. Biol. Chem.*, **275**, 35661–35664.
20. Dou, F., Netzer, W.J., Tanemura, K., Li, F., Hartl, F.U., Takashima, A., Gouras, G.K., Greengard, P. and Xu, H. (2003) Chaperones increase association of tau protein with microtubules. *Proc. Natl Acad. Sci. USA*, **100**, 721–726.
21. Cummings, C.J., Mancini, M.A., Antalffy, B., DeFranco, D.B., Orr, H.T. and Zoghbi, H.Y. (1998) Chaperone suppression of aggregation and altered subcellular proteasome localization imply protein misfolding in SCA1. *Nat. Genet.*, **19**, 148–154.
22. Auluck, P.K. and Bonini, N.M. (2002) Pharmacological prevention of Parkinson disease in Drosophila. *Nat. Med.*, **8**, 1185–1186.
23. Auluck, P.K., Chan, H.Y., Trojanowski, J.Q., Lee, V.M. and Bonini, N.M. (2002) Chaperone suppression of alpha-synuclein toxicity in a *Drosophila* model for Parkinson's disease. *Science*, **295**, 865–868.
24. Yang, Y., Nishimura, I., Imai, Y., Takahashi, R. and Lu, B. (2003) Parkin suppresses dopaminergic neuron-selective neurotoxicity induced by Pael-R in *Drosophila*. *Neuron*, **37**, 911–924.
25. Kitada, T., Asakawa, S., Hattori, N., Matsumine, H., Yamamura, Y., Minoshima, S., Yokochi, M., Mizuno, Y. and Shimizu, N. (1998) Mutations in the parkin gene cause autosomal recessive juvenile parkinsonism. *Nature*, **392**, 605–608.
26. Lewis, J., McGowan, E., Rockwood, J., Melrose, H., Nacharaju, P., Van Slegtenhorst, M., Gwinn-Hardy, K., Paul Murphy, M., Baker, M., Yu, X. *et al.* (2000) Neurofibrillary tangles, amyotrophy and progressive motor disturbance in mice expressing mutant (P301L) tau protein. *Nat. Genet.*, **25**, 402–405.
27. Marx, J. (2002) Cell biology. Ubiquitin lives up to its name. *Science*, **297**, 1792–1794.
28. Xia, W., Vilaboa, N., Martin, J.L., Mestril, R., Guo, Y. and Voellmy, R. (1999) Modulation of tolerance by mutant heat shock transcription factors. *Cell Stress Chaperones*, **4**, 8–18.
29. Whitesell, L., Mimnaugh, E.G., De Costa, B., Myers, C.E. and Neckers, L.M. (1994) Inhibition of heat shock protein HSP90-pp60v-src heteroprotein complex formation by benzoquinone ansamycins: essential role for stress proteins in oncogenic transformation. *Proc. Natl Acad. Sci. USA*, **91**, 8324–8328.
30. Zou, J., Guo, Y., Guettouche, T., Smith, D.F. and Voellmy, R. (1998) Repression of heat shock transcription factor HSF1 activation by HSP90 (HSP90 complex) that forms a stress-sensitive complex with HSF1. *Cell*, **94**, 471–480.
31. Marber, M.S., Mestril, R., Chi, S.H., Sayen, M.R., Yellon, D.M. and Dillmann, W.H. (1995) Overexpression of the rat inducible 70-kD heat stress protein in a transgenic mouse increases the resistance of the heart to ischemic injury. *J. Clin. Invest.*, **95**, 1446–1456.
32. Love, S., Saitoh, T., Quijada, S., Cole, G.M. and Terry, R.D. (1988) Alz-50, ubiquitin and tau immunoreactivity of neurofibrillary tangles, Pick bodies and Lewy bodies. *J. Neuropathol. Exp. Neurol.*, **47**, 393–405.
33. Dai, Q., Zhang, C., Wu, Y., McDonough, H., Whaley, R.A., Godfrey, V., Li, H.H., Madamanchi, N., Xu, W., Neckers, L.*et al.* (2003) CHIP activates HSF1 and confers protection against apoptosis and cellular stress. *EMBO J.*, **22**, 5446–5458.
34. Shimura, H., Schwartz, D., Gygi, S.P. and Kosik, K.S. (2004) CHIP-Hsc70 complex ubiquitinates phosphorylated Tau and enhances cell survival. *J. Biol. Chem.*, in press.
35. Wakabayashi, K., Oyanagi, K., Makifuchi, T., Ikuta, F., Homma, A., Homma, Y., Horikawa, Y. and Tokiguchi, S. (1994) Corticobasal degeneration: etiopathological significance of the cytoskeletal alterations. *Acta. Neuropathol. (Berl.)*, **87**, 545–553.
36. Yamada, T., McGeer, P.L. and McGeer, E.G. (1992) Appearance of paired nucleated, Tau-positive glia in patients with progressive supranuclear palsy brain tissue. *Neurosci. Lett.*, **135**, 99–102.
37. Verny, M., Duyckaerts, C., Delaere, P., He, Y. and Hauw, J.J. (1994) Cortical tangles in progressive supranuclear palsy. *J. Neural. Transm. Suppl.*, **42**, 179–188.
38. Yang, L. and Ksiezak-Reding, H. (1998) Ubiquitin immunoreactivity of paired helical filaments differs in Alzheimer's disease and corticobasal degeneration. *Acta. Neuropathol. (Berl.)*, **96**, 520–526.

Neuron, Vol. 36, 1007–1019, December 19, 2002, Copyright ©2002 by Cell Press

Parkin Protects against the Toxicity Associated with Mutant α-Synuclein: Proteasome Dysfunction Selectively Affects Catecholaminergic Neurons

Leonard Petrucelli,[1] Casey O'Farrell,[1] Paul J. Lockhart,[1] Melisa Baptista,[3] Kathryn Kehoe,[1] Liselot Vink,[1] Peter Choi,[2] Benjamin Wolozin,[2] Matthew Farrer,[1] John Hardy,[3] and Mark R. Cookson[3,4]

[1]Neurogenetics Laboratory
Mayo Clinic Jacksonville
Jacksonville, Florida 32224
[2]Department of Pharmacology
Loyola University Medical Center
Maywood, Illinois 60153
[3]Laboratory of Neurogenetics
National Institute on Aging
Bethesda, Maryland 20892

Summary

One hypothesis for the etiology of Parkinson's disease (PD) is that subsets of neurons are vulnerable to a failure in proteasome-mediated protein turnover. Here we show that overexpression of mutant α-synuclein increases sensitivity to proteasome inhibitors by decreasing proteasome function. Overexpression of parkin decreases sensitivity to proteasome inhibitors in a manner dependent on parkin's ubiquitin-protein E3 ligase activity, and antisense knockdown of parkin increases sensitivity to proteasome inhibitors. Mutant α-synuclein also causes selective toxicity to catecholaminergic neurons in primary midbrain cultures, an effect that can be mimicked by the application of proteasome inhibitors. Parkin is capable of rescuing the toxic effects of mutant α-synuclein or proteasome inhibition in these cells. Therefore, parkin and α-synuclein are linked by common effects on a pathway associated with selective cell death in catecholaminergic neurons.

Introduction

The identification of genes linked to familial forms of Parkinson's disease (PD) provides an important tool for modeling the pathways leading to neurodegeneration in this disorder. To date, eight linkages have been reported, with three genes identified as causal, or probably causal, in different families. Two of these encode proteins whose function is related to ubiquitin-dependent protein degradation through the proteasome (for review, see Hershko and Ciechanover, 1998). Parkin (OMIM 600116) is an E2-dependent E3 protein-ubiquitin ligase (Shimura et al., 2000; Zhang et al., 2000), and mutations in this gene are generally associated with recessive early onset parkinsonism (Kitada et al., 1998). *Parkin* mutations reported to date appear to be loss-of-function mutations reducing the ability of parkin to regulate degradation of substrate removal (Shimura et al., 2000; Zhang et al., 2000). One mutation in ubiquitin-C-terminal hydrolase (*UCHL1*, OMIM 191342) has been described (Farrer et al., 2000; Leroy et al., 1998), although pathogenicity of this mutation has not been fully established. However, polymorphic variability in *UCHL1* has been associated with altered risk for development of PD in case-control studies (Maraganore et al., 1999; Wintermeyer et al., 2000).

Mutations in α-*synuclein* have been reported in autosomal dominant pedigrees (OMIM 601508, Kruger et al., 1998; Polymeropoulos et al., 1997). Several pieces of evidence suggest that α-*synuclein* mutations and proteasome function may be related. Whether α-synuclein turnover is regulated by proteasome function is controversial, with both positive (Bennett et al., 1999; Tofaris et al., 2001) and negative (Ancolio et al., 2000; Paxinou et al., 2001) results reported. Forced overexpression of α-synuclein, especially mutant forms, sensitize PC12 (Stefanis et al., 2001; Tanaka et al., 2001), NT2, and SK-N-MC (Lee et al., 2001b) neuroblastoma cell lines to toxicity induced by the proteasome inhibitor lactacystin. The mechanism by which this occurs is not clear, but overexpression of mutant α-synuclein produces an inhibition of proteasome-associated proteolytic activities. The A30P mutant α-synuclein inhibits the postacidic proteasome activity by 25% and the trypsin-like and chymotrypsin-like activities by slightly smaller amounts, with wild-type α-synuclein having a much smaller effect (Tanaka et al., 2001). The A53T mutant form of α-synuclein also inhibits the chymotrypsin-like activity of the proteasome (Stefanis et al., 2001). Finally, it has been reported that an *O*-glycosylated form of α-synuclein found in human brain is ubiquitinated by parkin (Shimura et al., 2001), raising the possibility that loss of parkin function might result in α-synuclein accumulation. α-synuclein-positive Lewy bodies have been noted in a case of Parkin-related PD (Farrer et al., 2001).

Overall, the above studies suggest that proteasome inhibition might be a common link between the different genetic triggers of PD. Furthermore, there is evidence that proteasome function is impaired in sporadic PD (McNaught and Jenner, 2001). However, the hypothesis that proteasome dysfunction is an explanation for PD remains conjecture. For example, as cell loss in PD is not uniform, any attempt to link proteasome function to disease should account for selective vulnerability of specific subgroups of neurons. The selective vulnerability of different neuronal types to cell death or formation of the pathological hallmarks of the disease is complex (reviewed in Braak and Braak, 2000), but it is clear that functional loss of dopaminergic neurons in the substantia nigra (SN) *pars compacta* is important. The movement-related symptoms of PD patients are related to dopaminergic cell loss, and loss of these cells not only precedes symptom development, it is also progressive throughout the course of the disease (Pakkenberg et al., 1991).

In the present study we have explored the relationship between overexpression of α-synuclein and parkin with toxicity associated with proteasome inhibition. We have also used primary cell cultures to distinguish effects on

[4]Correspondence: cookson@mail.nih.gov

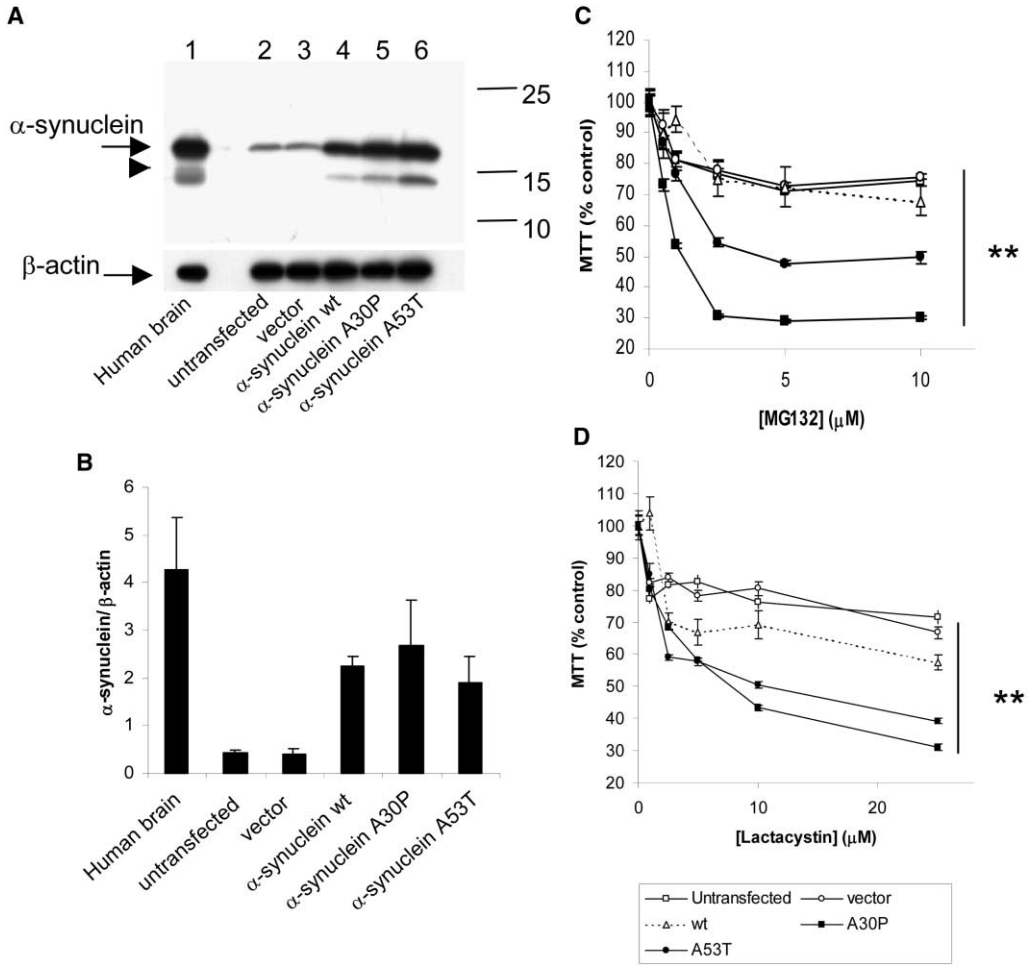

Figure 1. Effects of Proteasome Inhibitors on Cell Viability in M17 Cells Overexpressing α-Synuclein

(A and B) Stable clonal cell lines overexpressing α-synuclein were established and expression screened using Western blotting using monoclonal antibody 42. Untransfected cells (lane 2) or cells transfected with vector alone (lane 3) show moderate expression of α-synuclein compared to cells overexpressing wild-type (lane 4), A30P (lane 5), or A53T synuclein (lane 6). Human cerebral cortex extract was used as a positive control (lane 1). A reprobe of the same blot using β-actin is shown below to demonstrate similarity of loading across the lanes. Quantitation of α-synuclein expression is shown in (B) and is expressed as a ratio of the major synuclein band to β-actin (n = 4 serial passages of the cells, error bars represent the SEM).

(C and D) Overexpression of α-synuclein produces increased sensitivity to the proteasome inhibitor MG132 (C) or lactacystin (D). Cells were exposed to either inhibitor for 24 hr, after which cell viability was estimated using the MTT assay (see Experimental Procedures). Cell lines included untransfected cells (open squares) or cells transfected with empty vector (open circles), WT (open triangles), A30P (closed squares), or A53T (closed circles) α-synuclein. Results are expressed as a percentage of untreated cells for each clonal line (n = 8, each curve is representative of three or more experiments). Similar increased sensitivity to proteasome inhibition was seen in a second set of clonal lines. Statistical significance was estimated using two-way ANOVA using cell lines and concentration of inhibitors as independent variables. **$p < 0.001$ for differences between cell lines, both inhibitors having a significant effect on viability at $p < 0.001$. Representative data from one of three experiments.

tyrosine hydroxylase (TH)-positive neurons compared to TH-negative neurons. We show that parkin and mutant α-synuclein have opposite effects on neuronal cell death associated with impaired proteasome function and that parkin is capable of reducing toxicity associated with α-synuclein overexpression. We also show that knockdown of parkin increases the sensitivity of cells to proteasome inhibition, suggesting that loss-of-function mutations in parkin would cause cell death by the same mechanism as gain-of-function α-synuclein mutations. Furthermore, the effects of either mutant α-synuclein or proteasome inhibition are both selective for TH-positive neurons.

Results

Overexpression of α-Synuclein and Sensitivity to Proteasome Inhibitors

We used human M17 neuroblastoma cells to explore the relationship between mutant forms of α-synuclein and proteasome function. Cell lines stably overexpressing wild-type or either of the two mutants expressed about a 5-fold increased level of α-synuclein compared with untransfected cells (Figure 1A). Although the expression levels are high compared with untransfected cells, α-synuclein protein expression in human brain was 9-fold higher than untransfected M17 cells and approxi-

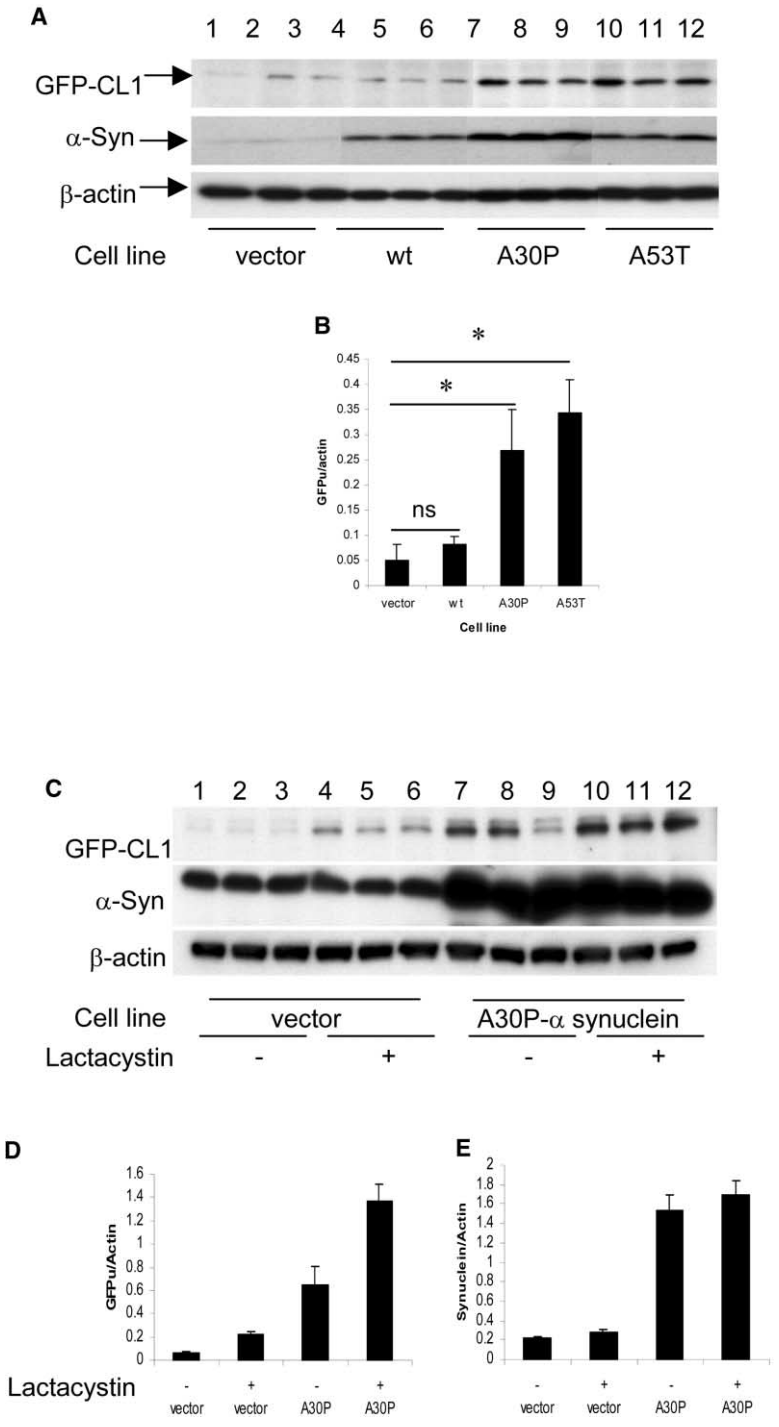

Figure 2. Measurements of Proteasome Activity in Living Cells

(A and B) Overexpression of mutant α-synuclein decreases proteasome activity. Stable cell lines (as in Figure 1) were transiently transfected with the GFP^u construct (see text for description of the construct). These included vector (lanes 1–3), cells expressing wild-type α-synuclein (4–6), A30P (7–9), or A53T (10–12) mutant α-synuclein. Protein extracts were blotted for GFP-CL1 peptide using anti-GFP (top panel) then reprobed sequentially for α-synuclein (middle panel) and β-actin (bottom panel). A semiquantitative analysis was performed by densitometry, correcting GFP-CL1 levels for β-actin. Each bar is the mean of the samples shown in (A) plus a duplicate set (hence n = 6), and error bars indicate the SEM. Both mutant forms of synuclein increased the amount of reporter construct, which was significant between cell lines at $p < 0.001$ by ANOVA.

(C–E) Additive effects of mutant α-synuclein expression and proteasome inhibition. (C) Vector (lanes 1–6) or A30P mutant α-synuclein cell lines (7–12) were transfected with GFP^u then, after 48 hr, treated with 5 μM lactacystin for 6 hr. Protein extracts were blotted for GFP, α-synuclein, and β-actin (top, middle, and bottom panels, respectively) and semiquantitative analysis for GFP immunoreactivity (D) or α-synuclein (E) normalized to β-actin for the same gel, bars are the mean of the samples shown in (C) plus a duplicate set (hence n = 6), and error bars indicate the SEM. Similar results were obtained in duplicate experiments.

mately 30% higher than the highest expressing clone of A30P cells. We also generated a second set of lines with similar levels of expression (data not shown).

We examined the sensitivity of these cell lines to toxicity induced by proteasome inhibition (Figure 1C). Exposure to 10 μM MG132 caused cell viability to be decreased to 74% ± 1% of untreated for untransfected cells and 76% ± 0.8% for vector cells (n = 8). For wild-type α-synuclein transfectants, a small increase in sensitivity was noted at the highest tested concentration, where cell viability was decreased to 68% ± 5%. Cells transfected with either of the mutant forms of α-synuclein were much more sensitive to MG132. The largest effect was seen in cells overexpressing A30P where cell viability was 30% ± 0.4% at 10 μM MG132. Overexpression of A53T α-synuclein decreased cell viability to 50% ± 1% at the same concentration. Similar results were seen with a second set of clones. For example, using two independent A30P-expressing clonal lines, cell viability after exposure to 10 μM MG132 was de-

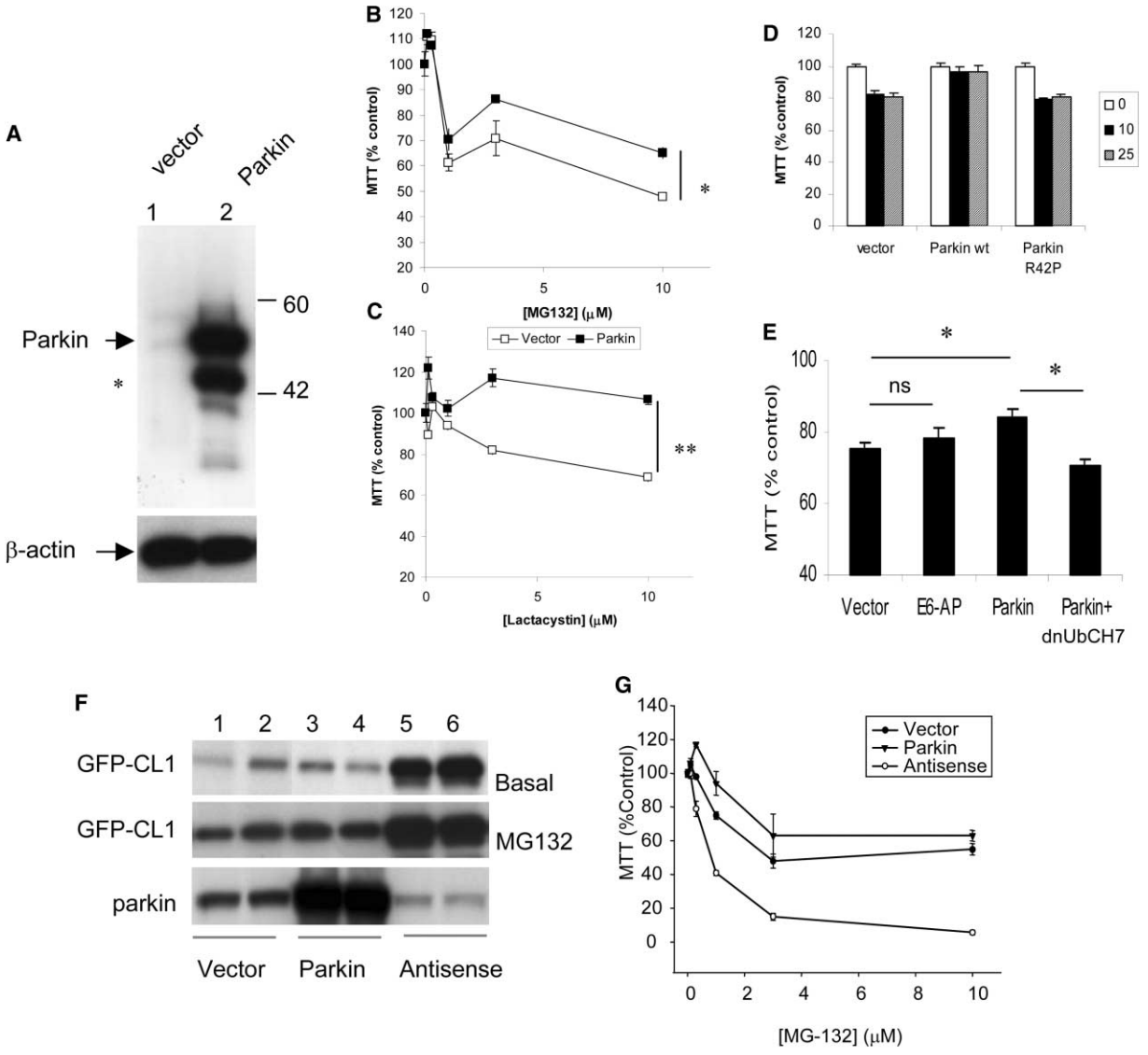

Figure 3. Effects of Proteasome Inhibitors on Cell Viability in M17 Cells Overexpressing Parkin

(A) Parkin protein was measured by Western blotting using a C-terminal antibody to human parkin in clonal lines transfected with vector (lane 1) or expression vector for human parkin (lane 2). Full-length parkin runs at ~50 kDa (arrow) although a C-terminal fragment (~42 kDa) is also noted in the overexpressing cell line (asterisk). Equal loading was demonstrated by reprobing the same blot with β-actin.

(B and C) Overexpression of parkin protects cells against the toxic effects of the proteasome inhibitor MG132 (B) or lactacystin (C). Cells stably transfected with parkin (open symbols) or vector (closed symbols) were exposed to inhibitors for 24 hr and cell viability assessed as in Figure 4. Statistical significance was estimated using two-way ANOVA using cell lines and concentration of inhibitors as independent variables. *$p < 0.05$; **$p < 0.001$ for differences between cell lines, both inhibitors having a significant effect on viability at $p < 0.001$. Similar protective effects of parkin overexpression were seen in two independent experiments (each $n = 8$).

(D) In an independent set of experiments, cells overexpressing mutant Parkin (R42P) were not protected from exposure to 10 μM (filled bars) or 25 μM (striped bars) lactacystin. ($n = 8$, representative of two experiments.)

(E) Cells were transfected with vector, the E3 ligase E6-AP, Parkin alone, or Parkin in the presence of a dominant-negative inhibitor of the E2 enzyme UbCH7 and exposed to 10 μM lactacystin. Cell death was quantified as above ($n = 8$) and expressed as a percentage of MTT conversion for transfected cells that had not been exposed to lactacystin. The differences between vector and parkin transfected cells were significant.

(F) Antisense knockdown of Parkin increases steady-state levels of heterologous substrates. M17 cells stably transfected with wild-type Parkin (lanes 3 and 4) or an antisense parkin construct (lanes 5 and 6) were transiently transfected with GFP^u reporter as above (upper panel) or transfected and then treated with MG132 (middle panel). Vector-only cells were included as controls (lanes 1 and 2, duplicate clonal lines). Parallel samples were blotted for parkin (lower panel) to demonstrate the level of overexpression and the effect of antisense knockdown. GFP-CL1 levels were unaffected by expression of parkin (similar effects were seen in two independent experiments), although antisense parkin cell lines did show an accumulation of GFP-CL1.

(G) MTT assays in the same cell lines show that cells transfected with antisense parkin (open circles) are more sensitive to MG132 toxicity compared to vector-only lines (closed circles) or cells transfected with WT parkin (closed triangles). Results are expressed as a percentage of untreated cells for each clonal line ($n = 8$, each curve is representative of two or more experiments).

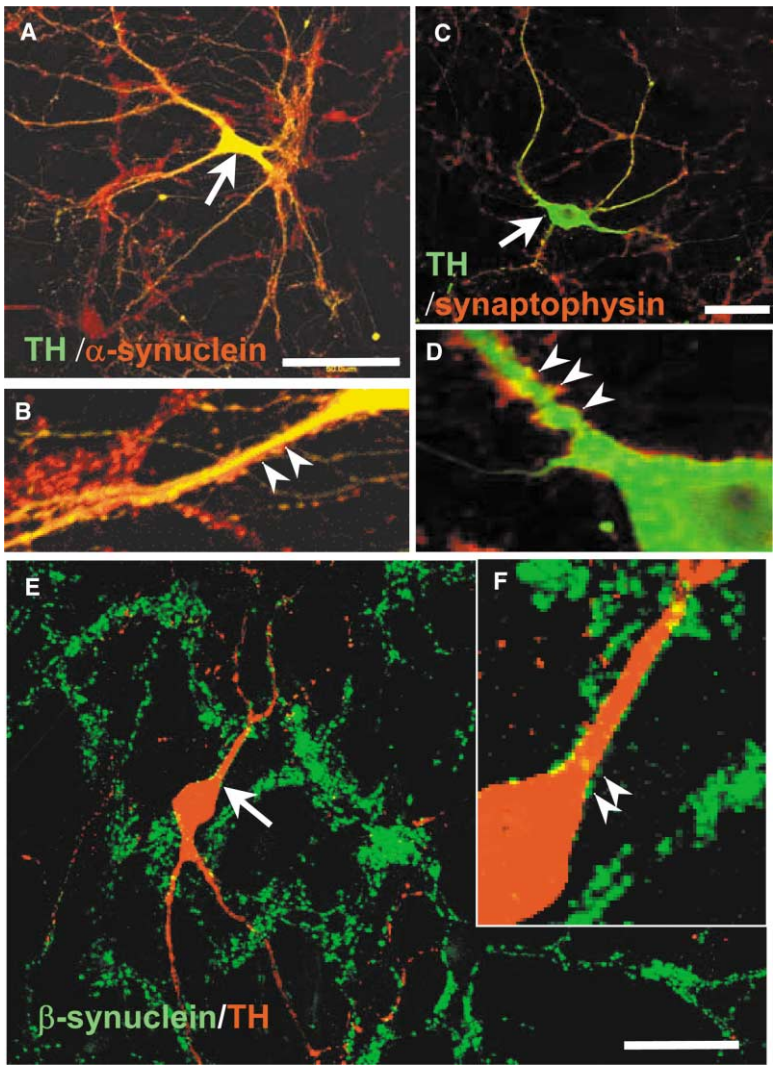

Figure 4. Characterization of α-Synuclein and β-Synuclein Expression in Primary Postnatal Midbrain Neurons

Primary neuronal cultures from postnatal mouse midbrain were stained with polyclonal antibodies to tyrosine hydroxylase (TH, green in [A]–[D]) and monoclonal antibodies to α-synuclein ([A] and [B] shows higher magnification) or synaptophysin ([C], higher magnification shown in [D]). The monoclonal antibody clone 42 (A and B) recognizes endogenous (mouse) α-synuclein. Staining for β-synuclein was performed using a polyclonal antibody (green in [E] and [F]) in combination with monoclonal anti-TH (red in [E] and [F]). All three proteins were expressed in both TH-positive (arrows) and TH-negative cells with similar patterns. Higher magnification of TH-positive cells (B, D, and F) demonstrated localization at the cell membrane, reminiscent of synaptic structures (arrowheads). All images were captured using a confocal microscope, and merged images of both channels are shown, yellow indicating overlap between the green and red channels. Scale bars represent 50 μm.

creased to 27% ± 1% in one clone and 30% ± 0.4% in the second. Consistent results were also obtained for two each of A53T and wild-type α-synuclein clones (data not shown). The differences between different clonal cell lines were significant ($p < 0.0001$) using two-way ANOVA, as was the effect of MG132 across all cell lines ($p < 0.0001$). We also exposed cells to the structurally unrelated inhibitor, lactacystin (Figure 1D). Lactacystin required concentrations of up to 25 μM to produce loss of cell viability to 70% (Figure 1D). Increased toxicity was noted in cell lines expressing either A30P or A53T α-synuclein. A small effect of wild-type α-synuclein was also seen. The differences between different clonal cell lines were significant ($p = 0.004$), as was the effect of lactacystin ($p < 0.0001$). Similar results were seen in experiments using a second set of clonal cell lines. Results presented here using MTT conversion are similar to previous reports using Trypan blue dye exclusion as a measure of cell death (Tanaka et al., 2001). To address the possibility that such effects might be due to inhibition of other proteases, we exposed cells to the cell-soluble calpain inhibitor E64d. This compound was without effect on cell viability up to 100 μM, which approached the limit of solubility (data not shown).

We next examined the mechanism by which mutant α-synuclein increases cellular sensitivity to proteasome inhibitors. We measured net proteasomal activity in living cells using the GFP^u reporter construct (Bence et al., 2001). When transfected into cells, the CL1 peptide (Gilon et al., 1998) sequence fused to GFP leads to rapid destruction of the protein, and in control cell lines we found only small amounts of GFP-CL1 peptide (Figure 2). The amount of reporter construct accumulation in cells transfected with wild-type α-synuclein was similar to that in vector-transfected cells but much higher in cells expressing A30P or A53T mutants (Figures 2A and 2B). The differences in amounts of GFP-CL1 between the cell lines were statistically significant ($p < 0.01$ by ANOVA). We also treated vector- or A30P-transfected cells with 5 μM lactacystin for 5 hr, which increased steady-state levels of the GFP-CL1 fusion protein. This effect was enhanced in the presence of A30P mutant α-synuclein (Figure 2D). Therefore, mutant α-synuclein inhibits proteasome function in a manner that is additive to the effect of pharmacological inhibition of the proteasome. There was no effect of lactacystin on steady-state α-synuclein levels in experiments where an increased GFP-CL1 reporter protein demonstrated unequivocally that

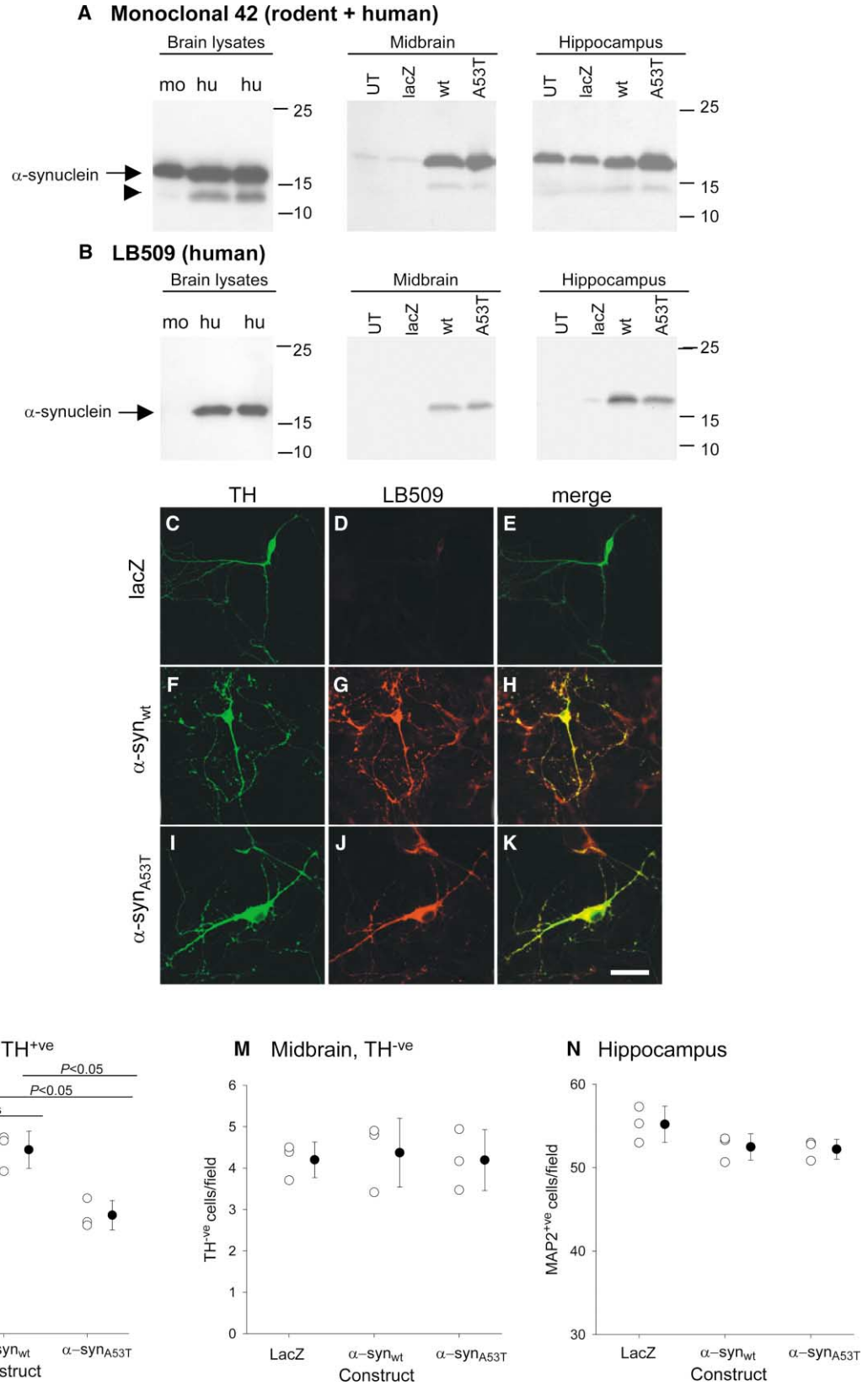

Figure 5. Overexpression of α-Synuclein in Primary Neurons

(A and B) Midbrain or hippocampal neurons were transduced with human α-synuclein (WT or A53T) and protein extracts (10 μg/lane) blotted with (A) either monoclonal 42 (recognizes rodent and human α-synuclein) or (B) LB509 (human α-synuclein only). Similar levels of expression were obtained with each of the viral constructs. Untransfected cells (UT) and cells transduced with a LacZ construct were used as controls.

there was proteasome inhibition (Figure 2E). Given the possible inhibitory effect of β-synuclein on α-synuclein toxicity (Hashimoto et al., 2001), we also examined β-synuclein expression in the same cell extracts. We were unable to detect β-synuclein protein in either basal conditions or after proteasome inhibition, although the antibodies used did detect expression of this protein in human brain (data not shown) and in primary mouse cultures (see below).

Manipulation of Parkin Expression Levels and Sensitivity to Proteasome Inhibitors

The above data demonstrate that the overexpression of mutant α-synuclein results in an increased sensitivity of cells to loss of viability induced by proteasome inhibition. We examined what effect increased parkin activity might have on the same parameters. Stable cell lines transfected with the parkin cDNA had substantially increased parkin protein expression (Figure 3A). Overexpression of parkin partially rescued cells from the toxic effects of MG132 (Figure 3B) or lactacystin (Figure 3C), with cell viability being 10%–20% higher in the parkin cell lines compared to controls at all doses of either compound. This effect was statistically robust ($p < 0.001$ for MG132, and $p < 0.004$ for lactacystin).

Further experiments confirmed that the observed rescue of parkin is dependent on its E3 ligase activity. A mutant form of parkin associated with loss of E3 ligase activity (R42P) was not able to rescue cells in an independent set of experiments (Figure 3D). Again, the differences between wild-type parkin and R42P parkin were statistically significant ($p < 0.001$ for differences between wild-type parkin and either vector alone or R42P). Coexpression of a dominant-negative E2 enzyme (UbCH7) also ameliorated the protective effect of parkin (Figure 3E). We also examined the effects of overexpression of a second E3 ligase, E6AP, which was not protective in these cells (Figure 3E). Experiments using the GFP^u construct demonstrated that there was no alteration in the amount of GFP-CL1 in the cells when transfected with parkin, either under basal conditions or after MG132 treatment (Figure 3F), although MG132 did increase GFP-CL1 levels in this experiment as in the experiments shown in Figure 2 . Parkin does not, therefore, act as an E3 ligase for this artificial proteasome reporter (see Discussion). However, the above experiments do not address what would occur if parkin activity within the cell was reduced, as occurs in ARJP. To model this effect, we generated cell lines with an antisense construct that had lower steady-state levels of parkin protein. This antisense knockdown of parkin does increase GFP^u levels within the cell, and MG132 has an additive effect (Figure 3F). This suggests that loss of parkin activity increases the level of heterologous substrates, presumably due to increased levels of parkin substrates competing for ubiquitination and/or proteasome-mediated degradation. Proteasome inhibitors are more toxic in cell lines transfected with an antisense parkin construct (Figure 3G).

Mutant α-Synuclein Triggers Selective Cell Death in Primary Neuronal Culture

Primary neuronal cultures from the midbrain of postnatal mice (Mena et al., 1997) were used to examine the effects of α-synuclein overexpression and proteasome inhibition on different neuronal groups. These cultures are predominantly from the nigral area and have a higher proportion of TH-positive catecholaminergic neurons than commonly used embryonic mesencephalic neuron preparations, with TH-positive cells representing about 20%–30% of the total neuronal population. The TH antibodies we used in these experiments recognized an appropriately sized band in extracts from whole mouse brain or from midbrain cultures but not in hippocampal cultures (data not shown). We characterized the expression of (mouse) α- and β-synuclein in these cells (Figure 4). Both TH-positive and TH-negative neurons expressed α-synuclein (Figures 4A and 4B) at the cell surface in a punctate pattern reminiscent of synaptic proteins such as synaptophysin (Figures 4C and 4D), similar to hippocampal neurons (Murphy et al., 2000). In addition, we also noted α-synuclein immunoreactivity in the cytoplasm. This was not limited to either TH-positive or TH-negative cells but was seen in many midbrain neurons. Expression of β-synuclein (Figures 4E and 4F) was also synaptic and seen in both cell populations at similar levels.

We next transduced primary midbrain cultures with wild-type or mutant α-synuclein and monitored expression by Western blotting or immunocytochemistry. Two monoclonal antibodies, clone 42 and LB509, were used to distinguish overexpressed human α-synuclein from endogenous mouse α-synuclein, respectively. Transduction with wild-type or mutant α-synuclein produced

Left-hand panels show controls using brain lysates from mouse (mo) or human (hu) cerebral cortex. Blotting using monoclonal antibody 42 yielded a major band at 19 kDa (arrow) plus a smaller degradation product with an apparent molecular weight of 16–17 kDa (arrowhead): this smaller product was not seen with LB509.

(C–K) Expression of human α-synuclein in catecholaminergic neurons. Primary midbrain catecholaminergic neurons (TH-positive, green) were transduced at multiplicities of infection (MOIs) of 5–10 with HSV1 expressing lacZ (C, D, and E) as a negative control or α-synuclein (WT, [F–H]; A53T, [I–K]). Transduction was demonstrated using a human specific monoclonal antibody LB509 (red), and more than 95% of cells were LB509 positive. Merged images are shown on the right of each set of photomicrographs. Scale bar in (K) represents 50 μm and applies to all panels. Representative data is shown from one of four experiments.

(L–M) Overexpression of mutant α-synuclein in primary midbrain neurons is associated with selective cell death of TH-positive cells. Cells were transduced with either LacZ (negative control), WT, or mutant (A53T) α-synuclein and cell numbers estimated by counting using TH and MAP2 staining. Although there was a significant reduction in TH-positive cell numbers (L), TH-negative cells in the midbrain (M) and hippocampal cells (N) were not affected. Each open circle is the average cell counts from one experiment with six fields counted in each of three cultures (hence $n = 18$): closed circles represent the mean from each of three experiments, with error bars representing the SEM between experiments. Statistical significance was assessed using one-way ANOVA with Student-Neuman-Kuells post-hoc tests between each group. ns, not significant.

similar levels of overexpression (Figures 5A and 5B). To confirm that TH-positive neurons in midbrain cultures were transduced, cells were costained for TH and human α-synuclein using LB509 (Figures 5C–5K). We estimated that after transduction at a multiplicity of infection (MOI) of 10, more than 95% of TH-positive neurons expressed human α-synuclein. TH-negative neurons were transduced at similarly high rates, showing almost 100% infectivity at MOIs of 5–10 (data not shown). Overexpression in this acute model does not result in the formation of microscopically visible α-synuclein aggregates (Figure 5J).

Cell counts were performed to assess whether the overexpressed α-synuclein induced any toxicity in TH-positive neurons. In each experiment, we counted six fields in each of three cultures. We also repeated the whole series three times with independent purifications of viral particles, and the data presented (Figure 5L) shows the interexperiment variation. We were able to demonstrate a clear toxic effect of A53T α-synuclein in TH-positive cells. We were not able to demonstrate an effect with wild-type α-synuclein under these conditions. TH-negative midbrain neurons (Figure 5M) or hippocampal neurons (Figure 5N) were unaffected by the presence of A53T α-synuclein.

TH-Positive Neurons Are Selectively Vulnerable to Proteasome Inhibition

We next examined whether proteasome inhibition was sufficient to produce selective neuronal cell loss in the same manner as α-synuclein overexpression. The numbers of TH-positive neurons in MG132 were decreased compared to controls, with remaining cells often showing shrinkage of cell bodies and retraction of neuritic processes (Figures 6A and 6B). Previous reports of cell death induced by proteasome inhibitors in the presence of mutant α-synuclein have given contradictory results on the mode of cell death, finding evidence for apoptosis (Tanaka et al., 2001) or autophagy (Stefanis et al., 2001). In our cultures exposed to proteasome inhibitors, counterstaining nuclei with Hoechst 33342 revealed that even in damaged cells the nuclei remained intact, unlike apoptosis. The numbers of TH-positive cells were significantly reduced at higher concentrations of lactacystin or MG132 (Figures 6C and 6E), while the number of TH-negative neurons was unaffected (Figures 6D and 6F). Using one-way ANOVA with Student-Newman-Kuells post-hoc test to evaluate the effects of proteasome inhibition on numbers of TH-positive cells remaining, MG132 had a significant ($p < 0.05$) effect at both 1 and 5 μM, whereas the effect of lactacystin was significant only at 10 μM. We also examined the effects of proteasome inhibitors on A53T α-synuclein-infected primary cultures (Figures 6G and 6H). The two treatments had an additive effect ($p < 0.01$ by ANOVA for all groups), although the loss of TH-positive cells was not complete after 24 hr, the time point used for this study. We examined cells transduced with A53T synuclein and treated with MG132 after staining with Hoechst 33342 (as in Figures 6A and 6B) and again did not find evidence for apoptosis (data not shown).

Parkin Rescues the Toxicity of Mutant α-Synuclein in Primary Neurons

We reasoned that as parkin protected cells against proteasome inhibition and mutant α-synuclein overexpression inhibited the proteasome then parkin might be protective against toxicity associated with overexpression of mutant α-synuclein. We repeated the experiments using A53T α-synuclein and coexpressed either lacZ as a control or parkin (Figures 7A and 7B). Cotransduction of parkin restored the number of counted neurons back to levels similar to cultures treated with lacZ alone. Using one-way ANOVA with post-hoc tests as above, the loss of TH-positive neurons was significantly different ($p < 0.05$) from controls and from cultures treated with parkin and α-synuclein ($p < 0.05$), but the difference between cotransduced cultures and control cells was not significant. Similarly to experiments in cell lines, Parkin was able to rescue to selective toxicity of MG132 to primary cells (Figures 7C and 7D).

Discussion

In the current study, we have examined manipulation of two genes that show association with familial PD on cellular sensitivity to proteasome inhibition and have examined aspects of neuronal selectivity. There was an increased sensitivity of cells overexpressing α-synuclein to proteasome inhibition, similar to previous reports (Lee et al., 2001b; Tanaka et al., 2001). Mutant α-synuclein also sensitizes cells to other insults (Junn and Mouradian, 2002; Ko et al., 2000; Lee et al., 2001b; Ostrerova-Golts et al., 2000; Zhou et al., 2000), but we and others (Stefanis et al., 2001; Tanaka et al., 2001) have demonstrated that one effect of mutant α-synuclein is to reduce the net proteasomal activity in living cells. Therefore, proteasome inhibition is likely to make a significant contribution to cell death induced by mutant α-synuclein. The inhibition of proteasome function by mutant α-synuclein may be a direct inhibition of proteasome activity, as α-synuclein can bind to one of the regulatory subunits of the proteasome (Ghee et al., 2000) or the presence of large amounts of misfolded or unfolded proteins, such as mutant α-synuclein, might inhibit the ubiquitin-proteasome pathway indirectly (Bence et al., 2001).

Overexpression of parkin protected against toxicity associated with reduced proteasome function. The lack of effect of the recessive R42P parkin mutation, which lacks ubiquitination activity (Shimura et al., 2001), demonstrates that mutant forms of parkin are unable to protect dopaminergic neurons against proteasome failure. Therefore, both genes implicated in familial PD alter the ability of neurons to tolerate reduced proteasome activity. We have shown that the E3 ligase activity of Parkin is required for protection, as a dominant-negative E2 mutant could ameliorate this effect. Experiments using the GFP^u reporter show that Parkin does not increase net proteasome activity, consistent with the role of this E3 ligase in controlling entry of target proteins into the proteasome via ubiquitination, and does not alter the steady-state levels of α-synuclein. Parkin is also protective in some other models of cell death, such as ER stress, but is not protective against all insults, including staurosporine (Imai et al., 2000). We suggest that parkin

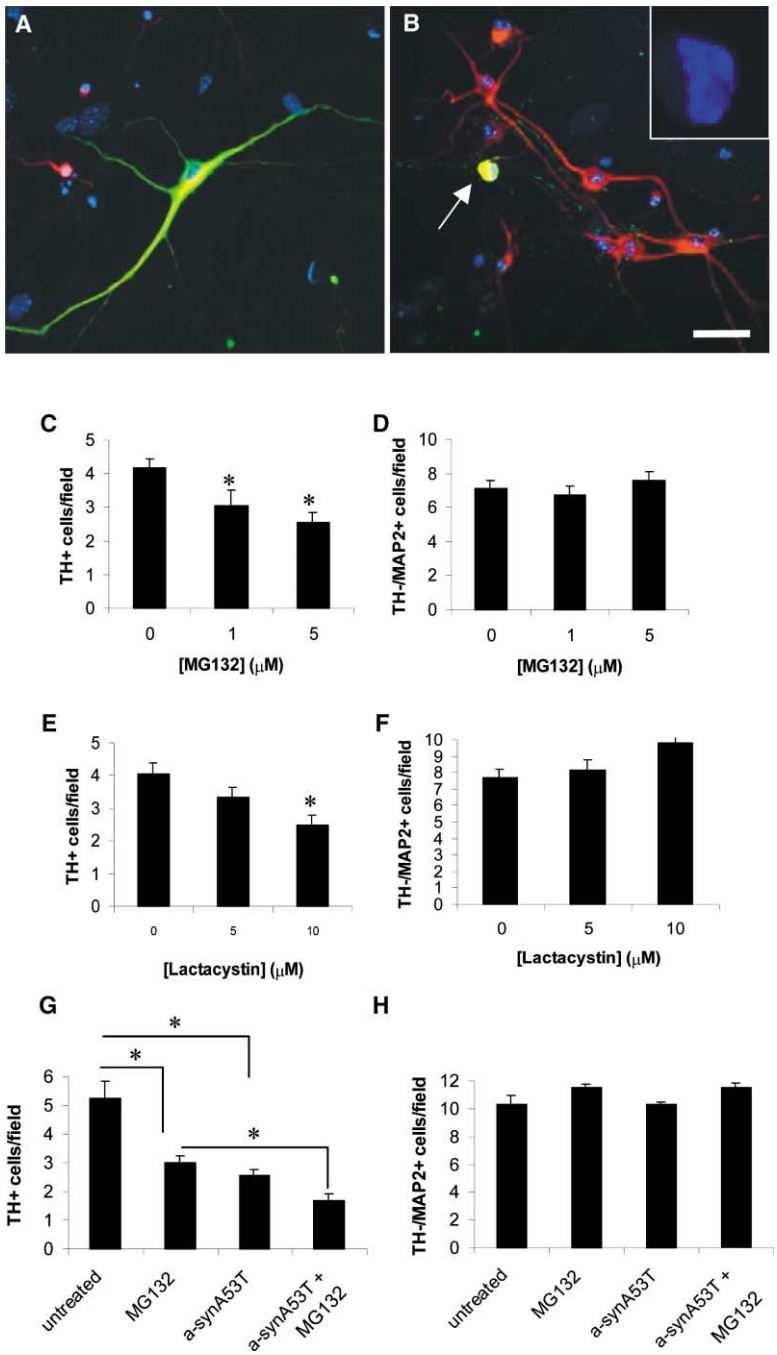

Figure 6. Catecholaminergic Neurons Are Preferentially Susceptible to Proteasome Inhibition in Primary Culture

(A and B) Primary midbrain cultures were left untreated (A) or exposed to 10 μM MG132 for 24 hr (B) and stained for MAP2 (red), TH (green), and Hoechst 33342 (blue) to demonstrate nuclear morphology. Exposure to the proteasome inhibitor caused TH-positive cells to become shrunken and retract processes, but nuclei remained intact (inset in [B]).

(C–F). Cell counts after exposure to MG132 (C and D) or lactacystin (E and F). Both inhibitors substantially affected the TH-positive neuronal population (C,E), whereas TH-negative/MAP2-positive neurons (D and F) were unaffected. Data are shown as cell counts from six randomly selected microscope fields in each of three replicate cultures (hence $n = 18$) and is representative of two to four independent experiments with different batches of primary cells. Statistical significance was assessed using one-way ANOVA with Student-Neuman-Kuells post-hoc tests between each group ($^*p < 0.05$).

(G and H) Additive effect of α-synuclein overexpression and proteasome inhibition. Primary cells as above were transduced with mutant α-synuclein as in Figure 5 for 24 hr then exposed to MG132 for a further 24 hr. Cell counts revealed a loss of TH-positive neurons (G) after either treatment but an additive effect of both treatments together ($^*p < 0.05$ by one-way ANOVA with Student-Newman-Kuells post-hoc test).

protects against the accumulation of its specific protein target(s). Accumulation of these downstream target proteins may also be promoted through ER stress due to a decreased ability of the cells for proper protein folding. The nature of the targets for parkin's E3 ligase activity is still under investigation, although several candidates have been reported (Chung et al., 2001; Imai et al., 2001; Shimura et al., 2001; Zhang et al., 2000). We also show that knockdown of parkin using a stable antisense construct increased sensitivity of cells to proteasome inhibition. This is, in many ways, a better model for loss-of-function mutations than overexpression of the wild-type protein. In ARJP, for example, homozygous large-scale deletions are predicted to reduce enzyme activity to extremely low levels and hence an antisense experiment is closer to this disease model than overexpression. In this experimental setting, there is a clear accumulation of heterologous substrates, as evidenced by accumulation of the GFP-CL1 reporter peptide, suggesting that loss-of-function alleles would decrease the ability of nigral neurons to regulate levels of proteasome substrates. It has been shown recently that proteasome inhibition in vivo damages nigral neurons (McNaught et al., 2002). Our results predict that loss of parkin function would have the same effect.

Both overexpression of mutant α-synuclein and pro-

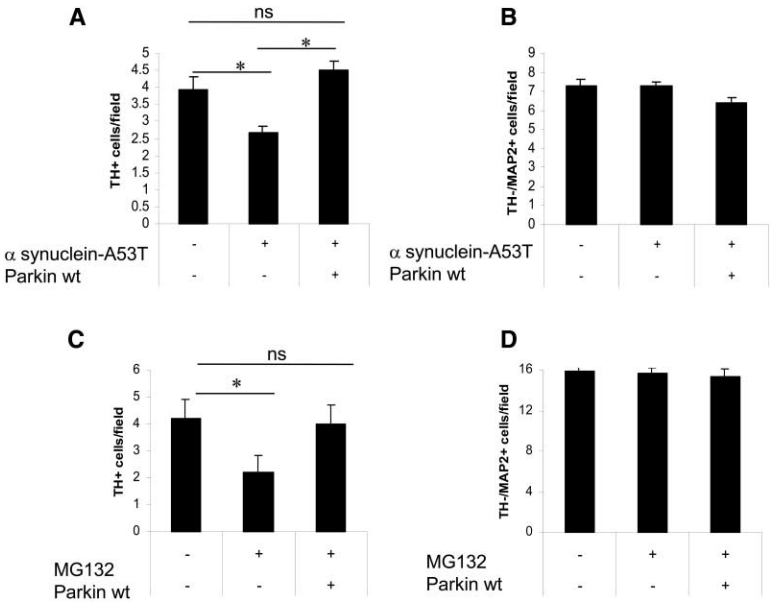

Figure 7. Parkin Rescues Toxicity Associated with Mutant α-Synuclein or Proteasome Inhibition in Primary Midbrain Cells

Primary midbrain neurons were transduced with both mutant α-synuclein and wild-type human parkin. Where either virus was absent (−), LacZ was substituted to keep the total number of viral particles similar. There was a significant reduction in the number of TH-positive neurons (A), which was ameliorated by coexpressing parkin. No effect on TH-negative cells was noted (B). Data are shown as cell counts from six randomly selected microscope fields in each of three replicate cultures (hence n = 18), and statistical significance was assessed using one-way ANOVA with Student-Neuman-Kuells post-hoc tests between each group (*$p < 0.05$; ns, not significant). Similar protective effects were noted using exposure to MG132 to induce toxicity (C and D) where selective toxicity to TH-positive cells was noted (C). The numbers of cell counts and statistical tests are as in (A) and (B).

teasome inhibition produce selective loss of TH-positive neurons. Therefore, proteasome inhibition is sufficient to mimic the effects of mutant α-synuclein. It is not the case that all catecholaminergic neurons are severely affected in PD, while all non-dopaminergic neurons are spared (Braak and Braak, 2000). Nonetheless, we have shown that the SN contains a population of TH-positive cells that are particularly sensitive to both proteasome inhibition and α-synuclein overexpression. The higher sensitivity of catecholaminergic neurons to damage induced by overexpression of mutant α-synuclein may be due to the ability of catecholamines to promote the formation of protofibrillar forms of α-synuclein (Conway et al., 2001). It has been suggested that α-synuclein protofibrils are a major toxic species of this protein, and mutations in α-synuclein also promote protofibril formation (Conway et al., 2000). Recently, it has been shown that, in cultured human dopaminergic neurons, dopamine is required for the toxic effects of mutant α-synuclein, supporting this hypothesis (Xu et al., 2002). We have not seen a protective effect of the same tyrosine hydroxylase inhibitor (α-methyl-*para*-tyrosine; AMPT) in the stable cell lines we used in this study, but this is confounded by a small toxic effect of AMPT alone in our hands (M.R.C. and M.B., unpublished data). In our experiments, mutant α-synuclein is more toxic to TH-positive cells than the wild-type protein. Overexpression of α-synuclein in embryonic mesencephalic cultures (Zhou et al., 2000) or human dopaminergic cells (Xu et al., 2002) produces a similar effect. In some mouse transgenic models, there is pathology associated with a substantial overexpression of wild-type α-synuclein, and there are reports of dopaminergic cell loss in some (Masliah et al., 2000) but not all (Matsuoka et al., 2001; Rathke-Hartlieb et al., 2001; VanDerPutten et al., 2000) models. In a *Drosophila* model, loss of dopaminergic neurons is also seen (Feany and Bender, 2000) with mutant α-synuclein having a more substantial effect than wild-type. Our data are similar to viral-mediated gene transfer experiments where mutant α-synuclein produces nigral cell loss (Kirik et al., 2002).

We did not find microscopically visible protein aggregates, nor did we see the formation of higher molecular weight species of α-synuclein as seen in some models (Lee et al., 2001a). We believe that this is compatible with the idea that protein aggregation to the extent of formation of insoluble fibrillar species is not a required step for α-synuclein toxicity. Soluble protein complexes appear to mediate the toxic effects of mutant α-synuclein in human dopaminergic cells (Xu et al., 2002). The formation of protein aggregates is clearly relevant to the human disease, as the formation of insoluble protein deposits in the form of Lewy bodies occurs in surviving neurons. Previous results using iron/dopamine-mediated toxicity have shown that although formation of protein aggregates and toxicity can be seen under similar conditions, these are dissociatable phenomena (Ostrerova-Golts et al., 2000). Proteasome inhibition might conceivably affect the fibrillization properties of α-synuclein through the phenomenon of "molecular crowding" (Ellis, 2001). Two recent studies have demonstrated that increasing the concentration of macromolecules in the immediate surroundings of α-synuclein increases its propensity to form protofibrillar and fibrillar species (Shtilerman et al., 2002; Uversky et al., 2002). By inhibiting proteasome function, concentrations of many cytosolic proteins will increase, thereby inducing a molecular crowding effect. Therefore, if formation of protofibrillar forms of α-synuclein is important for the toxicity of the mutant forms, proteasome inhibitors are likely to accelerate this process, without having an effect on net α-synuclein protein concentrations. Protection by parkin of TH-positive neurons exposed to either mutant α-synuclein or proteasome inhibition suggests that these two stresses damage cells by similar mechanisms. In the results reported here, antisense-mediated knockdown of parkin also increased levels of heterologous substrates, again potentially inducing accumulation of several toxic proteins and inducing a crowding effect.

The protective effect of parkin on loss of TH-positive neurons mediated by mutant α-synuclein demonstrates that these two proteins have interrelated effects. The

above data suggest that an increased sensitivity of cells to the toxic effects of proteasome inhibition link α-synuclein and parkin as well as providing an explanation for the selective loss of a subgroup of dopaminergic neurons in PD. Whether proteasome inhibition will provide a full explanation for neuronal damage in PD is not clear. There are several genes linked to familial PD that remain to be identified, and it will be critical to evaluate whether manipulations of these products also produces increased sensitivity to proteasome inhibition.

Experimental Procedures

Human Neuroblastoma Cell Lines

The production of stable cell lines overexpressing wild-type or mutant α-synuclein from parental BE (2)-M17 human dopaminergic neuroblastoma cells has been detailed elsewhere (Ostrerova-Golts et al., 2000). Full-length parkin cDNA was cloned into the same vector and transfections performed as described previously (Ostrerova-Golts et al., 2000). An antisense construct was made by placing the first 100 bp of coding sequence for parkin into pCDNA3.1 in the reverse orientation relative to the vector promoter. Stable clones were prepared as above and screened for reduced parkin expression. For the present study, clonal lines for both α-synuclein and parkin were made by limiting dilution and were maintained on 500 $\mu g\ mL^{-1}$ G418. Stable clonal lines were screened for α-synuclein expression by Western blotting using monoclonal antibody to α-synuclein (Clone 42, Transduction Labs). Cell lysates (10 μg total protein per lane) were separated on 16% SDS-PAGE gels (Novex) and transferred to Immobilon membranes (Immobilon, Inc). A soluble extract of adult human cerebral cortex was used as a positive control. After probing with primary antibody (1:1000), blots were developed with peroxidase-labeled secondary antibodies (Jackson Immunochemicals) using enhanced chemiluminescence substrates (Amersham). Blots were reprobed with β-actin (Sigma, clone AC15, 1:5000) to verify equal loading. Quantitation of α-synuclein expression was performed by capturing enhanced chemiluminescence using a CCD camera-based system (AlphaImager, Alpha Innotech Corp). Parkin expression was also monitored by Western blotting using a rabbit polyclonal antibody to the C terminus of parkin (Cell Signaling Technology, 1:2000 dilution). Cell viability was assessed using the MTT assay, as described previously (Cookson et al., 1998). For each experiment, 8 wells were used per concentration of either compound, and each experiment was repeated three times with similar results.

Measurement of Proteasome Function in Living Cells

Stable cell lines were transiently transfected with the GFP^u construct (Bence et al., 2001) and 24 hr later were treated with 5 μM lactacystin for 6 hr or left untreated as controls. Protein extracts and Western blotting were performed as above to measure steady-state amounts of GFP-CL1 fusion protein in the cells using a monoclonal antibody to GFP (Clontech). Blots were reprobed with monoclonal anti-α-synuclein and subsequently with monoclonal anti β-actin as described above.

Primary Cell Cultures

Primary cell cultures were prepared from postnatal mouse midbrain using methods described by Burke et al. (Burke et al., 1998). Briefly, midbrains containing SN and ventral tegmental area were dissected from 2-day-old postnatal mouse pups, using anatomical landmarks as described (Burke et al., 1998; Mena et al., 1997). Neurons from these areas were dissociated with papain and plated on top of preestablished cortical glia cell monolayers at a density of 80,000 cells per well in growth medium which had been preconditioned by adding to glial feeder layers 24 hr prior to plating neurons. Neurons from 3- to 4-week cultures were exposed for 24 hr to MG132 or lactacystin (Calbiochem) and toxicity assessed by staining for tyrosine hydroxylase (TH) and microtubule-associated protein 2 (MAP2). Cells were fixed and permeabilized with 4% paraformaldehyde in Dulbecco's phosphate-buffered saline (DPBS) containing 0.1% (w/v) saponin. After quenching (0.1 M glycine in DPBS, 20 min) and blocking (5% v/v goat serum plus 5% FBS in DPBS, 30 min), primary antibodies were applied overnight at 4°C. These were a combination of polyclonal antibody to TH (Chemicon, 1:200) and monoclonal anti-MAP2 (clone AP-20, Sigma) both at a dilution of 1:200. Secondary antibodies were goat anti-rabbit conjugated to Alexafluor488 (Molecular Probes) and goat anti-mouse conjugated to AlexaFluor 568. For estimations of cell numbers, six random microscope fields (using a 20× objective) were counted in each of three sister cultures, for a total of 18 fields per condition, counting all neuronal cells within each field. Each experiment was repeated two to four times with different batches of primary cells. For staining of α-synuclein, monoclonal anti-human α-synuclein LB509 (Zymed) or monoclonal anti-rodent α-synuclein (clone 42, listed above) were used in the above protocol at a dilution of 1:200. A polyclonal antibody to β-synuclein (Chemicon) was used at 1:500 in conjunction with monoclonal antibody to TH (also Chemicon, 1:200).

Viral Transduction

α-synuclein or parkin cDNAs were cloned into pHSVPrpUC and packaged into recombinant viral particles using 5dl1.2 helper virus and the 2-2 packaging cell line as described (Neve et al., 1997) and purified using sucrose gradients. A control virus expressing LacZ (from pHSVlacZ, Coopersmith and Neve, 1999) was prepared at the same time. Recombinant viruses were titred on human neuroblastoma cell lines. Primary cells were transduced with viral particles at a multiplicity of infection (MOI) of 10. In a small series of experiments, we extracted cultures grown in 6-well plates and blotted for α-synuclein as above.

Statistical Analyses

Differences in the responses of cell lines to proteasome inhibitors were evaluated using two-way analysis of variance (ANOVA) with cell line and concentration of each proteasome inhibitor as variables. For primary cell counts, one-way ANOVA with Student-Neuman-Kuells post-hoc test was used to assess differences between treatments with proteasome inhibitors or with transduction with different viral constructs. For each of these experiments, six fields were counted in each of three independent cultures, hence $n = 18$. In experiments comparing the toxicity associated with overexpression of α-synuclein, we repeated this whole set of experiments three times.

Acknowledgments

The authors would like to thank Dr. David Sulzer, Columbia University, for sharing the methods for culturing postnatal mouse midbrain neurons. We would also like to acknowledge the generous gifts of reagents for HSV-1 packaging from Dr. Rachael Neve, Harvard Medical School, Boston, and Neil Bence and Dr. Ron Kopito of Stanford University for the gift of the GFP^u plasmid. Dr. Ted Dawson, Johns Hopkins Medical Institute, kindly provided the dominant-negative UbCH7 construct. This work was supported by NINDS grants P01-NS40256 and RO1-NS41816-01.

Received: January 16, 2002
Revised: November 21, 2002

References

Ancolio, K., Alves da Costa, C., Ueda, K., and Checler, F. (2000). Alpha-synuclein and the Parkinson's disease-related mutant Ala53Thr-alpha-synuclein do not undergo proteasomal degradation in HEK293 and neuronal cells. Neurosci. Lett. *285*, 79–82.

Bence, N.F., Sampat, R.M., and Kopito, R.R. (2001). Impairment of the ubiquitin-proteasome system by protein aggregation. Science *292*, 1552–1555.

Bennett, M.C., Bishop, J.F., Leng, Y., Chock, P.B., Chase, T.N., and Mouradian, M.M. (1999). Degradation of alpha-synuclein by proteasome. J. Biol. Chem. *274*, 33855–33858.

Braak, H., and Braak, E. (2000). Pathoanatomy of Parkinson's disease. J. Neurol. Suppl. *247*, 3–10.

Burke, R.E., Antonelli, M., and Sulzer, D. (1998). Glial cell line-derived

neurotrophic growth factor inhibits apoptotic death of postnatal substantia nigra dopamine neurons in primary culture. J. Neurochem. *71*, 517–525.

Chung, K.K., Zhang, Y., Lim, K.L., Tanaka, Y., Huang, H., Gao, J., Ross, C.A., Dawson, V.L., and Dawson, T.M. (2001). Parkin ubiquitinates the α-synuclein-interacting protein, synphilin-1: implications for Lewy-body formation in Parkinson disease. Nat. Med. *7*, 1144–1150.

Conway, K.A., Lee, S.J., Rochet, J.C., Ding, T.T., Williamson, R.E., and Lansbury, P.T. (2000). Acceleration of oligomerization, not fibrillization, is a shared property of both alpha-synuclein mutations linked to early-onset Parkinson's disease: implications for pathogenesis and therapy. Proc. Natl. Acad. Sci. USA *97*, 571–576.

Conway, K.A., Rochet, J.-C., Bieganski, R.M., and Lansbury, P.T. (2001). Kinetic stabilization of the α-synuclein protofibril by a dopamine-α-synuclein adduct. Science *294*, 1346–1349.

Cookson, M.R., Ince, P.G., and Shaw, P.J. (1998). Peroxynitrite and hydrogen peroxide induced cell death in the NSC34 neuroblastoma x spinal cord cell line: Role of poly(ADP-ribose) polymerase. J. Neurochem. *70*, 501–508.

Coopersmith, R., and Neve, R.L. (1999). Expression of multiple proteins within single primary cortical neurons using a replication deficient HSV vector. Biotechniques *27*, 1156–1160.

Ellis, R.J. (2001). Macromolecular crowding: an important but neglected aspect of the intracellular environment. Curr. Opin. Struct. Biol. *11*, 114–119.

Farrer, M., Destee, T., Becquet, E., Wavrant-De Vrieze, F., Mouroux, V., Richard, F., Defebvre, L., Lincoln, S., Hardy, J., Amouyel, P., and Chartier-Harlin, M. (2000). Linkage exclusion in French families with probable Parkinson's disease. Mov. Disord. *15*, 1075–1083.

Farrer, M., Chan, P., Chen, R., Tan, L., Lincoln, S., Hernandez, D., Forno, L., Gwinn-Hardy, K., Petrucelli, L., Hussey, J., et al. (2001). Lewy bodies and parkinsonism in families with parkin mutations. Ann. Neurol. *50*, 293–300.

Feany, M.B., and Bender, W.W. (2000). A *Drosophila* model of Parkinson's disease. Nature *404*, 394–398.

Ghee, M., Fournier, A., and Mallet, J. (2000). Rat alpha-synuclein interacts with tat binding protein *1*, a component of the 26S proteasomal complex. J. Neurochem. *75*, 2221–2224.

Gilon, T., Chomsky, O., and Kulka, R.G. (1998). Degradation signals for ubiquitin system proteolysis in Saccharomyces cerevisiae. EMBO J. *17*, 2759–2766.

Hashimoto, M., Rockenstein, E., Mante, M., Mallory, M., and Masliah, E. (2001). beta-Synuclein inhibits alpha-synuclein aggregation: a possible role as an anti-parkinsonian factor. Neuron *32*, 213–223.

Hershko, A., and Ciechanover, A. (1998). The ubiquitin system. Annu. Rev. Biochem. *67*, 425–479.

Imai, Y., Soda, M., and Takahashi, R. (2000). Parkin supresses unfolded protein stress-induced cell death through its E3 ubiquitin-protein ligase activity. J. Biol. Chem. *275*, 35661–35664.

Imai, Y., Soda, M., Inoue, H., Hattori, N., Mizuno, Y., and Takahashi, R. (2001). An unfolded putative transmembrane polypeptide, which can lead to endoplasmic reticulum stress, is a substrate of Parkin. Cell *105*, 891–902.

Junn, E., and Mouradian, M.M. (2002). Human a-synuclein overexpression increases intracellular reactive oxygen species levels and susceptibility to dopamine. Neurosci. Lett. *320*, 146–150.

Kirik, D., Rosenblad, C., Burger, C., Lundberg, C., Johansen, T.E., Muzyczka, N., Mandel, R.J., and Bjorklund, A. (2002). Parkinson-like neurodegeneration induced by the targeted overexpression of α-synuclein in the nigrostriatal system. J. Neurosci. *22*, 2780–2791.

Kitada, T., Asakawa, S., Hattori, N., Matsumine, H., Yamamura, Y., Minoshima, S., Yokochi, M., Mizuno, Y., and Shimizu, N. (1998). Mutations in the parkin gene cause autosomal recessive juvenile parkinsonism. Nature *392*, 605–608.

Ko, L., Mehta, N.D., Farrer, M., Easson, C., Hussey, J., Yen, S., Hardy, J., and Yen, S.H. (2000). Sensitization of neuronal cells to oxidative stress with mutated human alpha-synuclein. J. Neurochem. *75*, 2546–2554.

Kruger, R., Kuhn, W., Muller, T., Woitalla, D., Graeber, M., Kosel, S., Przuntek, H., Epplen, J.T., Schols, L., and Riess, O. (1998). Ala30Pro mutation in the gene encoding alpha-synuclein in Parkinson's disease. Nat. Genet. *18*, 106–108.

Lee, H.J., Shin, S.Y., Choi, C., Lee, Y.H., and Lee, S.J. (2001a). Formation and removal of alpha-synuclein aggregates in cells exposed to mitochondrial inhibitors. J. Biol. Chem. *277*, 5411–5417.

Lee, M., Hyun, D., Halliwell, B., and Jenner, P. (2001b). Effect of the overexpression of wild-type or mutant alpha-synuclein on cell susceptibility to insult. J. Neurochem. *76*, 998–1009.

Leroy, E., Boyer, R., Auburger, G., Leube, B., Ulm, G., Mezey, E., Harta, G., Brownstein, M.J., Jonnalagada, S., Chernova, T., et al. (1998). The ubiquitin pathway in Parkinson's disease. Nature *395*, 451–452.

Maraganore, D.M., Farrer, M.J., Hardy, J.A., Lincoln, S.J., McDonnell, S.K., and Rocca, W.A. (1999). Case-control study of the ubiquitin carboxy-terminal hydrolase L1 gene in Parkinson's disease. Neurology *53*, 1858–1860.

Masliah, E., Rockenstein, E., Veinbergs, I., Mallory, M., Hashimoto, M., Takeda, A., Sagara, Y., Sisk, A., and Mucke, L. (2000). Dopaminergic loss and inclusion body formation in α-synuclein mice: implications for neurodegenerative disorders. Science *287*, 1265–1269.

Matsuoka, Y., Vila, M., Lincoln, S., McCormack, A., Picciano, M., LaFrancois, J., Yu, X., Dickson, D., Langston, W.J., McGowan, E., et al. (2001). Lack of nigral pathology in transgenic mice expressing human alpha-synuclein driven by the tyrosine hydroxylase promoter. Neurobiol. Dis. *8*, 535–539.

McNaught, K.S., and Jenner, P. (2001). Proteasomal function is impaired in substantia nigra in Parkinson's disease. Neurosci. Lett. *297*, 191–194.

McNaught, K.S., Bjorklund, L.M., Belizaire, R., Isacson, O., Jenner, P., and Olanow, C.W. (2002). Proteasome inhibition causes nigral degeneration with inclusion bodies in rats. Neuroreport *13*, 1437–1441.

Mena, M.A., Khan, U., Togasaki, D.M., Sulzer, D., Epstein, C.J., and Przedborski, S. (1997). Effects of wild-type and mutated copper/zinc superoxide dismutase on neuronal survival and L-DOPA-induced toxicity in postnatal midbrain culture. J. Neurochem. *69*, 21–33.

Murphy, D.D., Rueter, S.M., Trojanowski, J.Q., and Lee, V.M. (2000). Synucleins are developmentally expressed, and alpha-synuclein regulates the size of the presynaptic vesicular pool in primary hippocampal neurons. J. Neurosci. *20*, 3214–3220.

Neve, R.L., Howe, J.R., Hong, S., and Kalb, R.G. (1997). Introduction of the glutamate receptor subunit 1 into motor neurons in vitro and in vivo using a recombinant herpes simplex virus. Neuroscience *79*, 435–447.

Ostrerova-Golts, N., Petrucelli, L., Hardy, J., Lee, J.M., Farrer, M., and Wolozin, B. (2000). The A53T α-synuclein mutation increases iron-dependent aggregation and toxicity. J. Neurosci. *20*, 6048–6054.

Pakkenberg, B., Moller, A., Gundersen, H.J., Mouritzen Dam, A., and Pakkenberg, H. (1991). The absolute number of nerve cells in substantia nigra in normal subjects and in patients with Parkinson's disease estimated with an unbiased stereological method. J. Neurol. Neurosurg. Psychiatry *54*, 30–33.

Paxinou, E., Chen, Q., Weisse, M., Giasson, B.I., Norris, E.H., Rueter, S.M., Trojanowski, J.Q., Lee, V.M., and Ischiropoulos, H. (2001). Induction of alpha-synuclein aggregation by intracellular nitrative insult. J. Neurosci. *21*, 8053–8061.

Polymeropoulos, M.H., Lavedan, C., Leroy, E., Ide, S.E., Dehejia, A., Dutra, A., Pike, B., Root, H., Rubenstein, J., Boyer, R., et al. (1997). Mutation in the α-synuclein gene identified in families with Parkinson's disease. Science *276*, 2045–2047.

Rathke-Hartlieb, S., Kahle, P.J., Neumann, M., Ozmen, L., Haid, S., Okochi, M., Haass, C., and Schulz, J.B. (2001). Sensitivity to MPTP is not increased in Parkinson's disease-associated mutant alpha-synuclein transgenic mice. J. Neurochem. *77*, 1181–1184.

Shimura, H., Hattori, N., Kubo, S., Mizuno, Y., Asakawa, S., Minoshima, S., Shimuzu, N., Iwai, K., Chiba, T., Tanaka, K., and Suzuki,

T. (2000). Familial parkinson disease gene product, parkin, is a ubiquitin-protein ligase. Nat. Genet. *25*, 302–305.

Shimura, H., Schlossmacher, M.G., Hattori, N., Frosch, M.P., Trockenbacher, A., Schneider, R., Mizuno, Y., Kosik, K.S., and Selkoe, D.J. (2001). Ubiquitination of a new form of α-synuclein by parkin from human brain: implications for Parkinson's disease. Science *293*, 263–269.

Shtilerman, M.D., Ding, T.T., and Lansbury, P.T. (2002). Molecular crowding accelerates fibrillization of alpha-synuclein: could an increase in the cytoplasmic protein concentration induce Parkinson's disease? Biochemistry *41*, 3855–3860.

Stefanis, L., Larsen, K.E., Rideout, H.J., Sulzer, D., and Greene, L.A. (2001). Expression of A53T mutant but not wild-type α-synuclein in PC12 cells induces alterations of the ubiquitin-dependent degradation system, loss of dopamine release, and autophagic cell death. J. Neurosci. *21*, 9549–9560.

Tanaka, Y., Engelender, S., Igarashi, S., Rao, R.K., Wanner, T., Tanzi, R.E., Sawa, A.L., Dawson, V., Dawson, T.M., and Ross, C.A. (2001). Inducible expression of mutant alpha-synuclein decreases proteasome activity and increases sensitivity to mitochondria-dependent apoptosis. Hum. Mol. Genet. *10*, 919–926.

Tofaris, G.K., Layfield, R., and Spillantini, M.G. (2001). α-Synuclein metabolism and aggregation is linked to ubiquitin-independent degradation by the proteasome. FEBS Lett. *509*, 22–26.

Uversky, V.N., Cooper, E.M., Bower, K.S., Li, J., and Fink, A.L. (2002). Accelerated α-synuclein fibrillation in crowded milieu. FEBS Lett. *515*, 99–103.

VanDerPutten, H., Widerhold, K.-H., Probst, A., Barbieri, S., Misti, C., Danner, S., Kauffmann, S., Hofele, K., Spooren, W.P., Ruegg, M.A., et al. (2000). Neuropathology in mice expressing human α-synuclein. J. Neurosci. *20*, 6021–6029.

Wintermeyer, P., Kruger, R., Kuhn, W., Muller, T., Woitalla, D., Berg, D., Becker, G., Leroy, E., Polymeropoulos, M., Berger, K., et al. (2000). Mutation analysis and association studies of the UCHL1 gene in German Parkinson's disease patients. Neuroreport *11*, 2079–2082.

Xu, J., Kao, S.-Y., Lee, F.J.S., Song, W., Jin, L.-W., and Yankner, B.A. (2002). Dopamine-dependent neurotoxicity of α-synuclein: a mechanism for selective neurodegeneration in Parkinson disease. Nat. Med. *8*, 600–606.

Zhang, Y., Gao, J., Chung, K.K., Huang, H., Dawson, V.L., and Dawson, T.M. (2000). Parkin functions as an E2-dependent ubiquitin-protein ligase and promotes the degradation of the synaptic vesicle-associated protein, CDCrel-1. Proc. Natl. Acad. Sci. USA *97*, 13354–13359.

Zhou, W., Hurlbert, M.S., Schaack, J., Prasad, K.N., and Freed, C.R. (2000). Overexpression of human alpha-synuclein causes dopamine neuron death in rat primary culture and immortalized mesencephalon-derived cells. Brain Res. *866*, 33–43.

ELSEVIER

Neurobiology of Disease

www.elsevier.com/locate/ynbdi
Neurobiology of Disease 18 (2005) 492–498

Mitochondrial associated metabolic proteins are selectively oxidized in A30P α-synuclein transgenic mice—a model of familial Parkinson's disease

H. Fai Poon,[a] Mark Frasier,[b] Nathan Shreve,[a] Vittorio Calabrese,[c] Benjamin Wolozin,[b,1] and D. Allan Butterfield[a,d,e,*]

[a]*Department of Chemistry, University of Kentucky, Lexington, KY 40506-0055, USA*
[b]*Department of Pharmacology, Loyola University Medical Center, Maywood, IL 60153, USA*
[c]*Department of Chemistry, Section of Biochemistry, University of Catania, Catania, Italy*
[d]*Center of Membrane Sciences, University of Kentucky, Lexington, KY 40506-0059, USA*
[e]*Sanders-Brown Center on Aging, University of Kentucky, Lexington, KY 40536, USA*

Received 28 July 2004; revised 16 December 2004; accepted 22 December 2004
Available online 26 January 2005

Parkinson's disease (PD) is the most common neurodegenerative movement disorder and is characterized by the loss of dopaminergic neurons in the substantia nigra compacta. α-Synuclein is strongly implicated in the pathophysiology of PD because aggregated α-synuclein accumulates in the brains of subjects with PD, mutations in α-synuclein cause familial PD, and overexpressing mutant human α-synuclein (A30P or A53T) causes degenerative disease in mice or drosophila. The pathophysiology of PD is poorly understood, but increasing evidence implicates mitochondrial dysfunction and oxidative stress. To understand how mutations in α-synuclein contribute to the pathophysiology of PD, we undertook a proteomic analysis of transgenic mice overexpressing A30P α-synuclein to investigate which proteins are oxidized. We observed more than twofold selective increases in specific carbonyl levels of three metabolic proteins in brains of symptomatic A30P α-synuclein mice: carbonic anhydrase 2 (Car2), alpha-enolase (Eno1), and lactate dehydrogenase 2 (Ldh2). Analysis of the activities of these proteins demonstrates decreased functions of these oxidatively modified proteins in brains from the A30P compared to control mice. Our findings suggest that proteins associated with impaired energy metabolism and mitochondria are particularly prone to oxidative stress associated with A30P-mutant α-synuclein.

Keywords: Parkinson's disease; A30P; Oxidative stress; Lactate dehydrogenase; Enolase; Carbonic anhydrase; Alpha-synuclein; Protein oxidation

Introduction

Parkinson's disease (PD) is the second most common neurodegenerative disorder: approximately 1% of the population by age 65 is affected with PD (Eriksen et al., 2003). Loss of dopaminergic neurons in the substantia nigra compacta results in clinical symptoms of PD, such as bradykinesia, resting tremor, cogwheel rigidity, and postural instability. Although the majority of PD is sporadic, approximately 10% of PD are familial cases (Giasson and Lee, 2003). Mutations in α-synuclein, parkin, DJ-1, and PINK1 are all linked to early onset familial PD (Dawson and Dawson, 2003). In the case of α-synuclein, 4 different mutations have been identified in kindreds associated with familial PD: A53T, A30P, E46A, and genomic duplication (Kruger et al., 1998; Polymeropoulos et al., 1997).

Oxidative damage is a prominent pathological change in PD brains (Alam et al., 1997; Floor and Wetzel, 1998; Yoritaka et al., 1996). Toxicity associated with oxidative stress is exacerbated by overexpression of wild type or mutant α-synuclein (Ostrerova-Golts et al., 2000). Increasing evidence suggests that oxidative stress in PD might also be linked to mitochondrial dysfunction, excitotoxicity, and the toxic effects of nitric oxide, all of which are believed to be associated with cell death in PD brains (Jenner, 2003). Although the relationships of oxidative stress to PD are still unknown, basal protein oxidation is high in the substantia nigra of PD patients, and the levels of reactive carbonyls are increased in PD brains (Alam et al., 1997; Floor and Wetzel, 1998). Together, these data suggest that oxidative stress contributes significantly to the pathophysiology of PD.

Wild-type α-synucleins can bind to lipid membranes, inhibit enzymes such as phospholipase D2, protein kinase C and the dopamine transporter (reviewed in Goedert, 2001). However, α-synuclein has a strong tendency to aggregate, and most studies suggest that the accumulation of aggregated α-synuclein is toxic.

* Corresponding author. Department of Chemistry, Center of Membrane Sciences, and Sanders-Brown Center on Aging, University of Kentucky, Lexington, KY 40506-0055, USA. Fax: +1 859 257 5876.
E-mail address: dabcns@uky.edu (D.A. Butterfield).
[1] Current address: Department of Pharmacology, Boston University School of Medicine, Boston, MA 02118.
Available online on ScienceDirect (www.sciencedirect.com).

0969-9961/$ - see front matter © 2005 Elsevier Inc. All rights reserved.
doi:10.1016/j.nbd.2004.12.009

Expression of mutant α-synuclein cells produces increased levels of 8-hydroxyguanine, protein carbonyls, lipid peroxidation, and 3-nitrotyrosine, and markedly accelerated cell death in response to oxidative insult (Lee et al., 2001). These studies suggest that accelerated aggregation of mutant α-synucleins stimulates oxidative stress by loss of protective effect of the soluble α-synuclein (Li et al., 2001, 2002). In order to gain insight into the mechanism(s) by which loss of antioxidant ability caused by overexpression of A30P mutant α-synuclein leads to cell death, we used proteomics to identify the brain proteins that are significantly oxidatively modified in symptomatic mice with overexpression of a A30P mutation in α-synuclein compared to the brain proteins from the non-transgenic mice.

Methods

Animals

The animals used in this study were previously described. (Kahle et al., 2000; Neumann et al., 2002). The mice develop symptoms between 6 and 14 months. The symptoms begin with a tremor and progress to an end-stage phenotype characterized by muscular rigidity, postural instability and ultimately paralysis. Mice that progressed to end stage symptoms were sacrificed by cervical dislocation and their brains hemi-sectioned. Non-transgenic control mice were C57Bl/6 mice, and were also sacrificed at the same time as the symptomatic transgenic mice.

Sample preparation

Brain tissue extraction was performed as previously described by Sahara et al. (2002) with minor modifications. Left hemi-brains were weighed and homogenized in 3 volumes of TBS (TBS, pH 7.4, 1 mM EDTA, 5 mM sodium pyrophosphate, 30 mM glycerol 2-phosphate, 30 mM sodium fluoride, 1 mM EDTA) containing a protease inhibitor cocktail (Sigma-Aldrich, St. Louis, MO). Protein content was determined via the BCA method.

Two-dimensional gel electrophoresis

Samples of the proteins in the whole brains were prepared as previously described (Poon et al., 2004). Briefly, 200 μg of protein was applied to a pH 3–10 ReadyStrip™ IPG strip (Bio-Rad, Hercules, CA) for isoelectric focusing. The focused IEF strip was stored at −80°C until second dimension electrophoresis was performed.

For second dimension electrophoresis, Linear Gradient (8–16%) Precast criterion Tris–HCl gels (Bio-Rad) were used to separate proteins according to their molecular weight (MrW). Precision Protein™ Standards (Bio-Rad) were run along with the samples.

After electrophoresis, the gel was incubated in fixing solution for 20 min. Sypro Ruby stain was used to stain the gel for 2 h. The gels were placed in deionized water overnight for destaining.

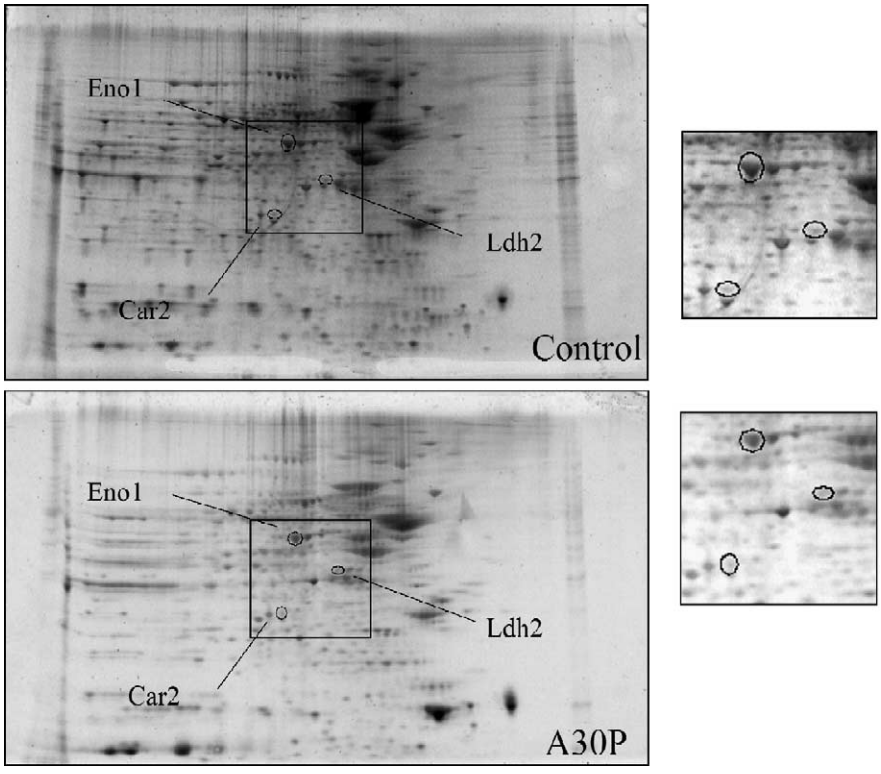

Fig. 1. Representative 2D gel electrophoresis pattern of proteins from mouse brain stem of control (top panel) and symptomatic A30P α-synuclein transgenic mice (bottom panel). The proteins after 2D electrophoresis from the brains of non-transgenic (control, left, top panel) mice and symptomatic A30P α-synuclein transgenic mice (left, bottom panel) described in this study are indicated. Panels on right show expanded of regions of the 2D gel from the mouse brain stems (outlined in the box). The right, top panel shows the expanded region of non-transgenic control brain stem, and the right bottom panel shows the expanded region of symptomatic A30P α-synuclein transgenic mouse brain stem.

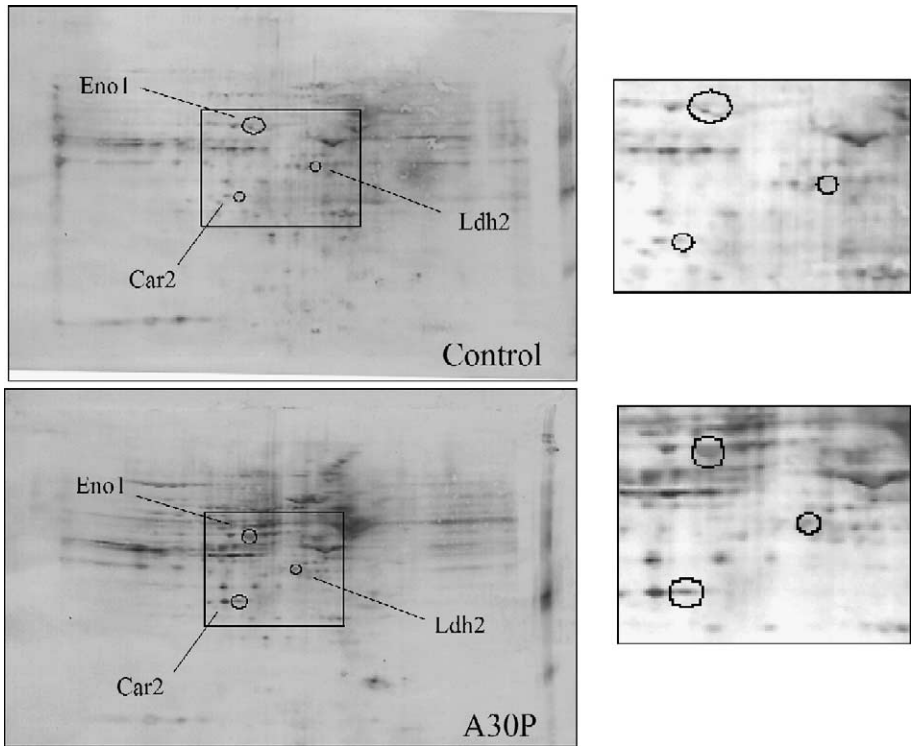

Fig. 2. Representative Western blots showing carbonyl-modified proteins from the brains of A30P α-synuclein transgenic mice and non-transgenic mice. Left-hand blots show carbonyl Western blots of brain lysates from A30P α-synuclein transgenic mice (bottom) and non-transgenic control mice (top). Arrows point to proteins showing significant changes in oxidative modification in the A30P mice brains. Right-hand blots show expansions of the blot outlined in the box. Carbonyl Western blot from the brain of non-transgenic mice is shown in the upper panel and A30P α-synuclein transgenic mice in the lower panel.

Western blotting

Western blotting for 2D gels was performed as previously described (Poon et al., 2004). 200 μg of the brain protein was incubated with 2,4-dinitrophenyl hydrazine (DNPH) at room temperature (25°C) for 20 min. The gels were prepared in the same manner as for 2D-electrophoresis. The proteins from the second dimension electrophoresis gels were transferred onto nitrocellulose paper (Bio-Rad) using a Transblot-Blot® SD semi-Dry Transfer Cell (Bio-Rad) at 15 V for 2 h. The 2,4-dinitrophenylhydrazone (DNP) adducts of the carbonyls of the brain proteins were detected immunochemically.

Image analysis

The gels and nitrocellulose blots were scanned and saved in TIF format using a Storm 860 Scanner (Molecular Dynamics) and Scanjet 3300C (Hewlett Packard), respectively. PDQuest (Bio-Rad) was used for matching and analysis of visualized protein spots among differential gels and oxyblots.

Statistics

The data of specific carbonyl level (intensity of carbonyl level divided by the intensity of protein level of an individual spot) of 6 animals per groups (6 in control group and 6 in A30P group) were analyzed by Student's t test. A value of $P < 0.05$ was considered statistically significant. Only the proteins that are considered significantly different by Student's t test were selected for identification.

Trypsin digestion

Samples were digested using the techniques previously described (Poon et al., 2004). Briefly, the selected protein spots were excised. The gel pieces were digested with 20 ng/μL modified trypsin (Promega, WI) in 25 mM NH_4HCO_3 with the minimal volume to cover the gel pieces. The gel pieces were chopped into smaller pieces and incubated at 37°C overnight in a shaking incubator.

Mass spectrometry

Digests (1 μL) were mixed with 1 μL α-cyano-4-hydroxy-*trans*-cinnamic acid (10 mg/mL in 0.1% TFA:ACN, 1:1, v/v). The mixture (1 μL) was deposited onto a fast evaporation

Table 1
Specific carbonyl level of oxidized proteins in A30P α-synuclein mice

Proteomics identified protein	Wild-type mice (A.U. ± SEM) (n = 6)	A30P α-synuclin transgenic mice (n = 6)	P value
Carbonic anhydrase 2 (Car2)	0.92 ± 0.19	2.22 ± 0.59	<0.05
Alpha-enolase (Eno1)	0.51 ± 0.09	0.93 ± 0.17	<0.05
Lactate dehydrogenase 2 (Ldh2)	0.29 ± 0.18	1.73 ± 0.63	<0.05

nitrocellulose matrix surface, washed twice with 2 μL 5% formic acid, and analyzed with a TofSpec 2E (Micromass, UK) MALDI-TOF mass spectrometer in reflectron mode. The mass axis was adjusted with trypsin autohydrolysis peaks (m/z 2239.14, 2211.10, or 842.51) as lock masses. The MALDI spectra used for protein identification from tryptic fragments were searched against the NCBI protein databases using the MASCOT search engine (http://www.matrixscience.com). Peptide mass fingerprinting used the assumption that peptides are monoisotopic, oxidized at methionine residues and carbamidomethylated at cysteine residues (Butterfield et al., 2003; Castegna et al., 2002, 2003, 2004). Up to 1 missed trypsin cleavage was allowed. Mass tolerance of 150 ppm was the window of error allowed for matching the peptide mass values.

Enzyme activity assay

Lactate dehydrogenase (LDH) enzymatic activity was determined by the method previously described (Stambaugh and Post, 1966; Zewe and Fromm, 1965). Briefly, the assay for the enzyme activity of LDH was performed in 100 μL Tris buffer (0.2 M Tris–HCl, 30 mM sodium pyruvate, 6.6 mM NADH, pH 7.3). The reaction was initiated by adding 5 μL of the samples (2 mg/mL). LDH activity was measured as the reduction of NADH to NAD^+. A decrease in absorbance at 340 nm was recorded as change in A_{340} min^{-1} by using a PowerWaveX® microtiter plated UV–VIS spectrophotometer (Bio-Tek Instruments, Winooki, VT).

Enolase activity assay was performed as described previously (Wagner et al., 2000) with modification. Enolase was added to 100 μL of assay mixture (20 mM Na_2HPO_4, pH 7.4, 400 mM KCl, 0.01 mM EDTA, 2 mM 2-phospho-D-glycerate) in a UV-transparent microtiter plate (Corning, MA). The enzymatic activity was determined by the change of absorption at A_{240} for 5 min.

Carbonic anhydrase activity is measured according to Anderson (Andersson et al., 1972) with modification. Briefly, a CO_2 saturated Tris buffer (pH 8.3, 0.2 M Tris–HCl, phenol red) decreased absorbance at 560 nm, is recorded upon addition of 5 μL of the 2 mg/mL samples. The maximum changes of absorbance are recorded.

Results

We used a parallel approach to investigate the effect of an A30P α-synuclein mutation on specific protein oxidation. Fig. 1 shows representative 2D-electrophoresis gels of brains homogenates from symptomatic A30P α-synuclein transgenic mice (A30P) and non-transgenic mice after Sypro Ruby staining. Fig. 2 shows representative 2D Western blots of the brains of symptomatic non-transgenic mouse and symptomatic A30P-α-synuclein transgenic mice. The specific carbonyl levels indicate the carbonyl level per unit mass of protein (Table 1).

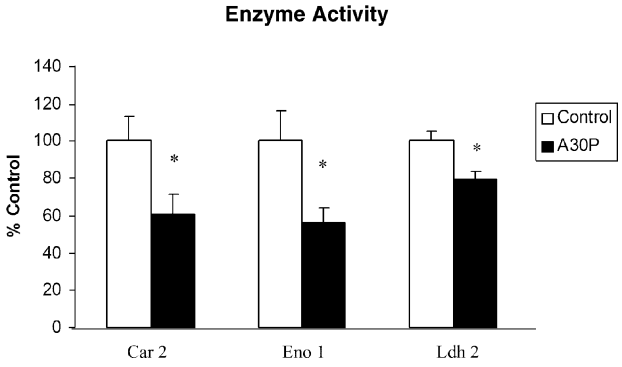

Fig. 3. Enzyme activities of Car2, Eno1, and Ldh2 in brain from A30P mice and non-transgenic control mice. All of the oxidatively modified proteins in A30P-transgenic mice brains show significant decreased activity as compared to that of the non-transgenic mice brains (n = 5–6),*$P \leq 0.05$.

In comparison to wild-type mice, three proteins in the brains of A30P α-synuclein transgenic mice were found to have significantly higher specific carbonyl levels. Only the specific carbonyl level of proteins that are different statistically were identified and reported here. These proteins were identified as carbonic anhydrase 2 (Car2), alpha-enolase (Eno1), and lactate dehydrogenase 2 (Ldh2). Prior results suggest that the accuracy of protein identification by mass spectrometry is equivalent to immunochemical identification (Castegna et al., 2002). The specific carbonyl levels of these proteins are summarized in Table 1. The summary of the mass spectrometry results for the proteins is listed in Table 2.

Oxidative modification of brain proteins leads to loss of their activity (Butterfield, 2004; Butterfield et al., 1997; Hensley et al., 1995; Lauderback et al., 2001; Sultana and Butterfield, 2004). To determine if these proteomic identified oxidatively modified brains proteins in the A30P α-synuclein mouse were dysfunctional, their enzymatic activities were analyzed. The activities of these enzymes in the A30P α-synuclein transgenic mice brains were significantly decreased when compared to the brain proteins from non-transgenic control (Fig. 3).

Discussion

A30P mutation accelerates synuclein aggregation (Conway et al., 1998; Li et al., 2001, 2002; Narhi et al., 1999) and aggregation increases vulnerability to oxidative insult (Lee et al., 2001). Moreover, the aggregation of α-synuclein occurs in parallel with symptoms in A30P α-synuclein transgenic mice (Neumann et al., 2002). Transgenic mice overexpressing α-synuclein develop an age-dependent accumulation of α-synuclein in neurons of the brain

Table 2
Summary of proteins identified by mass spectrometry

Identified protein	gi Accession #	# Peptides matched	% Coverage of matched peptides	pI, MrW (kDa)	Mowse score	Probability of a random identification hit
Carbonic anhydrase 2 (Car2)	gi|33243954	9	30	6.52, 29.1	75	3.16×10^{-80}
Alpha-enolase (Eno1)	gi|13637776	23	61	6.37, 47.4	208	1.58×10^{-21}
Lactate dehydrogenase 2 (Ldh2)	gi|6678674	11	36	5.7, 36.8	103	5.0×10^{-11}

stem (Giasson et al., 2002; Kahle et al., 2001), suggesting the α-synuclein aggregation-associated oxidative stress is involved in the pathology in the A30P α-synuclein transgenic mice.

Car2 is a Zn^{2+} metallo-enzyme that catalyzes reversible hydration of carbon dioxide (CO_2) to bicarbonate (HCO_3^-). Glia use this process to govern the pH shift associated with normal neuroactivity (Chesler and Kaila, 1992; Deitmer and Rose, 1996; Tong and Chesler, 1999). Moreover, Car2 shares high (68%) similarity in amino acid level to the mitochondrial counterpart carbonic anhydrase 5a (Car5a) and 5b (Car5b). One can speculate that they may couple or interact with each other to function in metabolic process, cellular transport, gluconeogenesis, and mitochondrial metabolism (Heck et al., 1994; Shah et al., 2000). Our study shows that Car2 is significantly oxidized in A30P α-synuclein mice and its activity is significantly decreased, suggesting its inactivation may lead to loss of the buffering system in brains with resulting in aggregation of synuclein and neurodegeneration.

Ldh2 is a subunit of lactate dehydrogenase (LDH). LDH is a glycolytic protein that catalyzes the reversible NAD-dependent interconversion of pyruvate to lactate. LDH isoform 5 (LDH-5) in astrocytes favors the formation of lactate (Bittar et al., 1996). Also, LDH-5 is more abundant in mitochondria than elsewhere in cells (Brooks et al., 1999), indicating that lactate is the predominant monocarboxylate oxidized by mitochondria for intracellular lactate transport (Kasischke et al., 2004). Here, we show that Ldh2 is significantly modified and inactivated by oxidative insults in A30P α-synuclein transgenic mice brains, suggesting oxidative inactivation of LDH may contribute to mitochondrial dysfunction in PD patients.

Eno1 is a subunit of enolase that interconverts 2-phosphoglycerate and phosphoenolpyruvate during glycolysis. The loss of the mitochondrial constituent-enriched cells is proportional to the total loss of immunoreactivity to neuronal specific enolase (NSE). Moreover, enolase and other glycolytic enzymes were identified in an intermembrane space/outer mitochondrial membrane fraction (Giege et al., 2003). These studies suggest enolase is present in mitochondria and contribute to mitochondria function. We show here that the specific carbonyl level of Eno1 is significantly increased and its activity is decreased in brains from A30P α-synuclein transgenic mice compared to that of non-transgenic mice, suggesting this oxidative inactivation may alter normal glycolysis and mitochondrial function in brains and contribute to the alteration of energy metabolism in PD.

The striking feature of Ldh2, Eno1 (possibly Car2) is that they are all associated with mitochondrial function. Increasing data implicate mitochondrial decrements and oxidation in PD (Schapira, 2001; Schapira et al., 1998; Sherer et al., 2002). Also, 1-methyl-4-phenyl-1,2,3,6-tetrahydropyridine (MPTP) and rotenone target the mitochondria with increased oxidative modification of proteins and α-synuclein aggregation (Ferrante et al., 1999; Pennathur et al., 1999; Sherer et al., 2003a,b). Moreover, DJ-1, PINK1, and parkin all appear to modulate mitochondrial function (Canet-Aviles et al., 2004; Palacino et al., 2004; Valente et al., 2004). The observation that each of the oxidatively modified brain proteins in A30P synuclein mice is associated with mitochondria provides strong evidence for the notion that mitochondrial dysfunction contributes to the toxicity of PD and implicates mitochondrial pathology in toxicity associated with aggregated synuclein.

Since impairment of energy production and mitochondrial dysfunction leads to neurodegeneration reminiscent of PD both in in vitro and in vivo studies (Benecke et al., 1993; Bouyer et al., 1984; Marey-Semper et al., 1993; Mizuno et al., 1989; Parker et al., 1989; Shoffner et al., 1991; Zeevalk et al., 1995, 1997), our current study suggests that the oxidative stress mediated impaired energy metabolism and mitochondrial dysfunction may be responsible, at least partially, for the neurodegeneration in the brains of A30P α-synuclein transgenic mice. Furthermore, this oxidative stress mediated impaired energy metabolism and mitochondrial dysfunction is brought about through the oxidative inactivation of Eno1, Ldh2, and Car2. We conclude, therefore, that the mitochondria dysfunction and impaired metabolism in familial PD may be associated with the oxidative inactivation of Eno1, Ldh2, and Car2.

Acknowledgments

The authors would like to thank Susan Debusca and Marcia Butterfield for assistance in the preparation of the manuscript. This work was supported in part by grants from NIH [AG-105119; AG-10836] to D.A.B. and from NIH [NS41786] and DAMD [17-01-1-0781] to B.W.

References

Alam, Z.I., Daniel, S.E., Lees, A.J., Marsden, D.C., Jenner, P., Halliwell, B., 1997. A generalised increase in protein carbonyls in the brain in Parkinson's but not incidental Lewy body disease. J. Neurochem. 69, 1326–1329.

Andersson, B., Nyman, P.O., Strid, L., 1972. Amino acid sequence of human erythrocyte carbonic anhydrase B. Biochem. Biophys. Res. Commun. 48, 670–677.

Benecke, R., Strumper, P., Weiss, H., 1993. Electron transfer complexes I and IV of platelets are abnormal in Parkinson's disease but normal in Parkinson-plus syndromes. Brain 116 (Pt. 6), 1451–1463.

Bittar, P.G., Charnay, Y., Pellerin, L., Bouras, C., Magistretti, P.J., 1996. Selective distribution of lactate dehydrogenase isoenzymes in neurons and astrocytes of human brain. J. Cereb. Blood Flow Metab. 16, 1079–1089.

Bouyer, J.J., Park, D.H., Joh, T.H., Pickel, V.M., 1984. Chemical and structural analysis of the relation between cortical inputs and tyrosine hydroxylase-containing terminals in rat neostriatum. Brain Res. 302, 267–275.

Brooks, G.A., Dubouchaud, H., Brown, M., Sicurello, J.P., Butz, C.E., 1999. Role of mitochondrial lactate dehydrogenase and lactate oxidation in the intracellular lactate shuttle. Proc. Natl. Acad. Sci. U. S. A. 96, 1129–1134.

Butterfield, D.A., 2004. Proteomics: a new approach to investigate oxidative stress in Alzheimer's disease brain. Brain Res. 1000, 1–7.

Butterfield, D.A., Hensley, K., Cole, P., Subramaniam, R., Aksenov, M., Aksenova, M., Bummer, P.M., Haley, B.E., Carney, J.M., 1997. Oxidatively induced structural alteration of glutamine synthetase assessed by analysis of spin label incorporation kinetics: relevance to Alzheimer's disease. J. Neurochem. 68, 2451–2457.

Butterfield, D.A., Boyd-Kimbel, D., Castegna, A., 2003. Proteomics in Alzheimer's disease; insights into mechanisms into neurodegeneration. J. Neurochem. 86, 1313–1327.

Canet-Aviles, R.M., Wilson, M.A., Miller, D.W., Ahmad, R., McLendon, C., Bandyopadhyay, S., Baptista, M.J., Ringe, D., Petsko, G.A., Cookson, M.R., 2004. The Parkinson's disease protein DJ-1 is neuroprotective due to cysteine-sulfinic acid-driven mitochondrial localization. Proc. Natl. Acad. Sci. U. S. A. 101, 9103–9108.

Castegna, A., Aksenov, M., Aksenova, M., Thongboonkerd, V., Klein, J.B., Pierce, W.M., Booze, R., Markesbery, W.R., Butterfield, D.A., 2002. Proteomic identification of oxidatively modified proteins in Alzheim-

er's disease brain. Part I: creatine kinase BB, glutamine synthase, and ubiquitin carboxy-terminal hydrolase L-1. Free Radical Biol. Med. 33, 562–571.

Castegna, A., Thongboonkerd, V., Klein, J.B., Lynn, B., Markesbery, W.R., Butterfield, D.A., 2003. Proteomic identification of nitrated proteins in Alzheimer's disease brain. J. Neurochem. 85, 1394–1401.

Castegna, A., Thongboonkerd, V., Klein, J.B., Lynn, B., Markesbery, W.R., Butterfield, D.A., 2004. Proteomic identification of oxidatively modified proteins in gracile axonal dystrophy mice. J. Neurochem. 88, 1540–1546.

Chesler, M., Kaila, K., 1992. Modulation of pH by neuronal activity. Trends Neurosci. 15, 396–402.

Conway, K.A., Harper, J.D., Lansbury, P.T., 1998. Accelerated in vitro fibril formation by a mutant alpha-synuclein linked to early-onset Parkinson disease. Nat. Med. 4, 1318–1320.

Dawson, T.M., Dawson, V.L., 2003. Molecular pathways of neurodegeneration in Parkinson's disease. Science 302, 819–822.

Deitmer, J.W., Rose, C.R., 1996. pH regulation and proton signalling by glial cells. Prog. Neurobiol. 48, 73–103.

Eriksen, J.L., Dawson, T.M., Dickson, D.W., Petrucelli, L., 2003. Caught in the act: alpha-synuclein is the culprit in Parkinson's disease. Neuron 40, 453–456.

Ferrante, R.J., Hantraye, P., Brouillet, E., Beal, M.F., 1999. Increased nitrotyrosine immunoreactivity in substantia nigra neurons in MPTP treated baboons is blocked by inhibition of neuronal nitric oxide synthase. Brain Res. 823, 177–182.

Floor, E., Wetzel, M.G., 1998. Increased protein oxidation in human substantia nigra pars compacta in comparison with basal ganglia and prefrontal cortex measured with an improved dinitrophenylhydrazine assay. J. Neurochem. 70, 268–275.

Giasson, B.I., Lee, V.M., 2003. Are ubiquitination pathways central to Parkinson's disease? Cell 114, 1–8.

Giasson, B.I., Duda, J.E., Quinn, S.M., Zhang, B., Trojanowski, J.Q., Lee, V.M., 2002. Neuronal alpha-synucleinopathy with severe movement disorder in mice expressing A53T human alpha-synuclein. Neuron 34, 521–533.

Giege, P., Heazlewood, J.L., Roessner-Tunali, U., Millar, A.H., Fernie, A.R., Leaver, C.J., Sweetlove, L.J., 2003. Enzymes of glycolysis are functionally associated with the mitochondrion in Arabidopsis cells. Plant Cell 15, 2140–2151.

Goedert, M., 2001. Alpha-synuclein and neurodegenerative diseases. Nat. Rev., Neurosci. 2, 492–501.

Heck, R.W., Tanhauser, S.M., Manda, R., Tu, C., Laipis, P.J., Silverman, D.N., 1994. Catalytic properties of mouse carbonic anhydrase V. J. Biol. Chem. 269, 24742–24746.

Hensley, K., Hall, N., Subramaniam, R., Cole, P., Harris, M., Aksenov, M., Aksenova, M., Gabbita, P., Wu, J.F., Carney, J.M., Lovell, M., Markesbery, W.R., Butterfield, D.A., 1995. Brain regional correspondence between Alzheimer's disease histopathology and biomarkers of protein oxidation. J. Neurochem. 65, 2146–2156.

Jenner, P., 2003. Oxidative stress in Parkinson's disease. Ann. Neurol. 53 (Suppl. 3), S26–S36 (discussion S36-28).

Kahle, P.J., Neumann, M., Ozmen, L., Muller, V., Jacobsen, H., Schindzielorz, A., Okochi, M., Leimer, U., van Der Putten, H., Probst, A., Kremmer, E., Kretzschmar, H.A., Haass, C., 2000. Subcellular localization of wild-type and Parkinson's disease-associated mutant alpha-synuclein in human and transgenic mouse brain. J. Neurosci. 20, 6365–6373.

Kahle, P.J., Neumann, M., Ozmen, L., Muller, V., Odoy, S., Okamoto, N., Jacobsen, H., Iwatsubo, T., Trojanowski, J.Q., Takahashi, H., Wakabayashi, K., Bogdanovic, N., Riederer, P., Kretzschmar, H.A., Haass, C., 2001. Selective insolubility of alpha-synuclein in human Lewy body diseases is recapitulated in a transgenic mouse model. Am. J. Pathol. 159, 2215–2225.

Kasischke, K.A., Vishwasrao, H.D., Fisher, P.J., Zipfel, W.R., Webb, W.W., 2004. Neural activity triggers neuronal oxidative metabolism followed by astrocytic glycolysis. Science 305, 99–103.

Kruger, R., Kuhn, W., Muller, T., Woitalla, D., Graeber, M., Kosel, S., Przuntek, H., Epplen, J.T., Schols, L., Riess, O., 1998. Ala30Pro mutation in the gene encoding alpha-synuclein in Parkinson's disease. Nat. Genet. 18, 106–108.

Lauderback, C.M., Hackett, J.M., Huang, F.F., Keller, J.N., Szweda, L.I., Markesbery, W.R., Butterfield, D.A., 2001. The glial glutamate transporter, GLT-1, is oxidatively modified by 4-hydroxy-2-nonenal in the Alzheimer's disease brain: the role of Abeta1-42. J. Neurochem. 78, 413–416.

Lee, M., Hyun, D., Halliwell, B., Jenner, P., 2001. Effect of the overexpression of wild-type or mutant alpha-synuclein on cell susceptibility to insult. J. Neurochem. 76, 998–1009.

Li, J., Uversky, V.N., Fink, A.L., 2001. Effect of familial Parkinson's disease point mutations A30P and A53T on the structural properties, aggregation, and fibrillation of human alpha-synuclein. Biochemistry 40, 11604–11613.

Li, J., Uversky, V.N., Fink, A.L., 2002. Conformational behavior of human alpha-synuclein is modulated by familial Parkinson's disease point mutations A30P and A53T. Neurotoxicology 23, 553–567.

Marey-Semper, I., Gelman, M., Levi-Strauss, M., 1993. The high sensitivity to rotenone of striatal dopamine uptake suggests the existence of a constitutive metabolic deficiency in dopaminergic neurons from the substantia nigra. Eur. J. Neurosci. 5, 1029–1034.

Mizuno, Y., Ohta, S., Tanaka, M., Takamiya, S., Suzuki, K., Sato, T., Oya, H., Ozawa, T., Kagawa, Y., 1989. Deficiencies in complex I subunits of the respiratory chain in Parkinson's disease. Biochem. Biophys. Res. Commun. 163, 1450–1455.

Narhi, L., Wood, S.J., Steavenson, S., Jiang, Y., Wu, G.M., Anafi, D., Kaufman, S.A., Martin, F., Sitney, K., Denis, P., Louis, J.C., Wypych, J., Biere, A.L., Citron, M., 1999. Both familial Parkinson's disease mutations accelerate alpha-synuclein aggregation. J. Biol. Chem. 274, 9843–9846.

Neumann, M., Kahle, P.J., Giasson, B.I., Ozmen, L., Borroni, E., Spooren, W., Muller, V., Odoy, S., Fujiwara, H., Hasegawa, M., Iwatsubo, T., Trojanowski, J.Q., Kretzschmar, H.A., Haass, C., 2002. Misfolded proteinase K-resistant hyperphosphorylated alpha-synuclein in aged transgenic mice with locomotor deterioration and in human alpha-synucleinopathies. J. Clin. Invest. 110, 1429–1439.

Ostrerova-Golts, N., Petrucelli, L., Hardy, J., Lee, J.M., Farer, M., Wolozin, B., 2000. The A53T alpha-synuclein mutation increases iron-dependent aggregation and toxicity. J. Neurosci. 20, 6048–6054.

Palacino, J.J., Sagi, D., Goldberg, M.S., Krauss, S., Motz, C., Wacker, M., Klose, J., Shen, J., 2004. Mitochondrial dysfunction and oxidative damage in parkin-deficient mice. J. Biol. Chem. 279, 18614–18622.

Parker Jr., W.D., Boyson, S.J., Parks, J.K., 1989. Abnormalities of the electron transport chain in idiopathic Parkinson's disease. Ann. Neurol. 26, 719–723.

Pennathur, S., Jackson-Lewis, V., Przedborski, S., Heinecke, J.W., 1999. Mass spectrometric quantification of 3-nitrotyrosine, *ortho*-tyrosine, and *o*,*o*′-dityrosine in brain tissue of 1-methyl-4-phenyl-1,2,3,6-tetrahydropyridine-treated mice, a model of oxidative stress in Parkinson's disease. J. Biol. Chem. 274, 34621–34628.

Polymeropoulos, M.H., Lavedan, C., Leroy, E., Ide, S.E., Dehejia, A., Dutra, A., Pike, B., Root, H., Rubenstein, J., Boyer, R., Stenroos, E.S., Chandrasekharappa, S., Athanassiadou, A., Papapetropoulos, T., Johnson, W.G., Lazzarini, A.M., Duvoisin, R.C., Di Iorio, G., Golbe, L.I., Nussbaum, R.L., 1997. Mutation in the alpha-synuclein gene identified in families with Parkinson's disease. Science 276, 2045–2047.

Poon, H.F., Castegna, A., Farr, S.A., Thongboonkerd, V., Lynn, B.C., Banks, W.A., Morley, J.E., Klein, J.B., Butterfield, D.A., 2004. Quantitative proteomics analysis of specific protein expression and oxidative modification in aged senescence-accelerated-prone 8 mice brain. Neuroscience 126, 915–926.

Sahara, N., Lewis, J., DeTure, M., McGowan, E., Dickson, D.W., Hutton, M., Yen, S.H., 2002. Assembly of tau in transgenic animals expressing

P301L tau: alteration of phosphorylation and solubility. J. Neurochem. 83, 1498–1508.

Schapira, A.H., 2001. Causes of neuronal death in Parkinson's disease. Adv. Neurol. 86, 155–162.

Schapira, A.H., Gu, M., Taanman, J.W., Tabrizi, S.J., Seaton, T., Cleeter, M., Cooper, J.M., 1998. Mitochondria in the etiology and pathogenesis of Parkinson's disease. Ann. Neurol. 44, S89–S98.

Shah, G.N., Hewett-Emmett, D., Grubb, J.H., Migas, M.C., Fleming, R.E., Waheed, A., Sly, W.S., 2000. Mitochondrial carbonic anhydrase CA VB: differences in tissue distribution and pattern of evolution from those of CA VA suggest distinct physiological roles. Proc. Natl. Acad. Sci. U. S. A. 97, 1677–1682.

Sherer, T.B., Betarbet, R., Greenamyre, J.T., 2002. Environment, mitochondria, and Parkinson's disease. Neuroscientist 8, 192–197.

Sherer, T.B., Betarbet, R., Kim, J.H., Greenamyre, J.T., 2003a. Selective microglial activation in the rat rotenone model of Parkinson's disease. Neurosci. Lett. 341, 87–90.

Sherer, T.B., Kim, J.H., Betarbet, R., Greenamyre, J.T., 2003b. Subcutaneous rotenone exposure causes highly selective dopaminergic degeneration and alpha-synuclein aggregation. Exp. Neurol. 179, 9–16.

Shoffner, J.M., Watts, R.L., Juncos, J.L., Torroni, A., Wallace, D.C., 1991. Mitochondrial oxidative phosphorylation defects in Parkinson's disease. Ann. Neurol. 30, 332–339.

Stambaugh, R., Post, D., 1966. A spectrophometric method for the assay of lactic dehydrogenase subunits. Anal. Biochem. 15, 470–480.

Sultana, R., Butterfield, D.A., 2004. Identification of oxidatively modified GST and MRP1 in Alzheimer's disease brain. Neurochem. Res. 29, 2215–2220.

Tong, C.K., Chesler, M., 1999. Endogenous pH shifts facilitate spreading depression by effect on NMDA receptors. J. Neurophysiol. 81, 1988–1991.

Valente, E.M., Abou-Sleiman, P.M., Caputo, V., Muqit, M.M., Harvey, K., Gispert, S., Ali, Z., Del Turco, D., Bentivoglio, A.R., Healy, D.G., Albanese, A., Nussbaum, R., Gonzalez-Maldonado, R., Deller, T., Salvi, S., Cortelli, P., Gilks, W.P., Latchman, D.S., Harvey, R.J., Dallapiccola, B., Auburger, G., Wood, N.W., 2004. Hereditary early-onset Parkinson's disease caused by mutations in PINK1. Science 304, 1158–1160.

Wagner, S., Breiteneder, H., Simon-Nobbe, B., Susani, M., Krebitz, M., Niggemann, B., Brehler, R., Scheiner, O., Hoffmann-Sommergruber, K., 2000. Hev b 9, an enolase and a new cross-reactive allergen from hevea latex and molds. Purification, characterization, cloning and expression. Eur. J. Biochem. 267, 7006–7014.

Yoritaka, A., Hattori, N., Uchida, K., Tanaka, M., Stadtman, E.R., Mizuno, Y., 1996. Immunohistochemical detection of 4-hydroxynonenal protein adducts in Parkinson disease. Proc. Natl. Acad. Sci. U. S. A. 93, 2696–2701.

Zeevalk, G.D., Derr-Yellin, E., Nicklas, W.J., 1995. Relative vulnerability of dopamine and GABA neurons in mesencephalic culture to inhibition of succinate dehydrogenase by malonate and 3-nitropropionic acid and protection by NMDA receptor blockade. J. Pharmacol. Exp. Ther. 275, 1124–1130.

Zeevalk, G.D., Manzino, L., Hoppe, J., Sonsalla, P., 1997. In vivo vulnerability of dopamine neurons to inhibition of energy metabolism. Eur. J. Pharmacol. 320, 111–119.

Zewe, V., Fromm, H.J., 1965. Kinetic studies of rabbit muscle lactate dehydrogenase. Ii. Mechanism of the reaction. Biochemistry 43, 782–792.